THERMODYNAMIC AND SPECTROSCOPIC INVESTIGATIONS OF NOVEL ANTIMICROBIAL PEPTIDES CONTAINING UNNATURAL AMINO ACIDS WITH MODEL MEMBRANE SYSTEMS

By
Amanda Laura Russell
April, 2011

Chair: Dr. Rickey P. Hicks
Major Department: Chemistry

With the over prescription and use of antibiotic drugs the evolution of drug resistant bacteria strains has become a world wide health crisis. In response to this crisis, the search for new drugs to kill bacteria via a novel mode of action has become of critical importance to modern medicine. Natural and synthetic antimicrobial peptides (AMPs) have exhibited a broad spectrum of activity against various infectious microorganisms while exhibiting little to no mammalian cell toxicity. It's because of this selectivity that AMPs are considered as a potential new source of therapeutics for drug-resistant bacteria. It is believed that the selectivity for bacteria cell membranes over host cells and the potency between different bacteria strains is derived from the ability of the AMPs to exploit the differences in chemical composition of various organism's membranes. The hypothesis guiding this research states: The physicochemical surface properties of the target cell's membrane interact with the 3D physicochemical surface properties of the approaching AMP inducing a conformational change onto the AMP maximizing the interactions between the two to facilitate AMP-membrane binding and the formation of pores leading to intracellular leakage and cell death. There are two binding interactions that are of interest, the S-state and I-state. The S-state, or surface state, refers to the binding of the peptide to the surface of the membrane, while the I-state involves the insertion of

the peptide into the bilayer. By understanding the interactions of various AMPs with different target cell membranes one can develop novel analogs with increased potency and selectivity for a particular strain of bacteria. This knowledge would eventually lead to the design of antimicrobial peptides used as pharmaceuticals to treat bacteria resistant to current antibiotics. In our laboratory we have developed a series of antimicrobial peptides that incorporate unnatural amino acids to impart specific physicochemical properties onto these peptides. Circular Dichroism (CD), isothermal titration calorimetry (ITC) and calcein leakage assays were conducted and it was determined that there are two distinctly different mechanisms of binding occurring between this series of peptides and zwitterionic and anionic membrane models. By understanding the interactions of various AMPs with different target cell membranes one can develop novel analogs with increased potency and selectivity.

THERMODYNAMIC AND SPECTROSCOPIC INVESTIGATIONS OF NOVEL ANTIMICROBIAL PEPTIDES CONTAINING UNNATURAL AMINO ACIDS WITH MODEL MEMBRANE SYSTEMS

By
Amanda Laura Russell

A Dissertation
Submitted to the Faculty of
East Carolina University
In Partial Fulfillment of the Requirements
For the Degree of Doctor of Philosophy
in the Department of Chemistry

East Carolina University, North Carolina
2011

THERMODYNAMIC AND SPECTROSCOPIC INVESTIGATIONS OF NOVEL ANTIMICROBIAL PEPTIDES CONTAINING UNNATURAL AMINO ACIDS WITH MODEL MEMBRANE SYSTEMS

By

Amanda Laura Russell

APPROVED BY:
DIRECTOR OF DISSERTATION:

_____

Rickey Hicks, Ph.D.

COMMITTEE MEMBER:

_____

Anne Spuches, Ph.D.

COMMITTEE MEMBER:

_____

Colin Burns, Ph.D.

COMMITTEE MEMBER:

_____

Anthony Kennedy, Ph.D.

COMMITTEE MEMBER:

_____

John Kenney, Ph.D.

CHAIR OF DEPARTMENT OF CHEMISTRY:

_____

Rickey Hicks, Ph.D.

DEAN OF THE GRADUATE SCHOOL:

_____

Paul Gemperline, Ph.D.

ACKNOWLEDGEMENTS

First, I would like to thank my advisor, Dr. Rickey Hicks, for all of his support, sharing his knowledge and encouraging me through my project. I am grateful for all of the analogies and for the “politically incorrect” humor. We both know being “politically correct” is overrated. Words cannot express how grateful I am. Dr. Anne Spuches served as committee member, but I am most grateful for her role as my mentor and friend. Her guidance and positivity has made even the toughest times bearable. A huge thank you to my committee members, Dr. Anthony Kennedy, Dr. Colin Burns and Dr. John Kenney, for their guidance and encouragement through the years. I could not have asked for a better committee. Thank you to East Carolina University and the Department of Chemistry for the opportunity and the faculty and staff for their friendly smiles and warm welcome. Thank you to the Bacterial Therapeutics Program 2.1 of the Defense Threat Reduction Agenct, contract # W81XWH-082-0095 for funding. want to thank

I am blessed to have met so many great people while here in Greenville. I truly believe school is an educational experience, academically and personally, and they all played a major part in making it a memorable journey. A special thanks to Brittany Williams for all of her hard work in the lab, taking care of Bailey and for being a great friend. I am also grateful for all of my friends in Charlotte that have always made it a point to continue our friendships, even with miles and weeks between us. I look forward to being apart of each others everyday lives.

My family has been my support system through the years to achieve my goals, even when they weren’t sure what those goals entailed. I want to thank my mom, dad, sister, brother-in-law, Aunt Laura and Uncle John for all of their love, support and encouragement. I owe everything I am to them. They are truly amazing and irreplaceable people. And thank you to my boyfriend, Ben, for handling the distance and miles apart better than I could have, or did.

TABLE OF CONTENTS

Page

AKNOWLEDGMENTS ii

LIST OF TABLES iv

LIST OF FIGURES vii

LIST OF ABBREVIATIONS xiv

CHAPTER ONE: INTRODUCTION 1

CHAPTER TWO: MATERIALS AND METHODS 38

CHAPTER THREE: COMPOUND 23 54

CHAPTER FOUR: SPACER # 1 88

CHAPTER FIVE: SPACER # 2 132

CHAPTER SIX: SPACER # 3 172

CHAPTER SEVEN: ROLE PLAYED BY NUMBER AND PLACEMENT OF POSITIVELY CHARGED CLUSTER 204

CHAPTER EIGHT: INACTIVE COMPOUNDS AS NEGATIVE CONTROLS 233

CHAPTER NINE: APPLICATION OF A RATIONAL DRUG DESIGN 243

CONCLUSIONS 284

LIST OF TABLES

Page

1.1 Amino acid sequences of the three most studied analogues of magainin……..11

1.2 Amino acid sequences of synthesized peptides containing three Tic-Oic Dipeptide units that are pertinent to this research……..18

2.1 The concentration of each peptide (μM) used for the binding studies with POPC and 4:1 POPC/POPG LUV membrane model via CD……....44

2.2 Sample calculation chart for the composition of samples used for the "pseudo" CD titration experiments……....47

2.3 The final concentration of each peptide (μM) used for the "pseudo" CD titration studies with POPC and 4:1 POPC/POPG membrane models……..47

2.4 The concentration of each peptide (μM) used during the full ITC titration studies……49

3.1 Broad spectrum antibacterial in vitro activity (μM) and hemolytic activity for compound **23**……54

3.2 In vitro antibacterial activity (μM) against Gram negative and other drug resistant bacteria strains for compound **23**……55

3.3 Thermodynamic data for compound **23** as determined from X_b vs c_m……..75

3.4 ΔH (kcal/mol) for single injection ITC experiments of compound **23**……..80

4.1 Amino acid sequences of compounds **23**, **36**, **29** and **37**……...89

4.2 Broad spectrum antibacterial in vitro activity (μM) and hemolytic activity for compounds **23**, **36**, **29** and **37**……...90

4.3 In vitro antibacterial activity (μM) against Gram negative and other drug Resistant bacteria strains for compounds **23**, **36**, **29** and **37**……..91

4.4 Thermodynamic data for compounds **23**, **36**, **29** and **37** as determined from X_b vs c_m……...113

4.5 ΔH (kcal/mol) for single injection experiments for compounds **23**, **36**, **29** and **37**……120

5.1 Amino acid sequences for compounds **23**, **43**, **53**, **45** and **56**……..133

5.2 Broad spectrum antibacterial in vitro activity (μM) and hemolytic activity for compounds **23**, **43**, **53**, **45** and **56**……...134

5.3 In vitro antibacterial activity (μM) against specific Gram negative and other drug resistant bacteria strains for compounds **23**, **43**, **53**, **45** and **56**……...134

5.4 Average distances between the side chain amine and the α-carbon of the Spacer #2 amino acid residues…….136

5.5 Thermodynamic data for compounds **23**, **43**, **53**, **45** and **56** as determined from X_b vs c_m ……..160

5.6 ΔH (kcal/mol) for single injection experiments for compounds **23**, **43**, **53**, **45** and **56**……..163

6.1 Amino acid sequences for compounds **23**, **50**, **51** and **52**……172

6.2 Broad spectrum antibacterial in vitro activity (μM) and hemolytic activity for compounds **23**, **50**, **51** and **52**…….173

6.3 In vitro antibacterial activity (μM) against specific Gram negative and other drug resistant bacteria strains for compounds **23**, **50**, **51** and **52**…….173

6.4 Thermodynamic data for compounds **23**, **50**, **51** and **52** as determined from X_b vs c_m ……..192

6.5 ΔH (kcal/mol) for single injection experiments for compounds **23**, **50**, **51** and **52**…….196

7.1 Amino acid sequences for compounds **23**, **64**, **39** and **61** ……...204

7.2 Broad spectrum antibacterial in vitro activity (μM) and hemolytic activity for compounds **23**, **64**, **39** and **61**…….205

7.3 In vitro antibacterial activity (μM) against specific Gram negative and other drug resistant bacteria strains for compounds **23**, **64**, **39** and **61**…….206

7.4 Thermodynamic data for compounds **23**, **64**, **39** and **61** as determined from X_b vs c_m ……..225

8.1 Amino acid sequences for compounds **23**, **14** and **34**……..233

8.2 Broad spectrum antibacterial in vitro activity (μM) and hemolytic activity for compounds **23**, **14** and **34**……...234

9.1 Average distances between the side chain amine and the α-carbon of the

Spacer #2 amino acid residues in rational drug design……267

9.2 Broad spectrum antibacterial in vitro activity (µM) and hemolytic activity for compound **46**……..270

9.3 In vitro antibacterial activity (µM) against specific Gram negative and other drug resistant bacteria strains for compound **46**……..271

LIST OF FIGURES

Page

1.1 Schematic diagram of toroidal pore mechanism.....5

1.2 Basic skeleton of AMPs containing three Tic-Oic dipeptide units Developed in our laboratory 14

1.3 Schematic diagram of an ITC instrument 20

1.4 Result of an ideal ITC experiment from the titration of lipid into peptide 22

1.5 Schematic of peptide-induced calcein leakage from liposomes 28

2.1 Chemical structures of SDS and DPC 38

2.2 Chemical structures of POPG and POPC 39

2.3 Chemical structure of calcein 39

2.4 Gel filtration column for the separation of calcein-encapsulate LUVs 42

2.5 Representative HT [V] values for compound **23** in POPC and 4:1 POPC/POPG LUVs 45

2.6 Representative absorbance spectra for compound **23** in POPC and 4:1 POPC/POPG LUVs 46

2.7 Representative emission spectra of peptide-induced calcein leakage.....51

3.1 CD spectra of tetrapeptides in 40 mM phosphate buffer 57

3.2 CD spectra of compound **23** in varying ratios of buffer and TFE 58

3.3 CD spectra of compound **23** in buffer, DPC and SDS.....59

3.4 CD spectra of compound **23** varying ratios of POPC to POPG.....60

3.5 CD spectra of compound **23** in buffer, POPC and 4:1 POPC/POPG LUVs.....62

3.6 CD spectra of separate compound **23** samples with solutions of increasing POPC LUV concentration.....65

3.7 CD spectra of separate compound **23** samples with solutions of increasing 4:1 POPC/POPG LUV concentration 67

3.8 Plots of CD intensity at 210 and 220 nm versus L/P rations for compound **23**.....68

3.9 Illustrative schematic of the full titration experiment of lipid into peptide.....70

3.10 Full titration ITC data for compound **23** with POPC and 4:1 POPC/POPG LUVs.....72

3.11 The plots of X_b versus c_f and X_b versus c_m for compound **23**.....74

3.12 Illustrative schematic of single injection ITC experiments for the titration of peptide into lipid.....76

3.13 Single injection ITC data for compound **23** into POPC and 4:1 POPC/POPG LUVs 77

3.14 Illustrative schematic of single injection ITC experiments for the titration of lipid into peptide.....78

3.15 Single injection ITC data for the titration of POPC and 4:1 POPC/POPC LUVs into compound **23**.....79

3.16 Calcein leakage of compound **23** for POPC and 4:1 POPC/POPG LUVs 81

3.17 Total calcein leakage for compound **23** from POPC and 4:1 POPC/POPG LUVs 82

4.1 CD spectra of compounds **23**, **36**, **29** and **37** in buffer 93

4.2 CD spectra of compounds **23**, **36**, **29** and **37** in SDS and DPC.....94

4.3 CD spectra of compounds **23**, **36**, **29** and **37** in POPC LUVs 96

4.4 CD spectra of compounds **23**, **36**, **29** and **37** in 4:1 POPC/POPG LUVs.....97

4.5 CD spectra of separate samples of compounds **23**, **36**, **29** and **37** with solutions of increasing POPC LUV concentration 99

4.6 CD spectra of separate samples of compounds **23**, **36**, **29** and **37** with solutions of increasing 4:1 POPC/POPG LUV concentration.....101

4.7 Full titration experiment for 4:1 POPC/POPG into compounds **23**, **36**, **29** and **37**.....103

4.8 Single injection ITC data for the titration of compounds **23**, **36**, **29** and **37** in 4:1 POPC/POPG LUVs 105

4.9 Single injection ITC data for the titration of 4:1 POPC/POPG LUVs into compounds **23**, **36**, **29** and **37**.....107

4.10 Full titration ITC experiment for POPC LUVs into compounds **23**, **36**, **29** and **37** 109

4.11 Plots for X_b against c_f for compounds **23**, **36**, **29** and **37**.....110

4.12 Plots for X_b against c_m for compounds **23**, **36**, **29** and **37**.....112

4.13 Single injection ITC data for the titration of compounds **23**, **36**, **29** and **37** into POPC LUVs 117

4.14 Single injection ITC data for the titration of POPC LUVs into compounds **23**, **36**, **29** and **37**.....119

4.15 Calcein leakage for compounds **23**, **36**, **29** and **37** from POPC LUVs.....122

4.16 Calcein leakage for compounds **23**, **36**, **29** and **37** from 4:1 POPC/POPG LUVs 123

4.17 Total calcein leakage for compounds **23**, **36**, **29** and **37** from POPC and 4:1 POPC/POPG LUVs 125

5.1 CD spectra of compounds **23**, **43**, **53**, **45** and **56** in buffer 135

5.2 CD spectra of compounds **23**, **43**, **53**, **45** and **56** in SDS and DPC 137

5.3 CD spectra of compounds **23**, **43**, **53**, **45** and **56** in POPC LUVs 139

5.4 CD spectra of compounds **23**, **43**, **53**, **45** and **56** in 4:1 POPC/POPG LUVs.....140

5.5 CD spectra of separate samples of compounds **23**, **43**, **53**, **45** and **56** with solutions of increasing POPC LUV concentration 142

5.6 CD spectra of separate samples of compounds **23**, **43**, **53**, **45** and **56** with solutions of increasing 4:1 POPC/POPG LUV concentration 144

5.7 Full titration ITC experiment for the titration of 4:1 POPC/POPG into compounds **23**, **43**, **53**, **45** and **56** 148

5.8 Single injection ITC experiments for the titration of compounds **23**, **43**, **53**, **45** and **56** into 4:1 POPC/POPG LUVs 150

5.9 Single injection ITC data for the titration of 4:1 POPC/POPG LUVs into compounds **23**, **43**, **53**, **45** and **56** 152

5.10 Full titration experiment for the titration of POPC LUVs into compounds **23**, **43**, **53**, **45** and **56**.....154

5.11 Plot of X_b against c_f for compounds **23**, **43**, **53**, **45** and **56**.....156

5.12 Plot of X_b against c_m for compounds **23**, **43**, **53**, **45** and **56** 158

5.13 Single injection ITC data for the titration of compounds **23**, **43**, **53**, **45** and **56** into POPC LUVs.....161

5.14 Single injection ITC data for the titration of POPC LUVs into compounds **23**, **43**, **53**, **45** and **56**.....162

5.15 Calcein leakage of compounds **23**, **43**, **53**, **45** and **56** from POPC LUVs 164

5.16 Calcein leakage of compounds **23**, **43**, **53**, **45** and **56** from 4:1 POPC/POPG LUVs.....166

5.17 Total calcein leakage for compounds **23**, **43**, **53**, **45** and **56** in POPC and 4:1 POPC/POPG LUVs 167

6.1 CD spectra of compounds **23**, **50**, **51** and **52** in buffer 174

6.2 CD spectra of compounds **23**, **50**, **51** and **52** in SDS and DPC 175

6.3 CD spectra of compounds **23**, **50**, **51** and **52** in POPC LUVs 176

6.4 CD spectra of compounds **23**, **50**, **51** and **52** in 4:1 POPC/POPG LUVs.....177

6.5 CD spectra of separate samples of compounds **23**, **50**, **51** and **52** with solutions of increasing POPC LUV concentration 178

6.6 CD spectra of separate samples of compounds **23**, **50**, **51** and **52** with solutions of increasing 4:1 POPC/POPG LUV concentration.....180

6.7 Full titration experiment for the titration of 4:1 POPC/POPG LUVs into compounds **23**, **50**, **51** and **52** 182

6.8 Single injection ITC data for the titration of compounds **23**, **50**, **51** and **52** into 4:1 POPC/POPG LUVs. 184

6.9 Single injection ITC data for the titration of 4:1 POPC/POPG LUVs into compounds **23**, **50**, **51** and **52** 186

6.10 Full titration experiment for the titration of POPC LUVs into Compounds **23**, **50**, **51** and **52**.....188

6.11 Plot of X_b against c_f for compounds **23**, **50**, **51** and **52**.....189

6.12 Plot of X_b against c_m for compounds **23**, **50**, **51** and **52**.....191

6.13 Single injection ITC data for the titration of compounds **23**, **50**, **51** and **52** into POPC LUVs....194

6.14 Single injection ITC data for the titration of POPC LUVs into compounds **23**, **50**, **51** and **52**....195

6.15 Calcein leakage for compounds **23**, **50**, **51** and **52** from POPC LUVs....197

6.16 Calcein leakage for compounds **23**, **50**, **51** and **52** from 4:1 POPC/POPG LUVs....198

6.17 Total calcein leakage for compounds **23**, **50**, **51** and **52** from POPC and 4:1 POPC/POPG LUVs....199

7.1 CD spectra of compounds **23**, **64**, **39** and **61** in buffer....207

7.2 CD spectra of compounds **23**, **64**, **39** and **61** in SDS and DPC....209

7.3 CD spectra of compounds **23**, **64**, **39** and **61** in POPC LUVs....210

7.4 CD spectra of compounds **23**, **64**, **39** and **61** in 4:1 POPC/POPG LUVs....211

7.5 CD spectra of separate samples of compounds **23**, **64**, **39** and **61** with solutions of increasing POPC LUV concentration....212

7.6 CD spectra of separate samples of compounds **23**, **64**, **39** and **61** with solutions of increasing 4:1 POPC/POPG concentration....214

7.7 Full titration experiment for the titration of 4:1 POPC/POPG LUVs into compounds **23**, **64**, **39** and **61**....217

7.8 Full titration experiment for the titration of POPC LUVs into compounds **23**, **64**, **39** and **61**....220

7.9 Plots of X_b against c_f for compounds **23**, **64**, **39** and **61**....222

7.10 Plots of X_b against c_m for compounds **23**, **64**, **39** and **61**....224

7.11 Calcein leakage for compounds **23**, **64**, **39** and **61** from POPC LUVs....227

7.12 Calcein leakage for compounds **23**, **64**, **39** and **61** from 4:1 POPC/POPG LUVs....228

7.13 Total calcein leakage for compounds **23**, **64**, **39** and **61** from POPC and 4:1 POPC/POPG LUVs....229

8.1 CD spectra of compounds **14** and **34** in buffer, SDS and DPC....235

8.2 CD spectra of separate samples of compounds **14** and **34** with solutions of increasing POPC LUV concentration 236

8.3 CD spectra of separate samples of compounds **14** and **34** with solutions of increasing 4:1 POPC/POPG LUV concentration....237

8.4 Full titration experiment for the titration of POPC LUVs into compounds **14** and **34**....238

8.5 Full titration experiments for the titration of 4:1 POPC/POPG LUVs into compounds **14** and **34**....239

8.6 Calcein leakage for compounds **14** and **34** from POPC and 4:1 POPC/POPG LUVs 240

9.1 Cartoon representation of the important structural and physicochemical Features to be incorporated into a new AMP....251

9.2 Structure of the Tic-Oic dipeptide conformationally restrained unit....254

9.3 Stereoview of the ChemDraw 3D minimum energy structures for five tetrapeptides....255

9.4 CD spectra of tetrapeptides in buffer....256

9.5 Representative novel C^{α}-tetrasubstituted α-amino acids developed by Grauer and Konig....257

9.6 Six alicyclic α-amino acids commercially available as either Fmoc or tBoc protected analogs or the free amino acids....258

9.7 Stereoviews of hexapeptides....260

9.8 Commercially available analogs of β-Leu and β-Phe....262

9.9 Partial listing of commercially available rigid spacers derived from benzoic acid 263

9.10 Some hydrophobic and tryptophan analogs used by Haug and coworkers 265

9.11 A partial list of commercially available hydrophobic amino acids which may be used to modify the electronic character of the aromatic ring of Phe 266

9.12 Analogs of the amino acid Lys with increased positive charge and side-chain bulk developed by Oh and Lee 268

9.13 Designed amino acid sequence incorporating the desired structural and physicochemical properties 270

9.14 CD spectra of compound **46** in buffer, SDS, DPC, POPC and

4:1 POPC/POPG LUVs 276

9.15 Calcein leakage for compound **46** from POPC and 4:1 POPC/POPG LUVs.....277

LIST OF ABBREVIATIONS

Ahx	6-Aminohexanoic acid
AMP	Antimicrobial peptide
βAla	Beta alanine
CD	Circular dichroism
Dab	Diaminobutyric acid
DPC	Dodecylphosphocholine
Dpr	Diaminopropionic acid
Gaba	Gamma aminobutyric acid
ITC	isothermal titration calorimetry
LUV	large unilamellar vesicles
MIC	minimum inhibitory concentration
MR	*Mycobacterium ranae*
Oic	Octahydroindolecarboxylic acid
Orn	ornithine
POPC	1-Palmitoyl-2-Oleoyl-*sn*-Glycero-3-Phosphocholine
POPG	1-Palmitoyl-2-Oleoyl-*sn*-Glycero-3-[Phospho-*rac*-(1-glycerol)] (Sodium Salt**)**
QSAR	Quantitative Structure Activity Relationship
Tic	Tetrahydroisoquinolinecarboxylic acid
SA	*Staphylococcus aureus*
SDS	Sodium dodecyl sulfate
ST	*Salmonella typhimurium*
SUV	small unilamellar vesicles

CHAPTER ONE: INTRODUCTION

General Background

Over the past two decades, infections caused by antibiotic-resistant bacteria have increased, while the number of new antibacterial agents approved in the United States has decreased. [1-3] Approximately 36 new antibacterial drugs were approved in the United States since 1988, however, only one new antibacterial drug was approved between 2006 and 2009.[1] The overuse of antibiotics has facilitated an increase in the evolution of resistance of several gram-positive and gram-negative pathogens that cause infection particularly in hospital environments. In a 2008 report, Rice grouped *Enterococcus faecium*, *Staphylococcus aureus*, *Klebsiella pneumoniae, Acinetobacter baumanii*, *Pseudomonas aeruginosa*, and *Enterobacter* species as the "ESKAPE" pathogens because they were the major cause of infections in hospitals in the United States due to their resistance to established antibacterial agents. [3] The Center for Disease Control reported that more people die from methicillin-resistant *S. aureus* (MRSA) infections in US hospital than HIV/AIDS and tuberculosis combined. [4] In a testimony by Spellberg to the House Committee on Energy and Commerce Subcommittee on Health on behalf of the Infectious Diseases Society of America, he stated that nearly 100,000 people die per year in the US as a result of antibiotic-resistant infections they acquired in hospitals. This number, however, does not take into account the number of deaths caused by infections acquired outside of a hospital setting. [Testimony of the Infectious Diseases Society of America (IDSA), entitled "Antibiotic Resistance: Promoting Critically Needed Antibiotic Research and Development and Appropriate Use ("Stewardship") of these Precious Drugs" presented by Brad Spellberg, MD, FIDSA, before the House Committee on Energy and Commerce Subcommittee on Health, June 9, 2010] This serious health crisis has lead to the necessity for a new generation of

pharmaceuticals with a novel mode of action against bacterial agents.[5] Antimicrobial peptides (AMPs), which are found as natural components of the innate immune system of a vast array of organisms, have emerged as possible new therapeutic agents to replace traditional antibiotics because of their broad spectrum activity against gram positive and negative bacteria, fungi and protozoa.[5-7] It is believed that by optimizing multiple parameters, including, but not limited to, the reduction of mammalian cell toxicity and the susceptibility to proteolytic degradation, AMPs have the potential to be developed as drugs to treat drug-resistant bacteria infections.[7, 8]

To date, there are over 1,700 naturally occurring peptides obtained from a variety of different species that have been identified and their amino acid sequences determined.[9] These peptides are listed in a database developed by Wang[9] and are classified by their biological activities such as antibacterial, anticancer, antiviral and antifungal. [9] Naturally occurring AMPs have been isolated from various living organisms including humans, [10] amphibians, [11] insects, mammals,[12] birds, fish and plants.[7, 8, 13-15] In addition to these, several thousand new AMPs have been engineered and produced synthetically.[8] AMPs are a part of the body's natural immune system and they protect the body in the event of exposure to infectious microorganisms[5, 14, 16] by either killing the microorganism, slowing its growth or aiding the body's other natural self-defense mechanisms.[7] In general, most AMPs consist of 10-50 amino acid residues and are highly positively charged, with a positive charge between +3 and +9, due to the incorporation of basic amino acids such as lysine and arginine. Due to their well defined regions of hydrophobic and hydrophilic character (~50% hydrophobic),[17] they are considered to be amphipathic molecules.[5, 8, 12, 13] As previously mentioned, AMPs are of great therapeutic interest as many AMPs have shown broad spectrum bioactivity against several different strains of bacteria

including Gram positive and Gram negative, mycobacterium, fungi and protozoa [5] while exhibiting very low mammalian toxicity.

AMPs are classified based on their amino acid composition and structure. The focus of this research is a class of linear, cationic, α-helical peptides. This subgroup contains approximately 290 peptides [7, 18] which are relatively short containing less than 40 amino acid residues, lack cysteine residues, and in some cases, contain a kink or hinge in the middle of the sequence.[7, 18, 19] These particular peptides are disordered in aqueous solutions, exhibiting characteristics of random coil conformation, however they adopt an ordered amphipathic secondary structure in the presence of a membrane environment, where all or part of the peptide is involved in an α-helix [7, 19-23] Generally, these AMPs exhibit minimum inhibitory concentrations (MIC) in the low-micromolar range. [7, 13, 14, 24] The MIC value represents the concentration of an AMP that will inhibit 50% of the growth for a microorganism.

Modes of Action

AMPs can be divided into two subclasses based on the mechanism of action by which they kill bacteria cells, non-membrane disruptors [16, 25, 26] and membrane disruptors. [7, 24, 25] The former, as the name suggests, does not involve the permeation of the cell membrane, but rather involves the translocation of peptides into the cytoplasmic area of the cell interrupting and/or inhibiting functions such as cell-wall synthesis, protein synthesis and metabolism.[7, 25, 27] The latter refers to those AMPs that cause cell lysis through the disruption of the integrity of the cell membrane. [5, 8, 28] Although the exact mechanism by which the cell is destroyed is not fully understood, there is a general agreement that the first target for any class of peptides is the negatively charged membranes of bacterial cells.[13, 15, 22, 24, 27, 29]

There are several proposed theories concerning the mechanism of action between peptides and membranes, but the attraction and attachment of the peptide to the surface of the membrane is the first step in either mechanism of action.[22] The positively charged residues of the peptide are attracted to the negatively charged phospholipids of the target cell by electrostatic interactions. [7, 14, 24] Once the peptide is bound to the surface via electrostatic interactions, the hydrophobic side-chains insert into the hydrophobic core of the membrane, anchoring the peptide to the membrane, inducing a conformation that maximizes the electrostatic and hydrophobic interactions while minimizing the repulsive forces. [17, 26] At low peptide concentrations the peptide is believed to align itself parallel to the surface of the membrane causing a thinning of the membrane which is a concentration dependent process (Surface or S-state). Once a particular peptide to lipid ratio is reached, which varies for both peptide and target lipid composition, the perpendicularly oriented peptides insert into the bilayer forming transmembrane pores (Insertion or I-state).[7, 30-32] The exact mechanism involving I-state formation could involve one of several accepted theories, including "carpet,"[33, 34] barrel stave,[7, 35, 36] and a toroidal pore mechanism.[35, 37, 38] The toroidal pore mechanism (**Figure 1.1**) is the most pertinent to our research.

The toroidal pore theory is a well understood mechanism for pore formation. As a peptide comes into contact with the membrane, it will orient itself in such a way as to adopt an α-helical conformation and align itself parallel to the surface (S-state).[16, 39] The hydrophobic residues of the bound peptide will cause local displacement of the lipid polar head groups introducing a strain onto the surface that will ultimately lead to thinning, displacement of head groups leading to a decrease in thickness of the bilayer, and destabilization of the membrane surface. As the concentration of peptide increases they aggregate to form complexes of 4-6 units, in a way such

that their polar residues are no longer exposed to the hydrocarbon chains and only associate with the polar head groups of the lipids.[16, 37] The peptides then change their orientation from parallel to perpendicular relative to the membrane surface.[7, 13, 40] Due to the destabilization caused by the membrane thinning, the oligomers are able to insert into the bilayer, forming a toroidal arrangement of peptides.[39] As the helical oligomers insert into the membrane, the polar head groups of the phospholipids are pulled into the pore inducing a continuous bending of the lipid monolayer through the pore.

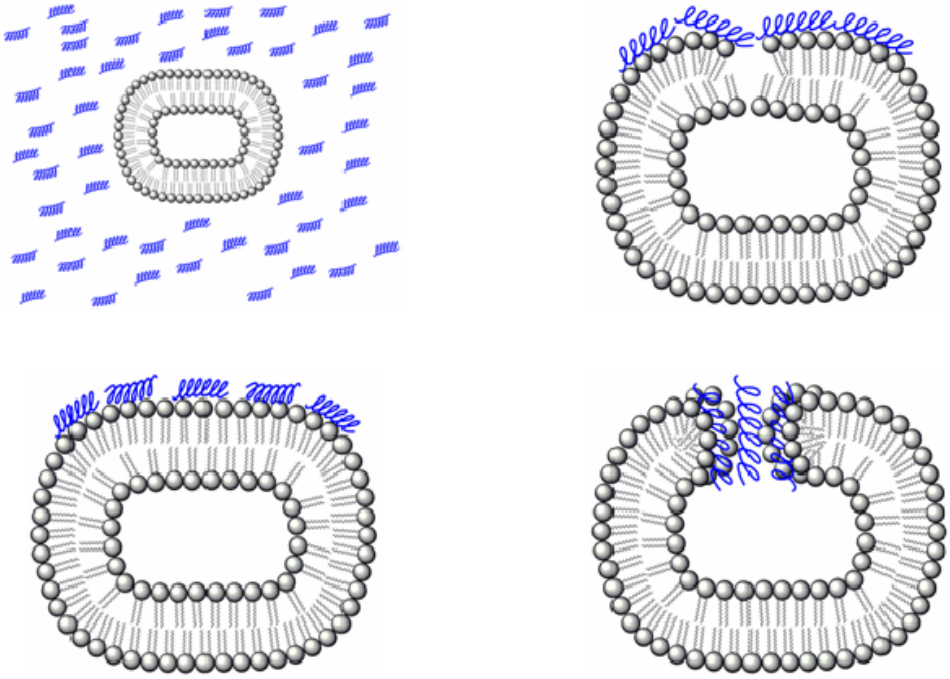

Figure 1.1: Schematic diagram of toroidal pore mechanism. Liposome surrounded by free peptide in bulk solution (top left). Peptide is pulled to membrane via electrostatic interactions and binds to the surface (bottom left). Peptides aggregate on the surface of the membrane, causing the disruption and rearrangement of lipid polar head groups (top right). Peptides insert into bilayer, pulling polar head groups into the pore (bottom right). Figure was adapted from Brogden.[7]

Because the hydrophobic side-chains are buried in the bilayer, the pore becomes lined with the hydrophilic faces of the peptides, as well as, the polar head groups of the monolayer that were pulled in. Finally, the outer and inner monolayers bend into each other becoming fused together causing a continuous bend from top to bottom. [7] Once the transmembrane pore is formed, the intracellular components can leak out or, upon disintegration of the pore, some of the peptides can enter the cytoplasmic leaflet of the membrane and target the intracellular components. Both result in cell lysis and death.[16] The main difference between this mechanism and that of the barrel stave model is that in the toroidal model, the peptides are always associated with the polar head groups of the monolayers, even when inserted into the core of the bilayer.[7, 16]

Membrane-disrupting peptides can be further classified as being cell-selective or non-cell selective.[41] The therapeutic usefulness of a peptide as a pharmaceutical agent is dependent upon its ability to differentiate between a bacterial cell and a mammalian host cell. While non-cell selective AMPs are toxic to both bacterial and mammalian cells, cell-selective AMPs are of high interest as they exhibit potent activity against bacterial cells while exhibiting much less activity against mammalian cells.[28, 41, 42]The first step of any binding mechanism is the attraction of the peptide to the membrane surface and it is believed that the driving force behind this affinity is the composition of the target cell's membrane.[8, 12, 14, 17, 24] The chemical composition of the membrane of mammalian red blood cells is very different from the chemical composition of membranes of bacterial cells. In general, mammalian red blood cells contain zwitterionic phospholipids having an overall neutral charge, while bacterial cell membranes contain a high percentage of anionic phospholipids having an overall negative charge.[43] The composition of bacterial cell membranes also varies between different strains. Gram-positive bacteria membranes are covered by a porous layer of peptidoglycan and are considered to be the easiest

membrane to penetrate. The membranes of Gram-negative bacteria are slightly more complex consisting of two lipid membranes containing lipopolysaccharides and porins.[14, 44] The bacterium with the most complex bacteria membrane, and therefore the hardest to penetrate and kill, is that of the mycobacterium which has a thick mycolate-rich outer coat. [16, 45]

Important Characteristics of AMPS

There are several physicochemical characteristics of AMPs that can affect antimicrobial activity and specificity. [7, 19, 46] They include size, charge, hydrophobicity, conformation, amphipathicity and polar angle where the charge, hydrophobicity, amphipathicity and conformation are closely related.[16] If the peptide is not long enough, it may be unable to span the width of the bilayer, making it impossible to form pores. Most active peptides range from as few as 10 amino acid residues to as many as 50. Shorter peptides offer a simpler synthesis, although, the truncation of a peptide to fewer than 20 amino acid residues results in an α-helical peptide that is unable to span a lipid bilayer. [24, 47] From a mechanistic perspective, this would explain the loss of activity. However, possessing the ability to span a bilayer is not a necessity as there are α-helical peptides with as few as 13 residues that retain antibacterial activity.[24, 48] In one study it was determined that 12-18 residues were the required length for activity, with optimal antibacterial/hemolytic properties ratio found at 14 residues.[18]

The importance of the sequence is not in the types of amino acids, but rather the patterns in distribution of the different types of residues within the sequence to give a variation of physicochemical properties. [18] Hydrophobic and charged residues are two major types of residues that play a major role in the activity of a peptide. The peptides focused on in this research are highly positively charged from +4 to +6 with the incorpotation of lysines, arginines

or other basic amino acids residues, as are most AMPs. The positive charges of basic amino acids are the driving force of the electrostatic interactions that attract the AMPs to the negatively charged surfaces of the bacterial cell membrane, thus, playing a major role in the activity and specificity of the AMP.[16] Several studies have shown a correlation between charge and potency.[12, 18, 49] Increasing the charge can increase both antibacterial and hemolytic activity, [50] however, a large increase in charge could also decrease the activity as it would prevent the peptide from adopting a structure which would promote binding.[51] Magainin studies showed that with an increase in charge, smaller, less stable and short lived pores are formed with a faster translocation across the membrane, thus causing an increase in hemolytic activity and a loss of antibacterial activity.[16] The suggested optimal charge for maximal lytic activity is +4.[52]

The overall percentage of hydrophobic residues in an active AMP, natural or synthetic, is approximately 50% and includes the incorporation of residues such as alanine, leucine, phenylalanine or tryptophan.[16, 18] The net hydrophobicity of the peptide is very important to the activity as it governs the attachment of the peptide to the surface and the extent of insertion into the bilayer.[16] However, an increase in hydrophobicity has been correlated to increased hemolysis and a decrease in cell selectivity.[53]

As previously mentioned, this class of AMPs adopts amphipathic α-helical conformations upon interaction with the surface of a target cell's membrane. The extent of the amphipathic helicity influences the peptides activity as well as its selectivity and reflects the relative abundance and placement of the charged and hydrophobic residues.[16] Approximate ratios of 1:1 to 1:2 of charged residues to hydrophobic residues appear optimal for such a structure.[18] It has been shown that by having the charged or hydrophobic residues confined to the N- or C-terminal segments, respectively, the peptide is inactive. For activity, a transversal amphipathic

arrangement of the residues is necessary, for example, polar and nonpolar regions running along the length of the peptide.[18] As the peptide is attracted to the surface of the membrane via electrostatic interactions, an amphipathic α-helix is adopted with polar residues dominating one face of the helix and the hydrophobic residues the other.[18] Such a conformation maximizes the attractive interactions while minimizing the repulsive interactions with the surface of the membrane.

The polar index, more commonly referred to as the polar angle, is the ratio of the polar to nonpolar regions of a peptide folded into an amphipathic helix. For example, for an α-helical peptide that contains two defined regions, one polar and the other nonpolar, the polar angle would be 180^{o}. By decreasing the segregation of these regions, the polar angle would be decreased in a proportional manner. Several studies have been conducted to investigate the role that the polar angle plays in the interaction of peptides with membranes. An increase in the hydrophobic surface area of the peptide, and therefore a smaller polar angle, resulted in an increase in the peptides ability to permeabiate membranes.[53-55] Although peptides with smaller polar angles induced greater membrane permeability, translocation and pore formation rates, these pores were also less stable. These studies lead to the conclusion that the hydrophilic and hydrophobic components of the peptide play very significant roles in the interaction and disruption of membranes.[16, 54] All of the above mentioned characteristics play an important role in the activity and selectivity of AMPs. Many of these parameters are very closely related and modifying any one of them, no matter how small, could result in a significant change in another parameter. As high helicity, high hydrophobicity and high amphipathicity have all been correlated to high hemolytic activity, [17, 56, 57] care should be taken when making any modifications as there are limits.[7]

Magainin

The magainin class of AMPs are secreted from the skin of the African clawed frog *Xenopus laevis* and have been classified as linear amphipathic α-helical AMPs.[39, 58] The magainins were of therapeutic interest as a broad-spectrum antibiotics because they are bactericidal, exhibiting potent activity against Gram-positive and Gram negative bacteria, fungicidal and virucidal, while exhibiting little mammalian toxicity.[8, 13, 39, 58] Although active in vitro, magainins were only effective in animal models at very high doses, greatly reducing their therapeutic usefulness. However, magainins have been extensively studied so as to gain a better understanding of their interactions with bacterial and mammalian cells in an effort to develop useful therapeutic agents.[59] Magainins consist of 21-26 amino acid residues with an overall positive charge of +3 to+5 and are soluble at high concentrations in aqueous solutions at physiological pH. The amino acid sequences for three of the most studied analogues of magain are given in **Table 1.1**. When interacting with membrane models, magainins adopt α-helical structures possessing a large hydrophobic moment; in other words, have a high probability of forming an amphipathic structure.[39, 60, 61] This class of AMPs has a broad nonpolar face and a narrow polar face with the positive charges of the lysine residues clustered together at the border of these two faces, characterizing magainins as well-defined α-helical amphipathic AMPs. It is believed that that their cytotoxic effects arise from the permeabilization of the negatively charged membrane by the toroidal mechanism previously mentioned.[39, 62-64]

Table 1.1: The amino acid sequences of the three most studied analogues of magainin.

Compound	Amino Acid Sequence
Magainin 1	G-I-G-K-F-L-H-S-A-G-K-F-G-K-A-F-V-G-E-I-M-K-S
Magainin 2	G-I-G-K-F-L-H-S-A-K-K-F-G-K-A-F-V-G-E-I-M-N-S
(Ala8,13,18)magainin-2-amide	G-I-G-K-F-L-H-A-A-K-K-F-A-K-A-F-V-A-E-I-M-N-S-NH2

The binding interactions of magainins and their analogues with model membranes have been extensively studied via NMR,[7, 65, 66] molecular modeling,[67] ITC,[39, 53, 58] CD,[65, 68] Neutron diffraction [69, 70] and fluorescence spectroscopy.[71, 72] Solid-state NMR spectroscopy has the capability of characterizing the secondary structure of an AMP as well as its orientation and penetration into lipid bilayers. NMR studies of magainin have determined that they are positioned parallel to the plane of the lipid bilayer at low peptide concentrations.[7, 20] Hicks and coworkers previously tested the hypothesis that the membrane's physicochemical surface interactions with the physicochemical surface of the AMP define organism selectivity using 2D NMR and molecular modeling.[67] Dodecylphosphocholine (DPC) micelles were used to mimic a simple model for zwitterionic cell membranes and sodium dodecylsulfate (SDS) micelles for anionic lipids. According to their 2D NMR and molecular modeling studies, (Ala^{8,13,18})magainin-2-amide adopts different conformations when in different membrane environments. In the presence of DPC micelles, an α-helical structure is adopted at residues 2-16 with four C-terminal residues converging to a loose β-turn like structure. For the SDS membrane, the α-helical structure involves residues 7-18 allowing for greater flexibility with C- and N-terminal residues. These conformational differences are attributed to the difference in electrostatic and hydrophobic interactions with the surfaces of the micelles. The SDS and DPC configurations determined by NMR were used to calculate Molecular Electrostatic Potential (MEP) maps to observe how the

electrostatic potential surface is affected by changes in conformation. The orientation of the peptide varied between membrane models, supporting the conclusion that magainin is cell-selective.[67]

As determined by ITC, the titration of the anionic lipid membrane model POPC/POPG into solutions of magainin 2-amide (M2a) can be divided into at least two steps.[39] The first step is the electrostatic attraction of the peptide to the membrane which increases the concentration of peptide immediately above the surface. This is followed by the hydrophobic adsorption of the peptide into the lipid bilayer. There is the presence of an endothermic enthalpy component with the first few injections of lipid into the peptide, low lipid-to-peptide ratios (L/P), which has been attributed to the transition from M2a pore formation to the disintegration of the pore. As the concentration of liposomes increases, resulting in an increase in the L/P ratio, the pore ↔ monomer equilibrium is shifted toward the M2a monomer phase, and the pore will disintegrate. The disintegration of a pore is an exothermic event and it compensates for the enthalpy consumed during pore formation.[39]

According to CD spectroscopy, magainin exhibits a random coil structure in aqueous buffer, but adopts an α-helix in the presence of an anionic membrane model. Using oriented CD and NMR spectroscopy, it was determined that at high L/P concentrations, the peptides are parallel in helical conformations on the surface of the membrane, but as the ratio decreases, the peptide becomes oriented perpendicular to the surface.[39, 73] Neutron diffraction coupled with fluorescence spectroscopy studies have shown that at high peptide concentration, pores are formed by bundles of helical peptides. The peptides of each pore are separated by lipids concluding that magainin causes membrane disruption through the formation of toroidal pores.[53, 70]

Novel AMPs

The broadband activity of magainin coupled with the in-depth understanding of its binding interactions with membrane models were the reasons it was used as a reference for the design of a new class of novel AMPs developed in the Hicks laboratory in the Department of Medicinal Chemistry, Division of Experimental Therapeutics at the Walter Reed Army Institute of Research in Silver Springs, Maryland.[13] These new compounds were designed to mimic the physicochemical properties of the magainins, more specifically their electrostatic surface potential maps. Although naturally occurring AMPs are of great therapeutic interest, there are several serious limitations to their therapeutic usefulness. Some of these factors include their rapid in vivo degradation, high production costs and their reduced activity in physiological conditions, as was the case with magainin.[29, 74] Efforts to overcome these problems while also retaining the biological activity of these peptides has resulted in the use of unnatural amino acids that mimic the residues incorporated in the natural pepties.[29]

The basic skeleton of each peptide synthesized in the Hicks lab is similar, containing between 15 and 21 natural and unnatural amino acid residues. Tic and Oic (**Figure 1.3** – red**)** are unnatural amino acids that were incorporated into the backbone as a dipeptide unit. Together these two unnatural amino acids induce a semi rigid conformation onto the peptide backbone.[13] Kyle and co-workers [75] used NMR to determine that placing the dipeptide unit D-Tic-L-Oic in positions *i*+1 and *i*+2 of a four amino acid sequence induces a β-turn. By strategically placing three of these unnatural dipeptide L-Tic-L-Oic units throughout the peptide and connecting them with amino acid spacers of defined properties of charge and hydrophobicity, it was believed that the 3D physicochemical properties of the peptide could be controlled.[76]

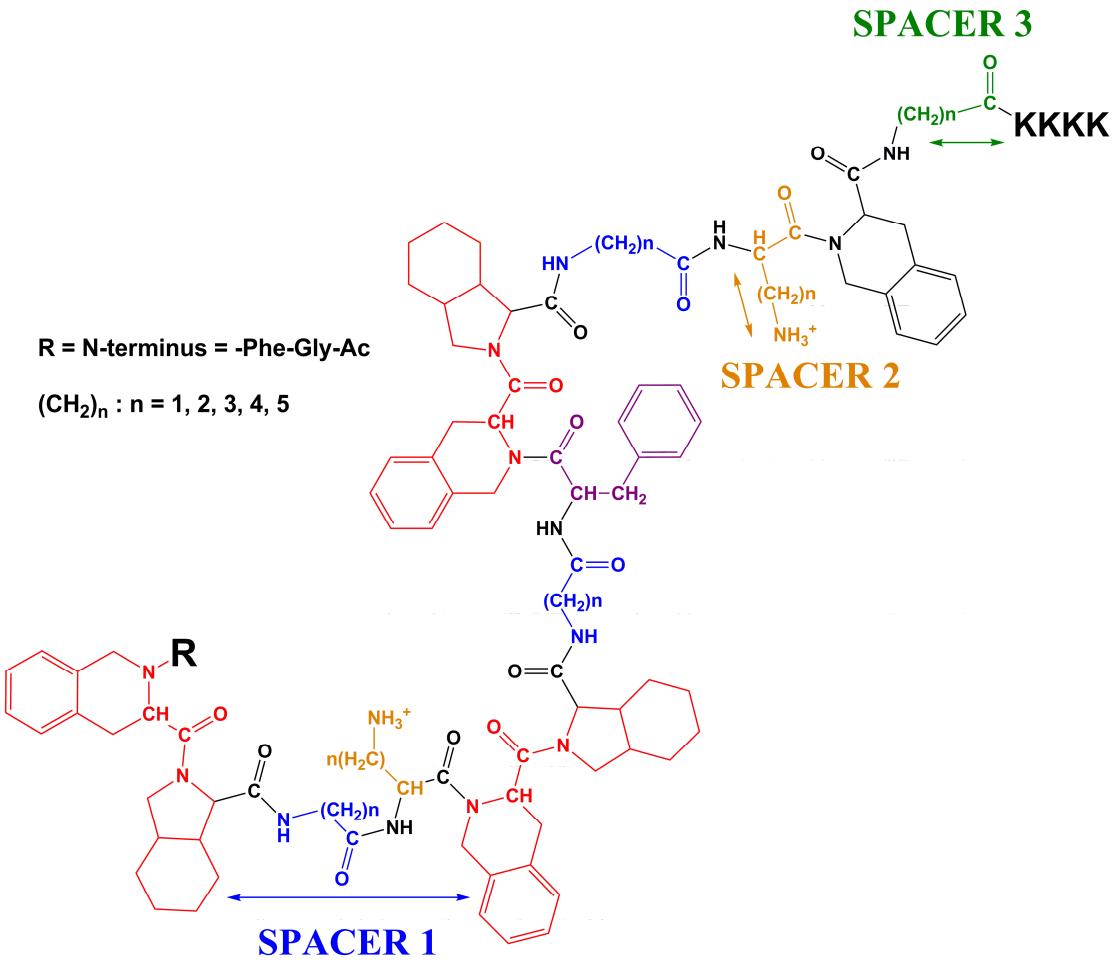

Figure 1.2: Diagram of the basic skeleton of AMPs containing three Tic-Oic dipeptide units developed in our laboratory.

In doing so, peptides could be designed with well-defined physicochemical properties in regards to acid/base properties, water solubility, and stereochemistry among others that maintain their conformational flexibility so as to allow them to adopt different conformations for different membranes.

In our lab, compound **23** (Ac-GF-Tic-Oic-GK-Tic-Oic-GF-Tic-Oic-GK-Tic-KKKK-$CONH_2$) was chosen as the reference because of its high in vitro activity against different bacteria strains and low hemolytic activity. Different modifications were designed to test the

significance of the Tic-Oic units, the distance between separate Tic-Oic units (**Figure 1.3** – spacer #1 in blue), the distance between the positive charge and the peptide backbone (**Figure 1.3** – spacer #2 in gold), the distance between the last Tic residue and the C-terminal Lys residues (**Figure 1.3** – spacer #3 in green), the need for a hydrophobic residue (**Figure 1.3** – purple) as well as the number and placement of a cluster of positive charge at either terminus.

The newly designed AMPs exhibited a broad range of antibacterial activity as well as hemolytic activity in cell culture. There were two sets of bacteria assays tested. The first set included *Salmonella typhimurium* (ATCC 13311) as the gram-negative and *Staphylococcus aureus* ME/GM/MTC (ATCC 33592) as a gram-positive screen. *Mycobacterium ranae* (ATCC 110) is a commercially available screen for mycobacterium and it is believed that it can provide insight into activity against tuberculosis.[10, 13, 17] *Bacillus subtillis* (ATCC 43223) was used as a screen for Bacillus anthraces.[10] Most of the observed MICs for these new peptides were as low as, if not lower, than those reported for other AMPs. The second series of bacteria assays consisted of several gram negative bacteria strains including *Acinetobacter baumanii* (ATCC 19606), clinical drug resistant isolate from Walter Reed *Acinetobacter baumanii* WRAIR, *Staphylococcus aureus* MRSA (ATTCC 33591), and the select agents *Yersinia pestis* (CO92), *Brucella melitensis* (16M), *Brucella abortus* (2308), *Brucella suis* (ATCC 23445), *Bacillus anthracis* AMES, *Francisella tularensis* (SCHU-S4), *Burkholderia mallei* (ATCC 23444) and *Burkholderia pseodomallei* (BURK003 1026b)**.** [77] The exact results for each peptide will be discussed further in their corresponding sections.

To determine the role the Tic-Oic unit played, compounds were synthesized that either deleted the Tic or Oic units completely or replaced them with glycine, or the less conformationally restrained phenylalanine.[13] Spacer #1 refers to the amino acid residues between

the Tic-Oic unit and the following positively charged or hydrophobic amino acid residues. They were systematically substituted with natural and unnatural amino acids to lengthen the peptide backbone in an attempt to investigate the effects of varying the distance between functional groups on selectivity and potency for the different bacterial strains. Compound **23** incorporated a one carbon spacer, glycine, in the backbone. Unnatural amino acids including β-alanine (βAla), γ-aminobutyric acid (Gaba) and 6-aminohexanoic acid (Ahx) were used to replace glycine in order to lengthen the chain from a one-carbon atom to two, three and five, respectively. Because the spacers control the distance between the Tic-Oic units as well as the distance between the positive and hydrophobic residues, they play a major role in determining the conformational flexibility of the peptide. An increase in spacer length adds conformational flexibility to the backbone, while the absence of a spacer causes a decrease in flexibility, inducing a helical conformation onto the peptide.

The positively charged amino acid of the peptide is referred to as spacer #2. It defines the distance from the side chain terminal amine group, the positive charge, to the peptide backbone. Analogues were synthesized to test the importance of this distance by incorporating the unnatural amino acids ornithine (Orn), diaminobutyric acid (Dab) and diaminopropionic acid (Dpr) to decrease the number of methylene groups from four, as with lysine in compound **23**, to three, two and one, respectively. Another possibility is the incorporation of arginine (Arg) which contains a guanidinium group at the end of its side-chain. In this planar group the positive charge is delocalized over two different nitrogen atoms, therefore allowing the positive charge to disperse more compared to the localized positive charge on the one nitrogen of the Lys side chain amino group. [78, 79]

Positively charged residues, as previously mentioned, are placed throughout the peptide backbone as Spacer #2, but there is also a cluster of positive charge at the C-terminus in our parent compound. For compound **23**, there are four lysine residues concentrated at the C-terminus. The positive charges are the driving force behind moving the peptide from the bulk solution to the surface of the membrane, thus, several analogues were synthesized changing the number of lysines grouped together as well as their location to help determine their significance. Analogues with 3 and 5 lysines at the C-terminus were synthesized, as well as an analog with four lysines at the N-terminus.

Spacer #3 refers to an amino acid between the last Tic residue and the lysine cluster at the C-terminus. This residue is not always included, but when it is included it usually consists of the same amino acid residue as Spacer #1. This particular spacer provides molecular flexibility between the last conformationally restrained dipeptide and the cluster of positively charged amino acid residues located at the C-terminus.

Most present day antibiotics kill bacteria via target:receptor interactions. For a peptide to interact with a receptor it must adopt a specific conformation with a specific stereochemistry that meets the special physicochemical requirements of the receptor. To insure that our peptides are not involved in a receptor mediated event and indeed kill the bacteria by disrupting the cell membrane two analogues were synthesized incorporating D-amino acids. By incorporating (D)-amino acids into the peptide backbone, we are changing the orientation of the peptide. If the peptide were to exhibit its antibiotic activity via a receptor mediated event, the change in stereochemistry and conformation would result in a loss in activity. However, these analogues exhibited the same activity as compound **23** which contains all (L)-amino acids,[13] proving they do not bind to a receptor.

Table 1.2: Amino acid sequences of previously synthesized peptides containing three Tic-Oic dipeptide units that are pertinent to this research

Compound	Amino Acid Sequence
14	Ac-GK-Tic-Oic-GLGKE-Tic-Oic-GLGK-Tic-Oic-ELMGER-$CONH_2$
23	Ac-GF-Tic-Oic-GK-Tic-Oic-GF-Tic-Oic-GK-Tic-KKKK-$CONH_2$
29	Ac-**Gaba**-F-Tic-Oic-**Gaba**-K-Tic-Oic-**Gaba**-F-Tic-Oic-**Gaba**-K-Tic-KKKK-$CONH_2$
34	Ac-GF-**G**-Oic-GK-**G**-Oic-GF-**G**-Oic-GK-**G**-KKKK-$CONH_2$
36	Ac- **βAla**-F-Tic-Oic-**βAla**-K-Tic-Oic-**βAla**-F-Tic-Oic-**βAla**-K-Tic-KKKK-$CONH_2$
37	Ac- **Ahx**-F-Tic-Oic-**Ahx**-K-Tic-Oic-**Ahx**-F-Tic-Oic-**Ahx**-K-Tic-KKKK-$CONH_2$
39	Ac-GF-Tic-Oic-GK-Tic-Oic-GF-Tic-Oic-GK-Tic-KKKK**K**-$CONH_2$
43	Ac-GF-Tic-Oic-G-**Orn**-Tic-Oic-GF-Tic-Oic-G-**Orn**-Tic-**Orn-Orn-Orn-Orn**-$CONH_2$
45	Ac-GF-Tic-Oic-G-**Dpr**-Tic-Oic-GF-Tic-Oic-G-**Dpr**-Tic-**Dpr-Dpr-Dpr-Dpr**-$CONH_2$
46	Ac-**βAla-Fpa**-Tic-Oic-**βAla-Dpr**-Tic-Oic-**βAla-Fpa**-Tic-Oic–**βAla-Dpr**-Tic-**Dpr-Dpr-Dpr-Dpr**-$CONH_2$
50	Ac-GF-Tic-Oic-GK-Tic-Oic-GF-Tic-Oic-GK-Tic-**βA**-KKKK-$CONH_2$
51	Ac-GF-Tic-Oic-GK-Tic-Oic-GF-Tic-Oic-GK-Tic-**Gaba**-KKKK-$CONH_2$
52	Ac-GF-Tic-Oic-GK-Tic-Oic-GF-Tic-Oic-GK-Tic-**Ahx**-KKKK-$CONH_2$
53	Ac-GF-Tic-Oic-G-**Dab**-Tic-Oic-GF-Tic-Oic-G-**Dab**-Tic-**Dab-Dab-Dab-Dab**-$CONH_2$
56	Ac-GF-Tic-Oic-G**R**-Tic-Oic-GF-Tic-Oic-G**R**-Tic-**RRRR**-$CONH_2$
61	Ac-**KKKK**-GF-Tic-Oic-GK-Tic-Oic-GF-Tic-Oic-GK-Tic-$CONH_2$
64	Ac-GF-Tic-Oic-GK-Tic-Oic-GF-Tic-Oic-GK-Tic-KKK-$CONH_2$

Instrumentation

Circular Dichroism

Circular Dichroism spectroscopy measures the differential absorbance of right- and left-circularly polarized light by a substance.[80, 81] The presence of an asymmetric chromophore is required for optical activity. For peptides, this chromophore is the amide bond. A chiral molecule interacts differently with right- and left-circularly polarized light at certain wavelengths due to differences in the extinction coefficients of the two polarized rays giving way to both positive and negative spectral components.[68, 81] It is the three-dimensional spatial orientation of the amide chromophores, which affects the spectrum of the peptide.[68] Circularly polarized light is obtained by the superposition of two perpendicular plane-polarized waves of equal amplitude and wavelength, but are 90^o out of phase. When the waves are 90^o out of phase, one wave is at its

peak when the other one is just crossing the zero line. When viewed along the direction of propagation, or looking toward the light source, the electric vector will appear to be following a circular path as the magnitude of the oscillation remains constant and the direction oscillates. If the electric vector is rotating in a clockwise direction, the light is said to be right-circularly polarized and for a counter-clockwise direction, left-circularly polarized.[81, 82]

Circular dichroism has been used to aid in the characterization of changes in the secondary structures of peptide in different membrane environments.[83, 84] Some of these secondary structures include α-helix, β-sheet, β-turn and random coil. These structures give characteristic spectra that, in an ideal situation, can be used to determine the percentage of each structure in other compounds.[81] However, due to the incorporation of un-natural amino acids and the lack of knowledge regarding these residues, quantifying the secondary structures of our peptides has proven to be difficult. We have, consequently, used CD as more of a qualitative tool and compared the overall changes in the spectra in comparison to each other. For instance, peptides that exhibit activity in the presence of bacteria cells, but show little to no activity in the presence of mammalian red blood cells should, theoretically, adopt different secondary structures in the presence of anionic and zwitterionic membrane models. Thus, we should observe different CD spectra in the presence of anionic and zwitterionic membrane models.

Isothermal Titration Calorimetry

Isothermal titration calorimetry (ITC) is a thermodynamic technique that monitors any chemical reaction initiated by the addition of a binding component and has been the method of choice for characterizing biomolecular interactions.[39, 58, 85-87] An isothermal titration calorimeter is a system with two identical cells, a reference and reaction cell, surrounded by an adiabatic

jacket to ensure that no heat is gained or lost to the system. The reference cell is filled with water or buffer and the reaction cell will contain the macromolecule solution. The two cells are equilibrated at the same temperature before the experiment starts. In general, a liquid solution of a "ligand" is titrated into the reaction cell which is filled with a liquid solution of the "macromolecule," in our case peptide and liposomes, respectively. The ligand is titrated using a syringe that continuously spins in order to ensure proper mixing and distribution of ligand, (**Figure 1.4**) There is a temperature change associated with the binding of the ligand to the macromolecule.[88]

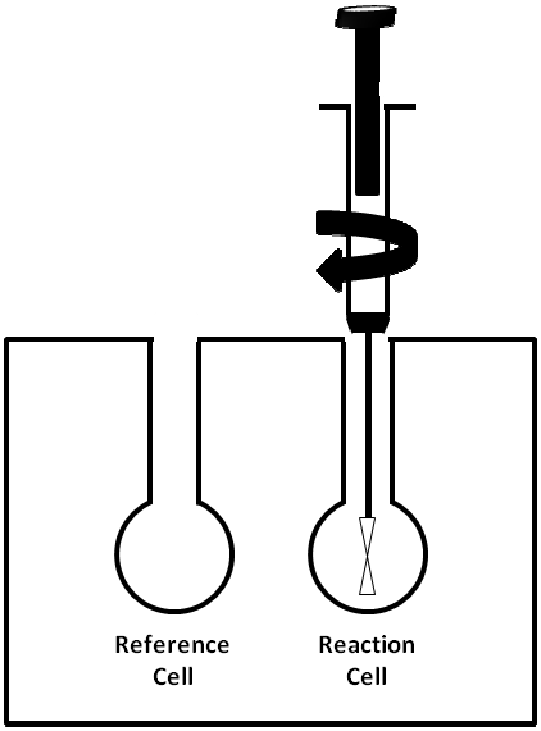

Figure 1.3: Schematic diagram of an ITC instrument. Figure adapted from Pierce et. al[88, 89] and the MicroCal User's Manual.[88]

The direct observable measured is the time-dependent input of power required to maintain equal temperatures in the cells. For an exothermic reaction, heat is evolved causing the

temperature in the sample cell to increase. The heat created by the reaction provides the heat needed to keep the cells the same temperature, thus, the feedback power is deactivated and a negative peak is produced.[88, 89] Exothermic reactions occur when components come together and bind, such as the electrostatic interactions of peptides on the membrane surface. For endothermic reactions, heat is absorbed and the reverse will occur. The feedback circuit will increase power to the sample cell to maintain equal temperatures and produces a positive peak. Examples of endothermic processes include the disruption of electrostatic interactions or liposome stability.[88, 89] Due to the fact that the differential power (DP) has units of power, the time integral of the peak yields a measurement of thermal energy, ΔH. The heat that is released or absorbed is directly proportional to the amount of binding that takes place between the ligand and macromolecule. As the amount of available macromolecule diminishes, so does the heat signal. Once the macromolecule solution becomes saturated the only signal observed is that of the heat of dilution.[88]

There are three different types of heat observed that contribute to the overall heat of reaction that should be accounted for. These observed heats include contributions from the dilution of the titrant and macromolecule, as well as a small contribution from stirring. Control experiments to account for the heats of dilution are performed by titrating peptide into a sample cell containing only buffer and vice versa. Identical control experiments should be performed with liposomes and buffer as well. The small contribution from stirring is taken into account automatically by the instrument.[89] The calorimeter has a long equilibration that takes place before the experiment starts. During this equilibration time, the syringe generates heat while stirring continuously. The calorimeter compensates for this heat.[88]

In an ideal case, one can obtain three pieces of thermodynamic data from a single experiment, the binding constant (K_b), the reaction stoichiometry (n), and the enthalpy (ΔH) of the binding association from one ITC experiment (**Figure 1.5**).[88, 90]

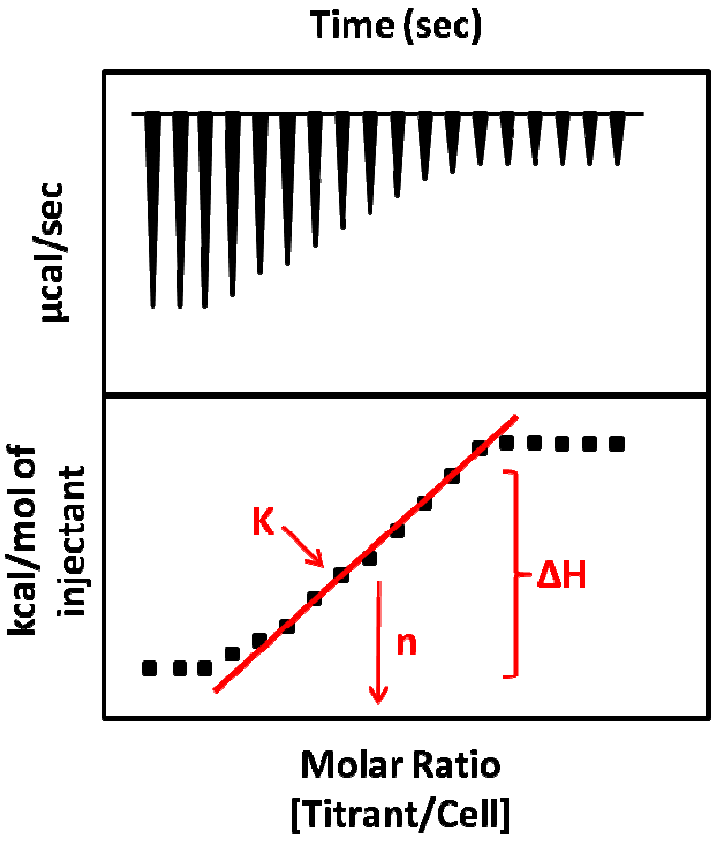

Figure 1.4: An ideal ITC experiment for the titration of lipid into peptide. The top panel shows the baseline-smoothed raw data plotted as mcal/sec versus against time. The bottom panel represents the integrated heat for each injection versus the molar ratio. The molar ratio for the experiment is the concentration of the lipid (titrant) compared to the concentration of the peptide (cell). Figure was adapted from Grossoehme et al.[91]

By using some simple equations and the experimentally determined enthalpy and binding constant, it is possible to determine the Gibbs free energy (ΔG) and entropy (ΔS) of the reaction. Using the binding constant (K_b) and the following **Equation 1.1**, one can calculate ΔG[89, 90]:

$$\Delta G = -RT\ln(55.5K) \quad (1.1)$$

where R is the gas constant (1.987 $cal \cdot K^{-1} \cdot mol^{-1}$) and T is the temperature in Kelvin. The factor 55.5 is the molar concentration of water and is incorporated to correct for the cratic contribution.[5, 92, 93] Now that ΔG is known, it's possible to calculate ΔS from the **Equation 1.2** below[89, 90]:

$$\Delta G = \Delta H - T\Delta S \quad (1.2)$$

Gibbs free energy can help predict how favorable or unfavorable a reaction is, whether it will proceed spontaneously or not. If $\Delta G > 0$, the forward reaction is energetically unfavorable and the reverse reaction is therefore energetically favored and will proceed spontaneously. If $\Delta G = 0$ the system is at equilibrium and there is no further change without external stimulus. If $\Delta G < 0$ then the forward reaction is energetically favorable and will proceed spontaneously. The enthalpy of a reaction, ΔH, is the heat evolved or absorbed by the reaction. A positive ΔH means the reaction is endothermic, absorbs heat, and is unfavorable. Endothermic reactions give off heat resulting in a negative ΔH and a favorable reaction. The second law of thermodynamics states that no process will occur spontaneously unless it is accompanied by an increase in the entropy of the universe. Entropy refers to the disorder of a system. A positive ΔS and a favorable reaction will go towards a more disordered outcome, for example, NaCl dissociating into Na^+ and Cl^-. The reverse of this reaction, the creation of salt, would be an unfavorable reaction with a negative ΔS.[94]

In order to obtain thermodynamic information mentioned above, the data must be fit to a model and there are two different models to consider. One model does not take into account the electrostatic interactions between the peptide and membrane surface, while the second does.[58, 86] The former model is the simpler of the two and involves the partitioning of the peptide between

the aqueous phase and the lipid membrane, if one assumes the following **Equation 1.3** from Wieprecht and Seelig [86] is a linear relationship:

$$X_b = K_p c_f \tag{1.3}$$

where X_b is the molar ratio of membrane-bound peptide per lipid, c_f is the concentration of free peptide in solution and K_p is the partition coefficient. The X_b and c_f can be calculated using the following equations. The standard molar reaction enthalpy, ΔH^0, is determined from the experimental data and **Equation 1.4**.[72, 86]

$$\Delta H^0 = \sum_i \delta h_i / (c^0_{pep} V_{cell}) \tag{1.4}$$

where δh_i are the raw heats of each injection in µcal after the heats of dilution have been subtracted, also known as the corrected heats, c^0_{pep} is the total peptide concentration (mol/mL) and V_{cell} is the volume of the calorimeter cell (1.4602 mL). Once the reaction enthalpy has been calculated, the binding isotherm is derived. After *i* injections, the fraction of peptide bound to lipid vesicles, $X^{(i)}_{P,b}$ can be found using the **Equation 1.5** below:[72, 90]

$$X^{(i)}_p = \frac{n^{(i)}_{P,b}}{n^0_{pep}} = \frac{\sum_{k=1}^{i} \delta h_k}{\Delta H^0 V_{cell} c^0_{pep}} \tag{1.5}$$

where $n^{(i)}_{P,b}$ is the molar amount of bound peptide after *i* injections, n^0_{pep} is the total amount of peptide in the calorimeter cell and $\sum_{k=1}^{i} \delta h_k$ is the sum of the first *k* reaction heats in µcals. The concentration of free peptide remaining in the bulk solution, $c^{(i)}_f$, after each injection is calculated by using **Equation 1.6** below[72, 86]

$$c_f^{(i)} = f_{dil}^{(i)} c_{pep}^0 \left[1 - X_p^{(i)}\right] \quad (1.6)$$

where $f_{dil}^{(i)}$ is the dilution factor. It takes into account the increase in volume after each injection of lipid vesicle[72, 86] and is defined **by Equation 1.7**. [86]

$$f_{dil}^{(i)} = \left(\frac{V_{cell}}{V_{cell} + V_{inj}}\right)^i \approx \frac{V_{cell}}{V_{cell} + iV_{inj}} \quad (1.7)$$

V_{inj} is the volume of each injection. The degree of binding, X_b , can then be defined as the fraction of bound peptide (mmol) per mole of total lipid in the cell and can is determined using **Equation 1.8** From Wieprecht and Seelig[72, 86]

$$X_b^{(i)} = \frac{n_{pep,b}^{(i)}}{n_L^{(i)}} = X_p^{(i)} \frac{c_{pep}^0 V_{cell}}{iV_{inj} c_L^0} \quad (1.8)$$

where c_L^0 is the concentration of the lipid stock solution that is injected into the calorimeter cell. A plot of X_b versus c_f should yield a linear curved that would fit the binding isotherm model described by **Equation 1.3**. However, this is not the case for our peptides as we observe a bending in the curves. Our peptides are positively charged and electrostatic interactions should be accounted for, which they are not using this particular model.

The second model, however, does consider electrostatic interactions. As mentioned, our peptides carry a positive charge and the net charge of the liposomes may be neutral or negative depending on if the model is zwitterionic or anionic making this model more relevant for our analysis. The negative charges of the membrane attracts the positively charged residues of the peptide resulting in increased peptide concentration at the surface of the membrane, c_m, in comparison to the bulk solution, c_f. [90] This being said, the following **Equation 1.9** [86, 95-97] is more appropriate for the analysis of our data

$$X_b = Kc_m \quad (1.9)$$

For negatively charged membranes, as the concentration of peptide at the surface increases, the surface potential and the electrostatic attractions between the membrane and peptide consequently decreases, resulting in a decrease in the degree of binding, X_b, and the downward-bending of the isotherm.[92, 95-97] A similar effect can be seen for neutral membranes. In the absence of peptides, the membrane surface potential is essentially zero. The binding of positively charged peptide on the surface of a neutral membrane causes the surface potential to become positively charged. This results in the repulsion of other peptides which becomes stronger as the peptide concentration on the surface increases, hence $c_m < c_f$.[86, 98, 99] In order to account for the electrostatic effects, the surface concentration c_m must be calculated. This value depends on the free peptide concentration in the bulk solution (c_f), the charge of the peptide (z) and the membrane surface potential (ψ_0) and it can be calculated using the following Boltzmann distribution (**Equation 1.10**)**.**

$$c_m = c_f \exp(-zF_0\psi_0/RT) \quad (1.10)$$

where F_0 is the Faraday constant and RT is the thermal energy (J/mol). Unfortunately, the membrane surface potential, ψ_0, cannot be measured directly and must be calculated based on its connection to the surface charge density, σ. The surface charge density for the binding of the electrically neutral POPC membrane with positively charged peptides can be calculated as follows according to **Equation 1.11**.[97, 99-101]

$$\sigma = (z_p e_0 X_b / A_L) / [(1 + X_b (A_P / A_L)] \quad (1.11)$$

where z_p is the effective valency of the peptide (+6 with 6 lysines), e_0 is the elementary electric charge (1.60218×10^{-16} mC), and A_L is the average surface area of a POPC

molecule (estimated to be 68 Å.)[97, 99-101] The cross-sectional area of the peptide, A_P, varies with peptide and can only be approximated from inspection with molecular modeling. The A_p for compound **23** was used for each of the peptides studied in these investigations. The ratio of A_P/A_L takes into account the possibility of penetration of the peptide into the membrane.[101] The surface charge density is linearly related to the extent of binding X_b, and once it has been calculated, the surface potential, ψ_0, can be calculated using the Gouy-Chapman theory described by **Equation 1.12**. (for reviews see Aveyard[102], and McLaughlin [103, 104])

$$\sigma^2 = 2000\varepsilon_0\varepsilon_r RT\sum_i c_i(e^{-z_i F_0\psi_0/RT} - 1) \qquad (1.12)$$

In **Equation 1.12**, c_i refers to the concentration of the *i*th electrolyte in the bulk aqueous phase, including buffer, peptide, and negatively charged phospholipids, and z_i is the signed valency associated with the *i*th species. The remaining symbols are constants. ε_0 is the electric permittivity of free space (8.8542 x 10^{-9}mF/m) and ε_r is the dielectric constant of water. By combining **Equations 1.8** and **1.9** and calculating the surface charge density from the experimentally obtained X_b, the membrane surface potential can be calculated using a number of computer programs such as Maxima, as used for our calculations. Once ψ_0 is known, c_M can be calculated. Plotting X_b versus c_m, the K can finally be obtained as it is the slope of the line. With the experimentally obtained ΔH and the calculated binding constant, K, ΔG and ΔS can be calculated using **Equations 1.1** and **1.2**.[89, 90]

Calcein Leakage Assays

Fluorescence is a spectrochemical method of analysis where the molecules of an analyte, or fluorophore, are excited by irradiation at a certain wavelength and emit radiation of a different

wavelength. The fluorophore for our research is calcein, which is encapsulated by liposomes at self-quenching concentrations. The solution of liposomes is treated with an AMP solution and the resulting fluorescence is measure as the calcein leaks out.

Calcein is self-quenching at very high concentrations, in other words, the fluorescence decreases with increasing calcein concentration. As can be seen in **Figure 1.6**, when at self-quenching concentrations, calcein is red and does not fluoresce. Once the liposomes are treated with peptide and leakage is induced, the calcein is diluted in the surroundings. Once the calcein is diluted below self-quenching concentrations and fluoresces. It is the increase in this fluorescence that is measured over a period of time.

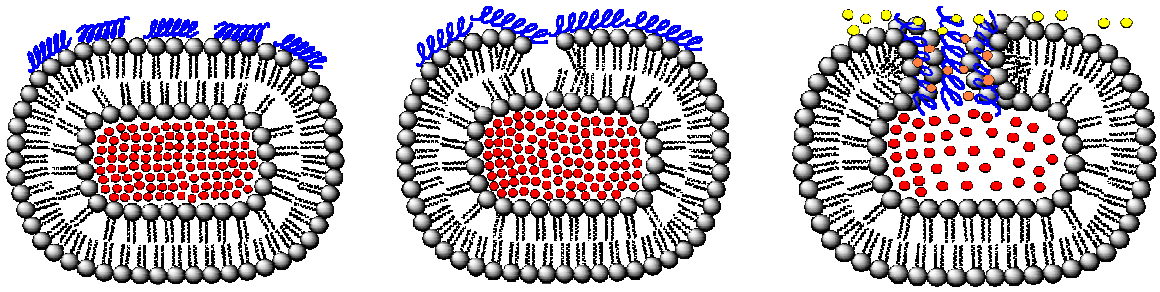

Figure 1.5: Schematic of peptide-induced calcein leakage from liposomes. Peptides bind to liposomes filled with calcein at self-quenching concentrations (left). As the peptide concentration increases, the membrane begins to disrupt (middle). At high peptide to lipid concentrations, the peptides insert into the bilayer causing calcein to leak into its surroundings (right). As the calcein is diluted, the concentration is decreased below self-quenching concentrations and fluoresces.

The AMP-induced leakage of fluorescent dyes entrapped in LUVs of different phospholipid compositions, such as calcein, is a widely used method for assessing the relative potency of peptides for disrupting the integrity of the lipid bilayer membranes and thus for predicting their antimicrobial and hemolytic activities. [12, 15, 105-110]

References

(1) Boucher, H. W.; Talbot, G. H.; Bradley, J. S.; Edwards, J. E.; Gilbert, D.; Rice, L. B.; Scheld, M.; Spellberg, B.; Bartlett, J. Bad bugs, no drugs: no ESKAPE! An update from the Infectious Diseases Society of America. *Clin. Infect. Dis.* **2009**, *48*, 1-12.

(2) Spellberg, B.; Guidos, R.; Gilbert, D.; Bradley, J.; Boucher, H. W.; Scheld, W. M.; Bartlett, J. G.; Edwards, J.,Jr The epidemic of antibiotic-resistant infections: a call to action for the medical community from the Infectious Diseases Society of America. *Clin. Infect. Dis.* **2008**, *46*, 155-164.

(3) Rice, L. B. Federal funding for the study of antimicrobial resistance in nosocomial pathogens: no ESKAPE. *J. Infect. Dis.* **2008**, *197*, 1079-1081.

(4) Boucher, H. W.; Corey, G. R. Epidemiology of methicillin-resistant Staphylococcus aureus. *Clin. Infect. Dis.* **2008**, *46 Suppl 5*, S344-9.

(5) Wen, S.; Majerowicz, M.; Waring, A.; Bringezu, F. Dicynthaurin (ala) Monomer Interaction with Phospholipid Bilayers Studied by Fluorescence Leakage and Isothermal Titration Calorimetry. *The Journal of Physical Chemistry B* **2007**, *111*, 6280-6287.

(6) Zasloff, M. Antimicrobial peptides of multicellular organisms. *Nature* **2002**, *415*, 389-395.

(7) Brogden, K. A. Antimicrobial Peptides: Pore formers or metabolic inhibitors in bacteria? *Nature Reviews.Microbiology* **2005**, *3*.

(8) Glukhov, E.; Stark, M.; Burrows, L. L.; Deber, C. M. Basis for selectivity of cationic antimicrobial peptides for bacterial versus mammalian membranes. *J. Biol. Chem.* **2005**, *280*, 33960-33967.

(9) Wang, G.; Li, X.; Wang, Z. APD2: the updated antimicrobial peptide database and its application in peptide design. *Nucleic Acids Res.* **2009**, *37*, D933-7.

(10) Ganz, T. Defensins: antimicrobial peptides of innate immunity. *Nature Reviews: Immunology* **2003**, *3*, 710-720.

(11) Simmaco, M.; Mignogna, G.; Barra, D. Antimicrobial peptides from amphibian skin: What do they tell us? *Peptide Science* **1998**, *47*, 435-450.

(12) Dathe, M.; Schumann, M.; Wieprecht, T.; Winkler, A.; Beyermann, M.; Krause, E.; Matsuzaki, K.; Murase, O.; Bienert, M. Peptide Helicity and Membrane Surface Charge Modulate the Balance of Electrostatic and Hydrophobic Interactions with Lipid Bilayers and Biological Membranes. *Biochemistry (N. Y.)* **1996**, *35*, 12612-12622.

(13) Hicks, R. P.; Bhonsle, J. B.; Venugopal, D.; Koser, B. W.; Magill, A. J. De Novo Design of Selective Antibiotic Peptides by Incorporation of Unnatural Amino Acids. *J. Med. Chem.* **2007**, *50*, 3026-3036.

(14) Dennison, S. R.; Wallace, J.; Harris, F.; Phoenix, D. A. Amphiphilic alpha-helical antimicrobial peptides and their structure/function relationships. *Protein Peptide Lett.* **2005**, *12*, 31-39.

(15) Tamba, Y.; Yamazaki, M. Single Giant Unilamellar Vesicle Method Reveals Effect of Antimicrobial Peptide Magainin 2 on Membrane Permeability. *Biochemistry (N. Y.)* **2005**, *44*, 15823-15833.

(16) Yeaman, M. R.; Yount, N. Y. Mechanisms of Antimicrobial Peptide Action and Resistance. *Pharmacol. Rev.* **2003**, *55*, 27-55.

(17) Toke, O. Antimicrobial peptides: New candidates in the fight against bacterial infections. *Peptide Science* **2005**, *80*, 717-735.

(18) Tossi, A.; Sandri, L.; Giangaspero, A. Amphipathic alpha-helical antimicrobial peptides. *Biopolymers* **2000**, *55*, 4-30.

(19) Gennaro, R.; Zanetti, M. Structural features and biological activities of the cathelicidin-derived antimicrobial peptides. *Peptide Science* **2000**, *55*, 31-49.

(20) Bechinger, B.; Zasloff, M.; Opella, S. J. Structure and orientation of the antibiotic peptide magainin in membranes by solid-state nuclear magnetic resonance spectroscopy. *Protein Sci.* **1993**, *2*, 2077-2084.

(21) Mendez-Samperio, P. The human cathelicidin hCAP18/LL-37: a multifunctional peptide involved in mycobacterial infections. *Peptides* **2010**, *31*, 1791-1798.

(22) Haney, E. F.; Hunter, H. N.; Matsuzaki, K.; Vogel, H. J. Solution NMR studies of amphibian antimicrobial peptides: Linking structure to function? *Biochimica et Biophysica Acta (BBA) - Biomembranes* **2009**, *1788*, 1639-1655.

(23) Jenssen, H.; Hamill, P.; Hancock, R. E. Peptide antimicrobial agents. *Clin. Microbiol. Rev.* **2006**, *19*, 491-511.

(24) Powers, J. -. S.; Hancock, R. E. W. The relationship between peptide structure and antibacterial activity. *Peptides* **2003**, *24*, 1681-1691.

(25) Peters, B. M.; Shirtliff, M. E.; Jabra-Rizk, M. Antimicrobial Peptides: Primeval Molecules or Future Drugs? *PLoS Pathogens* **2010**, *6*, 1-4.

(26) Liu, L.; Fang, Y.; Huang, Q.; Wu, J. A Rigidity-Enhanced Antimicrobial Activity: A Case for Linear Cationic alpha-Helical Peptide HP(2-20) and Its Four Analogues. *PLoS One* **2011**, *6*, e16441.

(27) Friedrich, C. L.; Moyles, D.; Beveridge, T. J.; Hancock, R. E. Antibacterial action of structurally diverse cationic peptides on gram-positive bacteria. *Antimicrob. Agents Chemother.* **2000**, *44*, 2086-2092.

(28) Dathe, M.; Meyer, J.; Beyermann, M.; Maul, B.; Hoischen, C.; Bienert, M. General aspects of peptide selectivity towards lipid bilayers and cell membranes studied by variation of the structural parameters of amphipathic helical model peptides. *Biochim. Biophys. Acta* **2002**, *1558*, 171-186.

(29) Ivankin, A.; Livne, L.; Mor, A.; Caputo, G. A.; DeGrado, W. F.; Meron, M.; Lin, B.; Gidalevitz, D. Role of the Conformational Rigidity in the Design of Biomimetic Antimicrobial Compounds. *Angewandte Chemie International Edition* **2010**, *49*, 8462-8465.

(30) Bechinger, B. Structure and Functions of Channel-Forming Peptides: Magainins, Cecropins, Melittin and Alamethicin. *J. Membr. Biol.* **1997**, *156*, 197-211.

(31) Wimmer, R.; Andersen, K. K.; Vad, B.; Davidsen, M.; Molgaard, S.; Nesgaard, L. W.; Kristensen, H. H.; Otzen, D. E. Versatile Interactions of the Antimicrobial Peptide Novispirin with Detergents and Lipids. *Biochemistry (N. Y.)* **2006**, *45*, 481-497.

(32) Lee, D. G.; Park, Y.; Jin, I.; Hahm, K.; Lee, H.; Moon, Y.; Woo, E. Structure-antiviral activity relationships of cecropin A-magainin 2 hybrid peptide and its analogues. *Journal of Peptide Science* **2004**, *10*, 298-303.

(33) Shai, Y.; Oren, Z. From "carpet" mechanism to de-novo designed diastereomeric cell-selective antimicrobial peptides. *Peptides* **2001**, *22*, 1629-1641.

(34) Pouny, Y.; Rapaport, D.; Mor, A.; Nicolas, P.; Shai, Y. Interaction of antimicrobial dermaseptin and its fluorescently labeled analogs with phospholipid membranes. *Biochemistry (N. Y.)* **1992**, *31*, 12416-12423.

(35) Yang, L.; Harroun, T. A.; Weiss, T. M.; Ding, L.; Huang, H. W. Barrel-stave model or toroidal model? A case study on melittin pores. *Biophys. J.* **2001**, *81*, 1475-1485.

(36) Ehrenstein, G.; Lecar, H. Electrically gated ionic channels in lipid bilayers. *Q. Rev. Biophys.* **1977**, *10*, 1-34.

(37) Yamaguchi, S.; Hong, T.; Waring, A.; Lehrer, R. I.; Hong, M. Solid-state NMR investigations of peptide-lipid interaction and orientation of a beta-sheet antimicrobial peptide, protegrin. *Biochemistry* **2002**, *41*, 9852-9862.

(38) Matsuzaki, K.; Murase, O.; Fujii, N.; Miyajima, K. An antimicrobial peptide, magainin 2, induced rapid flip-flop of phospholipids coupled with pore formation and peptide translocation. *Biochemistry* **1996**, *35*, 11361-11368.

(39) Wenk, M. R.; Seelig, J. Magainin 2 Amide Interaction with Lipid Membranes: Calorimetric Detection of Peptide Binding and Pore Formation. *Biochemistry (N. Y.)* **1998**, *37*, 3909-3916.

(40) Lee, M. T.; Hung, W. C.; Chen, F. Y.; Huang, H. W. Mechanism and kinetics of pore formation in membranes by water-soluble amphipathic peptides. *Proc. Natl. Acad. Sci. U. S. A.* **2008**, *105*, 5087-5092.

(41) Song, Y. M.; Park, Y.; Lim, S. S.; Yang, S. T.; Woo, E. -.; Park, S.; Lee, J. S.; Kim, J. I.; Hahm, K. -.; Kim, Y.; Shin, S. Y. Cell selectivity and mechanism of action of antimicrobial model peptides containing peptoid residues. *Biochemistry (N. Y.)* **2005**, *44*, 12094-12106.

(42) Shai, Y. Mechanism of the binding, insertion and destabilization of phospholipid bilayer membranes by α-helical antimicrobial and cell non-selective membrane-lytic peptides. *Biochimica et Biophysica Acta (BBA) - Biomembranes* **1999**, *1462*, 55-70.

(43) Papo, N.; Shai, Y. New Lytic Peptides Based on the d,l-Amphipathic Helix Motif Preferentially Kill Tumor Cells Compared to Normal Cellsâ€. *Biochemistry (N. Y.)* **2003**, *42*, 9346-9354.

(44) Giangaspero, A.; Sandri, L.; Tossi, A. Amphipathic alpha helical antimicrobial peptides. *Eur. J. Biochem.* **2001**, *268*, 5589-5600.

(45) Azuma, I.; Yamamura, Y.; Tanaka, Y.; Kosaka, K.; Mori, T. Cell wall of Mycobacterium lepraemurium strain Hawaii. *J. Bacteriol.* **1973**, *113*, 515-518.

(46) Boman, H. G. Peptide antibiotics and their role in innate immunity. *Annu. Rev. Immunol.* **1995**, *13*, 61-92.

(47) Zasloff, M.; Martin, B.; Chen, H. C. Antimicrobial activity of synthetic magainin peptides and several analogues. *Proc. Natl. Acad. Sci. U. S. A.* **1988**, *85*, 910-913.

(48) Zhang, L.; Rozek, A.; Hancock, R. E. Interaction of cationic antimicrobial peptides with model membranes. *J. Biol. Chem.* **2001**, *276*, 35714-35722.

(49) Matsuzaki, K.; Nakamura, A.; Murase, O.; Sugishita, K.; Fujii, N.; Miyajima, K. Modulation of Magainin 2-Lipid Bilayer Interactions by Peptide Charge. *Biochemistry (N. Y.)* **1997**, *36*, 2104-2111.

(50) Thompson, S. A.; Tachibana, K.; Nakanishi, K.; Kubota, I. Melittin-Like Peptides from the Shark-Repelling Defense Secretion of the Sole Pardachirus pavoninus. *Science* **1986**, *233*, 341-343.

(51) Tossi, A.; Scocchi, M.; Skerlavaj, B.; Gennaro, R. Identification and characterization of a primary antibacterial domain in CAP18, a lipopolysaccharide binding protein from rabbit leukocytes. *FEBS Lett.* **1994**, *339*, 108-112.

(52) Matsuzaki, K.; Yoneyama, S.; Miyajima, K. Pore formation and translocation of melittin. *Biophys. J.* **1997**, *73*, 831-838.

(53) Wieprecht, T.; Dathe, M.; Beyermann, M.; Krause, E.; Maloy, W. L.; MacDonald, D. L.; Bienert, M. Peptide Hydrophobicity Controls the Activity and Selectivity of Magainin 2 Amide in Interaction with Membranes. *Biochemistry (N. Y.)* **1997**, *36*, 6124-6132.

(54) Uematsu, N.; Matsuzaki, K. Polar angle as a determinant of amphipathic alpha-helix-lipid interactions: a model peptide study. *Biophys. J.* **2000**, *79*, 2075-2083.

(55) Dathe, M.; Wieprecht, T.; Nikolenko, H.; Handel, L.; Maloy, W. L.; MacDonald, D. L.; Beyermann, M.; Bienert, M. Hydrophobicity, hydrophobic moment and angle subtended by charged residues modulate antibacterial and haemolytic activity of amphipathic helical peptides. *FEBS Lett.* **1997**, *403*, 208-212.

(56) Chen, Y.; Mant, C. T.; Farmer, S. W.; Hancock, R. E. W.; Vasil, M. L.; Hodges, R. S. Rational Design of {alpha}-Helical Antimicrobial Peptides with Enhanced Activities and Specificity/Therapeutic Index. *J. Biol. Chem.* **2005**, *280*, 12316-12329.

(57) Oren, Z.; Hong, J.; Shai, Y. A Repertoire of Novel Antibacterial Diastereomeric Peptides with Selective Cytolytic Activity. *J. Biol. Chem.* **1997**, *272*, 14643-14649.

(58) Wieprecht, T.; Apostolov, O.; Seelig, J. Binding of the antibacterial peptide magainin 2 amide to small and large unilamellar vesicles. *Biophys. Chem.* **2000**, *85*, 187-198.

(59) Gottler, L. M.; Ramamoorthy, A. Structure, membrane orientation, mechanism, and function of pexiganan — A highly potent antimicrobial peptide designed from magainin. *Biochimica et Biophysica Acta (BBA) - Biomembranes* **2009**, *1788*, 1680-1686.

(60) Segrest, J. P.; Garber, D. W.; Brouillette, C. G.; Harvey, S. C.; Anantharamaiah, G. M. The amphipathic alpha helix: a multifunctional structural motif in plasma apolipoproteins. *Adv. Protein Chem.* **1994**, *45*, 303-369.

(61) Segrest, J. P.; Loof, H. D.; Dohlman, J. G.; Brouillette, C. G.; Anantharamaiah, G. M. Amphipathic helix motif: Classes and properties. *Proteins: Structure, Function, and Genetics* **1990**, *8*, 103-117.

(62) Matsuzaki, K.; Harada, M.; Funakoshi, S.; Fujii, N.; Miyajima, K. Physicochemical determinants for the interactions of magainins 1 and 2 with acidic lipid bilayers. *Biochimica et Biophysica Acta (BBA) - Biomembranes* **1991**, *1063*, 162-170.

(63) Juretic, D.; Hendler, R. W.; Kamp, F.; Caughey, W. S.; Zasloff, M.; Westerhoff, H. V. Magainin Oligomers Reversibly Dissipate .DELTA..mu.H+ in Cytochrome Oxidase Liposomes. *Biochemistry (N. Y.)* **1994**, *33*, 4562-4570.

(64) Westerhoff, H. V.; Juretić, D.; Hendler, R. W.; Zasloff, M. Magainins and the disruption of membrane-linked free-energy transduction. *Proceedings of the National Academy of Sciences of the United States of America* **1989**, *86*, 6597-6601.

(65) Corzo, G.; Escoubas, P.; Villegas, E.; Barnham, K. J.; He, W.; Norton, R. S. Characterization of unique amphipathic antimicrobial peptides from venom of the scorpian pandinus imperator. *Biochem. J.* **2003**, *359*, 35-45.

(66) Gesell, J.; Zasloff, M.; Opella, S. J. Two-dimensional 1H NMR experiments show that the 23-residue magainin antibiotic peptide is an alpha-helix in dodecylphosphocholine micelles, sodium dodecylsulfate micelles, and trifluoroethanol/water solution. *J. Biomol. NMR* **1997**, *9*, 127-135.

(67) Hicks, R. P.; Mones, E.; Kim, H.; Koser, B. W.; Nichols, D. A.; Bhattacharjee, A. K. Comparison of the conformation and electrostatic surface properties of magainin peptides bound to SDS and DPC micelles: Insight into possible modes on antimicrobial activity. *Biopolymers* **2003**, *68*, 459-470.

(68) Mulkerrin, M. G. In *Protein Structure Analysis Using Circular Dichroism;* Havel, H. A., Ed.; Spectroscopic Methods for Determining Protein Structures in Solution; VCH Publishers: New York, 1996; .

(69) He, K.; Ludtke, S. J.; Huang, H. W.; Worcester, D. L. Antimicrobial peptide pores in membranes detected by neutron in-plane scattering. *Biochemistry* **1995**, *34*, 15614-15618.

(70) Ludtke, S. J.; He, K.; Heller, W. T.; Harroun, T. A.; Yang, L.; Huang, H. W. Membrane pores induced by magainin. *Biochemistry* **1996**, *35*, 13723-13728.

(71) Matsuzaki, K.; Harada, M.; Handa, T.; Funakoshi, S.; Fujii, N.; Yajima, H.; Miyajima, K. Magainin 1-induced leakage of entrapped calcein out of negatively-charged lipid vesicles. *Biochimica et Biophysica Acta (BBA) - Biomembranes* **1989**, *981*, 130-134.

(72) Wieprecht, T.; Beyermann, M.; Seelig, J. Binding of Antibacterial Magainin Peptides to Electrically Neutral Membranes: Thermodynamics and Structure. *Biochemistry (N. Y.)* **1999**, *38*, 10377-10387.

(73) Ludtke, S. J.; He, K.; Wu, Y.; Huang, H. W. Cooperative membrane insertion of magainin correlated with its cytolytic activity. *Biochimica et Biophysica Acta (BBA) - Biomembranes* **1994**, *1190*, 181-184.

(74) Hancock, R. E.; Sahl, H. G. Antimicrobial and host-defense peptides as new anti-infective therapeutic strategies. *Nat. Biotechnol.* **2006**, *24*, 1551-1557.

(75) Kyle, D. J.; Blake, P. R.; Smithwick, D.; Green, L. M.; Martin, J. A.; Sinsko, J. A.; Summers, M. F. NMR and computational evidence that high-affinity bradykinin receptor antagonists adopt C-terminal beta-turns. *J. Med. Chem.* **1993**, *36*, 1450-1460.

(76) Bhonsle, J. B.; Venugopal, D.; Huddler, D. P.; Magill, A. J.; Hicks, R. P. Application of 3D-QSAR for Identification of Descriptors Defining Bioactivity of Antimicrobial Peptides. *J. Med. Chem.* **2007**, *50*, 6545-6553.

(77) Venugopal, D.; Klapper, D.; Srouji, A. H.; Bhonsle, J. B.; Borschel, R.; Mueller, A.; Russell, A. L.; Williams, B. C.; Hicks, R. P. Novel antimicrobial peptides that exhibit activity against select agents and other drug resistant bacteria. *Bioorg. Med. Chem.* **2010**, *18*, 5137-5147.

(78) Vogel, H. J.; Schibli, D. J.; Jing, W.; Lohmeier-Vogel, E. M.; Epand, R. F.; Epand, R. M. Towards a structure-function analysis of bovine lactoferricin and related tryptophan- and arginine-containing peptides. *Biochem. Cell Biol.* **2002**, *80*, 49-63.

(79) Haug, B. E.; Strom, M. B.; Svendsen, J. S. The medicinal chemistry of short lactoferricin-based antibacterial peptides. *Curr. Med. Chem.* **2007**, *14*, 1-18.

(80) Woody, R. W. In *Theory of Circular Dichroism of Proteins ;* Fasman, G. D., Ed.; *Circular Dichroism and the Conformational Analysis of Biomolecues*; Plenum Press: New York: 1996; pp 25.

(81) Kelly, S. M.; Price, N. C. The application of circular dichroism to studies of protein folding and unfolding. *Biochimica et Biophysica Acta (BBA) - Protein Structure and Molecular Enzymology* **1997**, *1338*, 161-185.

(82) Giancoli, D. C. In *Physics for Scientists and Engineers;* Prentice Hall: Upper Saddle River, NJ, 2000; .

(83) Glattli, A.; Daura, X.; Seebach, D.; van Gunsteren, W. F. Can One Derive the Conformational Preference of a Î²-Peptide from Its CD Spectrum? *J. Am. Chem. Soc.* **2002**, *124*, 12972-12978.

(84) Ladokhin, A. S.; Fernandez-Vidal, M.; White, S. H. CD spectroscopy of peptides and proteins bound to large unilamellar vesicles. *J. Membr. Biol.* **2010**, *236*, 247-253.

(85) Hunter, H. N.; Jing, W.; Schibli, D. J.; Trinh, T.; Park, I. Y.; Kim, S. C.; Vogel, H. J. The interactions of antimicrobial peptides derived from lysozyme with model membrane systems. *Biochimica et Biophysica Acta (BBA) - Biomembranes* **2005**, *1668*, 175-189.

(86) Wieprecht, T.; Seelig, J. Isothermal Titration Calorimetry for Studying Interactions between Peptides and Lipid Membranes. *Current Topics in Membranes* **2002**, *52*, 31-55.

(87) Jing, W.; Hunter, H. N.; Hagel, J.; vogel, H. J. The structure of the antimicrobial peptide Ac-RRWWRF-NH2 bound to micelles and its interacitons with phospholipid bilayers. *Journal of Peptide Research* **2003**, *61*, 219-229.

(88) MicroCal, L. In *VP-ITC MicroCalorimeter User's Manual;* .

(89) Pierce, M. M.; Raman, C. S.; Nall, B. T. Isothermal Titration Calorimetry of Protein-Protein Interactions. *Methods* **1999**, *19*, 213-221.

(90) Seelig, J. Titration calorimetry of lipid-peptide interactions. *Biochim. Biophys. Acta* **1997**, *1331*, 103-116.

(91) Grossoehme, N. E.; Spuches, A. M.; Wilcox, D. E. Application of isothermal titration calorimetry in bioinorganic chemistry. *JBIC, J. Biol. Inorg. Chem.* **2010**, *15*, 1183-1191.

(92) Wieprecht, T.; Beyermann, M.; Seelig, J. Thermodynamics of the coil–α-helix transition of amphipathic peptides in a membrane environment: the role of vesicle curvature. *Biophys. Chem.* **2002**, *96*, 191-201.

(93) Seelig, J. Thermodynamics of lipid-peptide interactions. *Biochim. Biophys. Acta* **2004**, *1666*, 40-50.

(94) Holde, K. E. V.; Johnson, W. C.; Ho, P. S. In *Principles of Physical Biochemistry;* Pearson Prentice Hall: 2006; .

(95) Seelig, J.; Nebel, S.; Ganz, P.; Bruns, C. Electrostatic and nonpolar peptide-membrane interactions. Lipid binding and functional properties of somatostatin analogs of charge z = +1 to z = +3. *Biochemistry (N. Y.)* **1993**, *32*, 9714-9721.

(96) Beschiaschvili, G.; Seelig, J. Peptide binding to lipid bilayers. Binding isotherms and .zeta.-potential of a cyclic somatostatin analog. *Biochemistry (N. Y.)* **1990**, *29*, 10995-11000.

(97) Beschiaschvili, G.; Seelig, J. Melittin binding to mixed phosphatidylglycerol/phosphatidylcholine membranes. *Biochemistry (N. Y.)* **1990**, *29*, 52-58.

(98) Altenbach, C.; Seelig, J. Calcium binding to phosphatidylcholine bilayers as studied by deuterium magnetic resonance. Evidence for the formation of a calcium complex with two phospholipid molecules. *Biochemistry (N. Y.)* **1984**, *23*, 3913-3920.

(99) Evans, R. W.; Williams, M. A.; Tinoco, J. Surface areas of 1-palmitoyl phosphatidylcholines and their interactions with cholesterol. *Biochem. J.* **1987**, *245*, 455-462.

(100) Seelig, A.; Allegrini, P. R.; Seelig, J. Partitioning of local anesthetics into membranes: surface charge effects monitored by the phospholipid head-group. *Biochimica et Biophysica Acta (BBA) - Biomembranes* **1988**, *939*, 267-276.

(101) Kuchinka, E.; Seelig, J. Interaction of melittin with phosphatidylcholine membranes. Binding isotherm and lipid head-group conformation. *Biochemistry (N. Y.)* **1989**, *28*, 4216-4221.

(102) Aveyard, R.; Haydon, D. A. In *An Introducation to the principles of surface chemistry;* Cambridge University Press: Great Britain, 1973; .

(103) McLaughlin, S. The Electrostatic Properties of Membranes. *Annu. Rev. Biophys. Biophys. Chem.* **1989**, *18*, 113-136.

(104) McLaughlin, S. Electrostatic potentials at membrane-solution interfaces. *Current Topics in Membranes and Transport* **1977**, *9*, 71.

(105) Abraham, T.; Marwaha, S.; Kobewka, D. M.; Lewis, R. N. A. H.; Prenner, E. J.; Hodges, R. S.; McElhaney, R. N. The relationship between the binding to and permeabilization of phospholipid bilayer membranes by GS14dK4, a designed analog of the antimicrobial peptide gramicidin S. *Biochim. Biophys. Acta* **2007**, *1768*, 2089-2098.

(106) Andrushchenko, V. V.; Aarabi, M. H.; Nguyen, L. T.; Prenner, E. J.; Vogel, H. J. Thermodynamics of the interactions of tryptophan-rich cathelicidin antimicrobial peptides with model and natural membranes. *Biochimica et Biophysica Acta (BBA) - Biomembranes* **2008**, *1778*, 1004-1014.

(107) Wieprecht, T.; Apostolov, O.; Beyermann, M.; Seelig, J. Membrane Binding and Pore Formation of the Antibacterial Peptide PGLa: Thermodynamic and Mechanistic Aspects. *Biochemistry (N. Y.)* **2000**, *39*, 442-452.

(108) Wieprecht, T.; Dathe, M.; Schumann, M.; Krause, E.; Beyermann, M.; Bienert, M. Conformational and Functional Study of Magainin 2 in Model Membrane Environments Using the New Approach of Systematic Double-D-Amino Acid Replacement. *Biochemisty* **1996**, *35*, 10844-10853.

(109) Wei, S.; Wu, J.; Kuo, Y.; Chen, H.; Yip, B.; Tzeng, S.; Cheng, J. Solution Structure of a Novel Tryptophan-Rich Peptide with Bidirectional Antimicrobial Activity. *J. Bacteriol.* **2006**, *188*, 328-334.

(110) Butko, P.; Huang, F.; Pusztai-Carey, M.; Surewicz, W. K. Membrane Permeabilization Induced by Cytolytic Î´-Endotoxin CytA from Bacillus thuringiensis var. israelensis; doi: 10.1021/bi960970s. *Biochemistry (N. Y.)* **1996**, *35*, 11355-11360.

CHAPTER TWO: MATERIALS AND METHODS

Materials

Monobasic and dibasic sodium phosphate, EDTA and sodium chloride (NaCl) were purchased from Fischer Scientific. Bis-tris and SDS (**Figure 2.1** – top) were obtained from Sigma-Aldrich. All chemicals were of analytical or reagent grade and used without further purification. POPC (**Figure 2.2** – bottom), POPG (**Figure 2.2** – top) and DPC (**Figure 2.1** – bottom) were purchased from Avanti Polar Lipids (Alabaster, AL). High purity calcein (**Figure 2.3**) was purchased from Invitrogen and used as obtained without further purification. All buffers and solutions were prepared using distilled water. Some peptides were purchased from the Peptide Core Facility in the School of Medicine of the University of North Carolina at Chapel Hill, Chapel Hill, NC. Other peptides were synthesized by the Division of Experimental Therapeutics, Walter Reed Army Institute of Research, Silver Spring, Maryland.

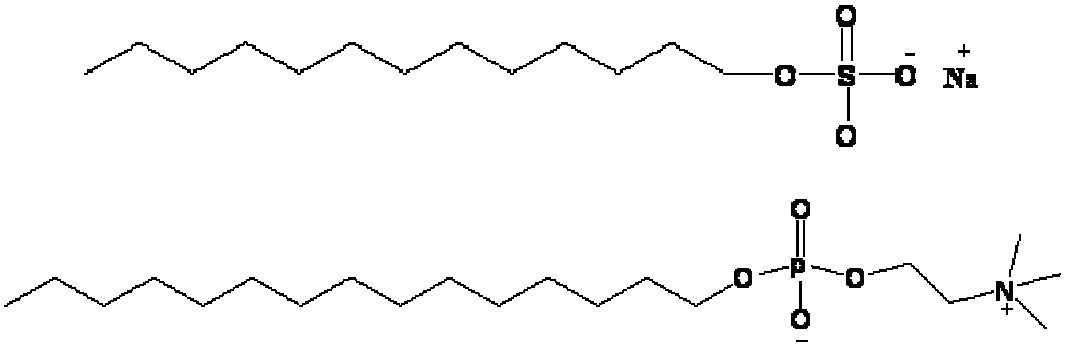

Figure 2.1: Chemical structures of lipids used for micelle membrane models. SDS (top) was used as a simple anionic model and DPC (bottom) was used as a simple zwitterionic model.

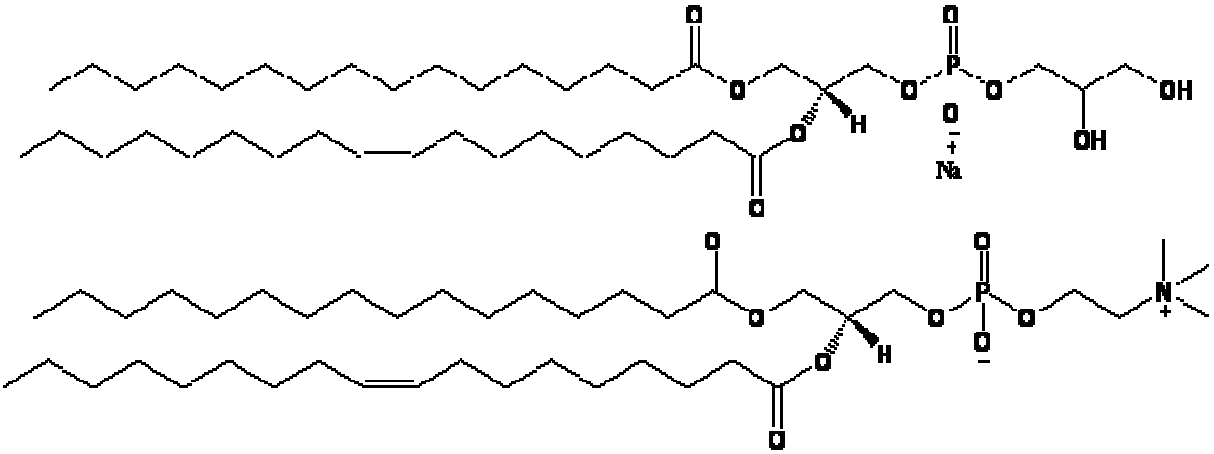

Figure 2.2: Chemical structures of lipids used for micelle membrane models. POPG (top) was used as the anionic component for the bilayer membrane models and POPC (bottom) was used as the zwitterionic component.

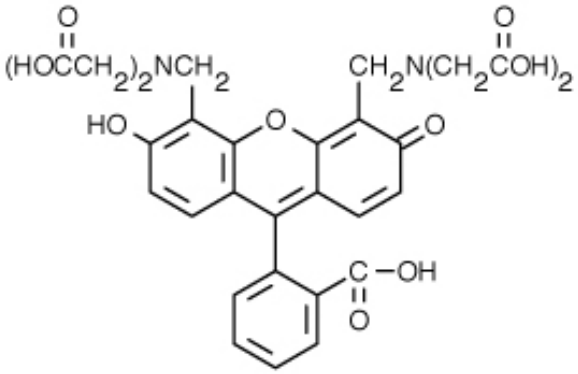

Figure 2.3: Chemical structure of calcein.

Biological Testing

Biological assays for the following bacteria strains were tested by MDS Pharma: *Salmonella typimurium* (ATCC 13311), *Staphylococcus aureus* ME/GM/MTC resistant bacteria (ATCC 33592), *Mycobacterium ranae* (ATCC 110) and *Bacillus subtillis* (ATCC 43223). Biological assays for the following select agents and other drug resistant bacteria were tested by the Division of Bacterial and Rickettsial Diseases at Walter Reed Army Institute of Research:

Acinetobacter baumanii (ATCD 19606), *Acinetobacter baumanii* (WRAIR), *Staphylcoccus aureus*-MRSA (ATCC 33591), *Yersinia pestis* (CO92), *Brucella melitensis* (16M), *Brucella abortus* (2308), *Brucella suis* (ATCC 23445), *Bacillus anthracis* (AMES), *Francisella tularensis* (SCHU-S4), *Burholderia mallei* (ATCC 23444) and *Burkholderia pseudomallei* (BURK003).

Preparation of Liposomes

POPC and 4:1 POPC/POPG Liposomes for CD and ITC experiments

For POPC LUVs, a defined amount of dried lipid was weighed and suspended in buffer (40 mM sodium phosphate, pH = 6.8) and spun for 30 minutes. The 4:1 POPC/POPG (mol to mol) LUVs were prepared by first dissolving a defined amount of POPC and POPG, separately, into chloroform. The lipids in chloroform were then mixed at a molar ratio of 4:1, vortexed and dried under a steady stream of nitrogen. Once dried, the mixed liposomes were suspended in the phosphate buffer and spun for 30 minutes. The liposomes used for CD and ITC were prepared by extrusion via a Mini-Extruder (Avanti Polar Lipid Inc).[1-3] The lipid solutions were passed 21 times through a stack of 4 polycarbonate support filters, with a 100 nm pore size polycarbonate membrane in the middle. Kennedy and co-workers[4] have previously reported that passing the liposome solution through the membrane 21 times as described resulted in a homogeneous population of LUVs with >95% of the particles falling into the size range of 70-100 nm.[4] The final lipid concentration was calculated based on the weight of the dried lipid.[5-10]

POPC and 4:1 POPC/POPG Liposomes for Dye Release Experiments

High purity calcein was dissolved in buffer (10 mM Bis-Tris, 150 mM NaCl, 1 mM EDTA, pH = 7.1) at self-quenching concentrations (70 mM). Once hydrated, the pH of the

calcein-containing buffer was adjusted using 3 mM NaOH. A defined amount of dried lipid was hydrated with the calcein-containing buffer to give a starting concentration of 35 mM and vortexed for one minute. POPC LUVs were used as obtained. The 4:1 POPC/POPG liposomes were made as described above. Both LUV solutions were prepared by the same extrusion process as described above and the final volume after extrusion was noted, approximately 300 µL. Unencapsulated calcein was removed by gel filtration on a Sephadex G50 column (eluent: buffer 10 mM Bis-Tris, 150 mM NaCl, 1 mM EDTA, pH = 7.1). Once the sample was added to the column, the fraction with the calcein-encapsulated liposomes separated out first as a band that was light orange in color. The unencapsulated calcein, along with liposomes containing no calcein, formed three bands, two yellow bands with a red one in the middle, **Figure 2.4**.

The fraction of calcein-encapsulated LUVs was collected and retained for fluorescence studies, taking note of the final volume. The final lipid concentration was calculated based on dilution by the column using the volumes before and after separation. To ensure self-quenching efficiency (Q) of each lipid solution, the following equation was used: $Q = [1- (F_0/F_T)] \times 100\%$ where F_0 and F_T are the fluorescences before and after treatment with 10uL of 10% Triton X, respectively. The minimum Q value used was 80%.[5-9, 11-14]

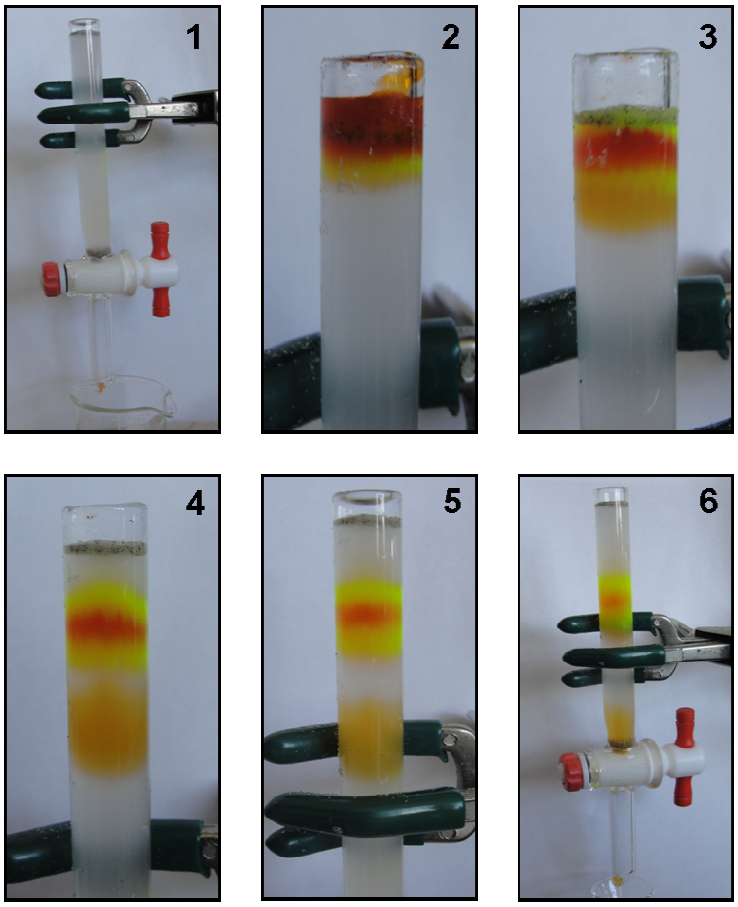

Figure 2.4: Gel filtration for the separation of calcein-encapsulated LUVs using a G50 Sephadex column (eluent: buffer 10 mM Bis-Tris, 150 mM NaCl, 1 mM EDTA, pH =7.1). 1) A clean column before the separation process has begun. 2) Recently extruded solution of calcein-encapsulated LUVs is added all at once to the top of the column. 3 – 5) Fraction containing only calcein-encapsulated LUVs separates out as an orange band. Free calcein and LUVs not containing calcein remain in yellow and red bands. 6) Separation is complete and fraction containing only calcein-encapsulated LUVs is collected.

Circular Dichroism

CD Parameters

All CD spectra were obtained by acquiring 8 scans from 260 to 178 nm on a Jasco J-815 spectrometer (equipped with Jasco SOFTWARE V) using a 0.1 mm pathlength cylindrical quartz cell (Starna Cells, Atascadero, CA) at a speed of 20 nm/min, a 1 nm bandwidth, a data pitch of

0.2 nm, response time 0.25 sec and 5 mdeg sensitivity at room temperature (~25ºC) in a continuous scanning mode. Contributions due to LUVs were eliminated by subtracting the lipid spectra of the corresponding peptide-free suspensions.[6, 7] All analysis of CD spectra were conducted after smoothing (Means-movement with convolution width of 5-25) and conversion to molar ellipticity using the JASCO Spectra Analysis program.[1, 14, 15]

Due to the high percentage of unnatural amino acids that are incorporated into our peptides, no quantitative estimation of secondary structural features is possible. Analysis of CD spectra will be limited to qualitative comparisons highlighting differences in the spectra of this series of compounds. Reference to α-helical or β-turn structures are based on comparisons with published CD spectra of peptides and are used only as a qualitative discussion.

Peptide in buffer and micelle environments

Conformations of the peptides were studied in several different environments. First, peptides were weighed and dissolved in 40 mM phosphate buffer (pH = 6.8) to give a final concentration of 1 mg/mL in order to observe their natural states. Binding studies were conducted by hydrating dried peptide with either 80 mM SDS or DPC micelles in 40 mM phosphate buffer (pH = 6.8) to give an overall peptide concentration of 1 mg/mL.

Peptide in LUV environments

Binding studies in the presence of LUVs were conducted by hydrating dried peptide with either 1.75 mM POPC or 4:1 POPC/POPG LUVs in 40 mM phosphate buffer (pH = 6.8). LUVs (100 nm liposomes) were selected instead of small unilamellar vesicles (SUVs) because they are considered to be more closely related to biological membranes. LUVs are not

subject to the increased curvature stress associated with SUVs [6, 16] resulting in metastability and an increase in irregular peptide binding.[16, 17] The exact concentrations of peptide used for these experiments are given in **Table 2.1**.

Table 2.1: The concentration (μM) used for each peptide of the different series for the interactions with POPC and 4:1 POPC/POPG LUV membrane models as studied by CD.

Compound	POPC	4:1 POPC/POPG
Parent		
23	200	200
Spacer 1		
23	75	100
36	75	100
29	75	100
37	75	100
Spacer 2		
23	75	200
43	100	200
53	100	200
45	100	200
56	100	200
Spacer 3		
23	75	200
50	100	200
51	100	200
52	100	200
Placement of Lys		
23	75	100
39	100	100
64	100	100
61	100	100
Negative Control		
23	200	100
14	200	100
34	200	75
All Unnatural Amino Acids		
23	75	100
46	100	100

The HT [V] values and UV spectra of compound **23** in the presence of 1.75, 7.0 and 10.5 mM POPC (left) and 4:1 POPC/POPG LUVs (right) are given in **Figures 2.5** and **2.6**, respectively. Compound **23** serves as the reference for interference caused by LUVs in CD studies. CD spectra should maintain a high tension (HT) voltage below 600 V for the study of peptides to ensure that the detector is not saturated. Also, work of Ladokhin and co-workers has shown that undistorted CD studies can be obtained in the presence of up to 3 mM LUVs above 200 nm and in the presence of 7 mM LUVs above 215 nm as long as the absorbance of the uncorrected (without subtraction of buffer) spectra remained below 1.5 AU.[16] Clearly the uncorrected (no subtraction of buffer etc.) absorbance at all three LUV concentrations remained below 1.5 AU at a wavelength above 200 nm which based on the work of Ladokhin and co-workers allows for a qualitative comparison of the CD spectra.[16] However, for the purpose of our studies in the presence of a constant LUV concentration, we will use 1.75 mM to ensure qualitative data below 200 nm.[16]

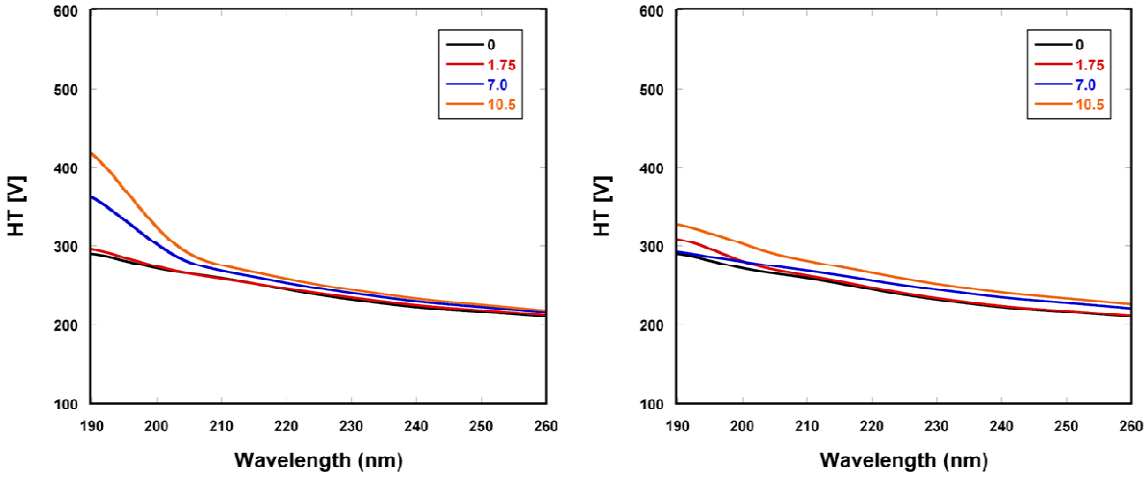

Figure 2.5: Representative HT [V] values of 75 µM compound **23** in POPC (left) and 100 µM compound **23** in 4:1 POPC/POPG LUVs (right).

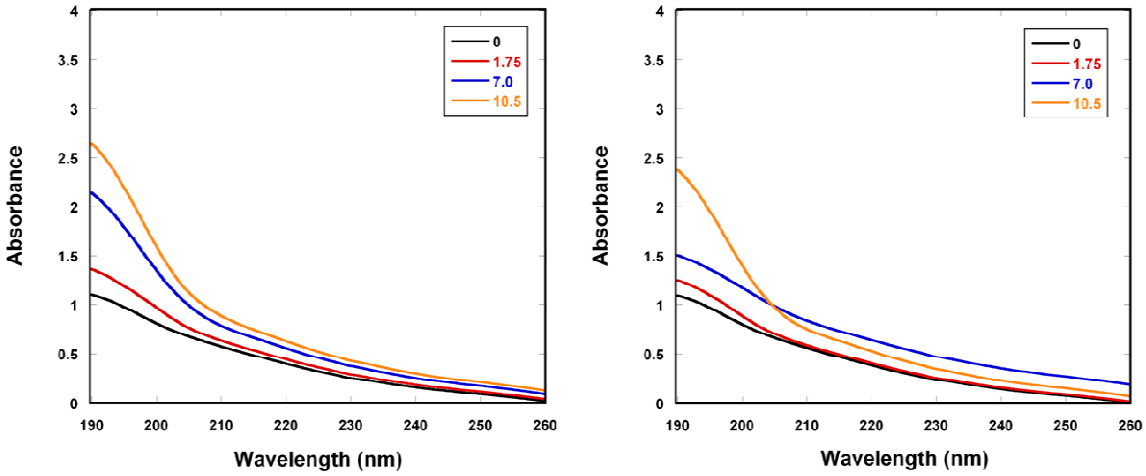

Figure 2.6: Representative optical density, absorbance values, of 75 µM compound **23** in POPC (left) and 100 µM compound **23** in 4:1 POPC/POPG LUVs (right).

CD "pseudo" titration experiments

CD spectra were recorded for separate peptide samples with increasing concentrations of liposomes using the parameters previously discussed.[2, 8] Stock solutions of peptide (150 – 400 µM) and liposomes (35 mM) were prepared. Separate samples were prepared by first, taking 100 µL of the peptide stock solution and diluting it with varying amounts (0-100 µL) of 40 mM sodium phosphate buffer, pH = 6.8. Corresponding volumes of the liposome stock solution were then added to give a final sample volume of 200 µL resulting in an overall peptide concentration that was half the concentration of the stock solution. A sample calculation chart of the "pseudo" titration samples can be seen below in **Table 2.2**. The final concentrations for each peptide used in the "pseudo" CD titrations are given in **Table 2.3**.

Table 2.2: Sample calculation chart for the composition of samples used for the "pseudo" CD titration experiments.

Sample	Total Vol[a]	Pep Vol[b]	Lip Vol[c]	Buf Vol[d]	[Pep][e]	[Lip][f]	L/P[g]
0	200	100	0	100	0.1	0	0
1	200	100	5	95	0.1	0.875	8.75
2	200	100	10	90	0.1	1.75	17.5
3	200	100	20	80	0.1	3.5	35
4	200	100	30	70	0.1	5.25	52.5
5	200	100	40	60	0.1	7	70
Total	1200	600	105	495			

[a] Total volume (µL) of sample. [b] Volume (µL) of peptide. [c] Volume (µL) of 35 mM lipid solution. [d] Volume (µL) of 40 mM phosphate buffer, pH = 6.8. [e] Final concentration (mM) of peptide in sample. [f] Overall concentration (mM) of lipid in sample. [g] Lipid to peptide ratio.

Table 2.3: The final peptide concentration (µM) used for the "pseudo" CD titration studies with POPC and 4:1 POPC/POPG LUV membrane models.

Compound	POPC	4:1 POPC/POPG
Parent		
23	200	200
Spacer 1		
36	75	100
29	75	100
37	75	200
Spacer 2		
43	100	200
53	100	200
45	200	200
56	100	100
Spacer 3		
50	100	200
51	100	200
52	100	200
Placement of Lys		
39	100	100
64	100	200
61	100	100
Negative Control		
14	100	100
34	200	75
All Unnatural Amino Acids		
46	100	100

Isothermal Titration Calorimetry

ITC Parameters

Data was acquired using a Microcal VP-ITC calorimeter (Microcal, Norhampton, MA). All experiments were run in 40 mM sodium phosphate buffer, pH = 6.8, and at a temperature of 25 ºC with a stirring speed of 220 rpm. All solutions were degassed for approximately 10 minutes under vacuum before running the experiments.

Full Titration Experiment

Full titrations refer to the ITC experiments that are carried out until only the heat of dilution was observed and all of the peptide is assumed bound. Experiments included 15 µL injections of 35 mM liposomes into excess peptide (50 – 200 µM). The exact peptide concentrations used are listed in **Table 2.4**. Injection durations were 30 s with 700-800 sec spacing between individual injections to ensure complete equilibration. The heat of dilution was determined by injecting LUV solutions into peptide-free buffer. This heat was subtracted from the heat evolved from the interactions between the liposomes and peptide. Data was analyzed with the Origin® software (version 7). ITC experiments were duplicated to ensure reproducibility.[1, 5, 6, 8, 9, 11, 18, 19]

Table 2.4: The concentration of each peptide (μM) used during the full ITC titration studies. The reaction cell was filled with the peptide solutions and titrated with either 35 mM POPC or 4:1 POPC/POPG LUVs in buffer.

Compound	POPC	4:1 POPC/POPG
Parent Compound		
23	200	200
Spacer 1		
36	50	50
29	100	100
37	50	200
Spacer 2		
43	200	200
53	200	200
45	200	300
56	100	100
Spacer 3		
50	50	200
51	100	200
52	100	200
Placement of Lys		
39	200	200
64	100	200
61	100	200
Negative Control		
14	100	100
34	200	50
All Unnatural Amino Acids		
46	100	200

Single Injection Experiments

Data from the full injection experiments with 4:1 POPC/POPG LUVs could not be fit to a current model, therefore, we were unable to obtain quantitative thermodynamic information. However, by performing single injection experiments we were able to determine the ΔH values that correspond to the two extremes of the peptide and lipid interaction, binding and membrane disruption and should not be confused with ΔH^0, the enthalpy of the entire reaction.

To determine the ΔH of binding at very high L/P ratios, dilute solutions of peptide (100 – 200 μM) were titrated into solutions of excess liposomes (15 – 30 mM). Single injection experiments were also performed in the opposite direction. Dilute solutions of liposomes (5 – 20 mM) were titrated into solutions of excess peptide (300 – 400 μM) to determine the ΔH of membrane disruption.[11, 19-24] The exact concentrations used for each experiment are included with the figure in the body of the text.

Calcein Leakage Assays

Peptide-induced calcein leakage was investigated using an ISS PC1 photon counting spectrofluorometer (ILC Technology) at an excitation wavelength of 494 nm and an emission wavelength of 518 nm. An aliquot of 1.0 mM peptide (10 – 50 μM) in buffer (10 mM Bis-Tris, 150 mM NaCl, 1 mM EDTA, pH = 7.1) was added to the cell (1.0 cm quartz cuvette) containing 2.5 mL of liposomes (36.6 μM) to give an overall peptide concentration of 4-20 μM. The intensity, F_I, was measured every minute for the first 20 minutes of the experiment and every 10 minutes after until the emission intensity leveled off, approximately 90 minutes. One hundred percent leakage, F_T, was determined with the addition of 10 μL of 10% (v/v) Triton X. The apparent percent leakage was calculated using the following equation: % leakage = $[(F_I - F_0)/F_T)]$ x 100 %, where F_0 and F_T are the fluorescence before introduction of peptide and after the addition of Triton X, respectively.[1, 5, 7, 12, 13, 25] Representative emission spectra as the time increases is given in **Figure 2.7**.

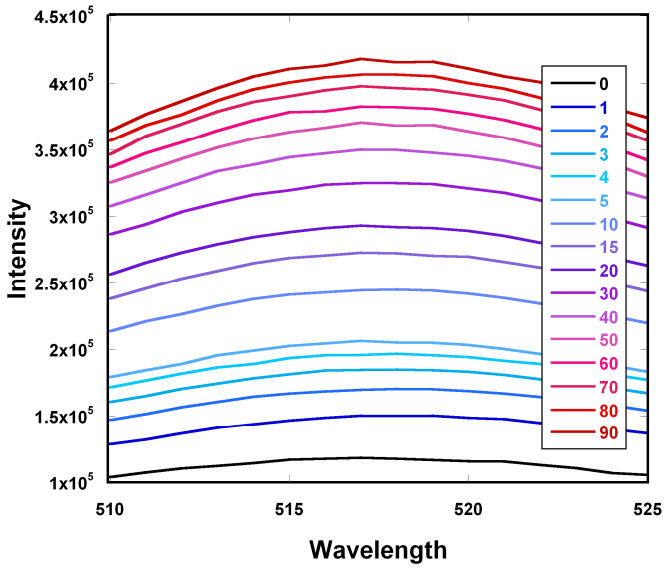

Figure 2.7: Representative spectra of peptide-induced calcein leakage as time increases. At 0 minutes (black), only calcein-encapsulated 4:1 POPC/POPG LUVs were present. An aliquot of the peptide stock solution was added. The fluorescence was measured every minute for the first 20, then every 10 minutes for a total of 90 minutes. The intensity increased with time.

References

(1) Wei, S.; Wu, J.; Kuo, Y.; Chen, H.; Yip, B.; Tzeng, S.; Cheng, J. Solution Structure of a Novel Tryptophan-Rich Peptide with Bidirectional Antimicrobial Activity. *J. Bacteriol.* **2006**, *188*, 328-334.

(2) Hunter, H. N.; Jing, W.; Schibli, D. J.; Trinh, T.; Park, I. Y.; Kim, S. C.; Vogel, H. J. The interactions of antimicrobial peptides derived from lysozyme with model membrane systems. *Biochimica et Biophysica Acta (BBA) - Biomembranes* **2005**, *1668*, 175-189.

(3) Thomas, C. J.; Surolia, N.; Surolia, A. Kinetic and thermodynamic analysis of the interactions of 23-residue peptides with endotoxin. *Biological Chemistry* **2001**, *276*, 35701-35706.

(4) Kennedy, A.; Hmel, P. J.; Seelbaugh, J.; Quiles, J. G.; Hicks, R.; Reid, T. J. Characterization of the transition in 1,2-dipalyitoyl-phosphatidylcholine LUVs by 1H NMR1*. *J. Liposome Res.* **2002**, *12*, 221-237.

(5) Wieprecht, T.; Apostolov, O.; Beyermann, M.; Seelig, J. Membrane Binding and Pore Formation of the Antibacterial Peptide PGLa: Thermodynamic and Mechanistic Aspects. *Biochemistry (N. Y.)* **2000**, *39*, 442-452.

(6) Wieprecht, T.; Apostolov, O.; Seelig, J. Binding of the antibacterial peptide magainin 2 amide to small and large unilamellar vesicles. *Biophys. Chem.* **2000**, *85*, 187-198.

(7) Dathe, M.; Schumann, M.; Wieprecht, T.; Winkler, A.; Beyermann, M.; Krause, E.; Matsuzaki, K.; Murase, O.; Bienert, M. Peptide Helicity and Membrane Surface Charge Modulate the Balance of Electrostatic and Hydrophobic Interactions with Lipid Bilayers and Biological Membranes. *Biochemistry (N. Y.)* **1996**, *35*, 12612-12622.

(8) Wen, S.; Majerowicz, M.; Waring, A.; Bringezu, F. Dicynthaurin (ala) Monomer Interaction with Phospholipid Bilayers Studied by Fluorescence Leakage and Isothermal Titration Calorimetry. *The Journal of Physical Chemistry B* **2007**, *111*, 6280-6287.

(9) Wieprecht, T.; Seelig, J. Isothermal Titration Calorimetry for Studying Interactions between Peptides and Lipid Membranes. *Current Topics in Membranes* **2002**, *52*, 31-55.

(10) Wieprecht, T.; Apostolov, O.; Beyermann, M.; Seelig, J. Thermodynamics of the α-helix-coil transition of amphipathic peptides in a membrane environment: implications for the peptide-membrane binding equilibrium. *J. Mol. Biol.* **1999**, *294*, 785-794.

(11) Wieprecht, T.; Beyermann, M.; Seelig, J. Thermodynamics of the coil–α-helix transition of amphipathic peptides in a membrane environment: the role of vesicle curvature. *Biophys. Chem.* **2002**, *96*, 191-201.

(12) Wieprecht, T.; Dathe, M.; Schumann, M.; Krause, E.; Beyermann, M.; Bienert, M. Conformational and Functional Study of Magainin 2 in Model Membrane Environments Using the New Approach of Systematic Double-D-Amino Acid Replacement. *Biochemisty* **1996**, *35*, 10844-10853.

(13) Tamba, Y.; Yamazaki, M. Single Giant Unilamellar Vesicle Method Reveals Effect of Antimicrobial Peptide Magainin 2 on Membrane Permeability. *Biochemistry (N. Y.)* **2005**, *44*, 15823-15833.

(14) Jing, W.; Hunter, H. N.; Hagel, J.; vogel, H. J. The structure of the antimicrobial peptide Ac-RRWWRF-NH2 bound to micelles and its interacitons with phospholipid bilayers. *Journal of Peptide Research* **2003**, *61*, 219-229.

(15) Bringezu, F.; Wen, S.; Dante, S.; Hauss, T.; Majerowicz, M.; Waring, A. The Insertion of the Antimicrobial Peptide Dicynthaurin Monomer in Model Membranes: Thermodynamics and Structural Characterizationâ€. *Biochemistry (N. Y.)* **2007**, *46*, 5678-5686.

(16) Ladokhin, A. S.; Fernandez-Vidal, M.; White, S. H. CD spectroscopy of peptides and proteins bound to large unilamellar vesicles. *J. Membr. Biol.* **2010**, *236*, 247-253.

(17) Ladokhin, A. S.; Selsted, M. E.; White, S. H. CD Spectra of Indolicidin Antimicrobial Peptides Suggest Turns, Not Polyproline Helix. *Biochemistry* **1999**, *38*, 12313-12319.

(18) Russell, A. L.; Kennedy, A. M.; Spuches, A. M.; Venugopal, D.; Bhonsle, J. B.; Hicks, R. P. Spectroscopic and thermodynamic evidence for antimicrobial peptide membrane selectivity. *Chem. Phys. Lipids* **2010**, *163*, 488-497.

(19) Abraham, T.; Lewis, R. N. A. H.; Hodges, R. S.; McElhaney, R. N. Isothermal Titration Calorimetry Studies of the Binding of a Rationally Designed Analogue of the Antimicrobial Peptide Gramicidin S to Phospholipid Bilayer Membranes. *Biochemistry (N. Y.)* **2005**, *44*, 2103-2112.

(20) Wieprecht, T.; Beyermann, M.; Seelig, J. Binding of Antibacterial Magainin Peptides to Electrically Neutral Membranes: Thermodynamics and Structure. *Biochemistry (N. Y.)* **1999**, *38*, 10377-10387.

(21) Bastos, M.; Bai, G.; Gomes, P.; Andreu, D.; Goormaghtigh, E.; Prieto, M. Energetics and Partition of Two Cecropin-Melittin Hybrid Peptides to Model Membranes of Different Composition. *Biophys. J.* **2008**, *94*, 2128-2141.

(22) Seelig, J. Titration calorimetry of lipid-peptide interactions. *Biochim. Biophys. Acta* **1997**, *1331*, 103-116.

(23) Wenk, M. R.; Seelig, J. Magainin 2 Amide Interaction with Lipid Membranes: Calorimetric Detection of Peptide Binding and Pore Formation. *Biochemistry (N. Y.)* **1998**, *37*, 3909-3916.

(24) Nomura, K.; Corzo, G. The effect of binding of spider-derived antimicrobial peptides, oxyopinins, on lipid membranes. *Biochimica et Biophysica Acta (BBA) - Biomembranes* **2006**, *1758*, 1475-1482.

(25) Won, A.; Ianoul, A. Interactions of antimicrobial peptide from C-terminus of myotoxin II with phospholipid mono- and bilayers. *Biochimica et Biophysica Acta (BBA) - Biomembranes* **2009**, *1788*, 2277-2283.

CHAPTER THREE: COMPOUND 23

Introduction

As mentioned in Chapter 1, we chose compound **23** with the amino acid sequence Ac-GF-Tic-Oic-GK-Tic-Oic-GF-Tic-Oic-GK-Tic-KKKK-$CONH_2$ as the reference peptide due to its previously reported high antibacterial activities against *Salmonella typhimurium*, *Staphylococcus aureus*, *Mycobacterium ranae* and *Bacillus subtillis* (**Table 3.1**).[1] Compound 23 was also tested in several select agent assays where it showed activity against *Acinetobacter baumanii* and *Bacillus anthracis* (**Table 3.2**).[2] This peptide also exhibited a therapeutically acceptable maximum tolerated dose of 125 mg/kg in a standard mouse toxicity model. [1] The parent compound, **23**, has been extensively studied via CD, ITC and fluorescence spectroscopy in the presence of anionic and zwitterionic micelle and bilayer membrane models.[3]

Table 3.1: Minimum inhibitory concentration (μM) and hemolytic activity of selected bacteria strains[1]

Compound	***Salmonella typhimurium***	***Staphylococcus aureus* ME/GM/TC resistant**	***Mycobacterium ranae***	***Bacillus subtillis***	**% hemolysis 100/25 μM**
23	10	3	10	1	14%

AMPs are known to exist in many different conformers depending on their local chemical environment.[4, 5] In the presence of membrane model systems these conformers include monomeric peptides in solution as well as surface bound (S-state) and membrane inserted (I-state) oligomers, the latter being associated with pore formation.[6-8] Previous computational studies conducted by Bhonsle and co-workers [9] has shown that compound **23** adopts a back to back turn conformation in the gas phase with an overall shape similar to a loose helical structure.

It is therefore reasonable to assume that compound **23** will adopt an ordered structure when in the presence of micelles or LUVs. In an effort to understand the observed biological cell selectivity and to improve the selectivity and potency of these peptides CD, calcein leakage assays and ITC were conducted to investigate the mechanisms of lipid binding of compound **23** to zwitterionic and anionic liposomes.

Table 3.2: Minimum inhibitory concentrations (μM) of specific Gram negative and other drug resistant bacteria strains.[2]

Compound	23
Acinetobacter baumanii ATCC 19606	3.2
Acinetobacter baumanii WRAIR	3.2
Staphylococcus aureus ATCC 33591	205
Yersinia pestis CO92	205
Brucella melitensis 16M	205
Brucella abortus 2308	205
Brucella suis 23444	205
Bacillus anthracis AMES	12.8
Francisella tularensis SCHUS4	100
Burkholderia mallei	205
Burkholderia pseudomallei	205

Results and Discussion

Structural Investigations of the Conformational Capacity of the Peptides

Importance of the order and stereochemistry of dipeptide unit. Three different tetra peptides were synthesized to observe the role of the Tic-Oic dipeptide unit in the secondary structures of the AMP developed in our laboratory. The amino acid sequences investigated were Ac-Ala-Tic-Oic-Ala-NH_2, Ac-Ala-D-Tic-Oic-Ala-NH_2, and Ac-Ala-Oic-D-Tic-Ala-NH_2, and their CD spectra are given in **Figure 3.1**. The CD spectra of the tetra peptide Ac-Ala-Tic-Oic-Ala-NH_2 (black) exhibited an ordered turn as indicated by the double minima at about 205 and 220 nm with a maximum at approximately 195 nm, which is consistent with the presence of β-turn and helical conformers. [10-12] The tetra peptide Ac-Ala-D-Tic-Oic-Ala-NH_2 (red) exhibited an ordered turn containing secondary structure as indicated by the double maxima in the CD spectrum at about 195 and 205 nm, and a minimum at 220 nm, which is consistent with the presence of possible β-turn conformers. [10-12] This observation is consistent with the NMR finding by Kyle and co-workers that when Tic and Oic are placed in positions i+1 and i+2 in a four sequence unit, a β-turn is induced. [13] The tetra peptide Ac-Ala-Oic-D-Tic-Ala-NH_2 (blue) exhibits a maximum in the CD spectrum at about 220 nm, and a minimum at about 198 nm, which is consistent with random coil conformers. [10, 12] These three CD spectra served as experimental evidence that given the proper stereochemistry the Tic-Oic dipeptide unit can serve as a turn inducing unit. The dipeptide L-Tic-L-Oic induced a predominately α-helical conformation while the inversion of the stereochemistry of the Tic residue from L to D induced a β-turn. When the order of the Tic-Oic dipeptide is reversed, the dipeptide no longer induces turn

or helical structures proving that the order and stereochemistry of the Tic-Oic dipeptide is important in stabilizing a stable secondary structure on the larger peptide.

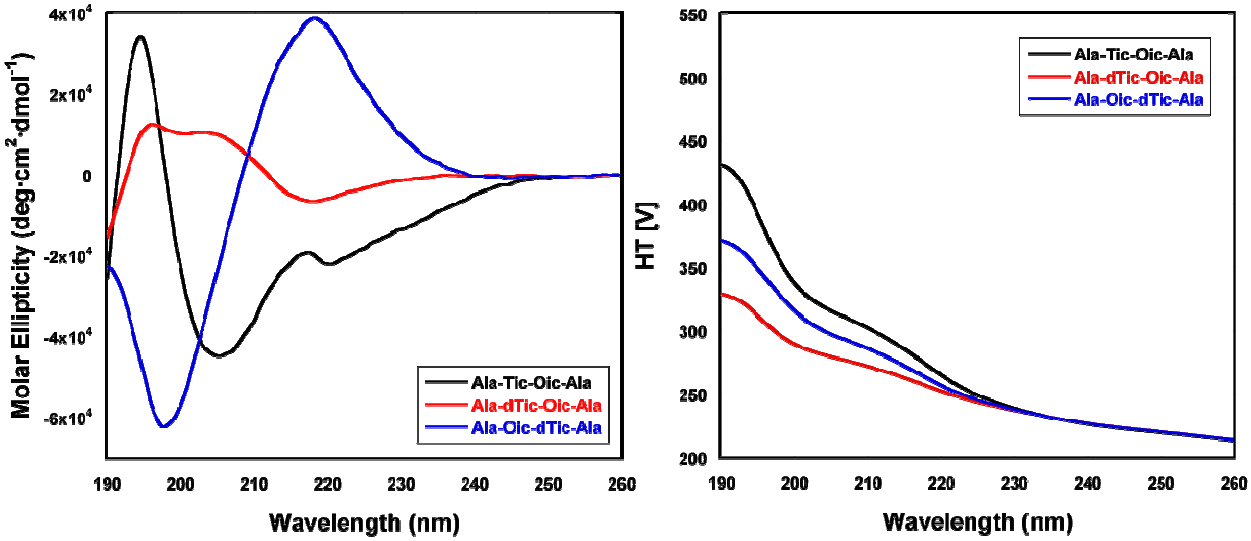

Figure 3.1: CD spectra of tetrapeptides (1 mg/mL) in 40 mM phosphate buffer (left), pH = 6.8, and their corresponding HT values (right). The sequences were Ac-Ala-Tic-Oic-Ala-NH_2 (black), Ac-Ala-D-Tic-Oic-Ala-NH_2 (red), and Ac-Ala-Oic-D-Tic-Ala-NH_2 (blue).

TFE studies. All of the peptides in this investigation contain three Tic-Oic dipeptide units and to evaluate the order inducing capacity of these peptides, a series of CD spectra of compound **23** in trifluoroethanol (TFE) were collected. TFE is an organic solvent which induces maximum helicity for short polypeptides.[14-17] **Figure 3.2** displays the CD spectra observed when Compound **23** (1 mg/mL) is dissolved in varying ratios of TFE in 40 mM phosphate buffer (pH = 6.8), ranging from 100% buffer (black) to 100% TFE (light blue)**.** The CD spectrum of Compound **23** in 100% phosphate buffer exhibits the most intense double minima at 210 and 220 nm, but the least intense below 200 nm, suggesting a mixture of β-turn and helical structures. As the % of TFE increases, the intensity of the two minima above 200 nm decreases while the opposite occurs below 200 nm. The increase of intensity below 200 nm coupled with the shift

from ~196 nm in 100% buffer to ~193 nm in TFE suggests that the percentage of α-helical conformers in solution is also increasing. This observation supports our hypothesis that the Tic-Oic dipeptide unit, in an order inducing environment such as TFE, will induce conformational changes to obtain a stable secondary structure.

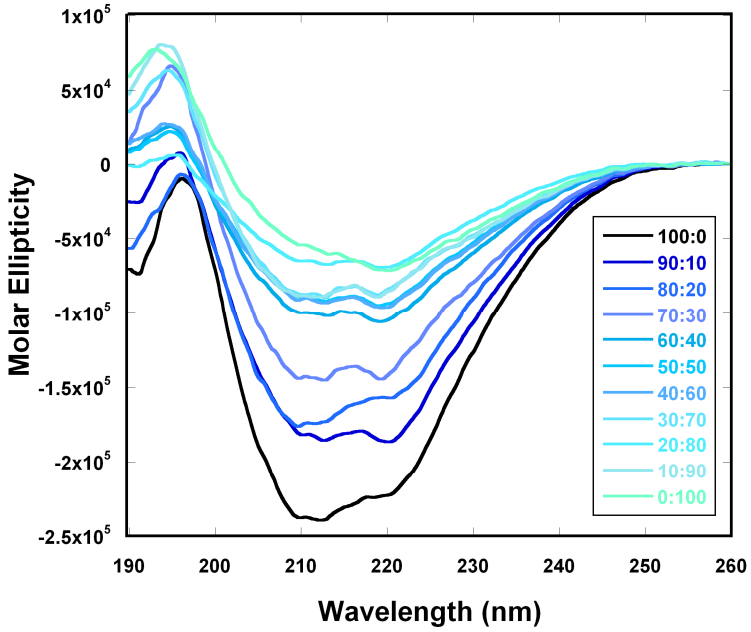

Figure 3.2: Far-UV Circular Dichroism spectra of Compound **23** (1 mg/mL) dissolved in varying ratios of 40 mM phosphate buffer (pH = 6.8) and TFE, from 0% (black) to 100% TFE (light blue).

Investigations of Secondary Structures Adopted by Compound **23**

*Compound **23** in buffer and micelle environments*. The CD spectra of compound **23** in 40 mM phosphate buffer, and in the presence of 80 mM DPC in buffer and 80 mM SDS in buffer are shown in **Figure 3.3**. In buffer, compound **23** exhibited a characteristic double minimum at about 210 and 220 nm which is consistent with the presence of helical and β-turn conformers.[10, 18] The CD spectra of compound **23** in the presence of DPC micelles displayed a shift in λ_{max} from approximately 195 to 190 nm and a shift in one of the minima from 210 to 203 nm. Also,

there was an increase in intensity at approximately 195 and 203 nm. The CD spectra of compound **23** in the presence of SDS and DPC micelles were very similar. However, there was a significant increase in intensity at the λ_{max} and the double minima in SDS as compared to DPC suggesting an increase in α-helical components of the peptide. Both of the CD spectra in DPC and SDS micelles were different from the spectrum in buffer indicating they do interact with the micelle surfaces. The observed differences intensity of the CD spectra indicate that S-state bound conformations of these peptides to SDS and DPC micelles were different, as expected.

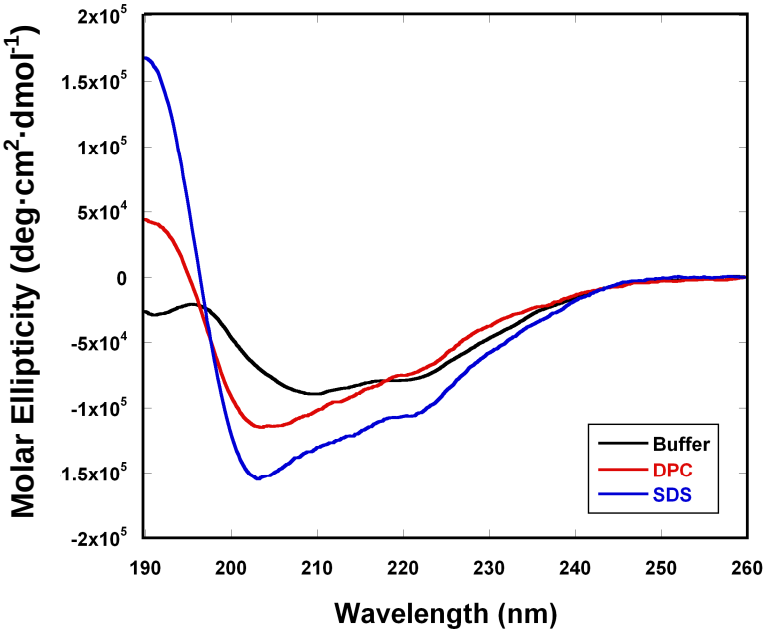

Figure 3.3: CD spectra of compound **23** (1 mg/mL) in 40 mM sodium phosphate buffer, pH = 6.8 (black), 80 mM DPC in buffer (red) and 80 mM SDS in buffer (blue).

Importance of anionic phospholipid concentration. All of the peptides were investigated in the presence of zwitterionic and anionic membrane model systems. As previously mentioned in Chapter 2, LUVs were chosen because they are not prone to the curvature stress and metastability issues that are common for SUVs.[18, 19] It has been documented that the extent of

the interaction between the peptides and the membrane model depends on the composition of the membrane. [20, 21] To confirm this hypothesis, spectral data was collected of compound **23** in the presence of 10 mM mixed POPC/POPG liposomes at various ratios of POPC and POPG. POPC vesicles were used to represent zwitterionic membranes, a simple model for eukaryotic membranes [22-24] and POPG was used as the anionic component of the model membranes for this study.[24, 25] The percent composition of the membrane model was varied from 100% POPG (black CD spectrum) to 100% POPC (light blue CD spectrum) in 10% increments (**Figure 3.4**). The CD spectra shown in **Figure 3.4** also confirmed our hypothesis that the total percentage of anionic lipid plays a major role in defining the membrane's physicochemical surface properties thus affecting the conformations and interactions. Changes in the anionic to zwitterionic phospholipid ratios in the membrane model result in different surface potentials, inducing different conformations onto the peptide so as to allow for binding.

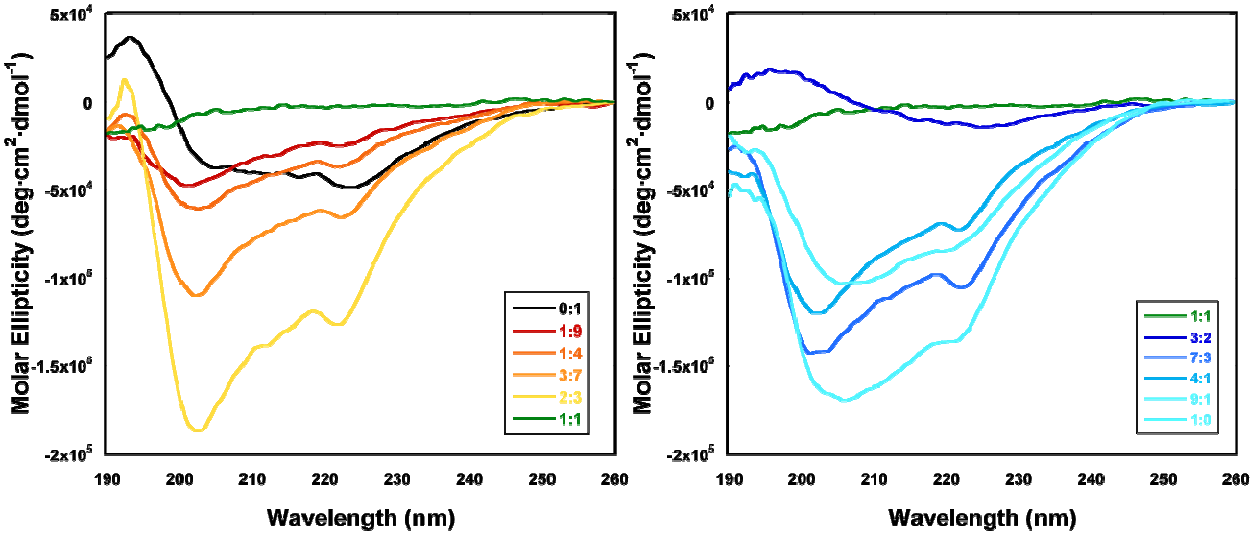

Figure 3.4: Far-UV CD spectra of compound **23** (1 mg/mL) in the presence of 10 mM POPC/POPG liposomes with varying ratios dissolved in 40 mM phosphate buffer (pH = 6.8). The percent composition of the liposomes is varied from 100% POPG (black CD spectrum) to 100% POPC (light blue CD spectrum) in 10% increments, with the highest POPG ratios on the left and highest POPC ratios on the left.

*Compound **23** in LUV environments*. The CD spectra of 75 µM compound **23** and 100 µM compound **23** in the presence of 1.75 mM POPC and 4:1 POPC/POPG LUVs are given in **Figure 3.5**, along with their corresponding HT values and absorbance for the uncorrected spectra (without subtraction of buffer). As previously discussed in Chapter 2, HT values should remain below 600 V and UV absorbance below 1.5 AU in order to exhibit undistorted CD spectra for qualitative comparison.[19] The spectra in the different membrane environments were different from the spectrum observed for this AMP in buffer leading to the conclusion that there is some interaction between the AMP and model membrane systems.

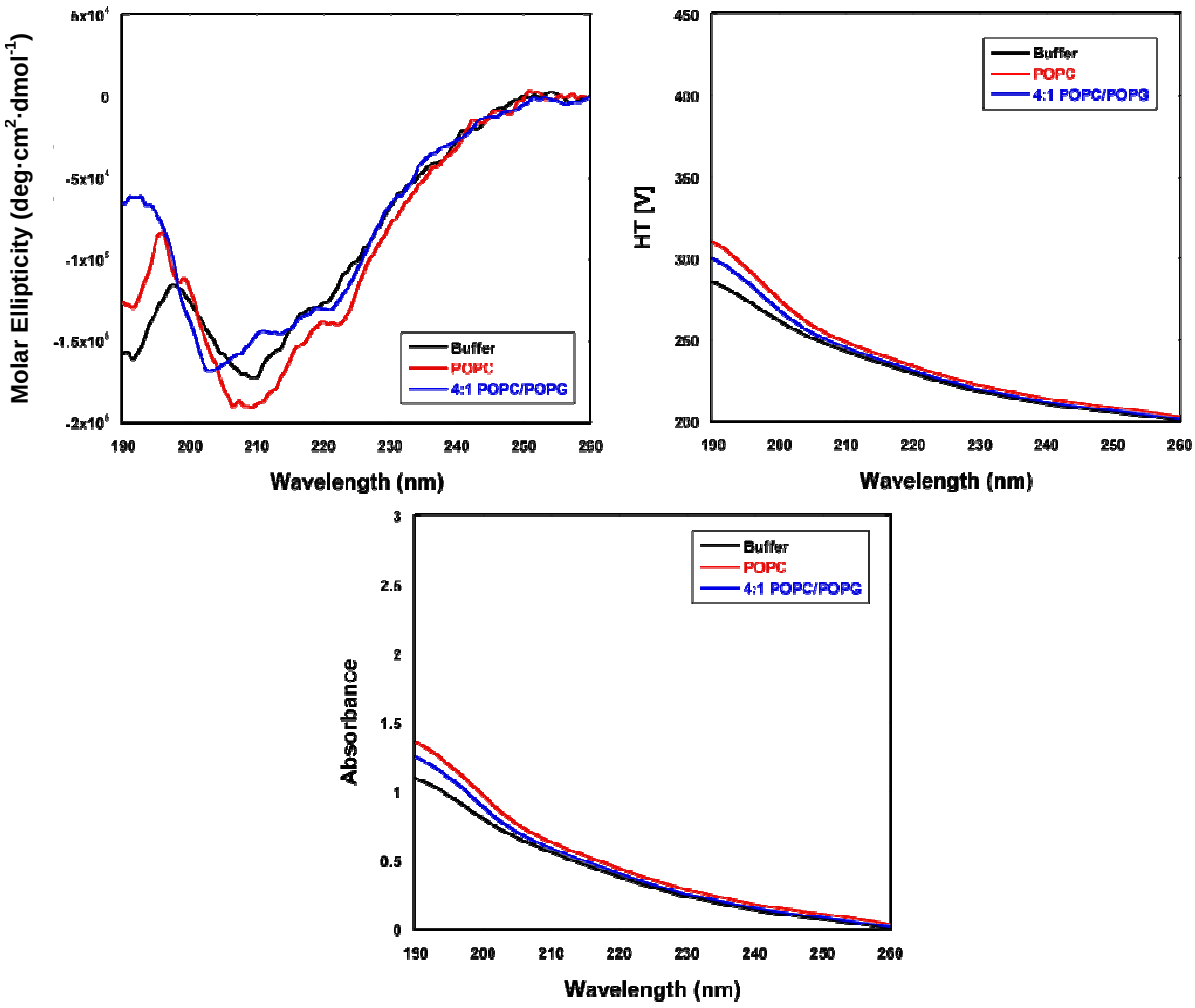

Figure 3.5: Far-UV CD spectra (top left) of 75 µM compound **23** in 1.75 mM POPC LUVs (red) and 100 µM compound **23** in 40 mM phosphate buffer (black), pH = 6.8, and 1.75 mM 4:1 POPC/POPG LUVs (blue). Corresponding HT [V] (top right) and absorbance spectra (bottom) were included.

For POPC LUVs, the increase in the intensity of the maximum at approximately 195 nm suggests that compound **23** adopts some type of β-turn or β-sheet like conformation. [10, 18] The CD spectra of compound **23** in POPC LUVs is also very different from the CD spectrum observed for this AMP in the presence of zwitterionic DPC micelles, particularly in regards to the absence of the positive maxima below 200 nm. This is expected since the CD spectrum in the

presence of POPC LUVs should include some I-state contribution while that of the spectra in DPC micelles should only consist of S-state conformations, thus, their spectra should be different.

The CD spectrum of compound **23** in the presence of anionic LUVs was different from the spectrum of the compound bound to the zwitterionic LUVs. These differences clearly indicated that this compound was adopting different conformations when interacting with the two different LUVs. The λ_{max} between 190 and 195 nm suggests that compound **23** is adopting some combination of α-helical and β-turn components in this environment.[10, 18] Therapeutically, this characteristic would allow for the design of analogs with greater selectivity for a particular membrane composition The CD spectra of this AMP in the presence of 4:1 POPC/POPG LUVs was also very different from the spectrum observed in the corresponding micelle membrane, SDS, more specifically, in the absence of the positive maxima below 200 nm. This was expected, as was the case with zwitterionic DPC and POPC, since in the presence of 4:1 POPC/POPG LUVs some contribution of the I-state will be observed in the CD spectra.

"Pseudo" CD titrations. It has been well document that the lipid to peptide ratio, L/P, plays a major role in determining pore formation. [26-28] In order to better understand the mechanism of action for this peptide, CD spectra of compound **23** were recorded at various liposome concentrations while maintaining a constant peptide concentration to determine conformational information regarding these structures. In the analysis of any data concerning a peptide binding to a liposome, it must be remembered that a large number of different possible states for the peptides are in equilibrium. These states vary from bulk solution, to surface bound, aggregating oligomers consisting of a various number of peptides and pore formation as well as any states corresponding to reverse processes.

The logic behind these experiments was to span the concentration range from low L/P ratios to high L/P ratios. When the peptide concentration is much higher than that of the liposome, a combination of peptide in bulk solution and pore forming peptides is favored, i.e. the peptide concentration is such that the resulting equilibrium of the liposome bound peptides would favor pore formation. At the other end of the liposome concentration range, high L/P, the peptide concentration would be low enough that the equilibrium would favor monomeric peptide or clusters of peptides that are too small to form pores on the surface of the liposome.

The CD spectra of compound **23** with increasing POPC concentrations is shown in **Figure 3.6**. The concentration of compound **23** was held constant at 200 μM and the POPC LUV concentration increased from 0.8 mM to 17 mM. In the presence of POPC LUVs, even at the lowest L/P ratio, dramatic changes were observed in both the shape and intensity of the CD spectra compared to the spectrum of the peptide in buffer alone. The CD spectrum of **23** in buffer exhibited a double minimum at about 210 and 220 nm, [10, 18] but upon addition of POPC LUVs this double minimum disappeared. As can be seen from the CD spectra, the shape and intensity remain relatively constant as the LUV concentration increased implying the adopted conformations and membrane interactions were not concentration dependant. As expected based on the work of Ladokhin and co-workers [19] the spectra at the higher POPC concentrations were distorted (i.e. increased noise) at the lower wavelengths, but were still very similar even at the highest POPC concentrations above 200 nm.

The similarity of the CD spectra with increasing POPC LUV concentrations suggests that all possible peptide states were in equilibrium and there was not a predominate state. This assumption is based on the dramatically different conformations observed in conformation in the presence of increasing anionic LUVs (**Figure 3.7**). Only two sets of conformers were observed,

peptide in bulk solution and the surface bound state (S-state), suggesting that for POPC LUVs, the S-state is dominant with a low probability of I-state formation. This observation is consistent with the reports by Marrink and co-workers [29] who conducted molecular dynamics simulations of magainin analog interactions with model membranes [29] indicating that the controlling factors for spontaneous pore formation was a critical peptide concentration and the propensity of the peptides to aggregate. [29] Since the CD spectra in the presence of POPC LUVs were essentially unchanged, regardless of the concentration of liposome, one can assume the conformations also remain relatively constant. This observation indicates that peptide oligomerization was not occurring on the surface of the zwitterionic LUVs as the oligomerization of peptides would result in changes in conformation.

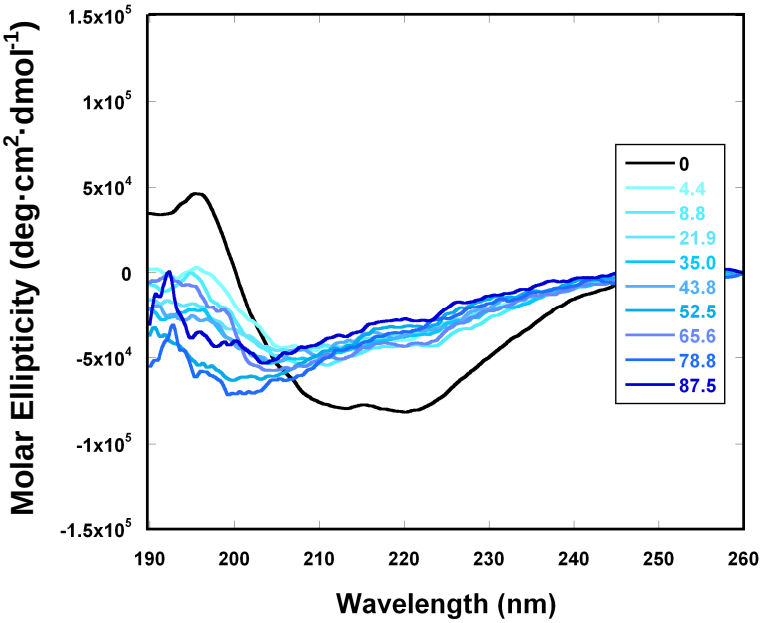

Figure 3.6: Far-UV CD spectra for separate samples of 200 µM compound **23** with increasing concentration of POPC LUVs. [30, 31] New samples were prepared at each LUV concentration in 40 mM sodium phosphate buffer; pH = 6.8. The numbers in the legend refer to the L/P ratios. Color intensity increases with liposome concentration.

Unfortunately, this did not allow for a conclusion to be made concerning the binding mechanism of compound **23** with POPC LUVs. This data suggests that there were no major changes in the peptide conformation occurring with increased POPC LUV concentration. It is impossible to characterize the exact conformations adopted by compound **23** upon binding to POPC LUVs due to the incorporation of the unnatural amino acids and the distortion below 200 nm; however, it was possible to make a few therapeutically important conclusions. One, it can be concluded that these peptides do interact with POPC LUVs in some manner because there were observable differences in the CD spectra in buffer and in the presence of POPC LUVs. Secondly, the interaction with POPC LUVs did not appear to be concentration dependant as the spectra did not change significantly with an increase in lipid concentrations.[26-28]

The introduction of 20% anionic lipids into the membrane model (4:1 POPC/POPG) resulted in large differences in the CD spectra of compound **23** compared to the CD spectrum in buffer and in the presence of varying concentrations of POPC liposomes. These differences were due solely to small changes in the electrostatic surface potential of the liposomes. This fact is highlighted by the CD data as shown in **Figure 3.4**. These representative spectra clearly show that conformers of the peptide in buffer are different from all spectra of the peptide in various 4:1 POPC/POPG LUV concentrations. The most interesting feature of this figure is the presence of three sets of spectra, indicative of three different conformational profiles.

At low L/P ratios, (**Figure 3.7** – spectra in blue) the negative molar ellipticity of the peaks at 210 and 220 nm gradually decrease toward a 'critical point' (**Figure 3.8**) which occurs at a L/P molar ratio of approximately 39:1 (**Figure 3.7** – spectrum in green). Having reached the 'critical point,' the decreasing pattern reverses and the negative intensities of both peaks gradually increase (**Figure 3.7** – spectra in red). Clearly, in the case of compound **23** interacting

with 4:1 POPC/POPG LUVs there were dramatic concentration dependant conformational changes occurring.

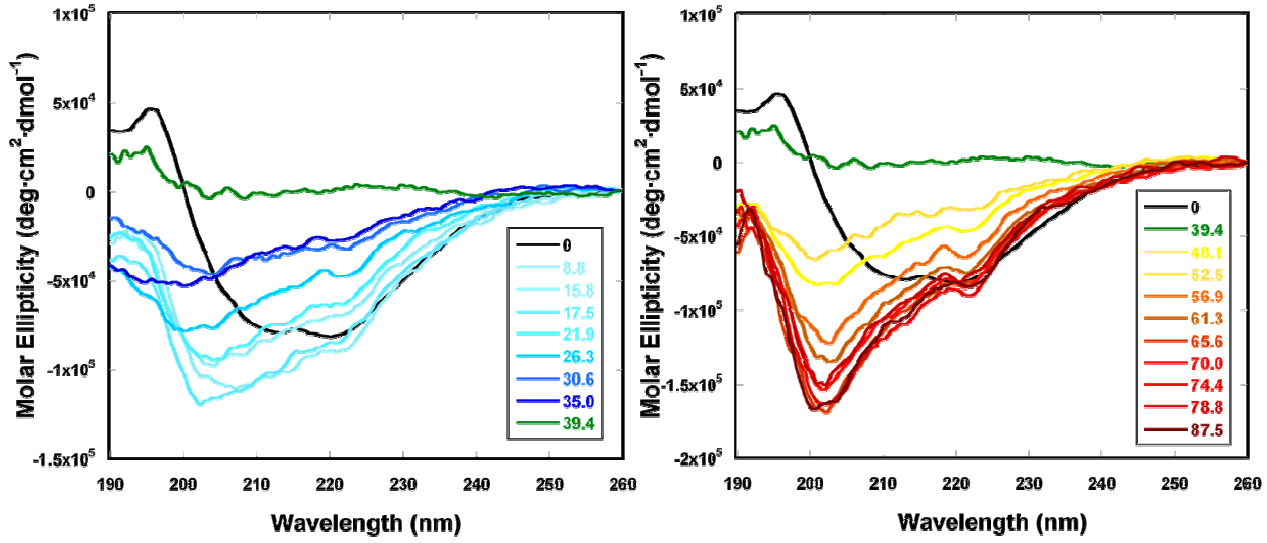

Figure 3.7: Far-UV CD spectra for separate 200 µM compound **23** samples in the presence of increasing concentrations of 4:1 POPC/POPG LUVs[30, 31] at low L/P ratios (left) and high L/P ratios (left). New samples were prepared at each liposome concentration in 40 mM sodium phosphate buffer, pH = 6.8. The numbers in the legend refer to the L/P ratios. Color intensity increases with liposome concentration.

In **Figure 3.8** the molar ellipticity intensity of the minima at 210 and 220 nm versus L/P ratios were plotted. Clearly, compound **23** interacts with 4:1 POPC/POPG LUVs in a dramatic concentration dependant manner. A maximum change in molar ellipticity occurred at a L/P ratio of approximately 39:1. With POPC LUVs, there was no concentration dependence observed in the molar ellipticity intensity of the minima at 210 and 220 nm. A similar decrease in the molar ellipticity for the antibacterial peptide PGLa with increasing lipid concentration to an end point of minimal intensity has been reported by Wieprecht and coworkers. [32] At this concentration they proposed that the peptide was completely bound to the liposome.[32] This observation is consistent with our hypothesis. Having reached the "critical point", at a L/P ratio of

approximately ~39:1, the pattern reversed and the negative intensities of both peaks gradually increased (**Figure 3.8** – right).

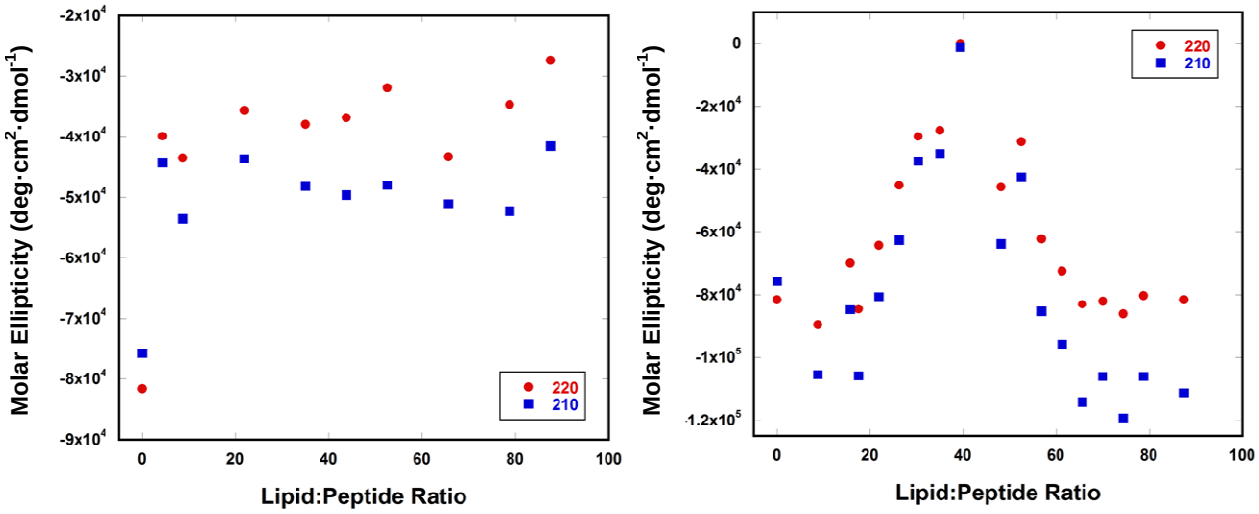

Figure 3.8: Plots of CD intensity at 210 and 220 nm versus L/P ratios for compound **23** in the presence of POPC (left) and mixed 4:1 POPC/POPG LUVs (right).

Although it was difficult to obtain quantitative data from the CD spectra due to the incorporation of unnatural amino acids, the groups of spectra may be attributed to different conformations adopted by the peptide in three different states. We postulated that at low L/P ratios, the relative concentration of peptide was such that essentially each liposome was saturated with peptide, thus the resulting spectra represents the peptide predominantly in two environments, namely solution state and the I-state. As the lipid concentration increases the free peptide concentration in bulk solution becomes negligible. This is the 'critical point' discussed earlier, which we hypothesize is predominantly I-state and this spectrum is un-ordered which is unexpected. However, previous molecular dynamics simulations [29] showed that for a magainin analog, the conformation of the peptides in the pore are not highly structured. Furthermore, Sengupta and co-workers predicted that the interaction of melittin with

dipalmitoylphosphatidylcholine bilayers resulted in disordered toroidal pores. [33] These observations are consistent with our data as we see an increase in disordered conformers close to the 'critical point'. Beyond the 'critical point,' as the lipid concentration increases further, a L/P ratio is reached such that the I-state is no longer statistically favored and various forms of the S-state dominate.

The differences in CD spectra of compound **23** in the presence of the two membrane models clearly indicate there are definitive "steps" in the mechanism of liposome binding to 4:1 POPC/POPG LUVs that are not observed for interaction with POPC liposomes. By exhibiting different interactions, these observations lead to two conclusions. One, compound **23** interacted with POPC and 4:1 POPC/POPG LUVs via different binding mechanisms suggesting some level of membrane selectivity. Secondly we can use these three individual "steps" to investigate in greater detail the overall mechanism of binding to 4:1 POPC/POPG LUVs.

ITC Studies

Full titration experiments. The use of isothermal titration calorimetry to study peptide-membrane interactions is a well documented technique. [30, 34, 35] As previously mentioned in Chapter 1, the titration of lipid into peptide would allow for the complete analysis of the thermodynamic parameters associated with the interaction, in an ideal case. These parameters include the binding constant (K_b), the enthalpy (ΔH), free energy (ΔG), the entropy (ΔS) and any heat capacity changes (c_p). [34, 36]

At the beginning of a full titration experiment, there is an excess of peptide in the cell. Small aliquots of LUVs are titrated into the cell and are saturated with peptide, removing some peptide from bulk solution. With a decrease in the peptide available for binding, the heats

involved with each injection will decrease until all of the peptide is removed from the bulk solution. Once the peptide is removed from the bulk solution, the only heat observed will be the heat of dilution. A schematic of the full titration experiment can be seen in **Figure 3.9**.

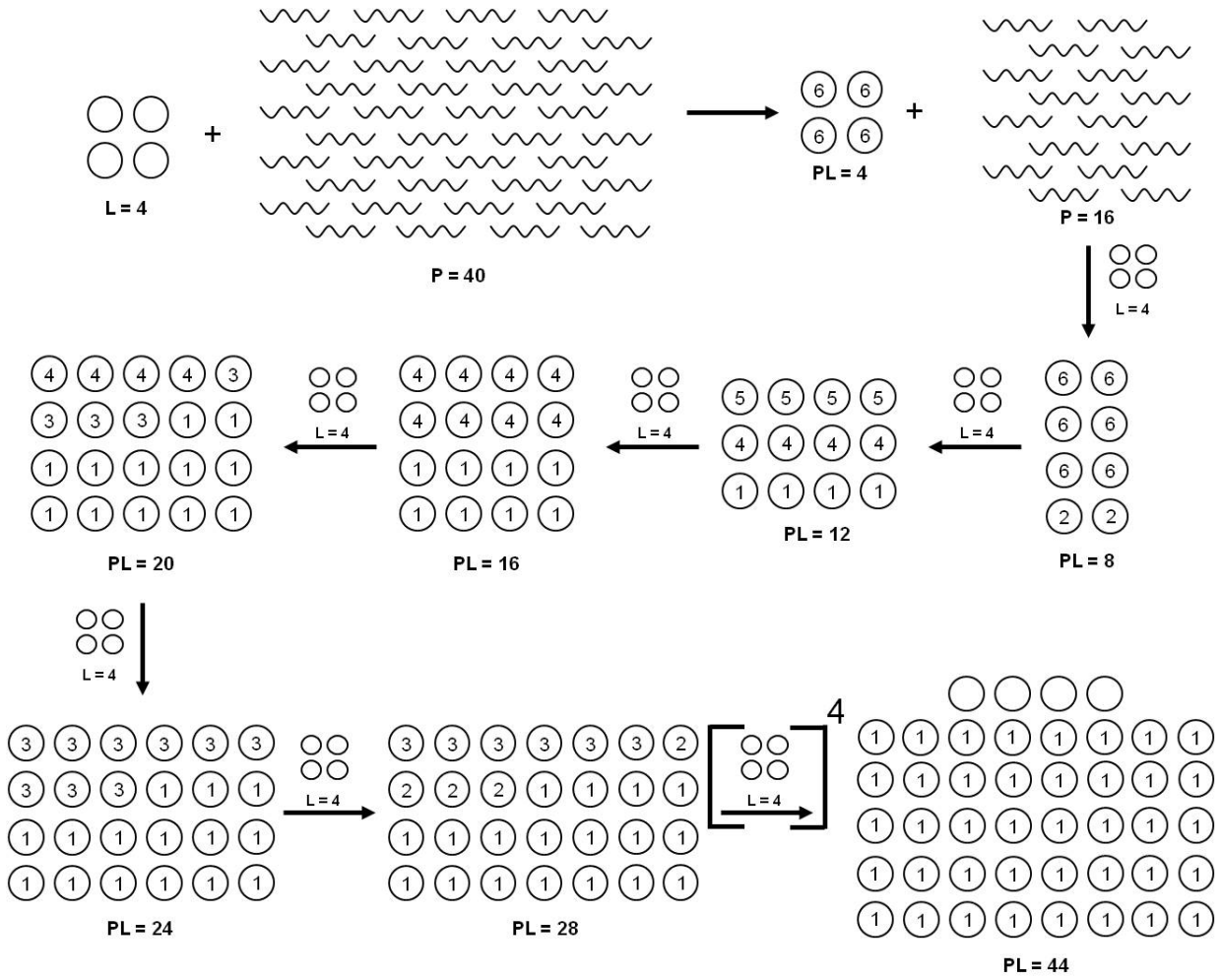

Figure 3.9: Illustrative schematic of the full titration experiment for the titration of lipid into peptide

The initial comparison of the thermograms obtained from the full titration experiment of the two different liposomes into compound **23** (over the same liposome concentration range as that used in the CD investigations) clearly revealed reproducible differences. The titration of **23** with 4:1 POPC/POPG LUVs (**Figure 3.10** – right) displayed a complex isotherm exhibiting two distinct phases. An endothermic phase was observed at low L/P ratios. This phase was followed by an exothermic component as the LUV concentration increased. Although this particular behavior is not very common it has been observed with other peptides. [24] Andrushchenko and co-workers[37] reported similar thermograms for mixed liposomes with the tryptophan-rich cathelicidin antimicrobial peptides, tritrpo4 and tritrpo6. [37] The behavior at low L/P ratios, an endothermic phase, has been attributed to processes such as pore formation, [32] peptide aggregation, [37] and changes in the phase properties of the lipids. [38] The isolated process of peptide binding to the liposome surface is thought to occur at high L/P ratios and was exhibited by the exothermic component. [39]

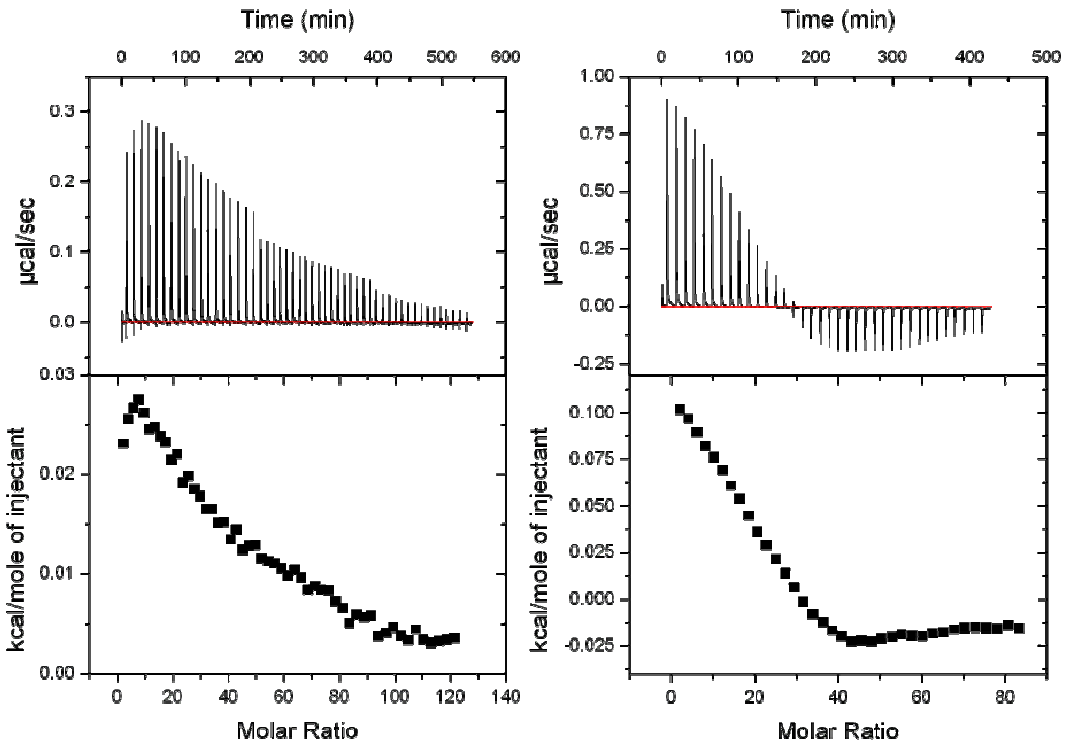

Figure 3.10: ITC data for the titration of 35 mM POPC (left) and 4:1 POPC/POPG LUVs (right) into 200 µM compound **23**.

There were also two other intriguing features of this thermogram. One was the point observed when the net heat flow is zero, in other words, where the isotherm crosses the x-axis. When the overall enthalpy of the reaction is zero, all of the contributions from the endothermic processes precisely balance out all of the contributions from the exothermic processes. Also, it is at this point in the titration that all of the free peptide is removed from bulk solution and assumed to be 100% bound. [40]

The second notable feature was the most exothermic point in the titration that occurred at a L/P ratio of ~40:1. This molar ratio corresponds to the CD spectra that bridge the two phases, which we attributed to the predominance of the I-state. It is important to note that this critical

point is absent from the thermogram and CD data for compound **23** in POPC LUVs. The exothermic heat changes associated with increasing concentrations of lipid after this point decreased until the heat of dilution was observed. This decrease in heat corresponded to the second set of spectral groupings observed in the 4:1 POPC/POPG LUVs CD studies (**Figure 3.7**) and indicated, what we believe to be, a shift of peptides from a predominantly I-state to various S-state configurations. It was because of the complexity of these competing interactions during the course of each titration that we were unable to fit our ITC data for mixed liposomes to current existing models, which would allow for the complete determination of thermodynamic parameters. [24, 37]

The titration of POPC LUVs into compound **23** (**Figure 3.10** – left) produced a relatively simple thermogram exhibiting a single endothermic phase.[413] Previous ITC studies have noted that a combination of several events can attribute to an endothermic phase. These events may include electrostatic interactions between the peptide and the membrane surface, disruption of polar head groups accompanied by the reorganization of lipids on the surface of the membrane, disruption of the solvation spheres on the surfaces of both the peptide and membrane and other less understood phenomena. [42]

A binding isotherm for compound **23** was developed as described previously in chapter 1. The plot of X_b versus c_f yielded a nonlinear binding isotherm for the binding of compound **23** to POPC LUVs (**Figure 3.11** – left**)** and did not fit the model presented by **Equation 1.3**. Because compound **23** is a positively charged peptide, electrostatic interactions should be accounted for. Therefore, the concentration of peptide at the surface of the membrane, c_m, was plotted against X_b, which yielded a linear binding isotherm (**Figure 3.11** – right) allowing for the binding constant K to be determined.[25, 39, 43] For compound **23**, ΔH^0 was determined experimentally and

the binding constant K was derived mathematically. From these two pieces of information a complete set of thermodynamic data was calculated for compound **23** using the **Equations 1.1** and **1.2**, previously discussed. The results for the thermodynamic analysis of compound **23** with POPC LUVs are given in **Table 3.3**.

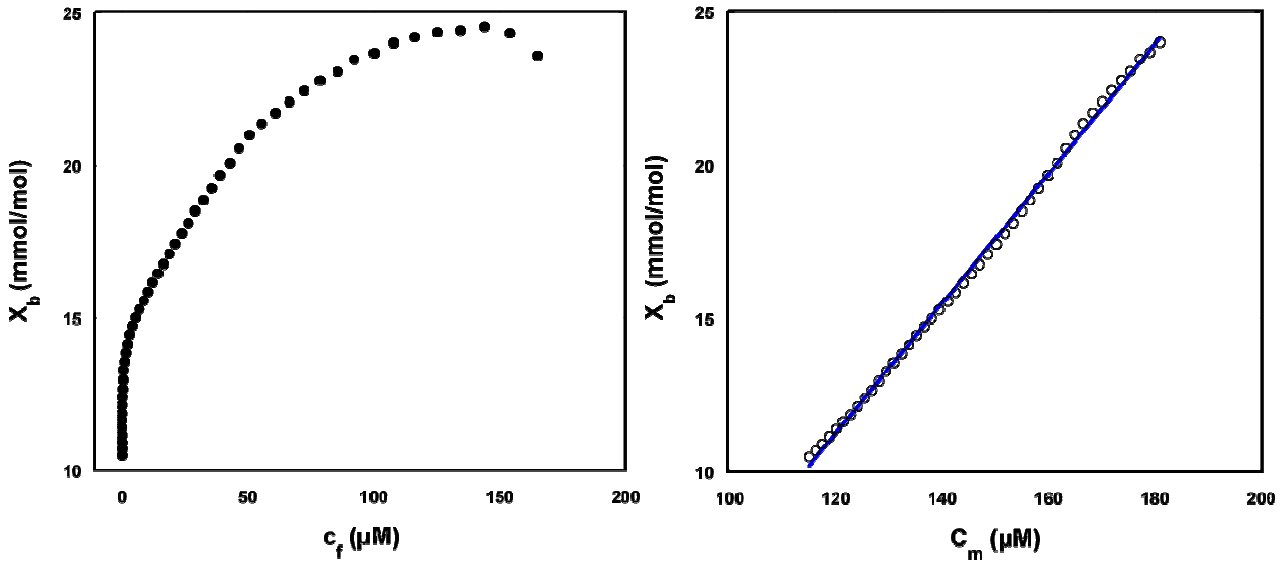

Figure 3.11: The degree of binding, X_b, of Compound **23** plotted against the concentration of free peptide in bulk solution, c_f, (left) and near the surface of the membrane, c_m (right).

The results for the thermodynamic analysis of compound **23** in the presence of POPC LUVs suggest a weak interaction. Although the ΔG and ΔS values were favorable, the ΔH and binding constant were not. The low value of the binding constant as compared to M2a suggests minimal binding. From a therapeutic standpoint, this is a very desirable quality.

Table 3.3: Thermodynamic data for a representative titration of 35 mM POPC into compound **23** at 25°C as derived from the equations discussed previously.

Compound	$\Delta H^{0,a}$ (kcal/mol)	K^b (M^{-1})	ΔG^c (kcal/mol)	ΔS^d (cal/mol·K)
23	0.7	211.0	-5.5	20.8
M2a[e]	-15.9	2000.0	-7.0	-29.4

[a] ΔH^0 values are directly measured binding enthalpies and calculated using **Equation 1.4**.
[b] Binding constants were generated from the lipid-into-peptide titrations using the model as described in the text.
[c] Free energies were calculated using **Equation 1.1**.
[d] Entropy was calculated using **Equation 1.2**.
[e] Thermodynamic parameters for Magainin analogue M2a as presented by Wieprecht et. al.[41]

Single injection experiments. The membrane selectivity between the different membrane models of compound **23** were further highlighted by the single injection ITC experiments, the titration of dilute samples of peptide into excess lipid and vice versa.[25, 44-46] By titrating relatively low concentrations of peptide into excess LUVs, we are able to determine the enthalpy of binding.[39, 44-46] At the beginning of this experiment, the reaction cell is filled with a large amount of liposome and a dilute sample of peptide is titrated into the cell resulting in high L/P ratios. Due to the excess liposomes under these conditions, the surface state, or S-state, predominates and it is assumed that all of the peptide binds to the liposome after each injection, leaving only peptide-free and bound lipid. These injections thus produce identical heats which are averaged to provide the ΔH for binding. A schematic of the single injection experiment for the titration of peptide into lipid is given below in **Figure 3.12**.

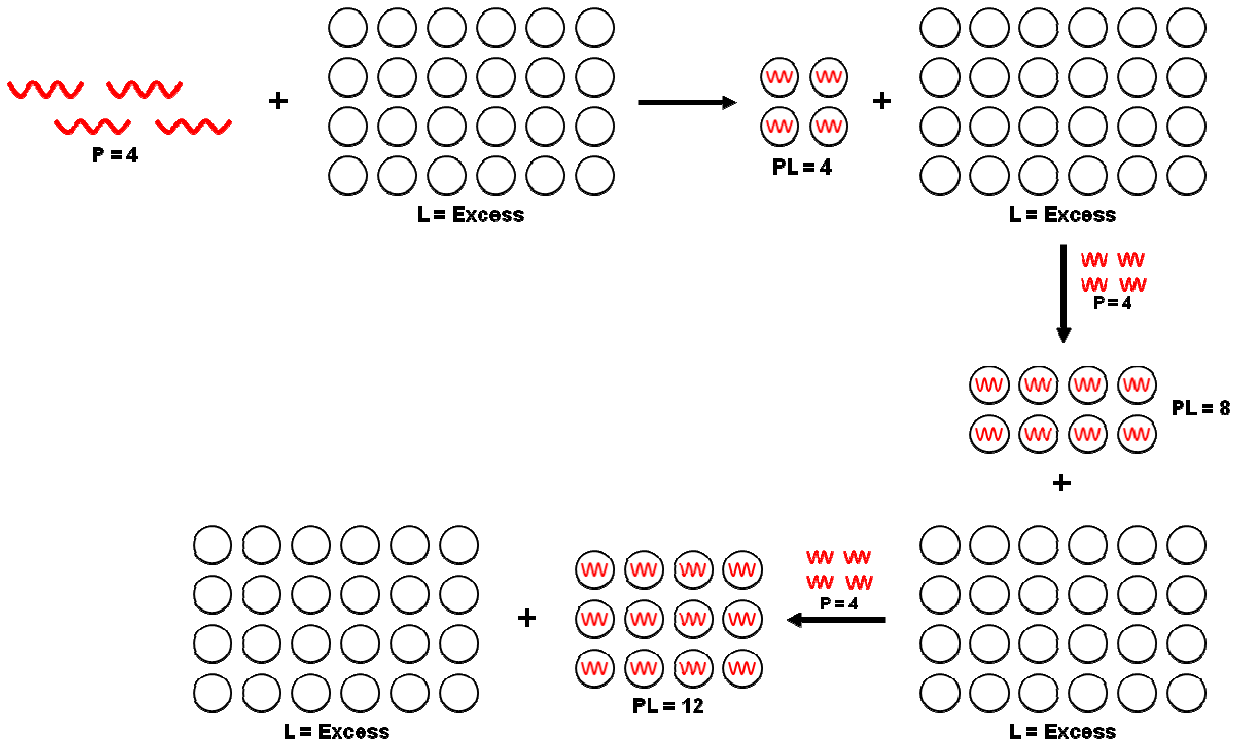

Figure 3.12: Schematic illustration of single injection experiments associated with the titration of dilute peptide solutions into excess liposome to determine the ΔH of binding.

The binding enthalpy obtained for the titration of compound **23** into POPC LUVs was +2.13 kcal/mol (**Figure 3.13** – left) and enthalpically disfavored. This was in contrast to the -1.02 kcal/mol obtained for the titration of the peptide into the 4:1 POPC/POPG LUVs (**Figure 3.13** – right) which indicated an enthalpically favored event. There are several possible factors that could contribute to the observed enthalpies of binding to both POPC and 4:1 POPC/POPG LUVs. These factors may include attractive and repulsive electrostatic interactions, conformational changes of the peptide, changes in Van der Waals contacts due to dehydration of both the peptide and membrane surfaces and the disruption of polar head groups on the surface of the liposome.[37, 39, 42] The major difference between the two membrane systems was the introduction of a greater negative charge on the surface of the mixed liposomes. The net charge

of compound **23** is highly positive (+6). We believe that the attractive electrostatic forces between the positive charges of the peptide and the negative charges of the 4:1 POPC/POPG LUVs contributed favorably to a net enthalpy of -1.02 kcal/mol.

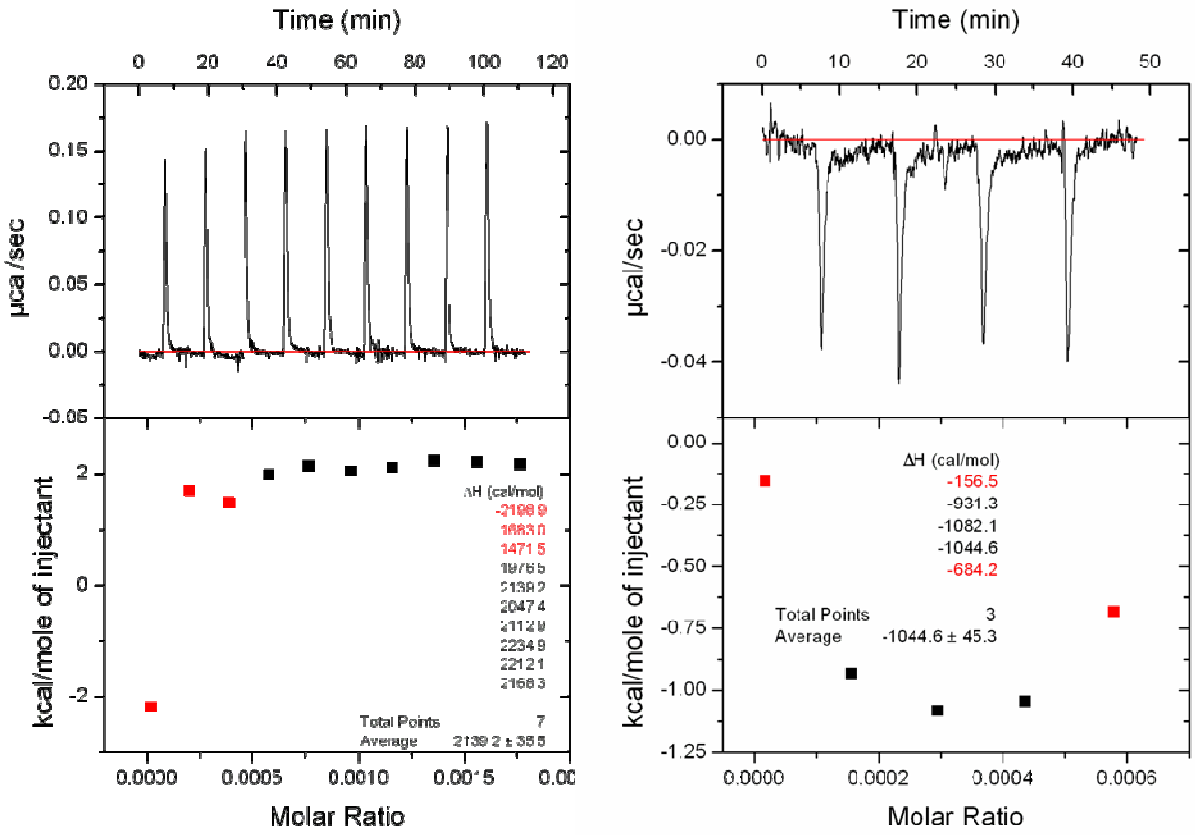

Figure 3.13: Single injection ITC data for the titration of 200 µM compound **23** into 15 mM POPC LUVs (left) and 15 mM 4:1 POPC/POPG LUVs (right). The data in red were discarded.

Reversing the direction of the single injection experiments for binding, and titrating dilute samples of LUVs (10 - 20 mM) into excess peptide (300 - 400 µM), allowed for the isolation of the heat associated with any membrane disrupting processes that may be taking place at low L/P ratios. [47] Only a few unbound liposomes were titrated into the cell at a time, thus,

becoming saturated with peptides which would exist predominantly in bulk solution and in the I-state. Each injection of liposomes would produce essentially identical heats which were averaged to provide the ΔH of the membrane disrupting processes associated with 4:1 POPC/POPG and POPC LUVs. An illustrative schematic of the single injection titration of dilute solutions of liposomes into excess peptides is given below in **Figure 3.14.**

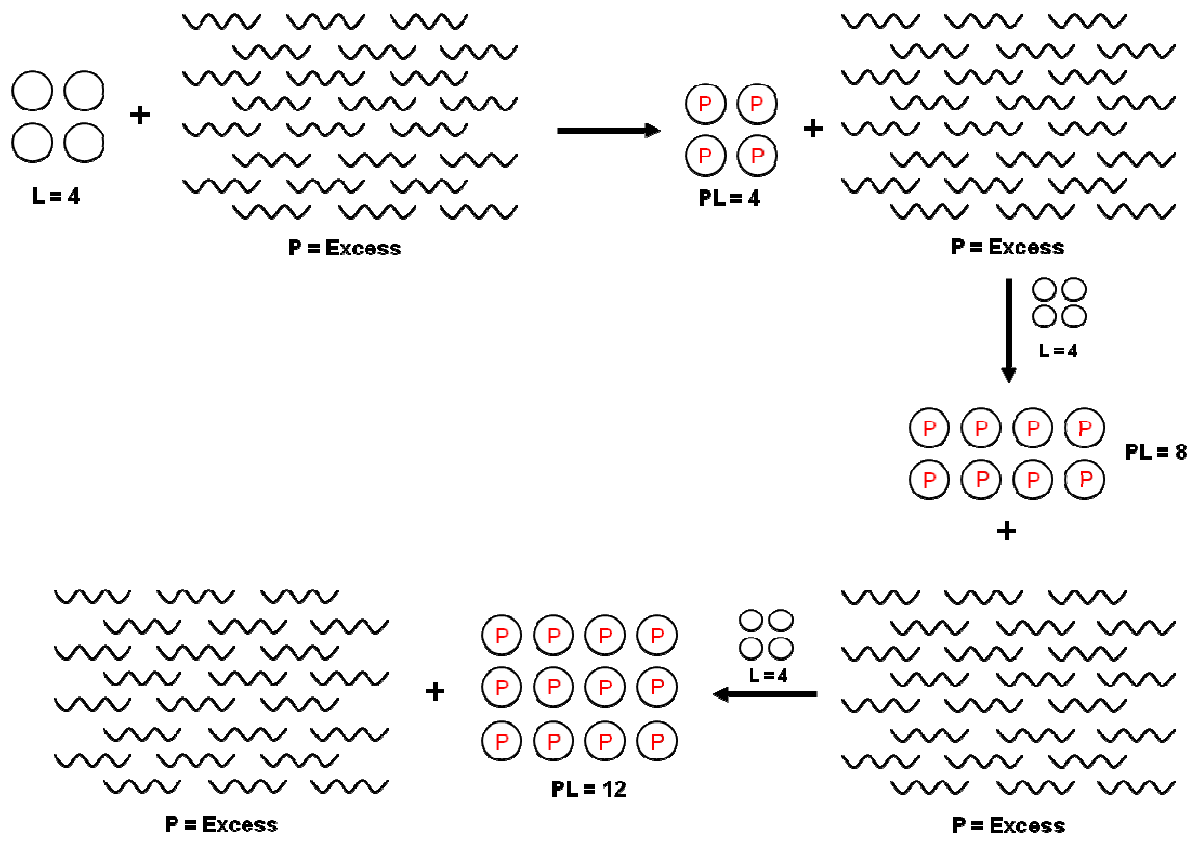

Figure 3.14: Illustrative **s**chematic of single injection experiments associated with the titration of dilute LUV solutions into excess peptide to determine the ΔH of membrane disrupting processes.

Single injection experiments to determine the ΔH values associated with membrane disruption for compound **23** in the presence of POPC (left) and 4:1 POPC/POPG LUVs is given in **Figure 3.15**. The enthalpy obtained for titration of POPC (left) into compound **23** was +0.042

kcal/mol and three times less than the +0.143 kcal/mol obtained for the 4:1 POPC/POPG LUVs (right). This series of single injection experiments involved several possible processes including binding, peptide conformational changes and aggregation, followed by possible pore formation. Our studies indicated that for compound **23** in both types of LUV models, the sum of these processes was endothermic and enthalpically disfavored. We attributed the larger endothermic enthalpy observed for the 4:1 POPC/POPG LUV to pore formation which is a highly endothermic process [39] and absent in the zwitterionic LUVs. All of the single injection data is summarized in **Table 3.4**.

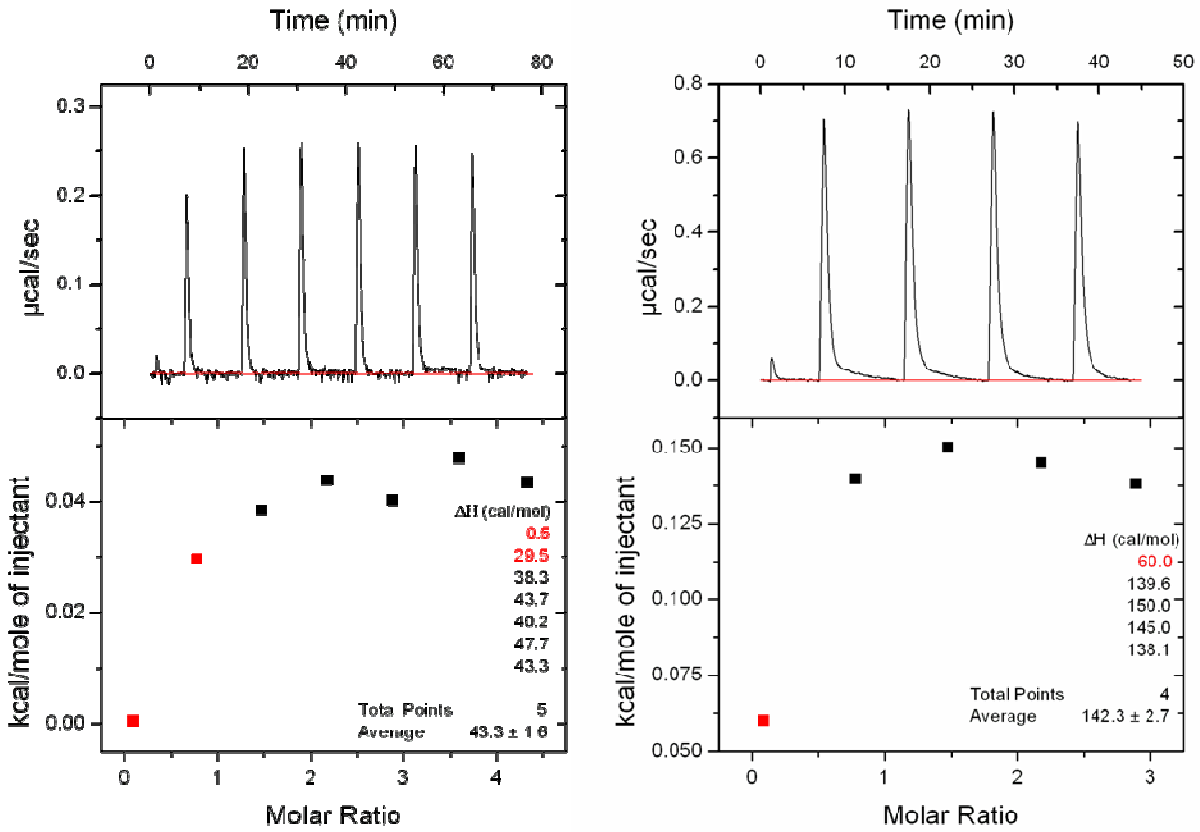

Figure 3.15: Single injection ITC data for the titration of 20 mM POPC (left) and 20 mM 4:1 POPC/POPG LUVs (right) into 300 µM compound **23**. The data in red was discarded.

Table 3.4: ΔH (kcal/mol) values for the binding and membrane disruption of 4:1 POPC/POPG and POPC LUVs as determined by single injection ITC experiments.

Compound	Compound into 4:1 POPC/POPG	4:1 POPC/POPG into Compound	Compound into POPC	POPC into Compound
23	-1.0 ± .04	0.14 ± .03	2.1 ± .04	0.04 ± 0

The ITC data further supports the hypothesis that there were two different mechanisms of interaction for POPC and 4:1 POPC/POPG LUVs. This is consistent with the observed selectivity of compound **23** for bacterial cells versus mammalian red blood cells determined previously through in vitro testing. [1]

Calcein Leakage Studies

It has been documented that compound **23** exhibits low micromolar antibacterial activity as well as activity against human red blood cells. [1] Peptide-induced calcein leakage monitored through fluorescence is well documented as a technique for probing AMP activity [37, 48] Leakage studies were conducted to evaluate the potential for compound **23** to induce leakage or form pores in POPC or 4:1 POPC/POPG LUVs.[49, 50] The data obtained from the fluorescence experiments of compound **23** and POPC LUVs (**Figure 3.16** – left) supports our earlier statement that the mechanism of interaction is not concentration dependant, as it can be observed that the calcein leakage from POPC LUVs is relatively low and appears to be insensitive to peptide concentration. The most likely cause of calcein leakage in the case of POPC LUVs is the rearrangement of the membrane lipids and polar head groups due to peptide binding and not pore formation, consequently resulting in the thinning of the surface of the membrane. [41 51]

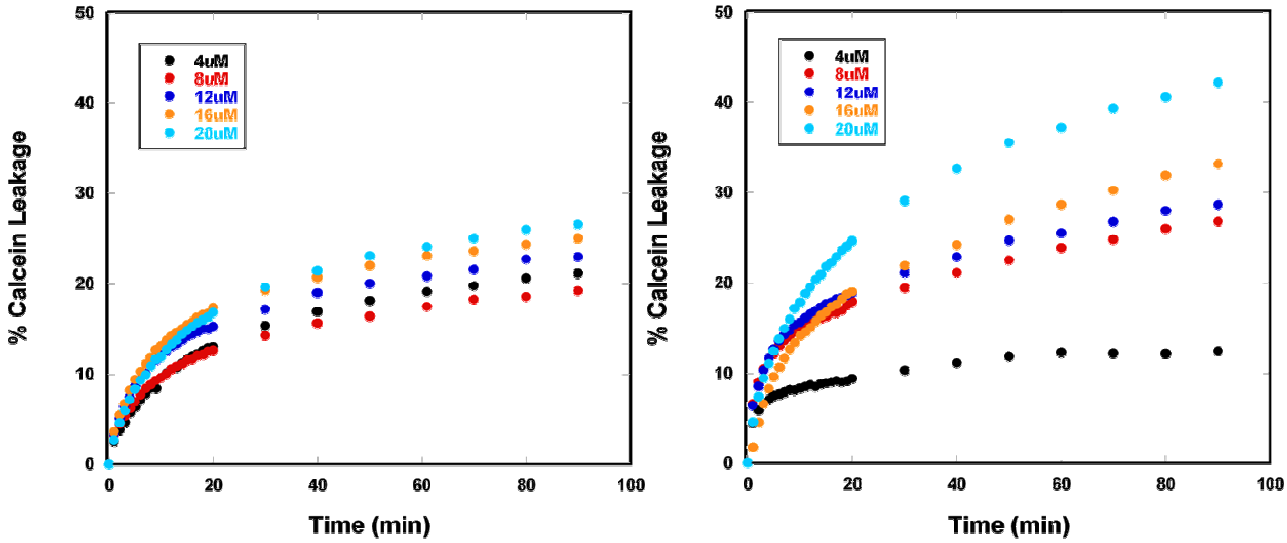

Figure 3.16: The time-dependent release of calcein from POPC (left) and 4:1 POPC/POPG (right) LUVs by increasing concentrations of compound **23** as measured by fluorescence.[52-54]

For 4:1 POPC/POPG LUVs, however, the magnitude of calcein leakage measured via fluorescence was much higher than that observed for POPC LUVs. Furthermore the induced calcein leakage for 4:1 POPC/POPG LUVs also appeared to be directly correlated with peptide concentration (**Figure 3.16** – right), as the peptide concentration increases so did the leakage. This concentration dependence may be explained in terms of a pore forming mechanism. The difference in concentration dependencies of compound **23** for the zwitterionic and anionic LUVs is highlighted when the maximum amount of leakage induced is plotted against the peptide concentration (**Figure 3.17**). As can be seen in the figure, the slope of the plot for POPC LUVs remains relatively constant while that of 4:1 POPC/POPG LUVs increases with increasing peptide concentration.

The increase of calcein leakage as the peptide concentration increases coupled with the leveling off of fluorescence over time suggests the formation of a transient pore as observed in earlier studies involving dynorphins and magainin. [51, 55, 56] This type of behavior is best explained

by the formation of transient pores during the initial bilayer insertion step, which then undergo a nucleation step followed by 'transient re-stabilization' of the lipid-peptide structure. [51] The net result is a leveling off of the observed leakage. [51, 57]

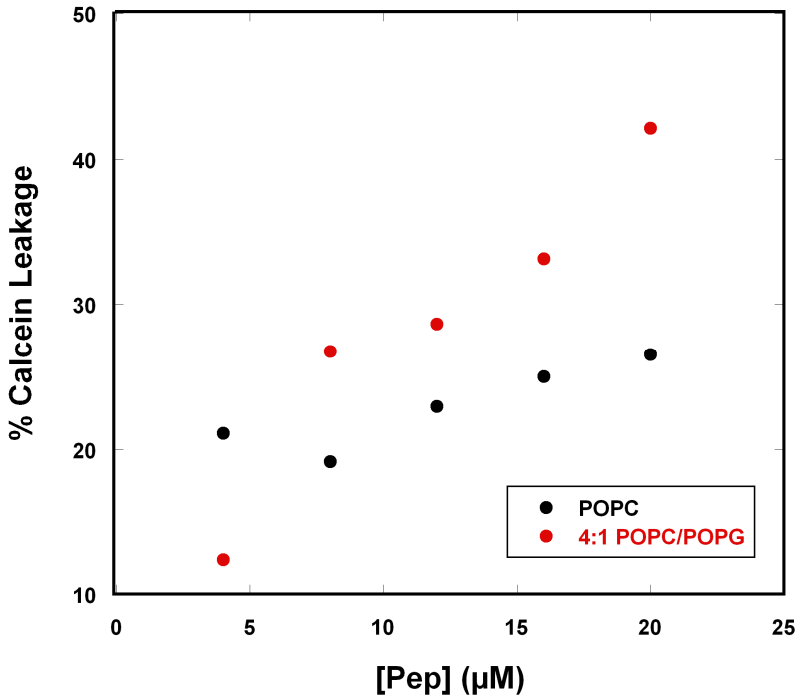

Figure 3.17: The total time-dependent release of calcein from POPC (black) and 4:1 POPC/POPG (red) LUVs by increasing concentrations of compound **23** as measured by fluorescence.

Conclusions

The conclusion that compound **23** interacted via different mechanisms with POPC and 4:1 POPC/POPG LUVs was supported by spectroscopic, thermodynamic and calcein leakage assay data. This peptide appeared to predominately interact with the surface of zwitterionic POPC LUVs (S-state), while all of the evidence supports the conclusion that a toroidal pore

mechanism dominates the interaction with 4:1 POPC/POPG LUVs (I-state). This study shows that a rational approach may be utilized to design biologically active and selective AMPs.

References

(1) Hicks, R. P.; Bhonsle, J. B.; Venugopal, D.; Koser, B. W.; Magill, A. J. De Novo Design of Selective Antibiotic Peptides by Incorporation of Unnatural Amino Acids. *J. Med. Chem.* **2007**, *50*, 3026-3036.

(2) Venugopal, D.; Klapper, D.; Srouji, A. H.; Bhonsle, J. B.; Borschel, R.; Mueller, A.; Russell, A. L.; Williams, B. C.; Hicks, R. P. Novel antimicrobial peptides that exhibit activity against select agents and other drug resistant bacteria. *Bioorg. Med. Chem.* **2010**, *18*, 5137-5147.

(3) Russell, A. L.; Kennedy, A. M.; Spuches, A. M.; Venugopal, D.; Bhonsle, J. B.; Hicks, R. P. Spectroscopic and thermodynamic evidence for antimicrobial peptide membrane selectivity. *Chem. Phys. Lipids* **2010**, *163*, 488-497.

(4) Hicks, R. P.; Mones, E.; Kim, H.; Koser, B. W.; Nichols, D. A.; Bhattacharjee, A. K. Comparison of the conformation and electrostatic surface properties of magainin peptides bound to SDS and DPC micelles: Insight into possible modes on antimicrobial activity. *Biopolymers* **2003**, *68*, 459-470.

(5) Hancock, R. E. W.; Lehrer, R. Cationic peptides: a new source of antibiotics. *Trends Biotechnol.* **1998**, *16*, 82-88.

(6) Bechinger, B. Structure and Functions of Channel-Forming Peptides: Magainins, Cecropins, Melittin and Alamethicin. *J. Membr. Biol.* **1997**, *156*, 197-211.

(7) Wimmer, R.; Andersen, K. K.; Vad, B.; Davidsen, M.; Molgaard, S.; Nesgaard, L. W.; Kristensen, H. H.; Otzen, D. E. Versatile Interactions of the Antimicrobial Peptide Novispirin with Detergents and Lipids. *Biochemistry (N. Y.)* **2006**, *45*, 481-497.

(8) Lee, D. G.; Park, Y.; Jin, I.; Hahm, K.; Lee, H.; Moon, Y.; Woo, E. Structure-antiviral activity relationships of cecropin A-magainin 2 hybrid peptide and its analogues. *Journal of Peptide Science* **2004**, *10*, 298-303.

(9) Bhonsle, J. B.; Venugopal, D.; Huddler, D. P.; Magill, A. J.; Hicks, R. P. Application of 3D-QSAR for Identification of Descriptors Defining Bioactivity of Antimicrobial Peptides. *J. Med. Chem.* **2007**, *50*, 6545-6553.

(10) Fuchs, P. F. J.; Bonvin, A. M. J. J.; Bochicchio, B.; Pepe, A.; Alix, A. J. P.; Tamburro, A. M. Kinetics and Thermodynamics of Type VIII β-Turn Formation: A CD, NMR, and Microsecond Explicit Molecular Dynamics Study of the GDNP Tetrapeptide. *Biophys. J.* **2006**, *90*, 2745-2759.

(11) Perczel, A.; Fasman, G. D. Quantitative analysis of cyclic beta-turn models. *Protein Sci.* **1992**, *1*, 378-395.

(12) Turner, J.; Cho, Y.; Dinh, N. N.; Waring, A. J.; Lehrer, R. I. Activities of LL-37, a cathelin-associated antimicrobial peptide of human neutrophils. *Antimicrob. Agents Chemother.* **1998**, *42*, 2206-2214.

(13) Kyle, D. J.; Blake, P. R.; Smithwick, D.; Green, L. M.; Martin, J. A.; Sinsko, J. A.; Summers, M. F. NMR and computational evidence that high-affinity bradykinin receptor antagonists adopt C-terminal beta-turns. *J. Med. Chem.* **1993**, *36*, 1450-1460.

(14) Sonnichsen, F. D.; Van Eyk, J. E.; Hodges, R. S.; Sykes, B. D. Effect of trifluoroethanol on protein secondary structure: an NMR and CD study using a synthetic actin peptide. *Biochemistry (N. Y.)* **1992**, *31*, 8790-8798.

(15) Haney, E. F.; Hunter, H. N.; Matsuzaki, K.; Vogel, H. J. Solution NMR studies of amphibian antimicrobial peptides: Linking structure to function? *Biochimica et Biophysica Acta (BBA) - Biomembranes* **2009**, *1788*, 1639-1655.

(16) Ng, D. P.; Deber, C. M. Deletion of a terminal residue disrupts oligomerization of a transmembrane alpha-helix. *Biochem. Cell Biol.* **2010**, *88*, 339-345.

(17) Luidens, M. K.; Figge, J.; Breese, K.; Vajda, S. Predicted and trifluoroethanol-induced alpha-helicity of polypeptides. *Biopolymers* **1996**, *39*, 367-376.

(18) Ladokhin, A. S.; Selsted, M. E.; White, S. H. CD Spectra of Indolicidin Antimicrobial Peptides Suggest Turns, Not Polyproline Helix. *Biochemistry* **1999**, *38*, 12313-12319.

(19) Ladokhin, A. S.; Fernandez-Vidal, M.; White, S. H. CD spectroscopy of peptides and proteins bound to large unilamellar vesicles. *J. Membr. Biol.* **2010**, *236*, 247-253.

(20) Dennison, S. R.; Wallace, J.; Harris, F.; Phoenix, D. A. Amphiphilic alpha-helical antimicrobial peptides and their structure/function relationships. *Protein Peptide Lett.* **2005**, *12*, 31-39.

(21) Toke, O. Antimicrobial peptides: New candidates in the fight against bacterial infections. *Peptide Science* **2005**, *80*, 717-735.

(22) Pouny, Y.; Rapaport, D.; Mor, A.; Nicolas, P.; Shai, Y. Interaction of antimicrobial dermaseptin and its fluorescently labeled analogs with phospholipid membranes. *Biochemistry (N. Y.)* **1992**, *31*, 12416-12423.

(23) Blondelle, S. E.; Lohner, K.; Aguilar, M. Lipid-induced conformation and lipid-binding properties of cytolytic and antimicrobial peptides: determination and biological specificity. *Biochimica et Biophysica Acta (BBA) - Biomembranes* **1999**, *1462*, 89-108.

(24) Jelokhani-Niaraki, M.; Hodges, R. S.; Meissner, J. E.; Hassenstein, U. E.; Wheaton, L. Interaction of Gramicidin S and its Aromatic Amino-Acid Analog with Phospholipid Membranes. *Biophys. J.* **2008**, *95*, 3306-3321.

(25) Wenk, M. R.; Seelig, J. Magainin 2 Amide Interaction with Lipid Membranes: Calorimetric Detection of Peptide Binding and Pore Formation. *Biochemistry (N. Y.)* **1998**, *37*, 3909-3916.

(26) Chen, F. Y.; Lee, M. T.; Huang, H. W. Evidence for membrane thinning effect as the mechanism for peptide-induced pore formation. *Biophys. J.* **2003**, *84*, 3751-3758.

(27) Almeida, P. F.; Pokorny, A. Mechanisms of Antimicrobial, Cytolytic, and Cell-Penetrating Peptides: From Kinetics to Thermodynamics. *Biochemistry (N. Y.)* **2009**, *48*, 8083-8093.

(28) Lee, M. T.; Hung, W. C.; Chen, F. Y.; Huang, H. W. Mechanism and kinetics of pore formation in membranes by water-soluble amphipathic peptides. *Proc. Natl. Acad. Sci. U. S. A.* **2008**, *105*, 5087-5092.

(29) Leontiadou, H.; Mark, A. E.; Marrink, S. J. Antimicrobial Peptides in Action. *J. Am. Chem. Soc.* **2006**, *128*, 12156-12161.

(30) Hunter, H. N.; Jing, W.; Schibli, D. J.; Trinh, T.; Park, I. Y.; Kim, S. C.; Vogel, H. J. The interactions of antimicrobial peptides derived from lysozyme with model membrane systems. *Biochimica et Biophysica Acta (BBA) - Biomembranes* **2005**, *1668*, 175-189.

(31) Wen, S.; Majerowicz, M.; Waring, A.; Bringezu, F. Dicynthaurin (ala) Monomer Interaction with Phospholipid Bilayers Studied by Fluorescence Leakage and Isothermal Titration Calorimetry. *The Journal of Physical Chemistry B* **2007**, *111*, 6280-6287.

(32) Wieprecht, T.; Apostolov, O.; Beyermann, M.; Seelig, J. Membrane Binding and Pore Formation of the Antibacterial Peptide PGLa: Thermodynamic and Mechanistic Aspects. *Biochemistry (N. Y.)* **2000**, *39*, 442-452.

(33) Sengupta, D.; Leontiadou, H.; Mark, A. E.; Marrink, S. Toroidal pores formed by antimicrobial peptides show significant disorder. *Biochimica et Biophysica Acta (BBA) - Biomembranes* **2008**, *1778*, 2308-2317.

(34) Wieprecht, T.; Seelig, J. Isothermal Titration Calorimetry for Studying Interactions between Peptides and Lipid Membranes. *Current Topics in Membranes* **2002**, *52*, 31-55.

(35) Jing, W.; Hunter, H. N.; Hagel, J.; vogel, H. J. The structure of the antimicrobial peptide Ac-RRWWRF-NH2 bound to micelles and its interacitons with phospholipid bilayers. *Journal of Peptide Research* **2003**, *61*, 219-229.

(36) Thomas, C. J.; Surolia, N.; Surolia, A. Kinetic and thermodynamic analysis of the interactions of 23-residue peptides with endotoxin. *Biological Chemistry* **2001**, *276*, 35701-35706.

(37) Andrushchenko, V. V.; Aarabi, M. H.; Nguyen, L. T.; Prenner, E. J.; Vogel, H. J. Thermodynamics of the interactions of tryptophan-rich cathelicidin antimicrobial peptides with model and natural membranes. *Biochimica et Biophysica Acta (BBA) - Biomembranes* **2008**, *1778*, 1004-1014.

(38) Epand, R. M.; Segrest, J. P.; Anantharamaiah, G. M. Thermodynamics of the binding of human apolipoprotein A-I to dimyristoylphosphatidylglycerol. *J. Biol. Chem.* **1990**, *265*, 20829-20832.

(39) Seelig, J. Titration calorimetry of lipid-peptide interactions. *Biochim. Biophys. Acta* **1997**, *1331*, 103-116.

(40) Abraham, T.; Lewis, R. N. A. H.; Hodges, R. S.; McElhaney, R. N. Isothermal Titration Calorimetry Studies of the Binding of the Antimicrobial Peptide Gramicidin S to Phospholipid Bilayer Membranes. *Biochemistry (N. Y.)* **2005**, *44*, 11279-11285.

(41) Wieprecht, T.; Apostolov, O.; Seelig, J. Binding of the antibacterial peptide magainin 2 amide to small and large unilamellar vesicles. *Biophys. Chem.* **2000**, *85*, 187-198.

(42) Abraham, T.; Lewis, R. N. A. H.; Hodges, R. S.; McElhaney, R. N. Isothermal Titration Calorimetry Studies of the Binding of a Rationally Designed Analogue of the Antimicrobial Peptide Gramicidin S to Phospholipid Bilayer Membranes. *Biochemistry (N. Y.)* **2005**, *44*, 2103-2112.

(43) Wieprecht, T.; Beyermann, M.; Seelig, J. Binding of Antibacterial Magainin Peptides to Electrically Neutral Membranes: Thermodynamics and Structure. *Biochemistry (N. Y.)* **1999**, *38*, 10377-10387.

(44) Bastos, M.; Bai, G.; Gomes, P.; Andreu, D.; Goormaghtigh, E.; Prieto, M. Energetics and Partition of Two Cecropin-Melittin Hybrid Peptides to Model Membranes of Different Composition. *Biophys. J.* **2008**, *94*, 2128-2141.

(45) Nomura, K.; Corzo, G. The effect of binding of spider-derived antimicrobial peptides, oxyopinins, on lipid membranes. *Biochimica et Biophysica Acta (BBA) - Biomembranes* **2006**, *1758*, 1475-1482.

(46) Wieprecht, T.; Beyermann, M.; Seelig, J. Thermodynamics of the coil–α-helix transition of amphipathic peptides in a membrane environment: the role of vesicle curvature. *Biophys. Chem.* **2002**, *96*, 191-201.

(47) Evans, R. W.; Williams, M. A.; Tinoco, J. Surface areas of 1-palmitoyl phosphatidylcholines and their interactions with cholesterol. *Biochem. J.* **1987**, *245*, 455-462.

(48) Medina, M. L.; Bolender, J. P.; Plesniak, L. A.; Chapman, B. S. Transient vesicle leakage initiated by a synthetic apoptotic peptide derived from the death domain of neurotrophin receptor, p75NTR. *Journal of Peptide Research* **2002**, *59*, 149-158.

(49) Mingeot-Leclercq, M. P.; Gallet, X.; Flore, C.; Van Bambeke, F.; Peuvot, J.; Brasseur, R. Experimental and conformational analyses of interactions between butenafine and lipids. *Antimicrob. Agents Chemother.* **2001**, *45*, 3347-3354.

(50) Sobko, A. A.; Kotova, E. A.; Antonenko, Y. N.; Zakharov, S. D.; Cramer, W. A. Effect of lipids with different spontaneous curvature on the channel activity of colicin E1: evidence in favor of a toroidal pore. *FEBS Lett.* **2004**, *576*, 205-210.

(51) Hugonin, L.; Vukojević, V.; Bakalkin, G.; Gräslund, A. Membrane leakage induced by dynorphins. *FEBS Lett.* **2006**, *580*, 3201-3205.

(52) Wieprecht, T.; Dathe, M.; Schumann, M.; Krause, E.; Beyermann, M.; Bienert, M. Conformational and Functional Study of Magainin 2 in Model Membrane Environments Using the New Approach of Systematic Double-D-Amino Acid Replacement. *Biochemisty* **1996**, *35*, 10844-10853.

(53) Wei, S.; Wu, J.; Kuo, Y.; Chen, H.; Yip, B.; Tzeng, S.; Cheng, J. Solution Structure of a Novel Tryptophan-Rich Peptide with Bidirectional Antimicrobial Activity. *J. Bacteriol.* **2006**, *188*, 328-334.

(54) Tamba, Y.; Yamazaki, M. Single Giant Unilamellar Vesicle Method Reveals Effect of Antimicrobial Peptide Magainin 2 on Membrane Permeability. *Biochemistry (N. Y.)* **2005**, *44*, 15823-15833.

(55) Matsuzaki, K.; Mitani, Y.; Akada, K.; Murase, O.; Yoneyama, S.; Zasloff, M.; Miyajima, K. Mechanism of Synergism between Antimicrobial Peptides Magainin 2 and PGLaâ€. *Biochemistry (N. Y.)* **1998**, *37*, 15144-15153.

(56) Benachir, T.; Lafleur, M. Study of vesicle leakage induced by melittin. *Biochimica et Biophysica Acta (BBA) - Biomembranes* **1995**, *1235*, 452-460.

(57) Arbuzova, A.; Schwarz, G. Pore-forming action of mastoparan peptides on liposomes: a quantitative analysis. *Biochimica et Biophysica Acta (BBA) - Biomembranes* **1999**, *1420*, 139-152.

CHAPTER FOUR: SPACER # 1

Introduction

Circular Dichroism, isothermal calorimetry and calcein fluorescence leakage experiments were conducted to provide insight into the mechanisms of binding for a series of antimicrobial peptides containing unnatural amino acids to zwitterionic and anionic lipids and micelles. The basic skeleton of the Tic-Oic dipeptide based AMP was previously given in **Figure 1.2** of chapter 1. Spacer #1, denoted by blue in **Figure 1.2**, defines the distance between successive Tic-Oic dipeptide units as well as the distances between the preceding Tic-Oic dipeptide units to either the following hydrophobic or positively charged residue. Spacer #1 is involved in defining the flexibility of any induced turn or helical structure.

One of the main advantages of incorporating unnatural amino acids into the peptide sequence is having the ability to maintain more control of the conformational flexibility. Incorporation of the conformationally restrained amino acids Tic and Oic in our compounds reduces the local flexibility of the peptide backbone, consequently reducing the total conformational freedom of the peptide during lipid binding. Incorporating different unnatural amino acids as Spacer #1 increases the number of methylene groups in the peptide backbone. By combining both conformationally restrained and conformationally flexible amino acids into the peptide backbone, it is possible to create regions of high and low molecular flexibility resulting in a semi-rigid peptide backbone with specific regions of hydrophobicity and charge. These modifications resulted in dramatic changes in the physicochemical surface properties within this series of AMPs on lipid binding.

The amino acid sequences for the peptides used to investigate the role played by Spacer #1 are given **Table 4.1**. Compound **23** contains the one-carbon spacer glycine with a distance of

2.46 Å between the carbonyl carbon atom and the amide nitrogen atom. Compound **36** contains a two carbon spacer, β-alanine, with average distance of 2.94 Å. Gaba in compound **29** is a three carbon spacer with average distance 4.68 Å and compound **37** contains the five carbon spacer, Ahx, with the longest average distance of 6.91 Å. The average distances were calculated using ChemDraw 3D version 10.0

Table 4.1: Amino acid sequences of the peptides used to study the role played by Spacer #1.[1]

Compound	Amino Acid Sequence
23	Ac-**G**F-Tic-Oic-**G**K-Tic-Oic-**G**F-Tic-Oic-**G**K-Tic-KKKK-$CONH_2$
29	Ac-**Gaba**-F-Tic-Oic-**Gaba**-K-Tic-Oic-**Gaba**-F-Tic-Oic-**Gaba**-K-Tic-KKKK-$CONH_2$
36	Ac-**βAla**-F-Tic-Oic-**βAla**-K-Tic-Oic-**βAla**-F-Tic-Oic-**βAla**-K-Tic-KKKK-$CONH_2$
37	Ac-**Ahx**-F-Tic-Oic-**Ahx**-K-Tic-Oic-**Ahx**-F-Tic-Oic-**Ahx**-K-Tic-KKKK-$CONH_2$

These modifications to Spacer #1 have shown to play a role in bacteria strain selectivity and potency. All four compounds exhibited very good *in vitro* MIC activity against *Salmonella typhimurium* (ATCC 13311), *Mycobacterium ranae* (ATCC 110), *Bacillus subtillis* (ATCC 43223), and *Bacillus anthracis* AMES. Compounds **23**, **36** and **37** exhibited very good in vitro MIC activity against *Staphylococcus aureus* ME/GM/TC resistant (ATCC 33592) while compound **29** was much less active (**Table 4.2**).[1]

However, as seen in **Table 4.3** compounds **23**, **36** and **29** exhibit much lower activity against several Gram Negative strains of bacteria except *Acinetobacter baumanii* (ATCC 19606), and *Acinetobacter baumanii* (drug resistant strain isolated at the Walter Reed Army Institute of Research).[2] Compound **37**, on the other hand, exhibited good to very good in vitro MIC activity against *Yersinia pestis*, *Brucella melitensis*, *Brucella abortus*, *Brucella suis* and *Francisella*

tularensis.[2] The observed differences in the in vitro activity of these AMPs support our hypothesis that the physicochemical surface properties presented by the AMP to the target cell can be engineered to obtain organism potency and selectivity. The most significant change that can be seen is the 2-3 fold differences in the hemolytic activity for these compounds, which implies changes in how these peptides interact with zwitterionic lipids.[1]

Table 4.2: Minimum inhibitory concentration (μM) of selected bacteria strains and hemolytic activity.[1]

Compound	***Salmonella typhimurium***	***Staphylococcus aureus* ME/GM/TC resistant**	***Mycobacterium ranae***	***Bacillus subtillis***	**% hemolysis 100/25 μM**
23	10 μM	3 μM	10 μM	1 μM	14%
36	10 μM	10 μM	1 μM	1 μM	24.4/ 7.4%
29	10 μM	100 μM	10 μM	1 μM	10.8/ 1.0%
37	10 μM	10 μM	3 μM	1 μM	44.7/ 26.6%

Table 4.3: Minimum inhibitory concentration (μM) of specific Gram negative and other drug resistant bacteria strains.[2]

Compound	23	36	29	37
Acinetobacter baumanii ATCC 19606	3.2	1.5	3.1	5.9
Acinetobacter baumanii WRAIR	3.2	6.2	3.1	2.9
Staphylococcus aureus ATCC 33591	205	200	196	187
Yersinia pestis CO92	205	200	196	23
Brucella melitensis 16M	205	200	196	95
Brucella abortus 2308	205	200	196	12
Brucella suis 23444	205	200	196	47
Bacillus anthracis AMES	12.8	25	12.5	1.5
Francisella tularensis SCHUS4	100	100	196	23.4
Burkholderia mallei	205	200	196	187
Burkholderia pseudomallei	205	200	196	187

Results and Discussion

CD Studies

CD spectroscopy is very sensitive and its use to monitor conformational changes in peptides and proteins is well documented.[3, 4] This investigation was divided into two phases. The first phase focused on surface binding (S-state) by only using SDS and DPC micelles. The second phase focused on membrane insertion (I-state) using liposomes membrane models.

The observed CD spectrum of a peptide, as previously mentioned, represents the linear combination of all of the different spectra due to conformers or states present in the sample [3, 5] including the peptide in the bulk solution, the surface bound and insertion states. Each of these states could exhibit a diversity of conformations. A change in shape and/or intensity of a CD spectrum for a peptide in the presence of micelles or liposomes implies that the peptide is adopting different conformations. This conformational change is a direct result of the different physicochemical interactions that are occurring between the AMP and the membrane model. As mentioned in chapter 2, any reference to secondary structures is used only for qualitative purposes due to the high percentage of unnatural amino acids.

CD spectra of Spacer #1 peptides in buffer and micelle environments. The CD spectra of compounds **23**, **36**, **29** and **37** in buffer are shown in **Figure 4.1**. Compound **23** exhibited a characteristic double minimum at approximately 210 and 220 nm, which is consistent with the presence of helical and β-turn conformers.[4, 6] Compounds **29**, **36**, and **37** exhibited a clear minima between 206 and 209 nm with a slight second minimum at approximately 222 nm suggesting the presence of α-helical components.[7, 8] The larger magnitude of the minima between 206 and 209 nm strongly suggests that, in buffer, these compounds also adopt a relatively high percentage of both unordered and β-turn structures[4, 9]. In addition, the maximum between 190 and 200 nm suggests a mixture of some β-sheet and α-helix.[10]

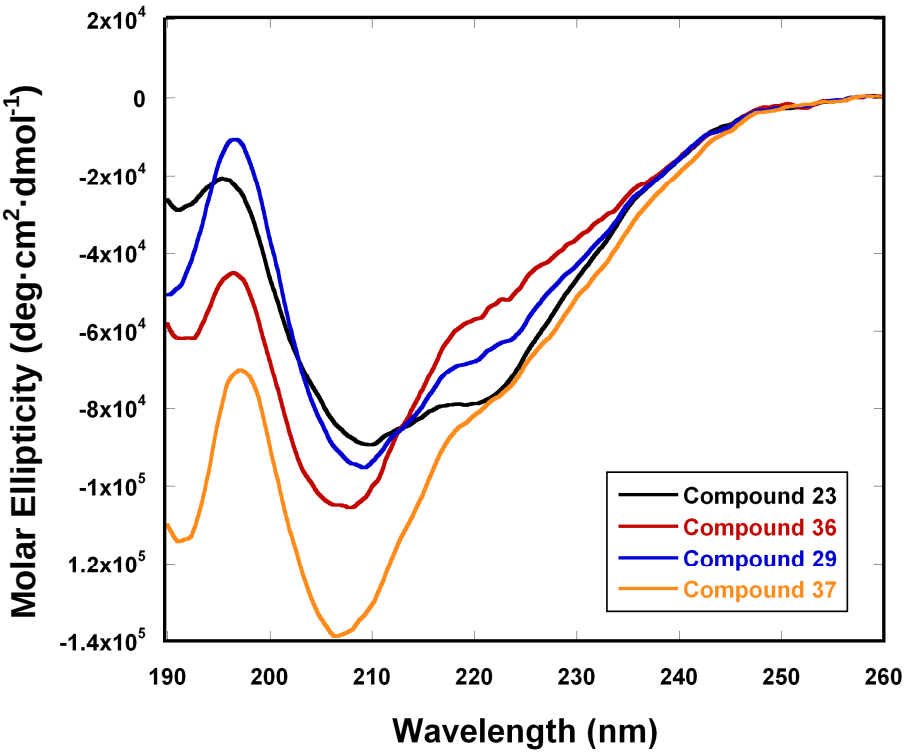

Figure 4.1: Far-UV CD spectra of compounds **23**, **36**, **29** and **37** (peptide concentration approximately 400 μM) dissolved in 40 mM phosphate buffer, pH = 6.8.

The CD spectra of these compounds in the presence of SDS micelles (**Figure 4.2** – left) showed an increase in the intensity of the λ_{max} at approximately 190 nm and the two minima at 205 and 220 nm suggesting a shift from a mixture of β-turn, α-helical and unordered features in buffer to a more dominate α-helical structure in SDS.[10, 11] The intensity of the maximum and minima decreased as the length of Spacer #1 increased indicating a reduction in α-helical components of the peptides.[4, 7, 8, 12]

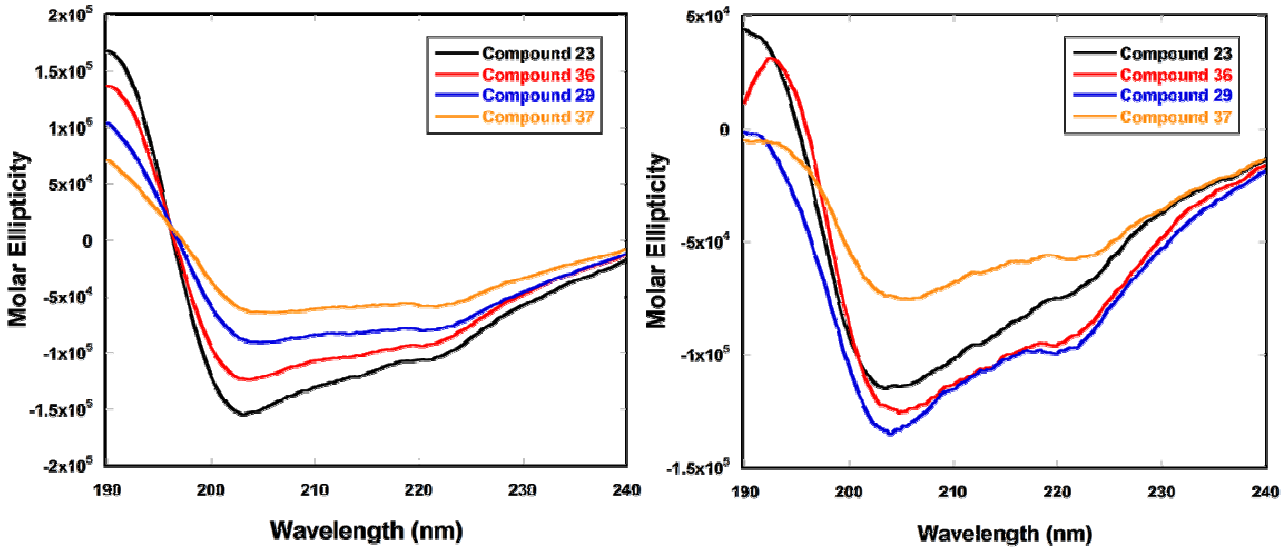

Figure 4.2: Far-UV CD spectra of compounds **23**, **36**, **29** and **37** in the presence of 80 mM SDS (left) and 80 mM DPC (right) micelles in 40 mM phosphate buffer, pH = 6.8.

The CD spectra of these compounds in the presence of DPC micelles (**Figure 4.2** – right) did not exhibit a clear trend as they did in SDS. In regards to changes in intensity, compounds **29** and **36**, with 3 and 2 carbon spacers, respectively, were very similar in intensity with the exception of the λ_{max} below 200 nm. Compound **36** exhibited a higher intensity than compound **29** below 200 nm. Compound **23** exhibited the greatest intensity below 200 nm but the least above 200 nm, with the exception of compound **37**. Although there was not a discernable trend between the intensities of the maxima below 200 nm and the spacer length, all four peptides decreased in intensity as compared to their corresponding spectra in SDS. This decrease in the intensity of the maxima below 200 nm is indicative of a reduction in the α-helical components of the peptide.[7, 8, 12] The intensity of the two minima above 200 nm varies, but unlike the case with SDS micelles, the intensity of the peaks in DPC micelles does not correlate directly with the length of the spacer. For compounds **23**, **36** and **29** the intensity of the peaks increased with

increasing spacer length. However, compound **37**, with the longest Spacer # 1 and therefore the most flexible peptide had the least intense maximum below 200 nm and the two minima above 200 nm. It is possible that this peptide is so flexible it can adopt many different conformations. There are also shifts in wavelengths when the peptides are in the DPC environment as compared to the buffer and SDS. The most significant shifts occur with the λ_{max} below 200 nm. As previously stated, the peptides consisted of mixture of β-turn and α-helical components in buffer due to the maxima at approximately 197 nm. These maxima shifted to approximately 190 – 192 nm for the four compounds suggesting an increase in the α-helical presence in DPC for all of the peptides. Also, one of the minima shifted from approximately 207 nm to approximately 202 nm in buffer and DPC, respectively. The shift to a lower wavelength for this minimum suggests a change from α-helical components to more unordered characteristics.[9] This observation coupled with the decrease in the intensity supports the conclusion that there was a decrease in the α-helical character of these peptides as compared to the buffer.[7, 8, 12] The observed differences in the shape and intensity of the CD spectra clearly indicated that the S-state bound conformations of these peptides in the presence of SDS and DPC micelles were, as expected, very different. However, the CD spectrum of each peptide in the same environment was similar in shape. The only notable difference within each series was the overall intensity of the individual spectrum indicating that the AMPs adopt similar binding conformations.

CD spectra of Spacer #1 peptides in LUV environments. The CD spectra of compounds **23**, **36**, **29** and **37** in the presence of 1.75 mM POPC liposomes are given in **Figure 4.3** (left) with their corresponding HT values (right). A LUV concentration of 1.75 mM does not produce an absorbance above 1.5 AU as discussed in Chapter 2 and 3. As such, the distortion caused by

this LUV concentration is minimal and does not interfere with qualitative comparisons of the data.[13] The four CD spectra in POPC LUVs were very similar in shape to their corresponding spectra in buffer with minimal shifts in their maximum and minima leading to the conclusion that if they were interacting with the POPC LUVs, it was a very weak interaction as shifts in the peaks are indicators of conformational change.[14, 15] The CD spectra of these peptides did exhibit some characteristics similar to each other. For instance, compounds **36** and **37** were similar in intensity and shape. All four compounds were similar in shape above 200 nm, but varied in their intensities. In most cases, however, the intensity of the minima at approximately 208 and 222 nm increased in the presence of POPC LUVs suggesting an interaction,[12] however, these intensities cannot be correlated to the length of Spacer #1.

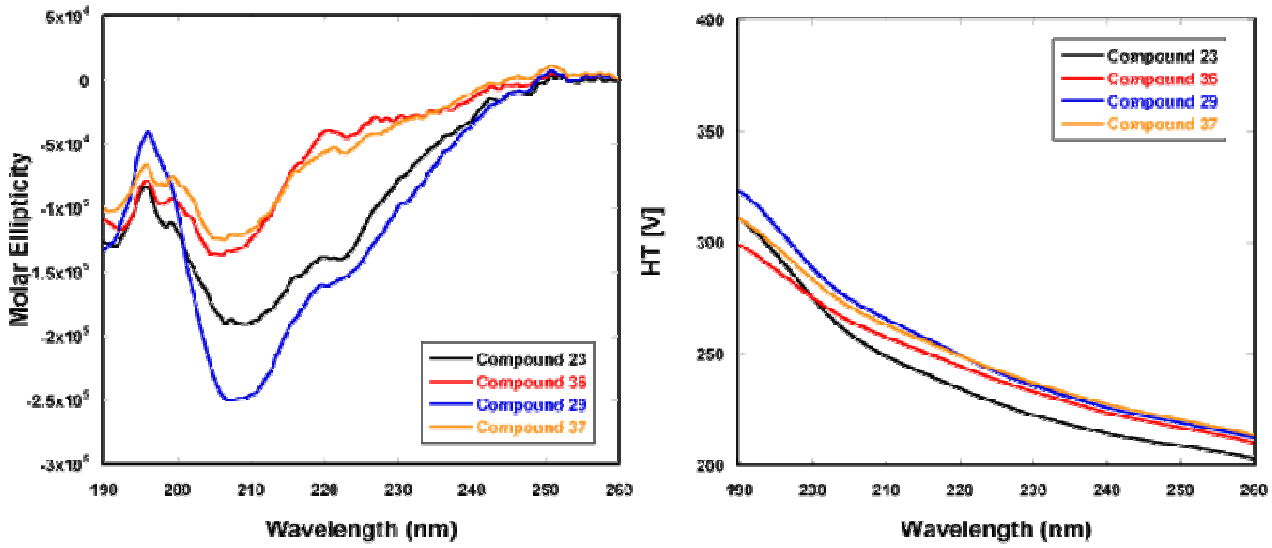

Figure 4.3: Far-UV CD spectra of 75 µM solutions of compounds **23, 36, 29** and **37** (left) in the presence of 1.75 mM POPC LUVs dissolved in 40 mM phosphate buffer (pH = 6.8) and their corresponding HT values (right).

The CD spectra of compounds **23**, **29**, **36** and **37** in the presence of 1.75 mM 4:1 POPC/POPG LUVs are given in **Figure 4.4** (left) with their corresponding HT values (right).

The CD spectrum of the compounds in this series in the presence of anionic liposomes were very different from their spectra in zwitterionic liposomes clearly indicating that these compounds adopt different conformations when interacting with the two different liposomes.[14-16] The intensity of the minima at approximately 205 nm can be correlated with the length of Spacer #1. The intensity of this peak decreases with an increase in the number of methylene groups in the spacer. Compound **23,** with no methylene groups, exhibited a greater intensity than compound **36** which contains one methylene group. Compounds **29** and **37** exhibited even less intense spectra. The overall shape and λ_{max} of the compounds were very similar to each other with the exception of compound **37**. This compound not only exhibited the weakest intensity, but had a completely different shape indicating that it adopts a different conformation than the other peptides when in the presence of 4:1 POPC/POPG LUVs.[15, 16]

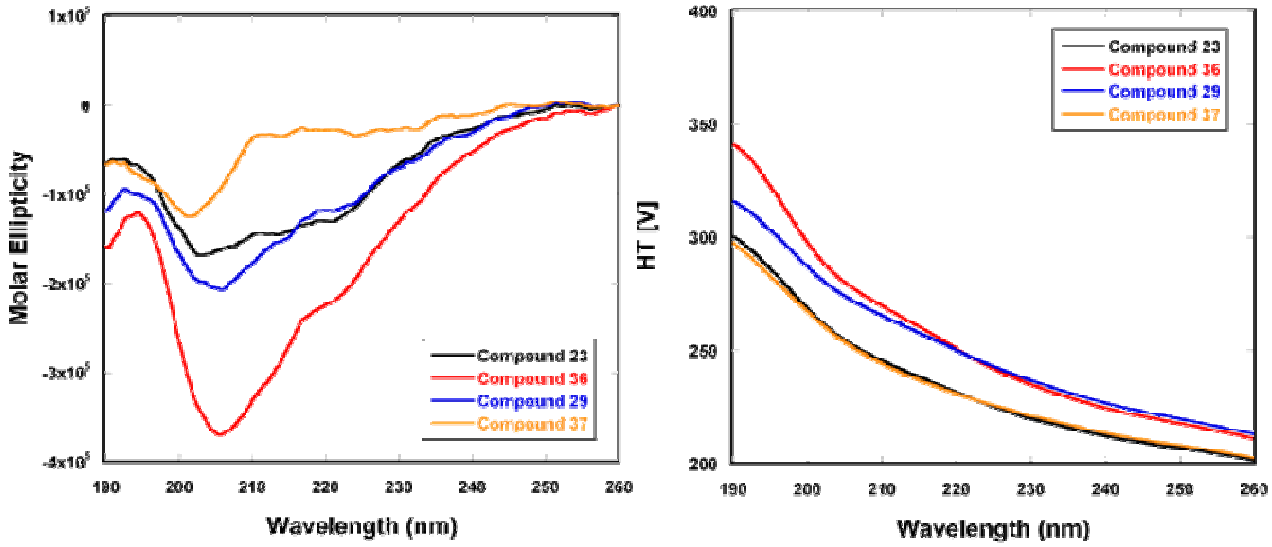

Figure 4.4: Far-UV CD spectra of 100 µM solutions of compounds **23, 36**, **29** and **37** in the presence of 1.75 mM 4:1 POPC/POPG LUVs (left) dissolved in 40 mM phosphate buffer (pH = 6.8) and their corresponding HT values (right).

The CD data for compounds **23**, **36**, **29** and **37** clearly indicated there was a difference, as expected, in the conformations observed for these peptides on interacting with zwitterionic and anionic liposomes. The changes in λ_{max} were relatively small although the changes in molar ellipticity could be large indicating a change in the degree of secondary structure present.

"Pseudo" CD Titrations. The conclusion that these AMPs interact differently with POPC and 4:1 POPC/POPG LUVs was further proven with "pseudo" titration experiments of increasing liposome concentrations as previously described. By preparing separate, but identical, samples of peptide and adding varying amounts of liposomes, we were able to observe the conformational changes associated with the transition from low L/P to high L/P ratios. As we previously reported, there was a dramatic difference in the CD behavior for compound **23** in the presence of POPC and 4:1 POPC/POPG liposomes.[17] Increasing the concentration of POPC LUVs while holding the concentration of the peptide constant resulted in very similar CD spectra. As can be seen in **Figure 4.5**, the CD spectra of these peptides did not vary much with the introduction of POPC LUVs suggesting that the interaction was not concentration dependent. Even at high L/P ratios, the spectra were very similar to the samples associated with low L/P ratios proposing an overall weak interaction with the membranes.[10]

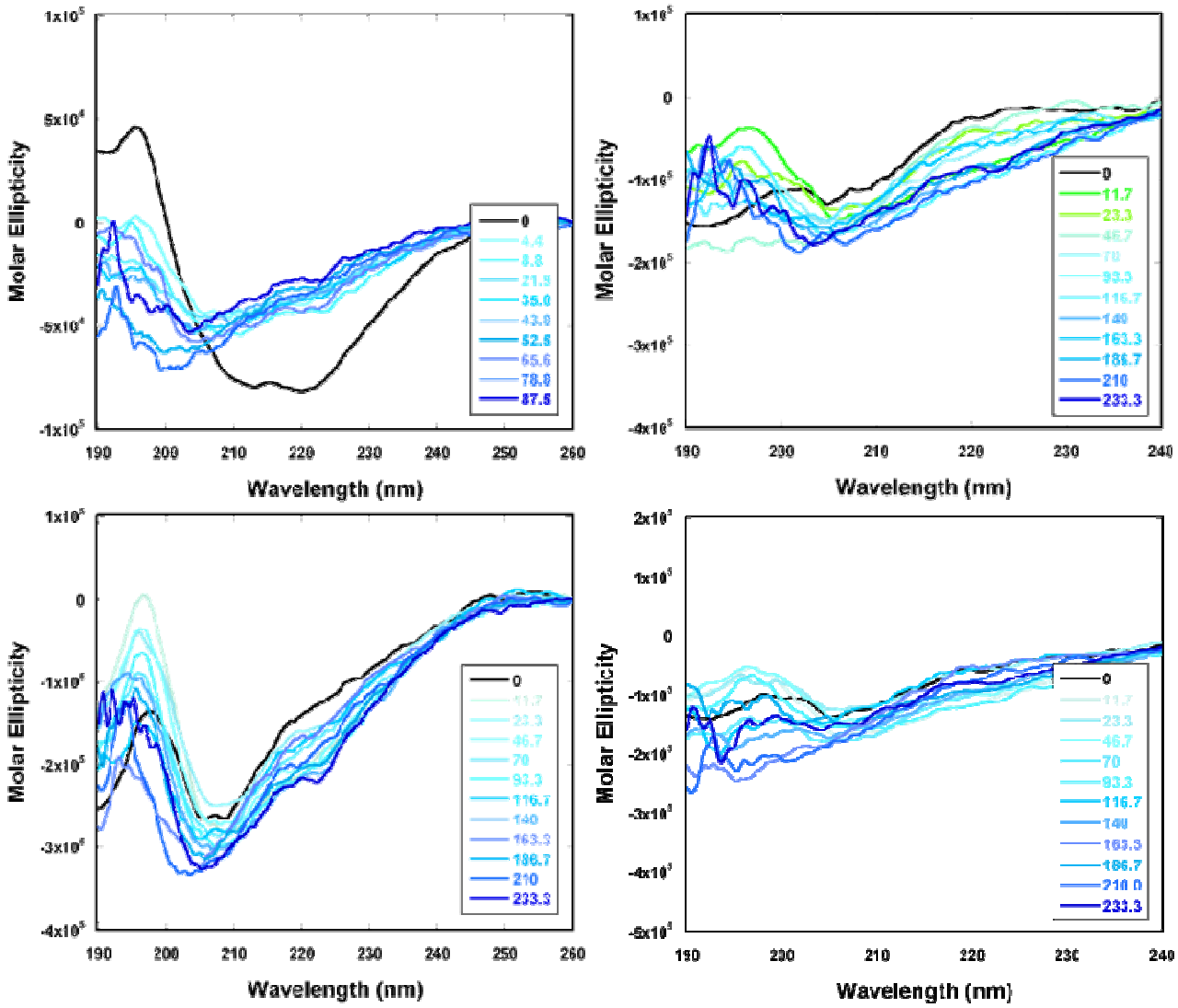

Figure 4.5: Far-UV CD spectra of separate samples of 200 µM compound **23** (top left) and 75 µM solutions of compounds **36** (top right), **29** (bottom left) and **37** (bottom right) with increasing concentrations of POPC LUVs.[18, 19]

However, vastly different CD spectra resulted from samples with increasing concentrations of 4:1 POPC/POPG LUVs (**Figure 4.6**). Increasing the anionic LUVs concentration yielded CD spectra that were very different in both intensity and shape from their corresponding spectrum in buffer. As the L/P ratio increased, the intensity decreased until a ratio

was met that exhibited an intensity of a constant-level. We refer to this as the "critical point" and it was at this point that all of the peptide was assumed to be bound. The L/P ratio that corresponds to this point was unique to each peptide. For compound **23** this ratio was approximately 39, for compound **36** it was 105, for compound **29** it was 70 and for compound **37** it was approximately 52. Once this "critical point" was reached, the trend of decreasing intensity was reversed and the intensity of the spectra increased.

The titration of 4:1 POPC/POPG LUVs into the peptide solutions resulted in three separate groupings of CD spectra. The first group yielded decreasing spectral intensity as the LUV concentration increased. At low L/P ratios, the relative concentration of peptide was such that each liposome was saturated with peptide. The resulting spectra represented the peptide free in solution and in the I-state (blue spectra).[17] The second group, which seemed to be limited to the transition point, consisted of 1 or 2 spectra which were very similar to each other and exhibited the lowest intensity. As the LUV concentration was increased, the amount of free peptide in bulk solution decreases and becomes negligible. We believe this corresponds to the 'critical point' discussed earlier, and hypothesize it is predominantly I-state (green spectra). The third and final grouping refers to the spectra after the "critical point" that continue to increase in intensity with increasing liposome concentration. [17] Beyond the 'critical point,' as the LUV concentration increases further, a P/L ratio is reached such that the I-state is no longer statistically favored and various forms of the S-state dominate (red spectra).[17]

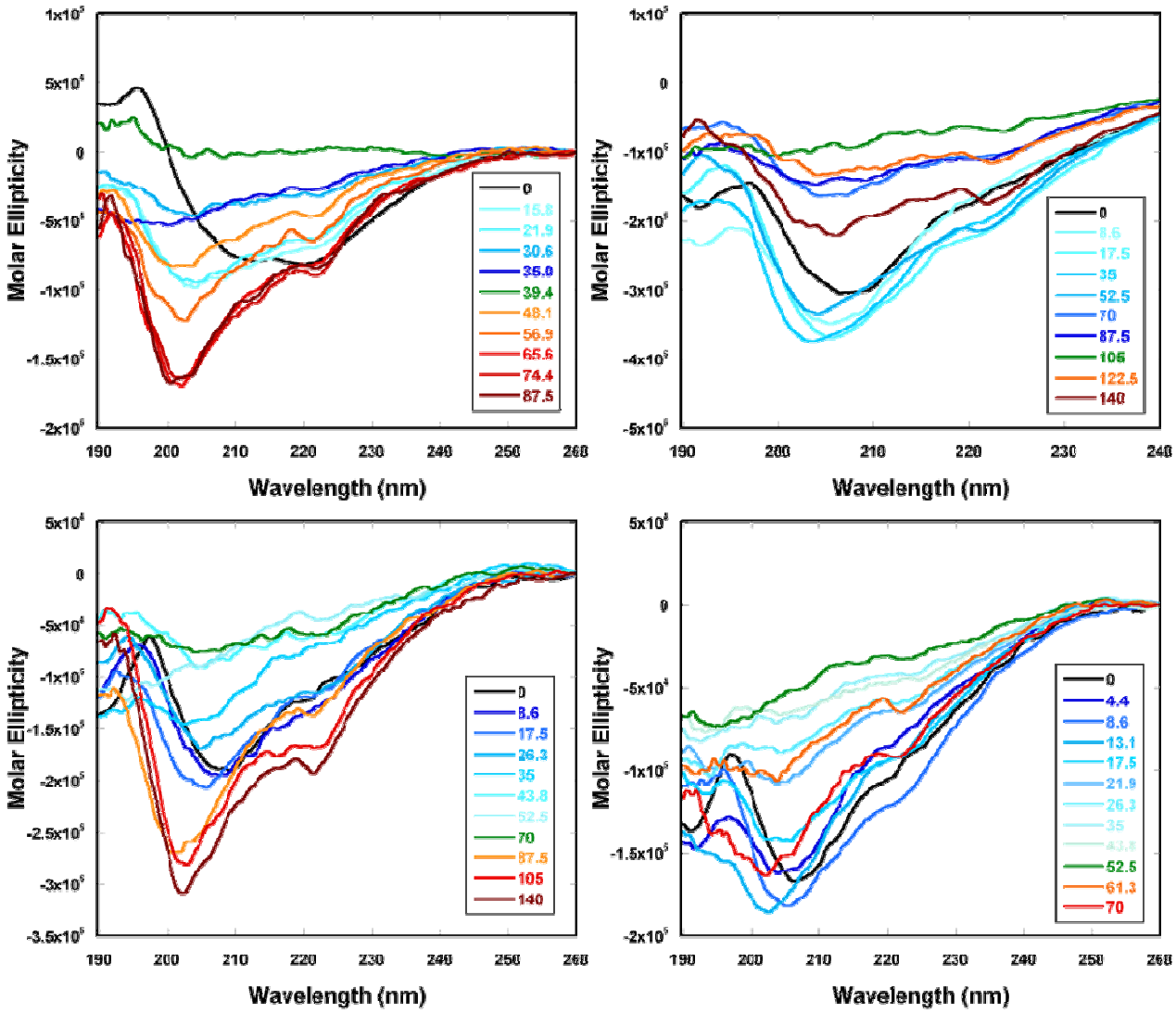

Figure 4.6: Far-UV CD spectra of separate samples of 200 µM solutions of compound **23** (top left) and **37** (bottom right) and 100 µM solutions of compounds **36** (top right) and **29** (bottom left) with increasing concentrations of 4:1 POPC/POPG LUVs. [18, 19]

ITC Studies

Anionic LUVs. ITC investigation for the titration of 4:1 POPC/POPG LUVs into compounds **23** (**Figure 4.7** – top left), **36** (**Figure 4.7** – top right), **29** (**Figure 4.7** – bottom left) and **37** (**Figure 4.7** – bottom right) produced complex 2-phase thermograms. Each peptide displayed an endothermic heat event followed by an exothermic event. With the exception of

compound **36**, as the spacer length increased, the magnitude of the endothermic heat event increased while the exothermic heat event subsequently decreased. Endothermic heat events are associated with several processes including the desolvation of the peptide and of the membrane surfaces, disruption of the polar lipid head groups and lipid:lipid interactions as well as the release of the water molecules from inside the vesicle.[20-23] With an increase in the length of the spacer, the conformational flexibility of the peptide and the overall space that the peptide occupies also increases. Consequently, the larger the space occupied by the peptide, the more disruption there is on the surface of the membrane. This increased disruption therefore increases the positive ΔH contributions. The magnitude of the cumulative endothermic heat components for compounds **23**, **29** and **37** were +0.80, +1.00 and +2.30 kcal/mol, respectively. Compound **36** absorbed the least amount of heat with +0.42 kcal/mol.[22-25]

Exothermic heats correspond with a process that favors binding. Processes that contribute to a negative ΔH include, but are not limited to, attractive electrostatic interactions, hydrogen bonding due to conformational changes of the peptide, increase in Van der Waals forces due to binding of the peptide to the membrane and the reorganization of the polar head groups and lipid:lipid interactions after binding.[11, 19, 21-23, 26] The exothermic component of the thermograms reached a maximum ΔH before subsequently decreasing into the heat of dilution for each peptide. As the length of the spacer increased, the maximum value that was reached by the exothermic component decreased. When the spacer length increases, the overall hydrophobic character of the peptide backbone also increases, thus allowing the peptide to associate more strongly through Van der Waal interactions with the hydrophobic core of the membrane bilayer. With stronger associations, the peptides are less likely to disassociate from one liposome in order to bind to another one. The process of leaving one liposome to bind with another resulted in the

exothermic component of the thermogram; therefore a decrease in this process would ultimately result in the decease of the magnitude of the exothermic component. The cumulative exothermic heat events released for compounds **23**, **29** and **37** were, respectively, -0.40, -0.17 and -0.05 kcal/mol.[22, 23, 25, 27] Compound **36**, as with the endothermic heat event, was an exception to this trend and produced -0.16 kcal/mol.

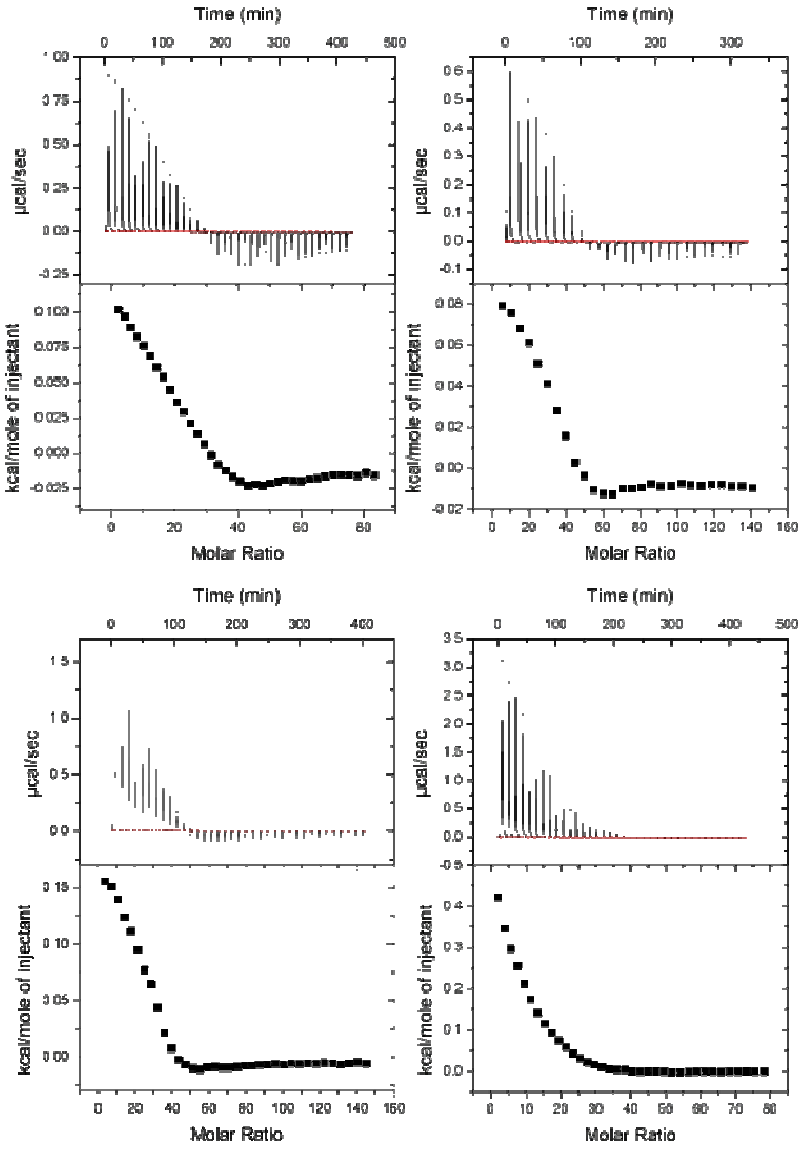

Figure 4.7: Full titration ITC experiment for the titration of 35 mM 4:1 POPC/POPG LUVs into 200 µM compound **23** (top left), 50 µM compound **36** (top right), 100 µM compound **29** (bottom left) and 200 µM compound **37** (bottom right).

Another intriguing feature of these pepties was the correlation between the most exothermic point of the ITC and the "critical point" of the CD titrations studies. The molar ratios obtained at each point were the same and were indicative of a transition from peptides in predominately I-states to those in S-states. These ratios are different for each peptide in this series, and decrease with increasing spacer length, with the exception of compound **36**.

As with compound **23**, we were unable to fit this data to known models so as to obtain a full set of thermodynamic data. However, single injection ITC experiments were conducted to determine the enthalpy (ΔH) values for the binding interaction as well as membrane disruption.[11, 22, 23, 25, 26, 28] These ΔHs should not be confused with ΔH^0, the enthalpy of the entire reaction, as they focus on the two extremes of the isotherm: binding and membrane disruption. To determine the ΔH of binding, dilute solutions of compounds **23**, **36**, **29** and **37** were titrated into concentrated solutions of 4:1 POPC/POPG LUVs (**Figure 4.8**) [25] to isolate the processes associated with high L/P ratios where the surface state, or S-state, predominates. An illustrative schematic can be seen in **Figure 3.12**. The ΔH for the binding of compounds **23**, **36**, **29** and **37** to anionic LUVs were -1.02, + 0.46, +1.2 and +1.8 kcal/mol, respectively. Compound **23** exhibited the most favorable enthalpic process of the peptides in this study while compounds **36**, **29** and **37** exhibited endothermic processes. These endothermic heat events can be explained in large part by the desolvation of the structured water molecules on the surfaces of the peptide and membrane. As the non-polar residues partition into the membrane, attaching the peptide to the surface, the water spheres surrounding both the peptide and membrane are disrupted. [26] As previously discussed with the full titration experiments, the increase in the length of the spacer for compounds **36**, **29** and **37** results in larger peptides which will cause more disruption on the surface of the membrane.

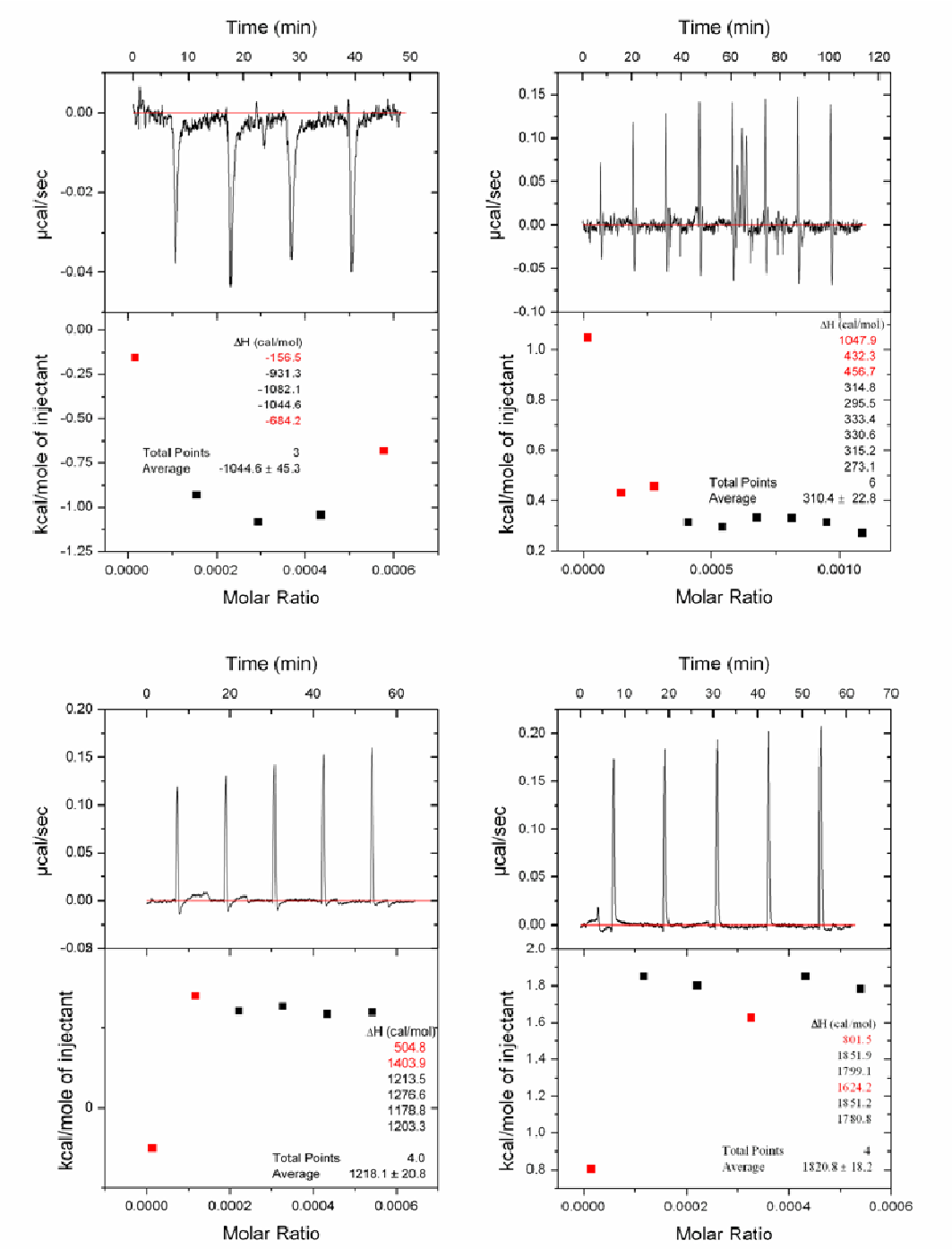

Figure 4.8: Single injection ITC experiments to determine the ΔH of binding. A dilute solution of 200 µM compound **23** (top left) was titrated into 15 mM 4:1 POPC/POPG LUVs. Dilute solutions of 250 µM compound **36** (top right), 200 µM compound **29** (bottom left) and 100 µM compound **37** (bottom right) were titrated into concentrated solutions of 20 mM 4:1 POPC/POPG LUVs to give high L/P ratios.[29]

Titrating dilute samples of lipid into excess peptide allowed for the isolation of heat associated with any membrane disrupting processes. In general, this process includes the saturation of the membrane surface followed by pore formation for 4:1 POPC/POPG LUVs. The LUVs were saturated upon injection into the reaction cell containing excess peptide so as to achieve L/P ratios where the peptide was present in two possible environments, bulk solution or the inserted state (I-state). An illustrative schematic can be seen in **Figure 3.14**. Single injection experiments for the titration of 4:1 POPC/POPG LUVs into the peptides (**Figure 4.9**) yielded enthalpy values ranging from +0.10 and +0.60 kcal/mol. These endothermic values can be explained in large part by the loss of water molecules on the surface of the peptide and membrane as the peptide inserted into the bilayer as well as the release of water molecules from the inside of the liposome due to the formation of a pore.[23] Also, the disruption of the lipid:lipid interactions of the bilayer upon insertion would contribute further to the endothermic heat event.[20, 23] All of the single injection data for the interactions between compounds **23**, **36**, **29** and **37** are summarized in **Table 4.5**.

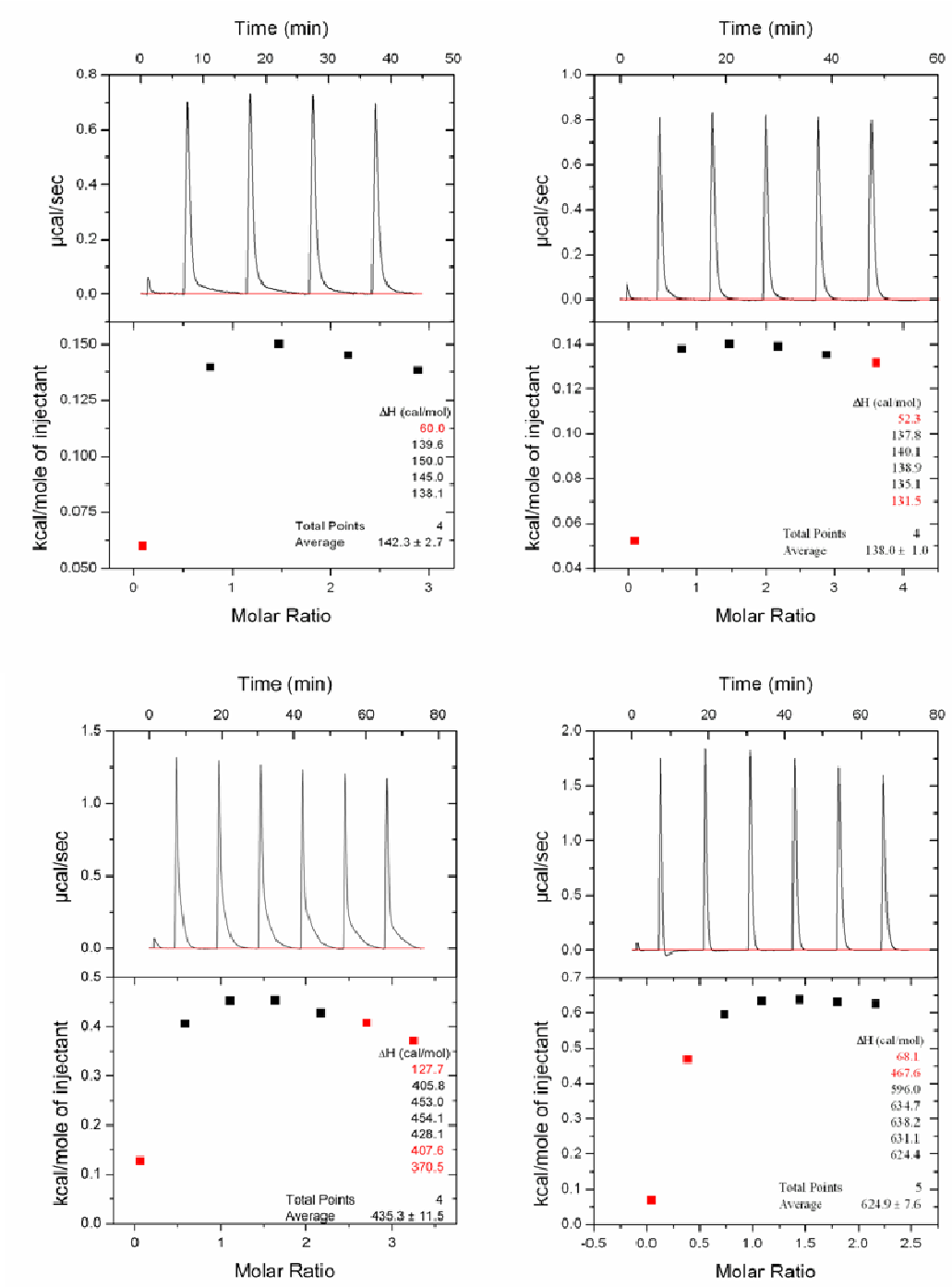

Figure 4.9: Single injection ITC experiments to determine the ΔH of membrane disruption. Dilute solutions of 20 mM 4:1 POPC/POPG LUVs were titrated into 300 µM solutions of compound **23** (top left) and **36** (top right). A 15 mM solution of 4:1 POPC/POPG LUVs was titrated into 300 µM compound **29** (bottom left) and 10 mM 4:1 POPC/POPG LUVs into 300 µM compound **37** (bottom right).

Zwitterionic LUVs. Full titrations of 35 mM POPC LUVs into compounds **23** (**Figure 4.10** - top left), **36** (F**igure 4.10 -** top right), **29** (**Figure 4.10 -** bottom left) and **37** (**Figure 4.10 -** bottom right) resulted in a single endothermic phase.[30] Previous ITC studies have reported [31] that an endothermic phase would be attributed to a combination of several events including electrostatic interactions between the peptide and the membrane surface, disruption of polar head groups accompanied by reorganization of lipids on the surface of the membrane, disruption of the solvation spheres on both the peptide and the membrane surfaces, and other less understood phenomena.[31] All of the titrations with POPC LUVs resulted in a continuous decrease of heat as the experiment progressed until only the heat of dilution was observed. The subsequent decrease of heat was due to the fact that with each addition of lipid, peptide became bound to the vesicles and removed from the bulk solution, thus, decreasing the amount of peptide available for binding. This process continued until no peptide was available for binding and thus was assumed to be 100% bound. The only heat observed after this point was the heat from dilution of lipid.[11, 19, 22-24, 28, 32] There were two observations of the thermograms that were indicative of weak binding between our peptides and POPC LUVs. One, there was minimal heat evolved upon titration of the peptide solutions with lipid.[31, 33] Also, weak binding was indicated by the high L/P molar ratios observed for complete binding of the peptides.[19, 22-24, 28] High ratios, ~120, 275, 250 and 300 for compounds **23**, **36**, **29** and **37** respectively, were required before all of the peptide was removed from the bulk solution.

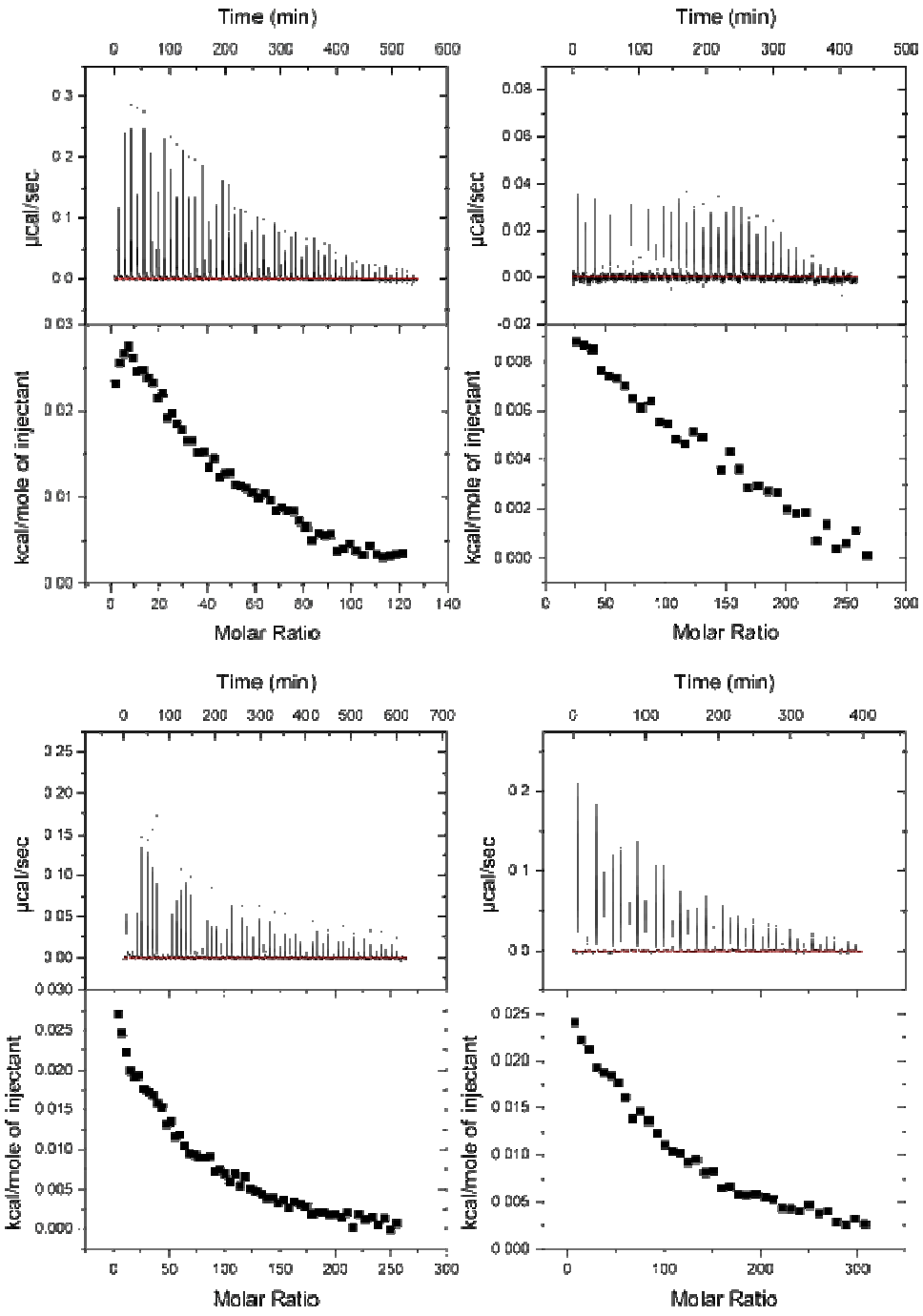

Figure 4.10: ITC experiment for the titration of 35 mM POPC LUVs into solutions of 200 µM compound **23** (top left), 50 µM compound **36** (top right), 100 µM compound **29** (bottom left) and 50 µM compound **37** (bottom right).

Although we were unable to obtain thermodynamic data for the titration of 4:1 POPC/POPG LUVs into peptides, this was not the case for the titration with POPC LUVs. A plot of the degree of binding, X_b, against c_f, that concentration of free peptide in bulk solution, yielded nonlinear binding isotherms compounds **23**, **36**, **29** and **37** in the presence of 35 mM POPC LUVs at 25°C (**Figure 4.11**).

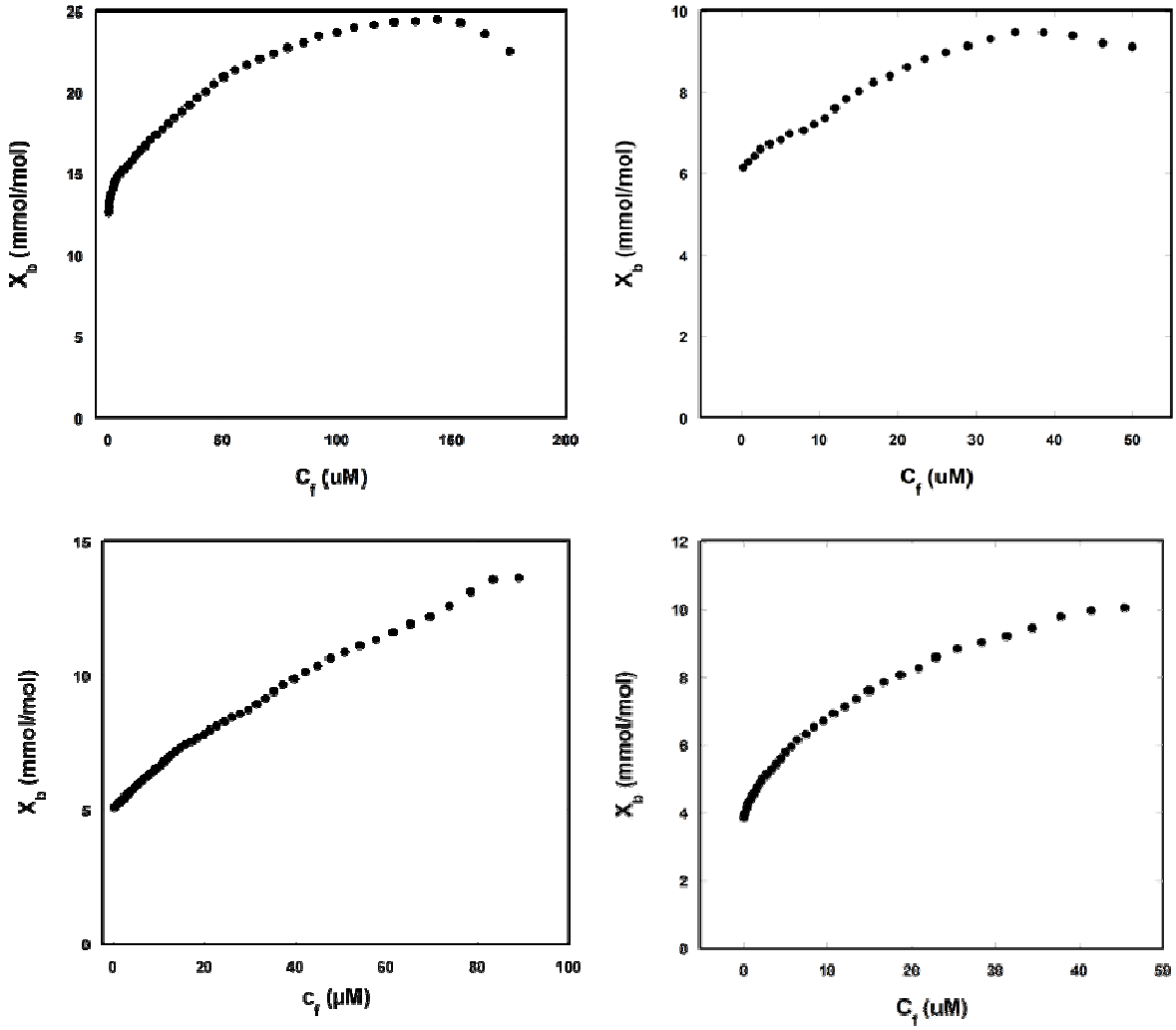

Figure 4.11: Plot for the degree of binding, X_b, as a function of the peptide concentration in bulk solution, c_f. The binding isotherms were derived from the titration of 35 mM POPC LUVs into compounds **23** (top left), **36** (top right), **29** (bottom left) and **37** (bottom right). X_b and c_f were calculated as described in chapter 1 of the text.[21, 26]

The nonlinear plots were due to the fact that the model, $X_b = K_p c_f$, does not account for the electrostatic interactions between the positively charged peptide and the localized regions of negative charge on the membrane surface. This results in an increase of peptide concentration at the surface of the membrane, c_m in comparison to the bulk solution, c_f.[26] Therefore, the more sophisticated surface partition equilibrium model, $X_b = Kc_m$, from **Equation 1.9** in Chapter 1[21, 32, 34, 35] is more appropriate for the analysis of our data. By plotting X_b versus c_m (**Figure 4.12**), the binding constant K can be obtained as it is the slope of the line. Knowing K_b allowed for the calculation of other thermodynamic data, including free energy (ΔG^0) and entropy (ΔS) from the **Equations 1.2** and **1.3** discussed earlier: $\Delta G^0 = -RT\ln(55.5K)$ and $\Delta G^0 = H - T\Delta S$.

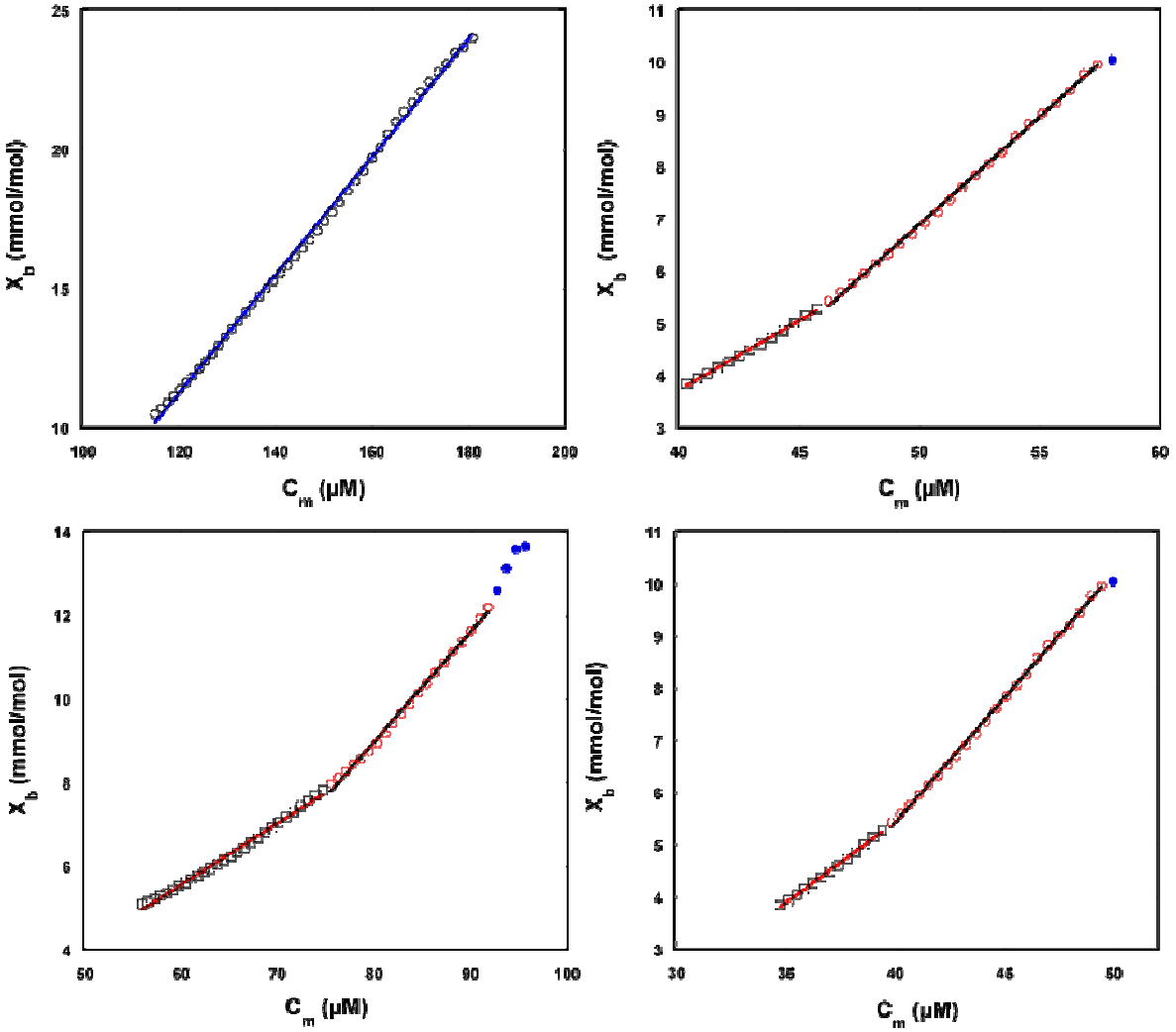

Figure 4.12: Plot for the degree of binding, X_b, as a function of the surface concentration of peptide, c_m. The binding isotherms were derived from the titration of 35 mM POPC LUVs into compounds **23** (top left), **36** (top right), **29** (bottom left) and **37** (bottom right). X_b and c_m were calculated as described in chapter 1 of the text.[21, 26]

Upon plotting c_m against X_b, a unique relationship was revealed between the binding constants and the spacer length. As seen in **Figure 4.12** one line was observed with compound **23**, where two intersecting lines were observed for compounds **36**, **29** and **37**. This intriguing observation has been attributed to the fact that compounds **36**, **29** and **37** contain unnatural amino acid spacers. Consequently, two sets of thermodynamic data were calculated for compounds **36**,

29 and **37**, one at lower peptide concentration and one at higher peptide concentration. The results for the thermodynamic analysis of compounds **23**, **36**, **29** and **37** with POPC liposomes are given in **Table 4.5**. As can be seen in **Table 4.5**, there is no discernable trend in ΔH^0, K or ΔG with regard to the length of Spacer #1. However, there is an obvious trend with the ΔS of the interactions as the entropy increases with the length of the spacer. The ΔS values become more positive as the spacer length increases.

Table 4.4: Thermodynamic data for a representative titration of 35 mM POPC into the peptides at 25°C as derived from the equations discussed previously.

Compound	$\Delta H^{0,a}$ (kcal/mol)	K^b (M^{-1})	ΔG^c (kcal/mol)	ΔS^d (cal/mol·K)
Lower Peptide Concentration				
23	na	na	na	na
36	0.04	265.2	-5.7	19.2
29	0.49	146.9	-5.3	19.5
37	0.19	309.0	-5.8	20.0
Higher Peptide Concentration				
23	0.67	211.0	-5.5	20.8
36	0.59	412.2	-5.9	21.9
29	0.95	262.7	-5.7	22.2
37	1.63	479.0	-6.0	25.7
Magainin-2-amide[e]				
M2a	-15.9	2000.0	-7.0	-29.4

[a] ΔH values were calculated using **Equation 1.4** from chapter 1 using the binding enthalpies measured directly from the experiment.
[b] K values were generated from the lipid-into-peptide titration using the calculations as described in chapter 1.
[c] ΔG values were calculated using **Equation 1.1** from chapter 1.
[d] ΔS was calculated using **Equation 1.2** from chapter 1.
[e] The thermodynamic parameters for the magainin analogue M2a as presented by Wieprecht et. al. [20, 30]

The increasing entropy can be explained by the molecular volume of the peptide. As the spacer length increases, the conformational flexibility and degrees of freedom for each peptide

also increases thereby causing the conformational space available to the peptide to increase dramatically. The magnitude of disruption caused on the surface of the membrane increases as the conformational space available for the peptide to sample increases. Association of the peptide with a membrane results in the desolvation of structured water molecules on both surfaces, contributing to the positive component of ΔS.[23, 36-38] Other positive ΔS contributors include the interruption of the polar head groups on the surface as well as the disruption of the lipid-to-lipid interactions upon binding.[23] Consequently, as the concentration of peptide increases so do the processes that disrupt the membrane surface, thus resulting in an increase of ΔS.[11, 19, 20, 23, 37, 39]

Traditional binding isotherms for peptides containing α-amino acids, such as compound **23** with a glycine spacer, exhibit straight lines.[11, 22, 26] However, for the peptides **36**, **29** and **37** which incorporate unnatural amino acids containing additional methylene groups in peptide backbone, resulted in two distinct intersecting lines. At this point, we have not been able to locate similar behavior in the literature. This unique observation could be due to the fact that β-peptides (compound **36**), γ-peptides (compound **29**) and ε-peptides (compound **37**) have expanded hydrogen bond ring sizes [40] which allow them to take on additional conformations that the α-amino acids such as the glycine of compound **23**, can not adopt. The longer the amino acid backbone the more flexible the peptide will be, thus allowing it to occupy a larger space.[40] The second line in the binding isotherm may represent a conformational transition un-available to α-amino acid containing peptides.

Examining the processes occurring in the full titration experiments could possibly offer an explanation for the observed behavior. As previously discussed, there is an excess of peptide in the cell at the beginning of the titration experiment. Small aliquots of liposomes were titrated into the cell and saturated with peptide, removing peptide from bulk solution with each titration.

As the peptide available for binding decreases, so do the heats associated with each injection until all of the peptide is removed from the bulk solution.[23] Low L/P ratios were observed at the beginning of the titration as the liposomes were saturated with peptide after each injection. At the end of the titration high L/P ratios were observed. An illustrative schematic can be seen in **Figure 3.9**. Depending on the L/P ratio, there are two types of conformational changes that the peptide may undergo. One involves the binding of peptide to a saturated liposome while the other involves a peptide-free liposome. As LUVs were titrated into the peptide solution, the peptides immediately adopt conformations to fit around the charged polar lipid head groups. At this point, the surface potential of the membrane becomes more positive resulting in the second type of conformational change which corresponds to the binding isotherm at higher peptide concentrations. With a change in the surface potential, the peptide must change conformation while in the bulk solution so as to bind with a liposome surface which is already saturated. As the L/P ratio increases, the peptides only undergo the conformational changes associated with binding to a peptide-free membrane surface. This process corresponds to the binding isotherm at lower peptide concentrations. Even though both processes occur with the binding of α-amino acids, we feel that the lack of conformational space available to α-amino acids relative to the others causes the two processes to be indistinguishable from each other.

Single injection experiments were also performed for the POPC liposomes in order to obtain representative ΔH values for low and high L/P ratios for the interaction between the peptides and zwitterionic models. Titrating minimal peptide into excess POPC lipid allowed for the isolation of the heat associated with the initial binding. For an illustrative schematic refer to **Figure 3.12**. For each of these peptides, this particular ΔH was endothermic with no obvious trend associated with an increase in spacer length. Compound **37** absorbed the most heat at +3.9

kcal/mol followed by compound **23**, **36** and **29** with +2.1, +1.6 and +1.1 kcal/mol, respectively (**Figure 4.13**). The fact that ΔH was positive rather than negative as observed in most "binding" events can be attributed to several processes including the desolvation of the water molecules on the surfaces of both the membrane and peptide, displacement of polar lipid head groups upon interaction with the peptide, disruption of the lipid:lipid interactions as the hydrophobic side chain inserted into the bilayer and any repulsive interactions between the positively charged side chains and the localized negative charge on the surface. The processes formerly mentioned contribute to positive ΔH values and thus counteract the negative ΔH of binding to produce an overall endothermic reaction.[11, 26, 31, 41] These differences in binding enthalpies reflect the global conformational and physicochemical changes that occur during the binding of each peptide to the surface of the liposomes. For example compound **37**, with the longest spacer Ahx, exhibited the greatest conformational flexibility and thus displayed the largest enthalpy changes.

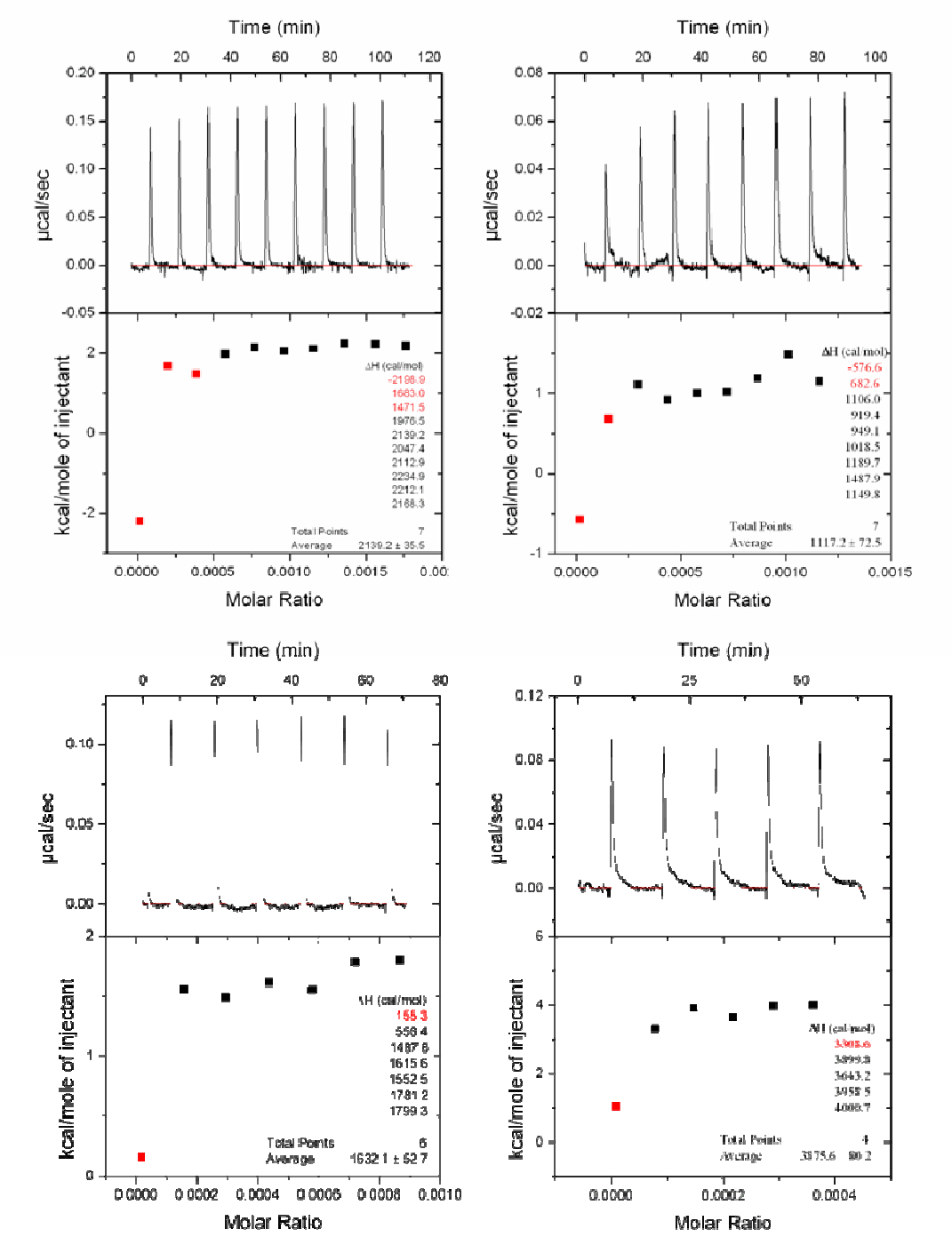

Figure 4.13: Single injection ITC experiments in order to determine the ΔH of binding for POPC LUVs. Dilute solutions of 200 µM compound **23** (top left), **36** (top right) and **29** (bottom left) were titrated into 15 mM solutions of POPC LUVs. A dilute solution of 100 µM compound **37** (bottom right) was titrated into 15 mM POPC LUVs to give high L/P ratios.[29]

The heat associated with membrane disruption was isolated by titrating dilute samples of POPC LUVs into excess peptide. Generally for the case of our peptides with POPC LUVs, this process includes the saturation of the membrane surface consequently causing leakage. Due to the low L/P ratio, the peptide will be observed in one of two possible environments, the bulk solution or in the inserted state (I-state). As the surface should be saturated with peptide, the I-state or other states involved in membrane disruption should predominate, producing injections of identical heats that were averaged. For an illustrative schematic refer to **Figure 3.14**. There was no discernable trend for the observed ΔHs affiliated with membrane disruption for this series of peptides and the spacer length. Compound **37** had the highest ΔH with +0.05 kcal/mol followed by compound **23** with +0.04 kcal/mol, compound **36** with +0.03 kcal/mol and compound **29** absorbed the least amount of heat with +0.02 kcal/mol (**Table 4.5**). One notable feature was the 4-10 fold decrease in the magnitude as compared to the ΔH of membrane disruption for 4:1 POPC/POPG LUV membrane models. This observation supports the conclusion that these peptides are selective towards anionic membranes over zwitterionic.

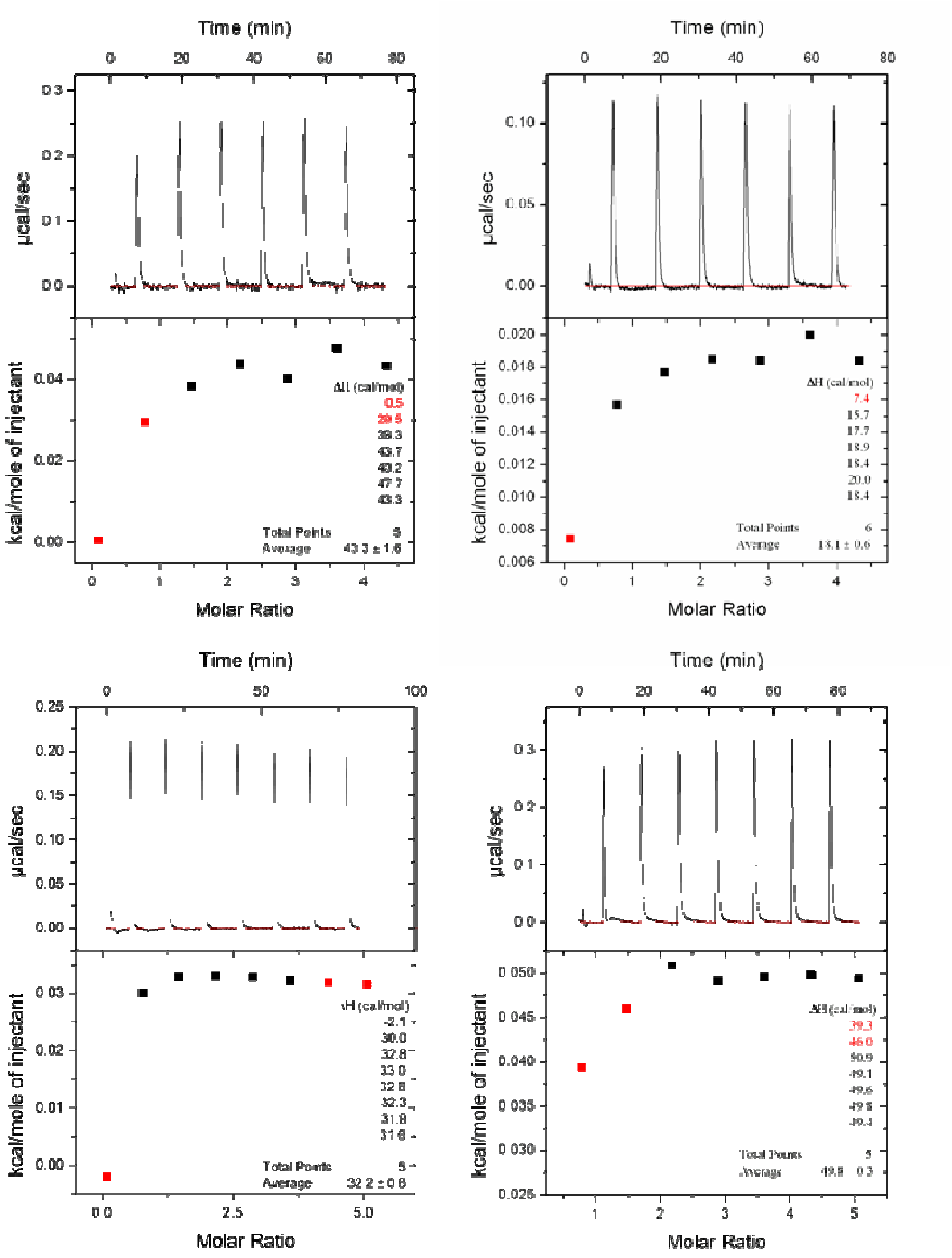

Figure 4:14: Single injection ITC experiments to determine the ΔH of membrane disruption for POPC LUVs. Dilute solutions of 20 mM 4:1 POPC/POPG LUVs were titrated into 300 µM solutions of compound **23** (top left), **36** (top right), **29** (bottom left) and **37** (bottom right).

The difference in ΔHs of the two different single injection experiments for POPC LUVs can be attributed to exothermic processes counteracting the positive ΔH contributions of the endothermic processes. At the low L/P ratios of the membrane disrupting processes, there are several peptides binding per lipid, thus increasing the negative ΔH component of the overall reaction. An increase in the negative component consequently causes an overall decrease in the positive.[22]

Table 4.5: ΔH (kcal/mol) values for the binding and membrane disruption of 4:1 POPC/POPG and POPC LUVs as determined by single injection ITC experiments.[23]

Compound	Compound into 4:1 POPC/POPG	4:1 POPC/POPG into Compound	Compound into POPC	POPC into Compound
23	-1.0 ± .04	0.14 ± .03	2.1 ± .04	0.04 ± 0
36	0.3 ± .02	0.14 ± .00	1.1 ± .07	0.02 ± 0
29	1.2 ± .02	0.44 ± .01	1.6 ± .05	0.03 ± 0
37	1.8 ± .02	0.62 ± .01	3.9 ± .08	0.05 ± 0

The different shapes of the anionic and zwitterionic thermograms, two phases versus one, are indicative of different mechanisms of action. This observation coupled with the large differences in the heats absorbed and/or released during the single injection experiments supports the hypothesis that this series of peptides is selective. There are several factors that contribute to the binding and membrane disruption enthalpies that are common to anionic and zwitterionic membrane models. In addition to changes in Van der Waals interactions due to the desolvation of both the peptide and membrane surfaces,[26, 31, 42] these factors include both repulsive and attractive electrostatic interactions, changes in conformation adopted by the peptide, disruption of polar head groups as well as lipid:lipid interactions on the outside and inside of the liposomes.[11, 19, 20, 22, 23] The only significant difference between the two model membrane

systems was the introduction of a greater negative charge on the surface of the 4:1 POPC/POPG mixed LUVs. This small increase in negative charge clearly played an important role in the interactions of the highly positively charged (+6) peptides and anionic membrane models, thus promoting selectivity.

Calcein leakage studies

Monitoring the fluorescence of peptide induced calcein leakage has been well documented as a technique for probing AMP activity.[42, 43] By introducing different concentrations of peptide to solutions of calcein-encapsulated POPC or 4:1 POPC/POPG LUVs, it was possible to determine the concentration dependency, if any, for the activity. It can be seen in **Figure 4.15** that these peptides did not appear to interact with POPC LUVs via a concentration dependent mechanism. There is not a significant difference in the leakage observed at 4 μM peptide and at 20 μM with any of the four peptides. It is hypothesized that the leakage observed was more than likely due to the displacement of the polar head groups as the peptides became bound. From the CD and ITC data, it is evident that there was a level of interaction taking place. As the peptide concentration increased, the increased displacement of polar lipid head groups resulted in the "thinning" of the membrane. Thus, one possible explanation for the leakage is due to a modified "carpet" mechanism rather than a pore.[20, 44, 45]

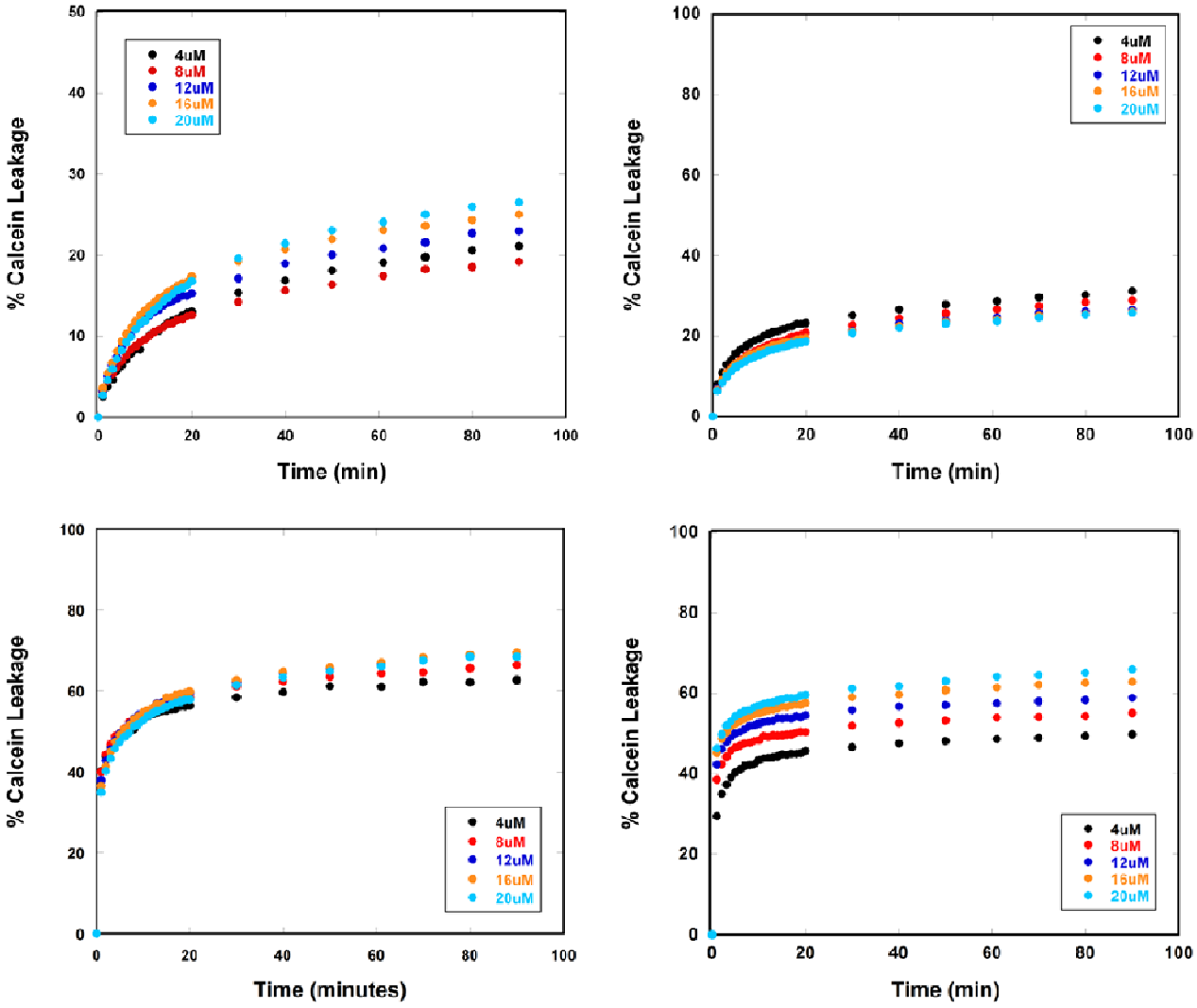

Figure 4.15: The time dependent release of calcein from POPC LUVs induced by increasing concentrations of compound **23** (top left), **36** (top right), **29** (bottom left) and **37** (bottom right) as measured by fluorescence.

It is evident in **Figure 4.16** that these peptides, with the exception of compound **36**, interact with the anionic membrane models via a concentration dependent manner. As the concentration of peptide increased so did the leakage, which maybe explained in the terms of a pore forming mechanism. [46-48] More specifically, the increase in leakage followed by a leveling off suggests a transient pore mechanism. [46, 49] During the initial insertion of the peptide into the

bilayer, the pore undergoes a nucleation step which is followed by a restabilization of the lipid-peptide structure, [46] consequently resulting in the leveling off of the observed leakage after a period of time unique to the peptide.[46, 50] The differences in the amount of leakage observed for each peptide can be explained by the varying selectivity of each peptide. In vitro data presented in **Tables 4.2** and **4.3** provided proof that these peptides are in fact selective against different gram-negative and other drug resistant bacteria strains.

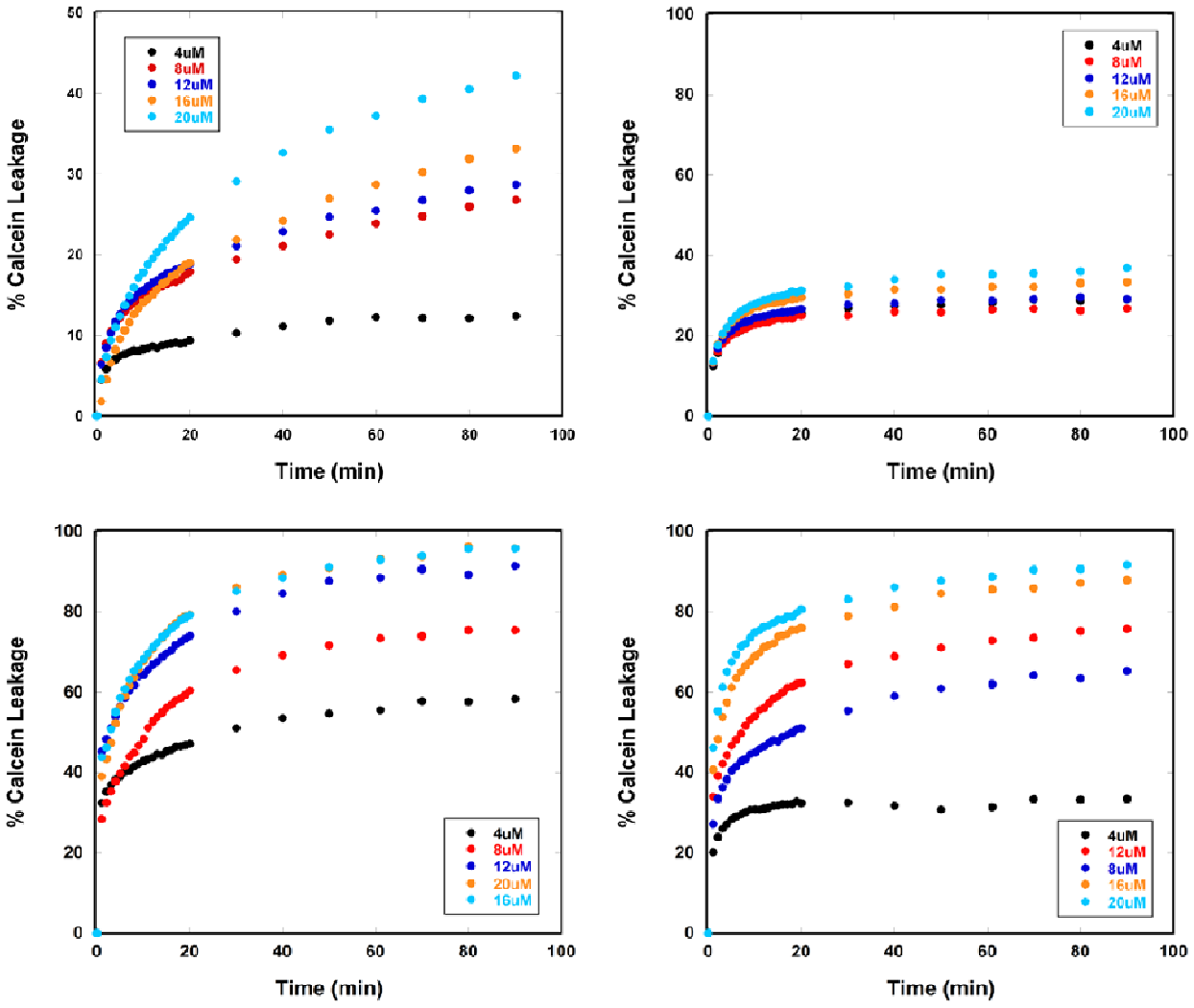

Figure 4.16: The time dependent release of calcein from 4:1 POPC/POPG LUVs induced by increasing concentrations of compound **23** (top left), **36** (top right), **29** (bottom left) and **37** (bottom right) as measured by fluorescence.

When comparing the total percent leakage caused by each peptide at the same concentration (**Figure 4.17**), compounds **29** and **37** exhibited a significant increase from POPC and 4:1 POPC/POPG LUVs as compared to compounds **23** and **36**. For POPC, this excess leakage was most likely due to the larger peptides displacing more polar head groups as they bind, thus increasing the extent of membrane thinning allowing leakage of the dye.[20, 44, 45] The best explanation for the increased leakage in the presence of 4:1 POPC/POPG LUVs at constant peptide and LUV concentrations is that compounds **29** and **37** form a larger number of pores. The increase in the spacer length results, ultimately in a larger peptide. With larger peptides, fewer peptides are needed to form pores capable of leakage. Due to the fact that the number of peptides available was held constant and fewer peptides were needed per pore, there were more peptides available to make more pores, thus leading to higher leakage. This conclusion was supported by the full titration ITC data for the titration of 4:1 POPC/POPG LUVs into the peptides. The larger peptides have smaller exothermic components, suggesting that we are observing peptides that remain bound to the liposome and do not dissociate from one membrane surface to associate with another.

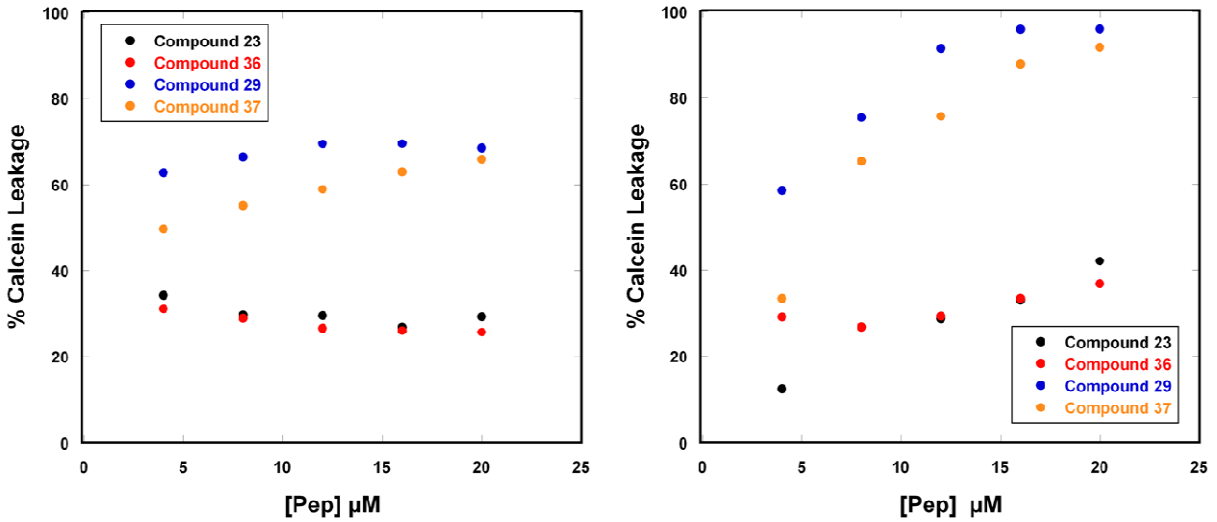

Figure 4.17: The total percent of calcein leakage from POPC (left) and 4:1 POPC/POPG LUVs induced by increasing concentrations of compounds **23**, **36**, **29** and **37** as measured by fluorescence.

Conclusions

The data presented in this chapter supports the hypothesis that this particular series of peptides exhibit selectivity and the lengthening of Spacer #1 does in fact play a role in the interactions with model membrane systems. CD spectra of compounds **23**, **36**, **29** and **37** clearly indicate that these peptides interact with zwitterionic and anionic micelles and liposomes differently, as expected. The conclusion that the different conformations adopted by the peptides in different membrane models as seen by CD are indicative of different mechanisms is supported by the ITC and calcein leakage studies. The change in the mechanism is believed to be a result of the changes in the physicochemical properties presented to the liposome surfaces by the modifications of spacer #1.

The ITC observed for these compounds is very different from the thermodynamic data that has been observed for natural AMPs.[18, 20-23, 25-27, 35, 41, 42, 51-53] We believe these differences are due, in large part, to the fact that our peptides incorporate a high percentage of unnatural

amino acids and were designed to have regions of limited conformational flexibility while the peptide backbones of most natural peptides are relatively flexible. As a whole, we believe that this group of peptides interacted with POPC LUVs via a modified version of the "carpet" mechanism, associating predominately with the surface, while forming pores in the presence of 4:1 POPC/POPG LUVs. We have also presented evidence suggesting that the peptides with the shorter spacers, compounds **23** and **36**, require a higher number of peptides to form a leakage inducing pore than compounds **29** and **37** with the longer backbones.

It was shown in **Figure 3.2** that compound **23** exhibited different CD spectra depending on the percentage of anionic lipids present in the liposomes. This particular observation supports our hypothesis that the chemical composition, and thus the surface physicochemical properties, of the lipid membrane plays a very important role in determining the conformation adopted by these peptides upon binding to the surface. Each strain of bacteria has small differences in the chemical composition of its cell membrane, thus presenting different physicochemical properties to the approaching peptide. We have provided spectroscopic and thermodynamic evidence supporting the conclusion that these peptides, with increasing spacer length, adopt different conformations and undergo different mechanisms of action depending on the membrane surface they are presented with. It is therefore reasonable to expect our peptides to be capable of interacting specifically with the membranes of various bacteria strains. The observed differences in biological activity (MIC values) between the various strains of bacteria as a function of spacer length can be explained by these peptides adopting different conformations on the membranes of the various bacteria strains. Some of these interactions are more favorable for pore formation than others, thus resulting in lower MIC values for that particular bacteria strain. This is clearly the case for compound **37** against the Gram Negative bacteria strains given in **Table 4.3**.

Therefore, it should be possible to design analogs which will exhibit selectivity for specific bacteria strains based on the chemical composition of their respective membranes.

References

(1) Hicks, R. P.; Bhonsle, J. B.; Venugopal, D.; Koser, B. W.; Magill, A. J. De Novo Design of Selective Antibiotic Peptides by Incorporation of Unnatural Amino Acids. *J. Med. Chem.* **2007**, *50*, 3026-3036.

(2) Venugopal, D.; Klapper, D.; Srouji, A. H.; Bhonsle, J. B.; Borschel, R.; Mueller, A.; Russell, A. L.; Williams, B. C.; Hicks, R. P. Novel antimicrobial peptides that exhibit activity against select agents and other drug resistant bacteria. *Bioorg. Med. Chem.* **2010**, *18*, 5137-5147.

(3) Glattli, A.; Daura, X.; Seebach, D.; van Gunsteren, W. F. Can One Derive the Conformational Preference of a Î²-Peptide from Its CD Spectrum? *J. Am. Chem. Soc.* **2002**, *124*, 12972-12978.

(4) Ladokhin, A. S.; Selsted, M. E.; White, S. H. CD Spectra of Indolicidin Antimicrobial Peptides Suggest Turns, Not Polyproline Helix. *Biochemistry* **1999**, *38*, 12313-12319.

(5) Berova, N.; Nakanishi, K.; Woody, R. W., Eds.; In *Circular Dichroism Principles and Applications;* Wiley-VCH: New York, 2000; .

(6) Fuchs, P. F. J.; Bonvin, A. M. J. J.; Bochicchio, B.; Pepe, A.; Alix, A. J. P.; Tamburro, A. M. Kinetics and Thermodynamics of Type VIII β-Turn Formation: A CD, NMR, and Microsecond Explicit Molecular Dynamics Study of the GDNP Tetrapeptide. *Biophys. J.* **2006**, *90*, 2745-2759.

(7) Glukhov, E.; Stark, M.; Burrows, L. L.; Deber, C. M. Basis for selectivity of cationic antimicrobial peptides for bacterial versus mammalian membranes. *J. Biol. Chem.* **2005**, *280*, 33960-33967.

(8) Imura, Y.; Nishida, M.; Matsuzaki, K. Action mechanism of PEGylated magainin 2 analogue peptide. *Biochim. Biophys. Acta* **2007**, *1768*, 2578-2585.

(9) Wang, P.; Bang, J.; Kim, H. J.; Kim, J.; Kim, Y.; Shin, S. Y. Antimicrobial specificity and mechanism of action of disulfide-removed linear analogs of the plant-derived Cys-rich antimicrobial peptide Ib-AMP1. *Peptides* **2009**, *30*, 2144-2149.

(10) Oglęcka, K.; Lundberg, P.; Magzoub, M.; Göran Eriksson, L. E.; Langel, Ü.; Gräslund, A. Relevance of the N-terminal NLS-like sequence of the prion protein for membrane perturbation effects. *Biochimica et Biophysica Acta (BBA) - Biomembranes* **2008**, *1778*, 206-213.

(11) Wieprecht, T.; Beyermann, M.; Seelig, J. Binding of Antibacterial Magainin Peptides to Electrically Neutral Membranes: Thermodynamics and Structure. *Biochemistry (N. Y.)* **1999**, *38*, 10377-10387.

(12) Christiaens, B.; Grooten, J.; Reusens, M.; Joliot, A.; Goethals, M.; Vandekerckhove, J.; Prochiantz, A.; Rosseneu, M. Membrane interaction and cellular internalization of penetratin peptides. *European Journal of Biochemistry* **2004**, *271*, 1187-1197.

(13) Ladokhin, A. S.; Fernandez-Vidal, M.; White, S. H. CD spectroscopy of peptides and proteins bound to large unilamellar vesicles. *J. Membr. Biol.* **2010**, *236*, 247-253.

(14) Olofsson, A.; Borowik, T.; Gröbner, G.; Sauer-Eriksson, A. E. Negatively Charged Phospholipid Membranes Induce Amyloid Formation of Medin via an α-Helical Intermediate. *J. Mol. Biol.* **2007**, *374*, 186-194.

(15) Sanavio, B.; Piccoli, A.; Gianni, T.; Bertucci, C. Helicity propensity and interaction of synthetic peptides from heptad-repeat domains of herpes simplex virus 1 glycoprotein H: A circular dichroism study. *Biochimica et Biophysica Acta (BBA) - Proteins & Proteomics* **2007**, *1774*, 781-791.

(16) Richardson, J. M.; Makhatadze, G. I. Temperature Dependence of the Thermodynamics of Helix–Coil Transition. *J. Mol. Biol.* **2004**, *335*, 1029-1037.

(17) Russell, A. L.; Kennedy, A. M.; Spuches, A. M.; Venugopal, D.; Bhonsle, J. B.; Hicks, R. P. Spectroscopic and thermodynamic evidence for antimicrobial peptide membrane selectivity. *Chem. Phys. Lipids* **2010**, *163*, 488-497.

(18) Hunter, H. N.; Jing, W.; Schibli, D. J.; Trinh, T.; Park, I. Y.; Kim, S. C.; Vogel, H. J. The interactions of antimicrobial peptides derived from lysozyme with model membrane systems. *Biochimica et Biophysica Acta (BBA) - Biomembranes* **2005**, *1668*, 175-189.

(19) Wen, S.; Majerowicz, M.; Waring, A.; Bringezu, F. Dicynthaurin (ala) Monomer Interaction with Phospholipid Bilayers Studied by Fluorescence Leakage and Isothermal Titration Calorimetry. *The Journal of Physical Chemistry B* **2007**, *111*, 6280-6287.

(20) Wieprecht, T.; Apostolov, O.; Seelig, J. Binding of the antibacterial peptide magainin 2 amide to small and large unilamellar vesicles. *Biophys. Chem.* **2000**, *85*, 187-198.

(21) Wieprecht, T.; Seelig, J. Isothermal Titration Calorimetry for Studying Interactions between Peptides and Lipid Membranes. *Current Topics in Membranes* **2002**, *52*, 31-55.

(22) Wenk, M. R.; Seelig, J. Magainin 2 Amide Interaction with Lipid Membranes: Calorimetric Detection of Peptide Binding and Pore Formation. *Biochemistry (N. Y.)* **1998**, *37*, 3909-3916.

(23) Abraham, T.; Lewis, R. N. A. H.; Hodges, R. S.; McElhaney, R. N. Isothermal Titration Calorimetry Studies of the Binding of a Rationally Designed Analogue of the Antimicrobial

Peptide Gramicidin S to Phospholipid Bilayer Membranes. *Biochemistry (N. Y.)* **2005**, *44*, 2103-2112.

(24) Nomura, K.; Corzo, G. The effect of binding of spider-derived antimicrobial peptides, oxyopinins, on lipid membranes. *Biochimica et Biophysica Acta (BBA) - Biomembranes* **2006**, *1758*, 1475-1482.

(25) Bastos, M.; Bai, G.; Gomes, P.; Andreu, D.; Goormaghtigh, E.; Prieto, M. Energetics and Partition of Two Cecropin-Melittin Hybrid Peptides to Model Membranes of Different Composition. *Biophys. J.* **2008**, *94*, 2128-2141.

(26) Seelig, J. Titration calorimetry of lipid-peptide interactions. *Biochim. Biophys. Acta* **1997**, *1331*, 103-116.

(27) Nomura, K.; Corzo, G. The effect of binding of spider-derived antimicrobial peptides, oxyopinins, on lipid membranes. *Biochimica et Biophysica Acta (BBA) - Biomembranes* **2006**, *1758*, 1475-1482.

(28) Wieprecht, T.; Beyermann, M.; Seelig, J. Thermodynamics of the coil–α-helix transition of amphipathic peptides in a membrane environment: the role of vesicle curvature. *Biophys. Chem.* **2002**, *96*, 191-201.

(29) Brogden, K. A. Antimicrobial Peptides: Pore formers or metabolic inhibitors in bacteria? *Nature Reviews.Microbiology* **2005**, *3*.

(30) Wieprecht, T.; Apostolov, O.; Beyermann, M.; Seelig, J. Membrane Binding and Pore Formation of the Antibacterial Peptide PGLa: Thermodynamic and Mechanistic Aspects. *Biochemistry (N. Y.)* **2000**, *39*, 442-452.

(31) Abraham, T.; Lewis, R. N. A. H.; Hodges, R. S.; McElhaney, R. N. Isothermal Titration Calorimetry Studies of the Binding of the Antimicrobial Peptide Gramicidin S to Phospholipid Bilayer Membranes. *Biochemistry (N. Y.)* **2005**, *44*, 11279-11285.

(32) Seelig, J.; Nebel, S.; Ganz, P.; Bruns, C. Electrostatic and nonpolar peptide-membrane interactions. Lipid binding and functional properties of somatostatin analogs of charge z = +1 to z = +3. *Biochemistry (N. Y.)* **1993**, *32*, 9714-9721.

(33) Al-Kaddah, S.; Reder-Christ, K.; Klocek, G.; Wiedemann, I.; Brunschweiger, M.; Bendas, G. Analysis of membrane interactions of antibiotic peptides using ITC and biosensor measurements. *Biophys. Chem.* **2010**, *152*, 145-152.

(34) Beschiaschvili, G.; Seelig, J. Peptide binding to lipid bilayers. Binding isotherms and .zeta.-potential of a cyclic somatostatin analog. *Biochemistry (N. Y.)* **1990**, *29*, 10995-11000.

(35) Beschiaschvili, G.; Seelig, J. Melittin binding to mixed phosphatidylglycerol/phosphatidylcholine membranes. *Biochemistry (N. Y.)* **1990**, *29*, 52-58.

(36) Seelig, J. Thermodynamics of lipid-peptide interactions. *Biochim. Biophys. Acta* **2004**, *1666*, 40-50.

(37) Freire, E. Do enthalpy and entropy distinguish first in class from best in class? *Drug Discov. Today* **2008**, *13*, 869-874.

(38) Meier, M.; Seelig, J. Thermodynamics of the Coil ⇆ β-Sheet Transition in a Membrane Environment. *J. Mol. Biol.* **2007**, *369*, 277-289.

(39) Shimokhina, N.; Bronowska, A.; Homans, S. W. Contribution of Ligand Desolvation to Binding Thermodynamics in a Ligand?Protein Interaction. *Angewandte Chemie* **2006**, *118*, 6522-6524.

(40) Vasudev, P. G.; Chatterjee, S.; Shamala, N.; Balaram, P. Structural Chemistry of Peptides Containing Backbone Expanded Amino Acid Residues: Conformational Features of beta, gamma, and Hybrid Peptides. *Chem. Rev.* **2011**, *111*, 657-687.

(41) Epand, R. M.; Segrest, J. P.; Anantharamaiah, G. M. Thermodynamics of the binding of human apolipoprotein A-I to dimyristoylphosphatidylglycerol. *J. Biol. Chem.* **1990**, *265*, 20829-20832.

(42) Andrushchenko, V. V.; Aarabi, M. H.; Nguyen, L. T.; Prenner, E. J.; Vogel, H. J. Thermodynamics of the interactions of tryptophan-rich cathelicidin antimicrobial peptides with model and natural membranes. *Biochimica et Biophysica Acta (BBA) - Biomembranes* **2008**, *1778*, 1004-1014.

(43) Medina, M. L.; Bolender, J. P.; Plesniak, L. A.; Chapman, B. S. Transient vesicle leakage initiated by a synthetic apoptotic peptide derived from the death domain of neurotrophin receptor, p75NTR. *Journal of Peptide Research* **2002**, *59*, 149-158.

(44) Chen, F. Y.; Lee, M. T.; Huang, H. W. Evidence for membrane thinning effect as the mechanism for peptide-induced pore formation. *Biophys. J.* **2003**, *84*, 3751-3758.

(45) Almeida, P. F.; Pokorny, A. Mechanisms of Antimicrobial, Cytolytic, and Cell-Penetrating Peptides: From Kinetics to Thermodynamics. *Biochemistry (N. Y.)* **2009**, *48*, 8083-8093.

(46) Hugonin, L.; Vukojević, V.; Bakalkin, G.; Gräslund, A. Membrane leakage induced by dynorphins. *FEBS Lett.* **2006**, *580*, 3201-3205.

(47) Matsuzaki, K.; Yoneyama, S.; Miyajima, K. Pore formation and translocation of melittin. *Biophys. J.* **1997**, *73*, 831-838.

(48) Benachir, T.; Lafleur, M. Study of vesicle leakage induced by melittin. *Biochimica et Biophysica Acta (BBA) - Biomembranes* **1995**, *1235*, 452-460.

(49) Matsuzaki, K.; Mitani, Y.; Akada, K.; Murase, O.; Yoneyama, S.; Zasloff, M.; Miyajima, K. Mechanism of Synergism between Antimicrobial Peptides Magainin 2 and PGLaâ€. *Biochemistry (N. Y.)* **1998**, *37*, 15144-15153.

(50) Arbuzova, A.; Schwarz, G. Pore-forming action of mastoparan peptides on liposomes: a quantitative analysis. *Biochimica et Biophysica Acta (BBA) - Biomembranes* **1999**, *1420*, 139-152.

(51) Wieprecht, T.; Apostolov, O.; Beyermann, M.; Seelig, J. Thermodynamics of the α-helix-coil transition of amphipathic peptides in a membrane environment: implications for the peptide-membrane binding equilibrium. *J. Mol. Biol.* **1999**, *294*, 785-794.

(52) Thomas, C. J.; Surolia, N.; Surolia, A. Kinetic and thermodynamic analysis of the interactions of 23-residue peptides with endotoxin. *Biological Chemistry* **2001**, *276*, 35701-35706.

(53) Heerklotz, H.; Seelig, J. Detergent-like action of the antibiotic peptide surfactin on lipid membranes. *Biophys. J.* **2001**, *81*, 1547-1554.

CHAPTER FIVE: SPACER # 2

Introduction

This chapter discusses the use of a combination of CD spectroscopy, ITC and calcein fluorescence leakage assays to investigate the role played by Spacer #2 (**Figure 1.2 –** gold). Spacer #2 defines the distance between the polypeptide backbone and the positively charged side chain amine. The residue is also involved in determining the overall surface charge density of the peptide as well as the distance between the membrane surface and the backbone of the peptide.[1] The number of methylene groups in the side chain of Spacer #2 decreases from four with Lys in compound **23**, to three with Orn in compound **43**, to two with Dab in compound **53** and to one methylene with Dpr in compound **45**. The sequences are given in **Table 5.1**. These studies were designed to provide a better understanding of how the physicochemical properties of the peptide influence the mechanism of binding with several zwitterionic and anionic membrane model systems. We have already discussed the logic of incorporating un-natural amino acids into the peptide sequence of an AMP as there are several advantages over an AMP consisting exclusively of naturally occurring amino acids. Here we will focus on the importance of the positively charged amino acid residue. By decreasing the length of the side chain, the positive charge density will reside closer to the backbone resulting in less flexibility during binding which is more important in binding with zwitterionic lipids than anionic.

A fifth AMP was included in this particular series. Compound **56** replaces the Lys residue of compound **23** with Arg, an amino acid residue containing a guanidinium group, a planar group with the positive charge delocalized over two different nitrogen atoms. This

delocalization allows for the positive charge to disperse more than the localized positive charge of the one nitrogen of the Lys side chain.[2, 3]

Table 5.1: Amino acid sequences of the peptides used to study the role of spacer #2.

Compound	Amino Acid Sequence
23	Ac-GF-Tic-Oic-G-**K**-Tic-Oic-GF-Tic-Oic-G-**K**-Tic-**K-K-K-K**-$CONH_2$
43	Ac-GF-Tic-Oic-G-**Orn**-Tic-Oic-GF-Tic-Oic-G-**Orn**-Tic-**Orn-Orn-Orn-Orn**-$CONH_2$
45	Ac-GF-Tic-Oic-G-**Dpr**-Tic-Oic-GF-Tic-Oic-G-**Dpr**-Tic-**Dpr-DprDpr-Dpr**-$CONH_2$
53	Ac-GF-Tic-Oic-G-**Dab**-Tic-Oic-GF-Tic-Oic-G-**Dab**-Tic-**Dab-Dab-Dab-Dab**-$CONH_2$
56	Ac-GF-Tic-Oic-G-**Arg**-Tic-Oic-GF-Tic-Oic-G-**Arg**-Tic-**Arg-Arg-Arg-Arg**-$CONH_2$

The in vitro activity of these peptides against several common bacterial strains[1] as well as several gram negative and drug-resistant strains[4] can be seen in **Tables 5.2** and **5.3**, respectively. The activities of this series of compounds were compared to the activity of compound **23** as it has shown broad spectrum activity with minimal hemolysis. Compound **43**, with 3 methylene groups, had increased activity in 8 of the 15 bacterial assays tested in comparison to compound **23**, and retained similar MIC values in the remaining 7. The next shortest spacer, compound **53**, had improved activity in one bacterial assay, lost activity in 4 and retained activity in 10 assays. Compound **45** with the shortest chain had decreased activity in 8 of the 15 assays, the same in 5 and slightly increased activity in 2 concluding that compound **45** is the least active peptide of this series. These results lead to the assumption that as the spacer length decreases, so does the activity. Compound **56** with the guanidinium group was similar to compound **43** in that they both contain three methylene groups. The activity of compound **56**, overall, was very similar to that of compound **23**.

Table 5.2: Minimum inhibitory concentration (μM) of selectra bacteria strains and hemolytic activity.[1]

Compound	*Salmonella typhimurium*	*Staphylococcus aureus* ME/GM/TC resistant	*Mycobacterium ranae*	*Bacillus subtillis*	% hemolysis 100/25 μM
23	10	3	10	1	14%
43	3	3	10	0.3	not tested
45	3	10	100	1	not tested
53	30	10	10	not tested	not tested

Table 5.3: Minimum inhibitory concentration (μM) of specific Gram negative and other drug resistant bacteria strains.[4]

Compound	23	43	53	45	56
Acinetobacter baumanii ATCC 19606	3.2	6.6	3.4	3.6	5.98
Acinetobacter baumanii WRAIR	3.2	6.6	3.4	3.6	24
Staphylococcus aureus ATCC 33591	205	53	220	114	96
Yersinia pestis CO92	205	26.5	220	228	192
Brucella melitensis 16M	205	106	220	288	192
Brucella abortus 2308	205	106	220	288	192
Brucella suis 23444	205	106	220	288	192
Bacillus anthracis AMES	12.8	0.82	6.8	14.8	5.98
Francisella tularensis SCHUS4	100	106	220	228	192
Burkholderia mallei	205	212	220	228	192
Burkholderia pseudomallei	205	212	220	228	192

CD Studies

CD spectra of Spacer #2 peptides in buffer and micelle environments. CD spectra of compounds **23, 43**, **53**, **45** and **56** can be seen in 40 mM phosphate buffer, pH = 6.8 (**Figure 5.1**). All of the peptides exhibited a characteristic α-helical structure with double minima at approximately 208 and 222 nm.[5-9] There also appeared to be the presence of some β-turn components due to the maxima between 195 and 200 nm.[10-12] Overall, the CD spectra of each compound in buffer were very similar in shape with varying intensities that appeared to be random and not associated with the decrease in the side-chain length of the positive residue. The average distances between the side chain amine and the α-carbon of the peptide backbone for each of the Spacer #2 amino acid residues were calculated using ChemDraw 3D, Cambridge Software and are given in **Table 5.4.** Although the distance for Arginine is not listed, we assumed it to be approximately the same distance as Orn from compound **43** as they both contain three methylene groups in their side-chains.

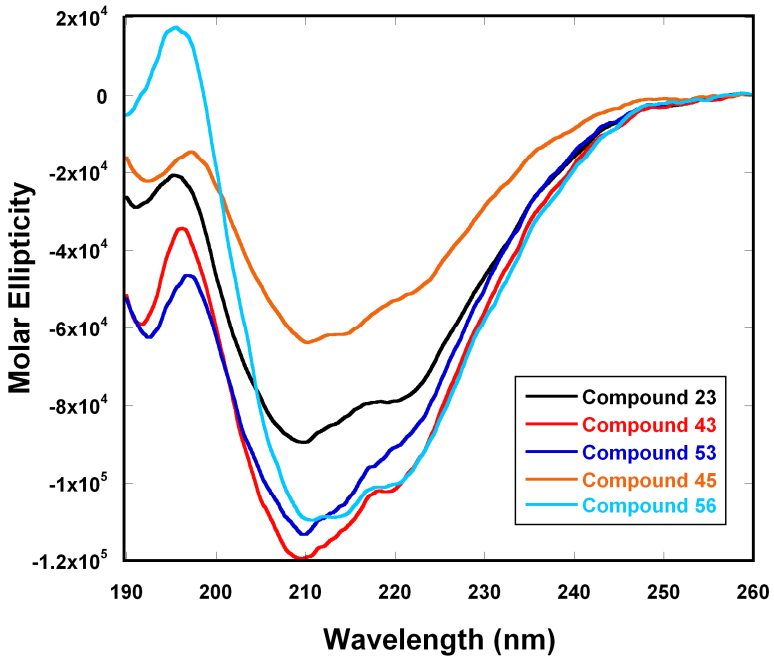

Figure 5.1: Far-UV CD spectra of compounds **23**, **43**, **53**, **45** and **56** (1 mg/mL) in 40 mM phosphate buffer, pH = 6.8.

Table 5.4: Average distances between the side chain amine and the α-carbon of the Spacer #2 amino acid residues.

Peptide ID	23	43	53	45
Residue	Lys	Orn	Dab	Dpr
Average distance	4.76 Å	3.55 Å	2.99 Å	2.56 Å
# of carbons in side-chain	4	3	2	1

In the presence of the negatively charged SDS micelles (**Figure 5.2** – left), all of peptides exhibited a shift in λ_{max} from approximately 195 to 190 nm as well as an increase in intensity. Both of these observations are indicative of an increase in α-helicity.[6, 8, 13, 14] All of the compounds, with the exception of compound **45**, exhibited the very similar shape with different intensities. The compounds with the longer side-chains, **23** and **43**, exhibited very similar intensities below 200 nm but compound **23** was slightly less intense above 200 nm. Compound **53** was less intense at the maximum below 200 nm and at both minima indicating less helical structure.[6, 8, 14] The shift in the minima from approximately 208 to 202 nm suggests an increase in the unordered components of the peptides.[8, 12, 15]

Compound **45**, with the shortest side-chain, exhibited a change in shape from the other peptides at approximately 200 nm which suggests a different interaction with the surface of the anionic membrane. A loss in the intensity at 190 and 202 nm also suggests a loss in ordered structure.[6, 8, 13] This could be due to the extremely short side-chain not allowing enough flexibility for the peptide to adopt the same secondary structures as the other peptides in this series. However, the shape of each spectrum in SDS micelles differed from the corresponding spectrum in buffer indicating that these peptides interact with the surface of the anionic micelle

membrane as they adopted different conformations.[5, 14] This interaction would be expected as the peptides are all highly positively charged.

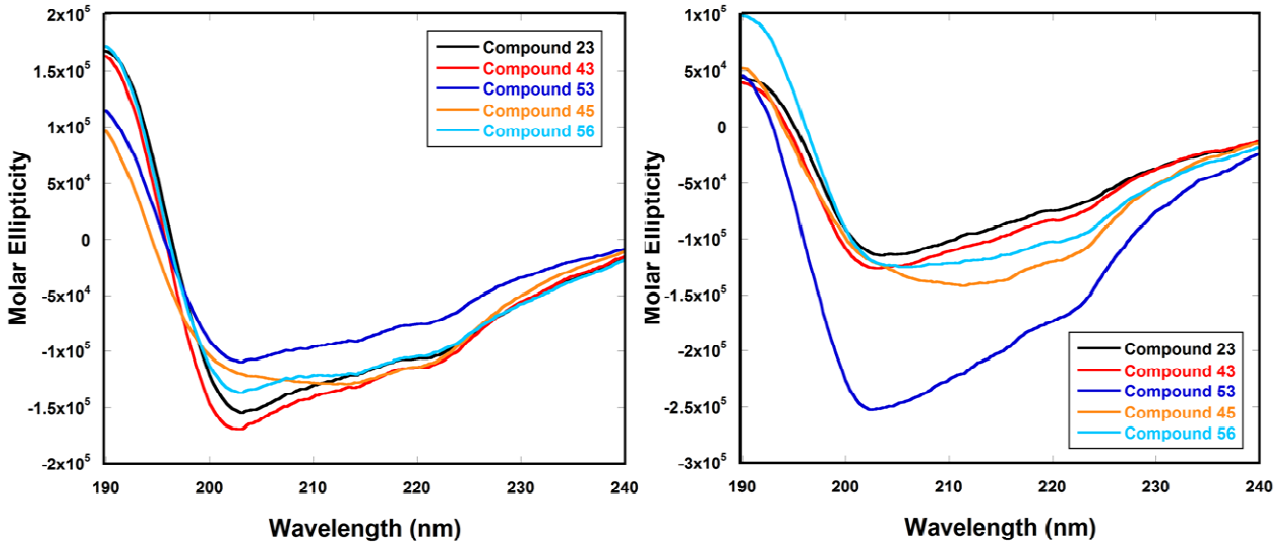

Figure 5.2: Far-UV CD spectra of compounds **23**, **43**, **53**, **45** and **56** in the presence of 80 mM SDS (left) and 80 mM DPC (right) in 40 mM phosphate buffer, pH = 6.8.

As seen in **Figure 5.2** (left)**,** when in the presence of zwitterionic DPC micelles, the shape and intensities of the CD spectra followed the same trend as they did for SDS with shifts to 190 nm and double minima at approximately 202 and 222 nm. Compounds **23** and **43** were essentially identical and very similar to compound **56** which had a slight increase in the intensities at 190 and 222 nm. Compound **53** exhibited the same shape, but the intensity of the spectra was extremely different. The intensity of compound **45** was similar to that of compounds **23** and **43**, but displayed a different shape. The minimum at the lower wavelength was obscured between 205 and 215 nm and not well defined as was the case for the other peptides. As a series,

each spectrum in DPC was significantly different from their corresponding spectra in buffer concluding some level of interaction was occurring. Although the spectra were similar in shape to those in SDS, the intensity was lower, with the exception of compound **53**, indicating less helical componenents.[6, 13, 14]

CD spectra of Spacer #2 peptides in LUV environments. The CD spectra of the five peptides in the presence of 1.75 mM POPC LUVs, the simple zwitterionic membrane model, are presented in **Figure 5.3**. Minimal changes were observed with regards to the intensity and location of the λ_{max} of the spectra in POPC LUVs as compared to buffer. For the double minima above 200 nm, there was no significant shift in the wavelengths, but there were observable changes in the intensities. For compounds **23**, **43** and **53** the intensities increased at approximately 208 nm, remained relatively constant for **56**, while significantly decreasing for compound **45**. The second minimum at approximately 222 nm increased in intensity for compound **23**, remained relatively unchanged for compounds **43** and **53**, decreased for compound **56** and disappeared for compound **45**. The decrease in the intensity of the double minima appeared to increase with the increase in spacer length. This increase in ellipticity of the two α-helical characteristics is indicative of an increase in the ordered structure.[6, 7, 14] As the spacer length increased, the peptide becomes more flexible allowing it to adopt such conformations. Compound **45**, however, does not appear to be ordered as it contains a minimum below 200 nm.[8, 12, 15, 16]

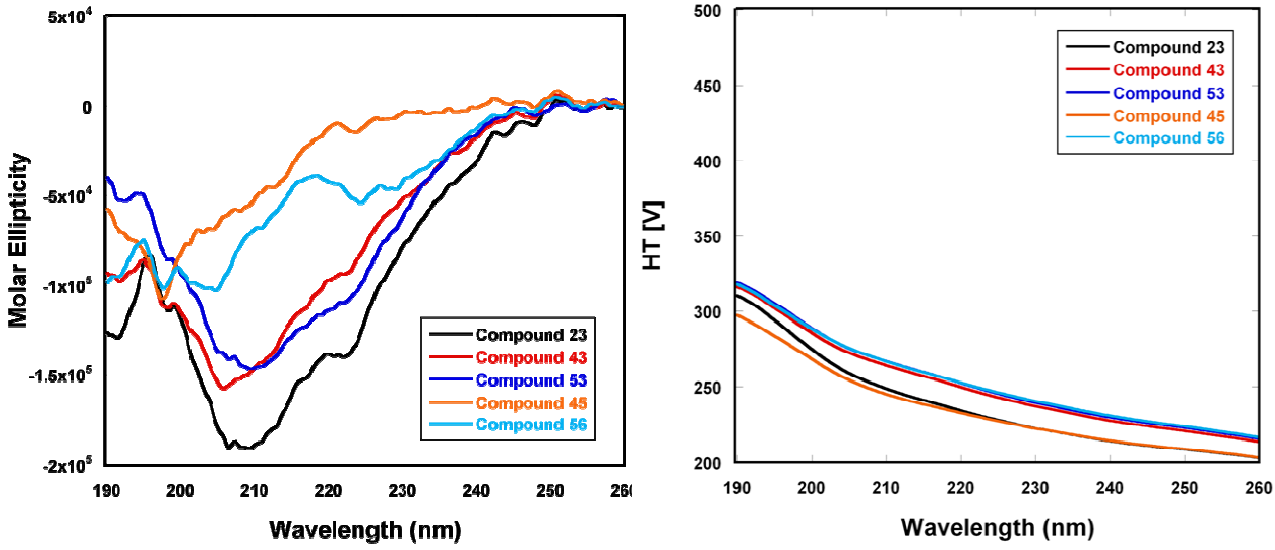

Figure 5.3: Far-UV CD spectra of compounds **23**, **43**, **53**, **45** and **56** in 1.75 mM POPC (left) in 40 mM phosphate buffer, pH = 6.8, and their corresponding HT values (right).

When compared to their spectra in the presence of DPC micelles , these compounds had obvious similarities and differences depending on the peptide. As a whole, there was a significant decrease in the intensity of the maximum below 200 nm suggesting a decrease in α-helicity.[6, 13, 14] However, this observation may be compensated by the shift in minimum from approximately 202 nm in the presence of DPC micelles, a combination of unordered and α-helical components,[8, 15, 16] to 208 nm in POPC LUVs, a characteristic of pure α-helicity.[6, 8, 9] The intensity of both minima increased for compounds **23** and **43**, however, decreased for compounds **53** and **56**. Compound **45** was completely different from its ordered conformation in DPC micelles suggesting different S-state and I-state conformations. Also, compound **45** was not only different from its own spectra in buffer and DPC micelles, but it was also completely different from the spectra of the other peptides. This observation leads to the assumption that compound **45** interacts with zwitterionic bilayers via a completely different mechanism.

As for the spectra of the peptides in the presence of the anionic membrane models, 4:1 POPC/POPG LUVs (**Figure 5.4)**, all of the peptides exhibited a downfield λ_{max} shift, as well as shifts in the minima from approximately 208 to 200 nm when compared to the spectra in buffer. The former suggests an increase in α-helicity[7, 17] while the latter is indicative of a combination of α-helical and unordered structures.[8, 12] Compound **23**, as previously discussed, had an overall increase in the intensity of the spectra supporting the conclusion that it was adopting α-helical characteristics. Overall, the intensity changes of compounds **43**, **53**, **45** and **56** proved minimal.

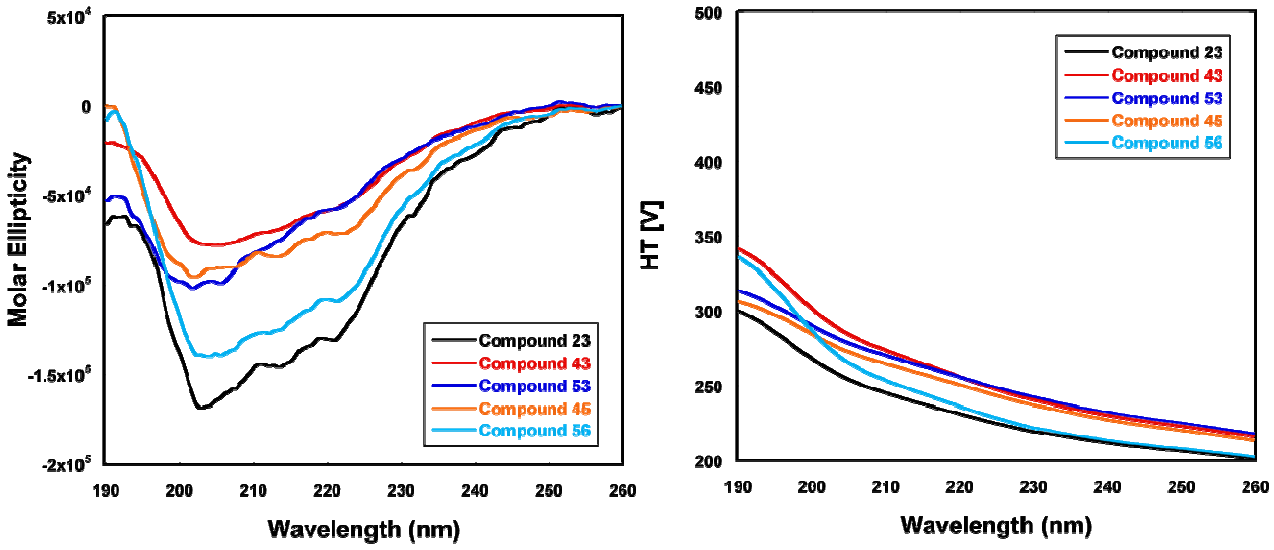

Figure 5.4: Far-UV CD spectra of compounds **23**, **43**, **53**, **45** and **56** in 1.75 mM 4:1 POPC/POPG LUVs in 40 mM phosphate buffer, pH = 6.8, and their corresponding HT values (right).

When compared to the spectra in the presence of SDS micelles, there were significant changes in the intensity of the λ_{max}. Each compound exhibited a decrease in the intensity from SDS micelles to the POPC/POPG bilayer, proposing a decrease in the helical characteristic of the

peptides.[6, 14] This could be due to the fact that these peptides were inserting into the bilayer and losing some of their α-helical component.

"Pseudo" CD Titrations. Pseudo titrations of the peptides with POPC LUVs are given in **Figure 5.5** for compounds **23**, **43**, **53**, **45** and **56**. Although the CD spectra for compounds **23** and **45** in the varying POPC LUV concentrations were clearly different from their spectra in buffer, and compounds **43, 53** and **56** were very similar, overall, the CD spectra did not appear to vary much in conformation when POPC LUV was added. The lack of variation in conformations suggests that the interaction between these peptides and the POPC LUV membrane models was not concentration dependent.[18-20] The spectra at low L/P ratios were very similar to the samples associated with high L/P ratios.

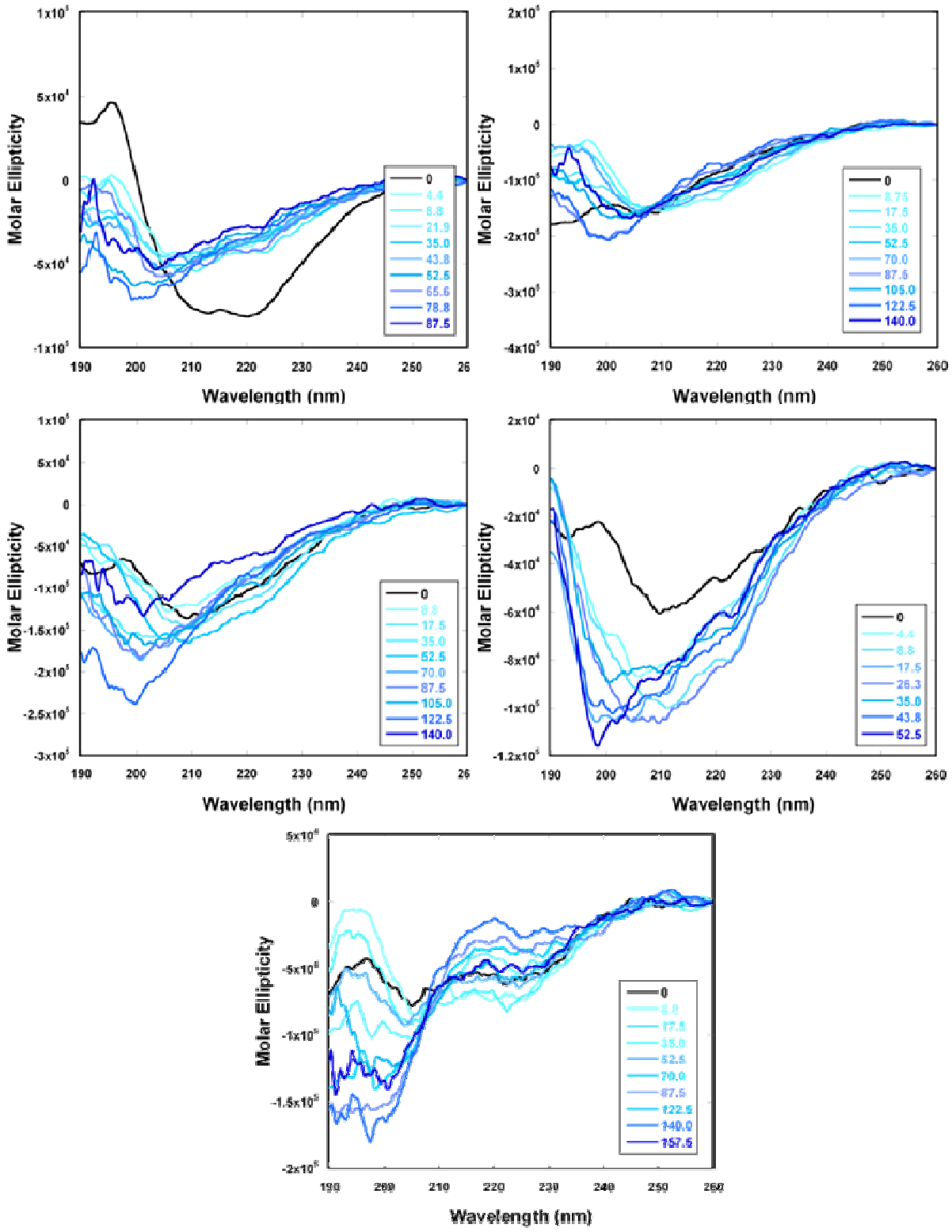

Figure 5.5: Far-UV CD spectra of separate samples of 200 µM compound **23** (top left) and 45 (middle right) and 100 µM solutions of compounds **43** (top right), **53** (middle left) and **56** (bottom) with increasing concentrations of POPC LUVs.[21, 22]

The “pseudo” titrations of these peptides with 4:1 POPC/POPG LUVs (**Figure 5.6**) yielded a very different outcome. The CD spectra of each peptide changed dramatically in shape and intensity from their spectra in buffer with the first introduction of anionic LUVs. The intensity of the spectra for each peptide at low L/P ratios (blue spectra) decreased with increasing LUV concentration. Intensity continued to decrease until a critical ratio was reached in which it became constant (green spectrum). The peptide is assumed to be completely membrane bound at this P/L ratio, which is unique to each peptide.[23, 24] Intensity of the spectra returned with the continuous addition of anionic liposomes (red spectra) and as the L/P continued to decrease. The blue group of spectra is associated with low L/P ratios and there for membrane disrupting processes while the red spectra correspond with high L/P ratios and binding.

A different trend, however, was observed for compounds **45** and **56**. The CD spectra for compound **45** were different from the spectrum in buffer, but the intensity changes of the two minima were minimal with no clear spectra associated with the transition from low to high L/P ratios, or I-state to S-state. Without this observable transition, it is believed that compound **45** does not favor pore formation. Compound **56**, on the other hand, exhibited several different groupings of spectra in comparison to the groups before and after the “critical point” for the compounds **23**, **43** and **53**. There was no discernable increasing or decreasing trend of the spectra as the L/P ratio increased before or after the spectra corresponding to the transition from predominately I-state to S-state (green spectrum). The complexity of the different processes occurring has been attributed to the delocalized positive charge of the guanidinium group, and at this point, cannot be described further.

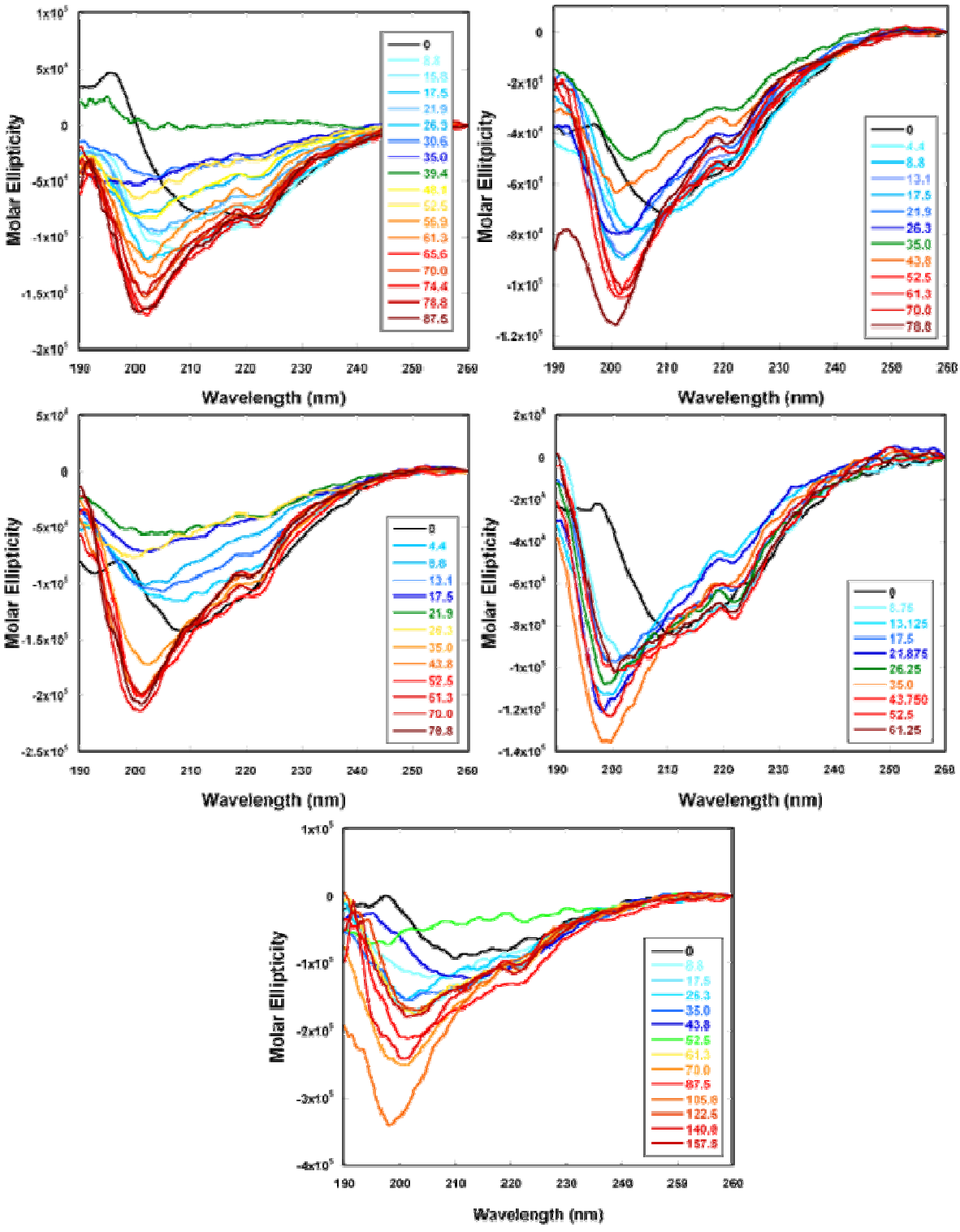

Figure 5.6: Far-UV CD spectra of separate samples of 200 µM compound **23** (top left), **43** (top right), **53** (middle left) and **45** (middle right) and 100 µM solutions of compound **56** (bottom) with increasing concentrations of 4:1 POPC/POPG LUVs.[21, 22]

ITC Studies

Anionic LUV environments. Titrating 4:1 POPC/POPG LUVs into the peptides (**Figure 5.7**) resulted in an endothermic reaction followed by a transition to an exothermic reaction. Overall, the appearance of the thermograms for compounds **23**, **43**, **53** and **56** were very similar. Endothermic phases have been attributed to a combination of several events including electrostatic interactions, the disruption of polar lipid head groups, disruption of the solvation spheres and several other less understood phenomena. The previously mentioned processes are involved with pore formation.[24-27] As the concentration of LUVs continues to increase, the thermogram shifts from an endothermic heat event to an exothermic which has been attributed to the transition from pore formation to pore disintegration. Due to the increased L/P ratios associated with the exothermic phase, the enthalpy of pore disintegration also corresponds to binding processes.[23, 25, 26]

The exothermic phase of each thermogram exhibited a maximum exothermic heat event which was followed by a continuous decrease in ΔH as the L/P ratio increased and the experiment progressed.[22, 27-30] The L/P ratio at the maximum exothermic injection refers to the point in the titration when the processed involved shifts from predominately I-state to S-state[9, 22, 25, 27, 29] and correlates back to the "critical point" (**Figure 5.6** – green spectra) in the "pseudo" CD titrations with 4:1 POPC/POPG LUVs. The endothermic heat event corresponds to low L/P ratios and the blue spectra from the CD titrations while the exothermic phase refers to high L/P and the red spectra.

Compound **45,** with the shortest spacer, exhibited a very different thermogram with the shortest and weakest endothermic component followed by a rapid transition into a very strong exothermic phase. Due to the magnitude of the exothermic component of compound **45**, it is

believed that it favors binding interactions over pore formation.[22, 25, 25, 27] This conclusion is supported by the single set of CD spectra for the "pseudo" titration and the decreased biological activity as compared to the other peptides.

As per the case for the previously discussed peptides, the complexity of this data made it impossible to fit using a current model. However, we were able to make some hypothesis about the meaning of the thermograms. Compounds **23** and **43** were very similar. The sums of their endothermic components[9, 25, 27, 31] had very similar total ΔHs, as well as the most, with approximately +0.80 and +0.90 kcal/mol, respectively, with compound **43** absorbing the most heat. Because endothermic components have been associated with pore formation[9, 25] coupled with the fact that the thermograms did not transition from the endothermic to the exothermic component until a L/P molar ratio of approximately 30, suggests that they both favor pore formation. Compound **43** had the larger cumulative endothermic component, therefore, was the more active of the two. This data coincides with the bioactivity as well as the CD data. In addition, both compounds **23** and **43** produced the least amount of heat for the exothermic component, supporting the idea that they favor pore formation.

Compound **53** absorbed approximately +0.65 kcal/mol followed by compound **45** with the least at 0.01 kcal/mol. Although the sums of the endothermic components for compounds **53** and **45** exhibited the least amount of heat, they produced the most exothermic heat. The cumulative exothermic heat for compound **53** was approximately -0.57 kcal/mol while compound **45** produced the most "binding" heat with -1.44 kcal/mol.[22, 25, 26, 32, 33] This information coupled with the low molar ratios required to transition from the endothermic to the exothermic phase suggests that they favor binding over pore formation for anionic membrane

models.[27] This conclusion is supported by the bioactivity data as they are less active than compounds **23** and **43**.

Compound **56** produced a cumulative endothermic ΔH of less magnitude, with the exception of compound **45**, than the other peptides with approximately +0.39 kcal/mol, but this was compensated with a larger cumulative exothermic component of -0.55 kcal/mol.[25, 27] Two possible explanations for this suggests two different mechanisms for compound **56**, both of which are focused on the role of the guanidinium group at the end of the Spacer #2 side-chain. If compound **56** were involved in pore formation, the decrease in the endothermic component as compared to the other peptides could be attributed to the large positive entity partaking in stronger binding through attractive electrostatic interactions.[22, 25-27] Stronger binding causes an increase in the negative ΔH component, counteracting the positive ΔH produced by pore formation, thus decreasing the overall positive ΔH.[25] The second theory relates compound **56** predominately with surface interactions rather than pore formation and suggests that when the peptide binds to the surface of the membrane, the polar head groups are displaced farther apart to allow for the positively charged guanidinium group.[24] Here again, the negative ΔH of binding counteracts the positive ΔH associated with the disruption of the polar head groups.[25] However, a large enough displacement of the head groups could allow for the leakage of the contents via a "thinning" mechanism similar to the "carpet" model. [18, 19, 24]

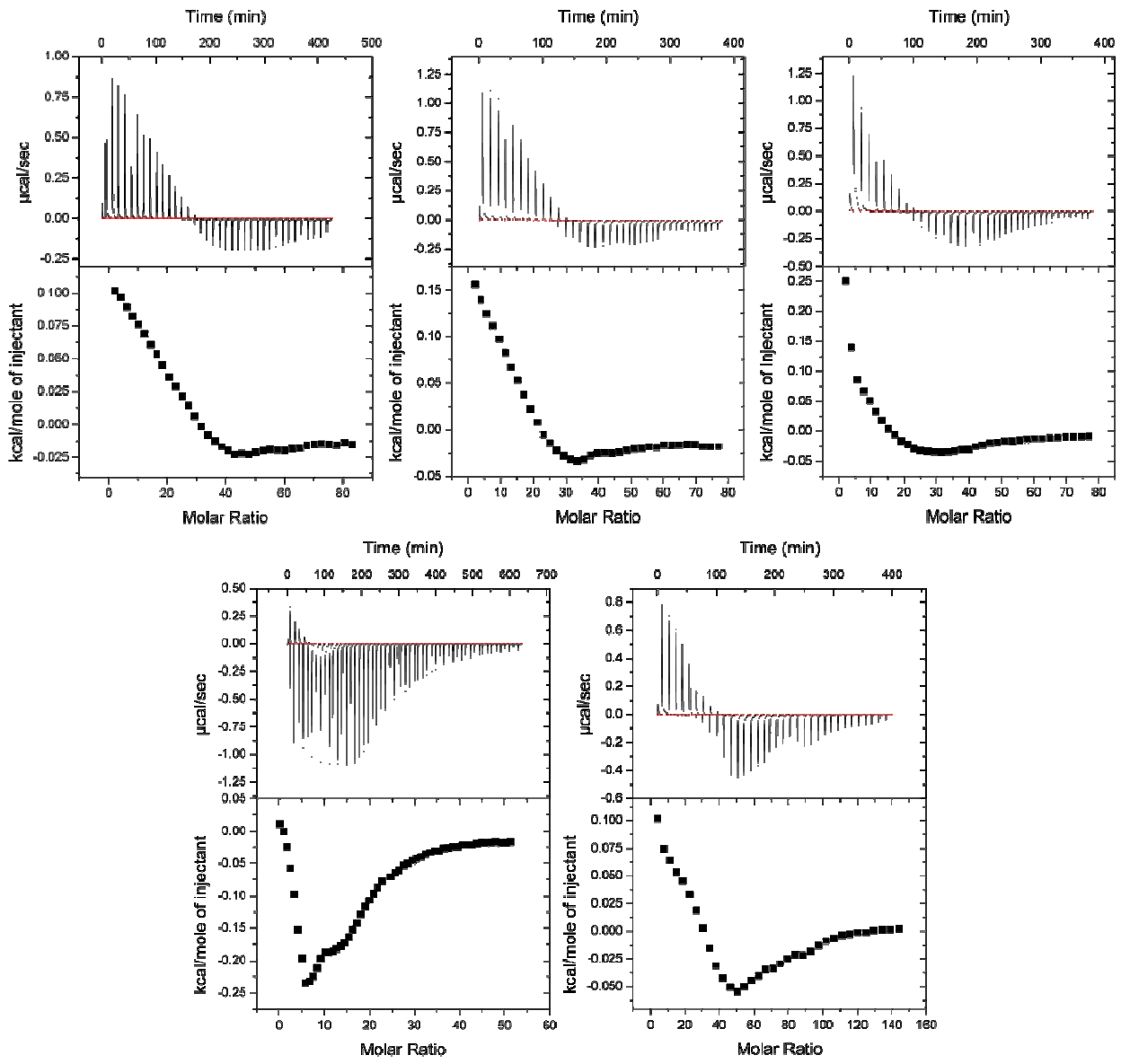

Figure 5.7: Full titration ITC experiment for the titration of 35 mM 4:1 POPC/POPG LUVs into 200 µM compound **23** (top left), compound **43** (top middle), and compound **53** (top right) and 300 µM compound **45** (bottom left) and 100 µM compound **56** (bottom right).

Quantitative data was collected regarding the ΔH associated with binding and pore formation via the single injection experiments previously discussed.[9, 25, 27-29, 33] When titrating dilute peptide solutions into excess lipid to determine the ΔH of binding, compound **56** released

the highest amount of heat with -2.84 kcal/mol. This could be attributed to the larger positively charged side chain which will increase the attractive electrostatic interactions.[25, 27, 33] Compound **43**, the most active peptide with regards to bioactivity, produced the second highest ΔH for binding. Compounds **53** and **45** were very similar and compound **23** produced the lowest ΔH for binding. This could be attributed to the fact that the longer spacer, lysine, allows compound **23** to occupy a larger volume. An increased volume would cause more disruption on the surface of the membrane, thus producing a larger positive ΔH component to counteract the negative ΔH of binding.[24, 25, 27]

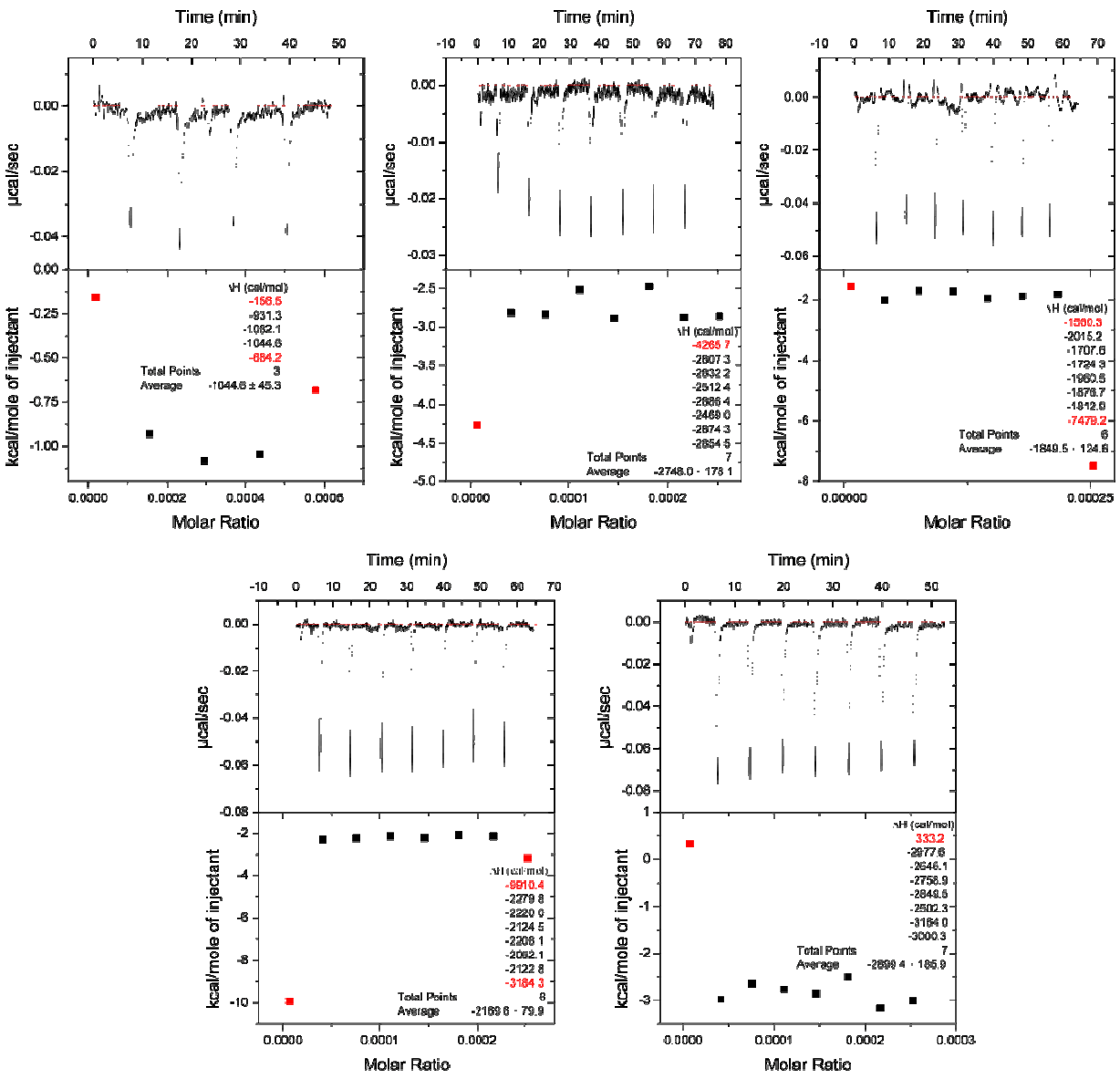

Figure 5.8: Single injection ITC experiments to determine the ΔH of binding for 4:1 POPC/POPG LUVs. A dilute solution of 200 µM compound **23** (top left) was titrated into 15 mM 4:1 POPC/POPG LUVs. Dilute solutions of 100 µM compounds **43** (top middle), **53** (top right), **45** (bottom left) and **56** (bottom right) were titrated into concentrated solutions of 20 mM 4:1 POPC/POPG LUVs to give high L/P ratios.

The titration of these peptides with dilute samples of 4:1 POPC/POPG LUVs proved to give very similar results in regards to the ΔH of pore formation (**Figure 5.9**), with the exception

of compound **45**. The peptide with the shortest positively charged side chain exhibited the least amount of heat, consequently producing injection peaks with both negative and positive components. The split injection peaks suggests that pore formation was not the dominate interaction for this compound.[25, 26]

The guanidinium group of compound **56** also played a large role in the increased ΔH associated with the pore formation. Due to the increased size of the positive charge, more disruption would be caused to the surface of the membrane and the lipid:lipid interactions upon formation of a pore.[24, 27] In addition to the disruption of the membrane composition, larger enthalpies would be involved with the desolvation of both membrane and peptide hydration shells.[22, 27, 34, 35] All of the fore mentioned processes are associated with pore formation and would contribute to the greater positive ΔH. The single injection data for this series in the presence of both zwitterionic and anionic LUVs is summarized in **Table 5.6**.

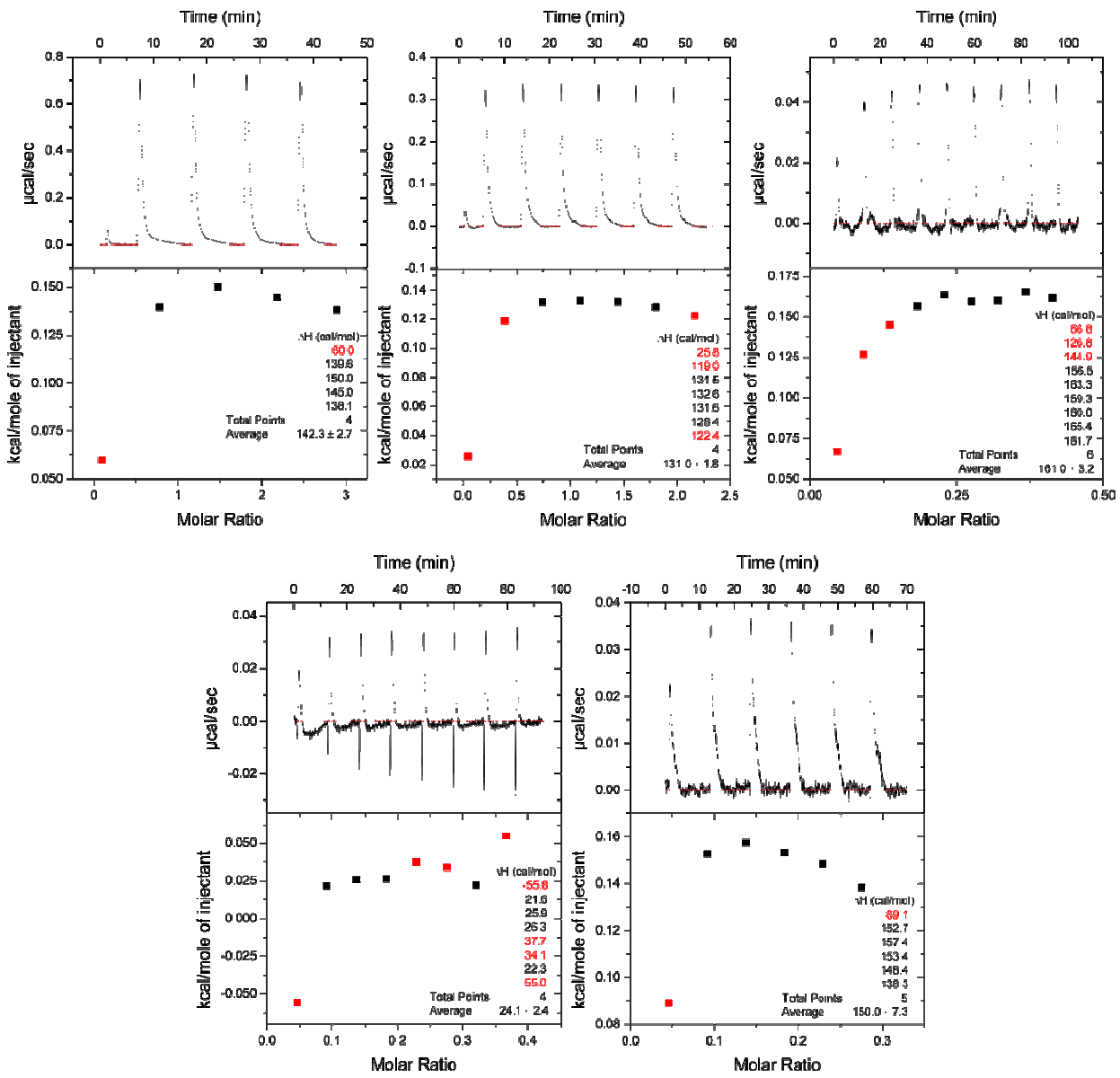

Figure 5.9: Single injection ITC experiments to determine the ΔH of membrane disruption for 4:1 POPC/POPG LUVs. Dilute solutions of 20 mM 4:1 POPC/POPG LUVs were titrated into 300 µM solutions of compound **23** (top left). A 10 mM solution of 4:1 POPC/POPG LUVs was titrated into 300 µM solutions of compounds **43** (top middle), **53** (top right), **45** (bottom left) and **56** (bottom right).

Zwitterionic LUV environments. The titration of POPC LUVs into compounds **23**, **43**, **53** and **56** (**Figure 5.10**) resulted in one endothermic reaction which required large L/P molar ratios

to reach completion. As POPC LUVs were titrated into the peptide solutions, the peptide will be pulled out of solution, decreasing the amount of peptide available left to bind, if binding occurs.[22, 27-30] The above mentioned compounds all required a L/P molar ratio of approximately 120 or more before all of the peptide was assumed bound and removed from the bulk solution. These high molar ratios suggest weak interaction between these compounds and POPC liposomes.[9, 22, 25, 27] However, compound **45** (**Figure 5.10**) reached one hundred percent binding, assumed, at a molar ratio of approximately 50 indicating that the shorter spacer interacts more effectively with zwitterionic liposomes.[27] From a therapeutic perspective, this is undesirable.

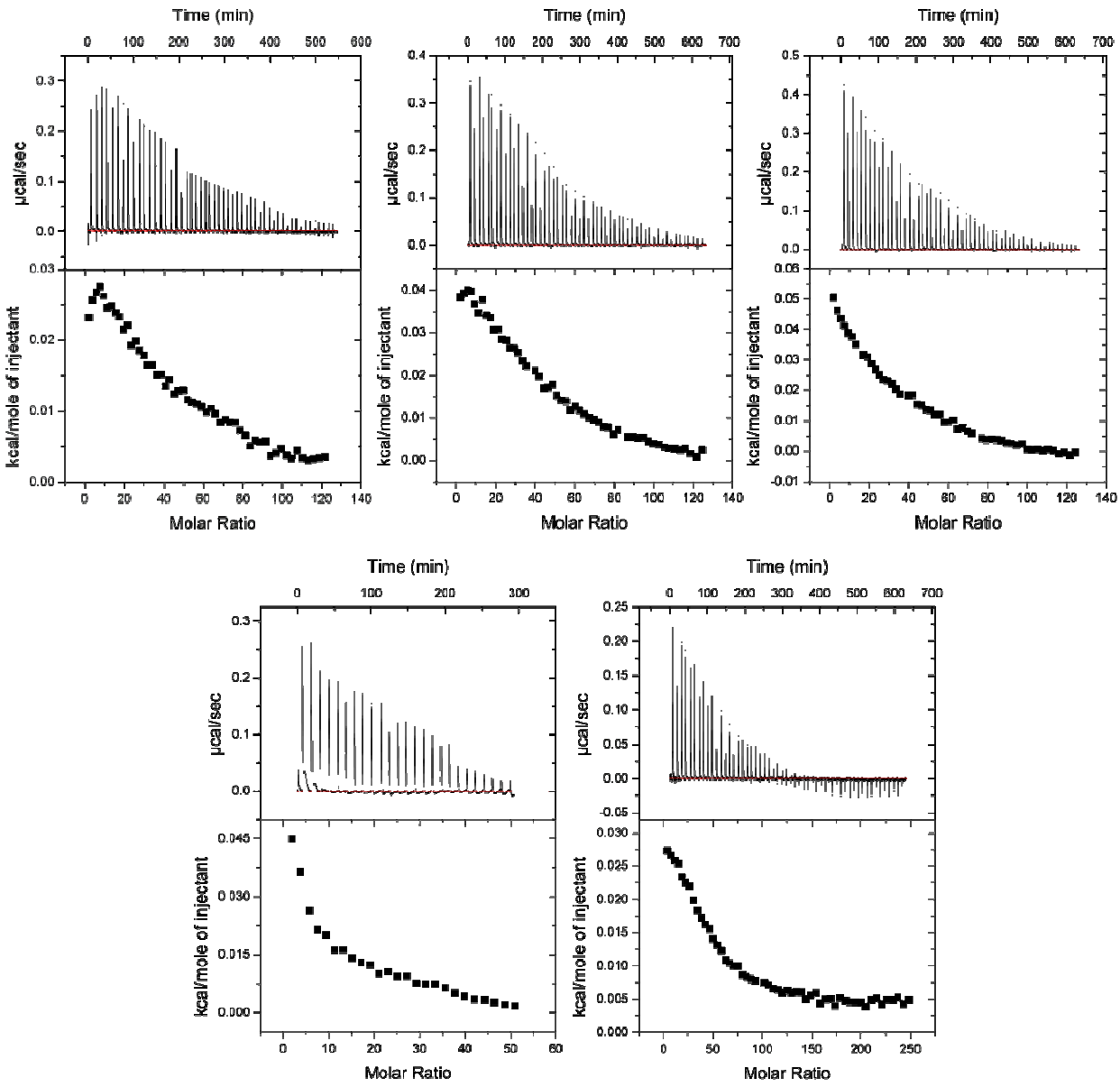

Figure 5.10: Full titration ITC experiment for the titration of 35 mM POPCLUVs into 200 µM compound **23** (top left), **43** (top middle), **53** (top right) and **45** (bottom left) and 100 µM compound **56** (bottom right).

Binding isotherms for the titration with POPC LUVs were developed as previously described by **Equations 1.3** – **1.12** using the experimentally measured ΔH^0 values. With the exception of compound **45**, the plots for the degree of binding, X_b, against the concentration of

peptide free in solution, c_f, did not yield linear relationships as the electrostatic interactions were not accounted for using the model from **Equation 1.9**. The downward bend of these plots has been attributed to the repulsion of the peptides by the membrane bound peptides as the charge of the membrane surface increases.[9, 36] As the spacer length decreases, the relationship between X_b and c_f became more linear suggesting that the compounds were participating in a different mechanism. One explanation is that the peptide is pulled so close to the surface of the membrane, it is adsorbed into the phospholipid head groups and the positively charged face is not exposed to the incoming peptides, thus decreasing the repulsion. The lack of bending for the compounds with the shorter side chains further supports this theory.

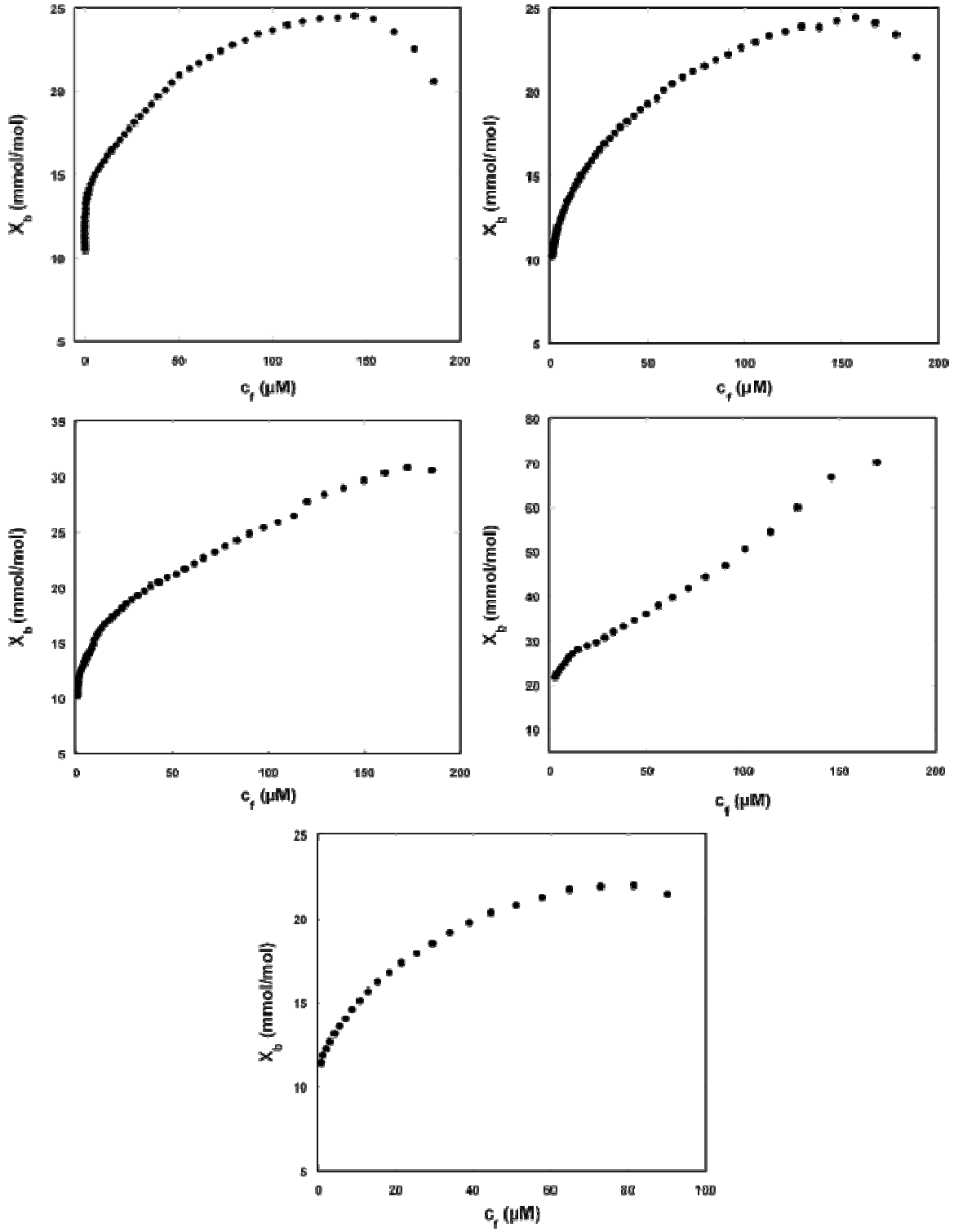

Figure 5.11: Plot for the degree of binding, X_b, as a function of the peptide concentration in bulk solution, c_f. The binding isotherms were derived from the titration of 35 mM POPC LUVs into compounds **23** (top left), **43** (top middle), **53** (top right), **45** (bottom left) and **56** (bottom right). X_b and c_f were calculated as described in chapter 1 of the text.[26, 32]

To factor in the electrostatic interactions between the peptides and membranes that cause an increase in the concentration of peptide immediately above the membrane surface, c_m, the more sophisticated surface partition equilibrium model was used.[23] The peptide concentration at the surface of the membrane was calculated using the equations presented in chapter 1 and a maximum peptide cross-sectional area of 342.4 $Å^2$ for each peptide. Plotting X_b against c_m yielded complex linear relationships with the degree of binding increasing as the length of the spacer decreased. As can be seen in **Figure 5.12**, compounds **23** and **43** exhibited one single line while compounds **43**, **53** and **56** were divided into two distinct phases. The division of the relationship was more distinct with the shorter spacers and compound **56** with the larger positive body, suggesting different mechanisms. This observation supports the theory discussed earlier in regards to the linearity of the X_b versus c_f plots increasing with the decrease in spacer length. The phase at the lower peptide concentration could correspond, as suggested with spacer #1, to the conformational changes the peptides undergo when binding to a peptide-free liposome. As the peptide concentration increases and becomes bound to the surface, the peptides remaining free in solution must undergo an additional change in order to maneuver around the bound peptides. The binding isotherm at higher peptide concentrations could correspond to this additional conformational change. The slopes of the lines were taken as the binding constants, K, and were then used in combination with their corresponding ΔH^0 values to calculate the ΔG and ΔS of the interactions **(Table 5.5)**.

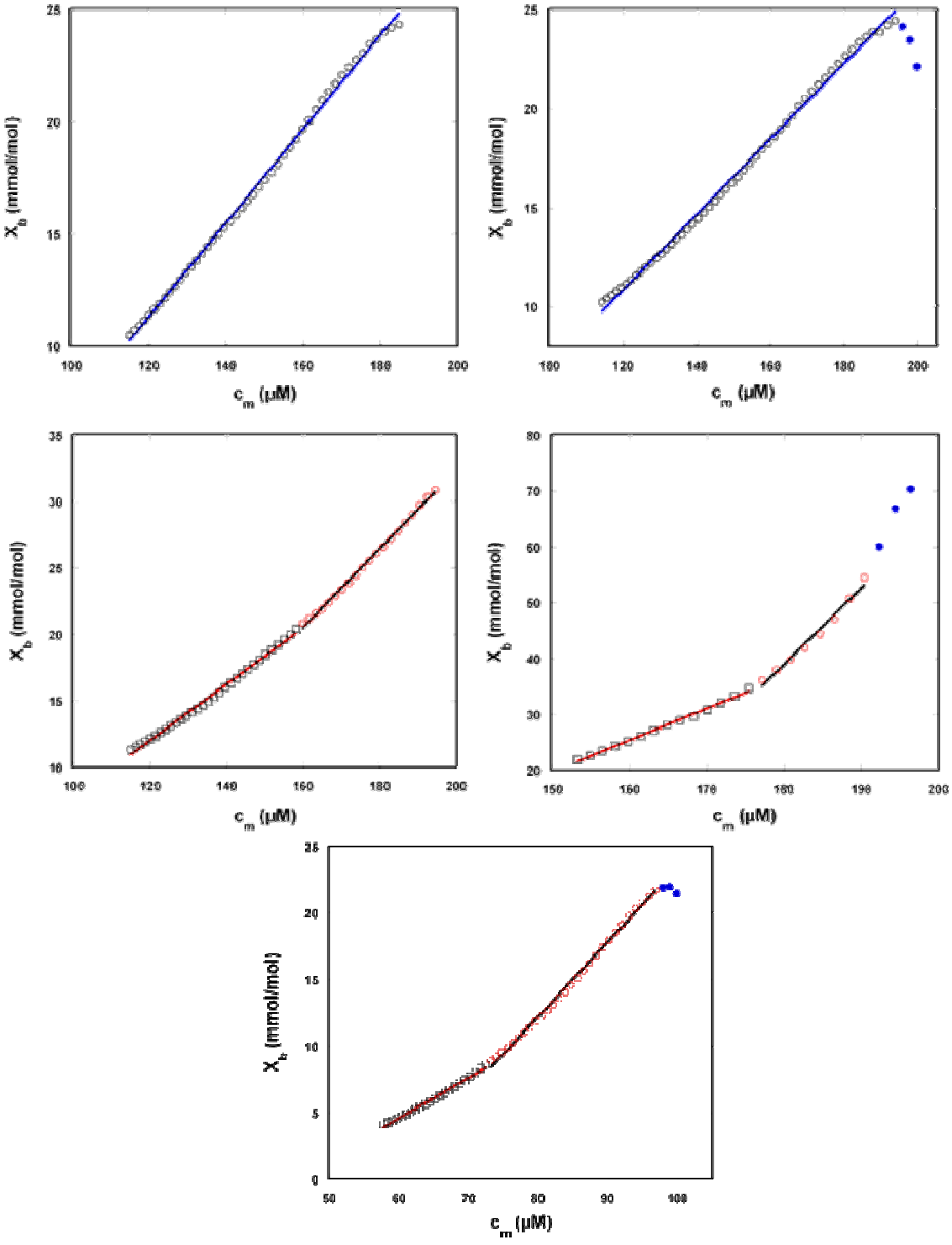

Figure 5.12: Plot for the degree of binding, X_b, as a function of the membrane surface concentration of peptide, c_m. The binding isotherms were derived from the titration of 35 mM POPC LUVs into compounds **23** (top left), **43** (top middle), **53** (top right), **45** (bottom left) and **56** (bottom right). X_b and c_f were calculated as described in Chapter 1 of the text.[26, 32]

In the case of POPC LUVs, a therapeutically relevant compound would produce the least favorable thermodynamic parameters. For this series of peptides, compound **43** has proven to interact the least with zwitterionic membranes, in a thermodynamic matter of speaking. Compound **43** exhibited the least favorable ΔG and lowest K and ΔS values. In comparison, compound **45** interacted the most favorably with POPC LUVs concluding that it would not be a desirable therapeutic agent. Overall, based on the thermodynamic data derived from the binding isotherms, the decreasing spacer length has a negative effect on the binding with POPC LUVs. Increasing the size of the positive charge increased binding constants and entropy in comparison to compound **23** and **43**, however, it still exhibited a more favorable interaction than compound **45**, possibly due to electrostatic repulsions.

Table 5.5: Thermodynamic data for a representative titration of 35 mM POPC into the peptides at 25°C as derived from the equations discussed previously.

Compound	$\Delta H^{0,a}$ (kcal/mol)	K^b (M^{-1})	ΔG^c (kcal/mol)	ΔS^d (cal/mol·K)
Lower Peptide Concentration				
23	na	na	na	na
43	na	na	na	na
53	0.51	211.27	-5.54	20.33
45	0.15	569.50	-6.13	21.09
56	-0.23	304.17	-5.76	18.57
Higher Peptide Concentration				
23	0.67	211.00	-5.54	20.84
43	1.26	190.68	-5.48	22.64
53	0.98	296.02	-5.74	22.57
45	0.22	1364.50	-6.65	23.06
56	1.02	561.70	-6.12	23.98
Magainin 2 amide[e]				
M2a[e]	-15.9	2000.0	-7.0	-29.4

[a] ΔH values were calculated using **Equation 1.4** from chapter 1 using the binding enthalpies measured directly from the experiment.
[b] K values were generated from the lipid-into-peptide titration using the calculations as described in chapter 1.
[c] ΔG values were calculated using **Equation 1.1** from chapter 1.
[d] ΔS was calculated using **Equation 1.2** from chapter 1.
[e] The thermodynamic parameters for the magainin analogue M2a as presented by Wieprecht et. al. [28]

Single injection experiments for the titration of dilute samples of peptide into zwitterionic LUVs (**Figure 5.13**) yielded ΔH values that became more negative, favorable, as the side-chain length decreased. Binding interactions involve both positive and negative contributions to the ΔH values, but the more dominant process will be observed.[25, 27] The increased negativity of the ΔH of binding as the spacer length decreases supports the previous conclusion that the shorter side-chains allow for more favorable binding with POPC LUVs, a therapeutically unfavorable event. This trend could be attributed to the ability for the peptide to position itself closer to the membrane surface, thus allowing for the hydrophobic side-chains to insert and bind.

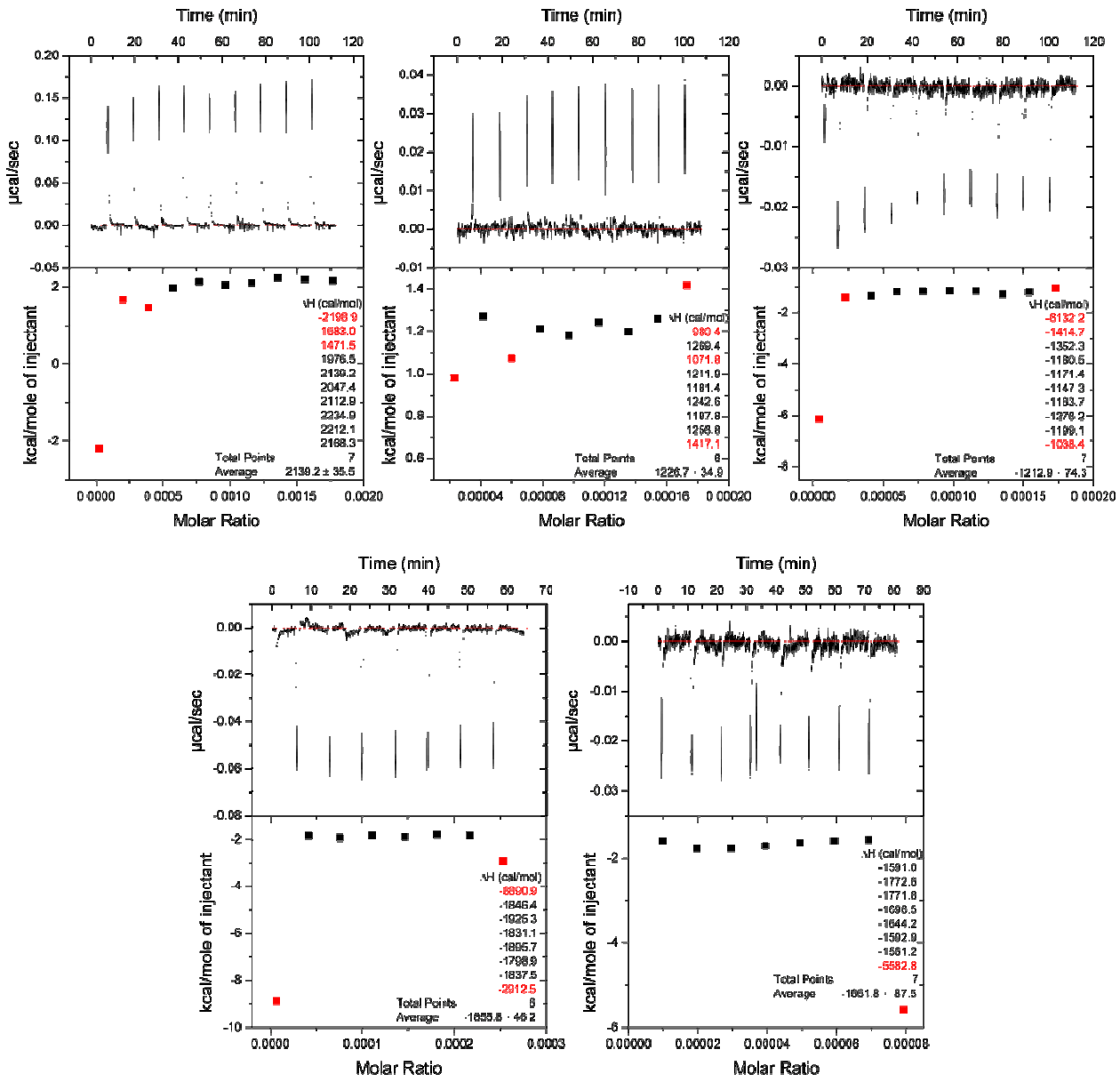

Figure 5.13: Single injection ITC experiments to determine the ΔH of binding for POPC LUVs. A dilute solution of 200 µM compound **23** (top left) was titrated into 15 mM POPC LUVs. Dilute solutions of 100 µM compounds **43** (top middle), **53** (top right) and **45** (bottom left) were titrated into 30 mM POPC LUVS. A dilute solution of 100 µM compound **56** (bottom right) was titrated into 35 mM POPC LUVs to give high L/P ratios.

There was not a significant change in the ΔH associated with membrane disruption for POPC LUVs (**Figure 5.14**), but there was an increase, once again, with the decrease in spacer

length. One must remember that every pore forming process is accompanied by a thermodynamically counteracting binding process.[25] Keeping this in mind, it is quickly realized that the ΔH for pore formation would be much greater, especially in the case of compound **45.** The positive ΔH for pore formation required to overcome the -3.02 kcal/mol associated with binding would be very large. The single injection experiment data is summarized in **Table 5.6**.

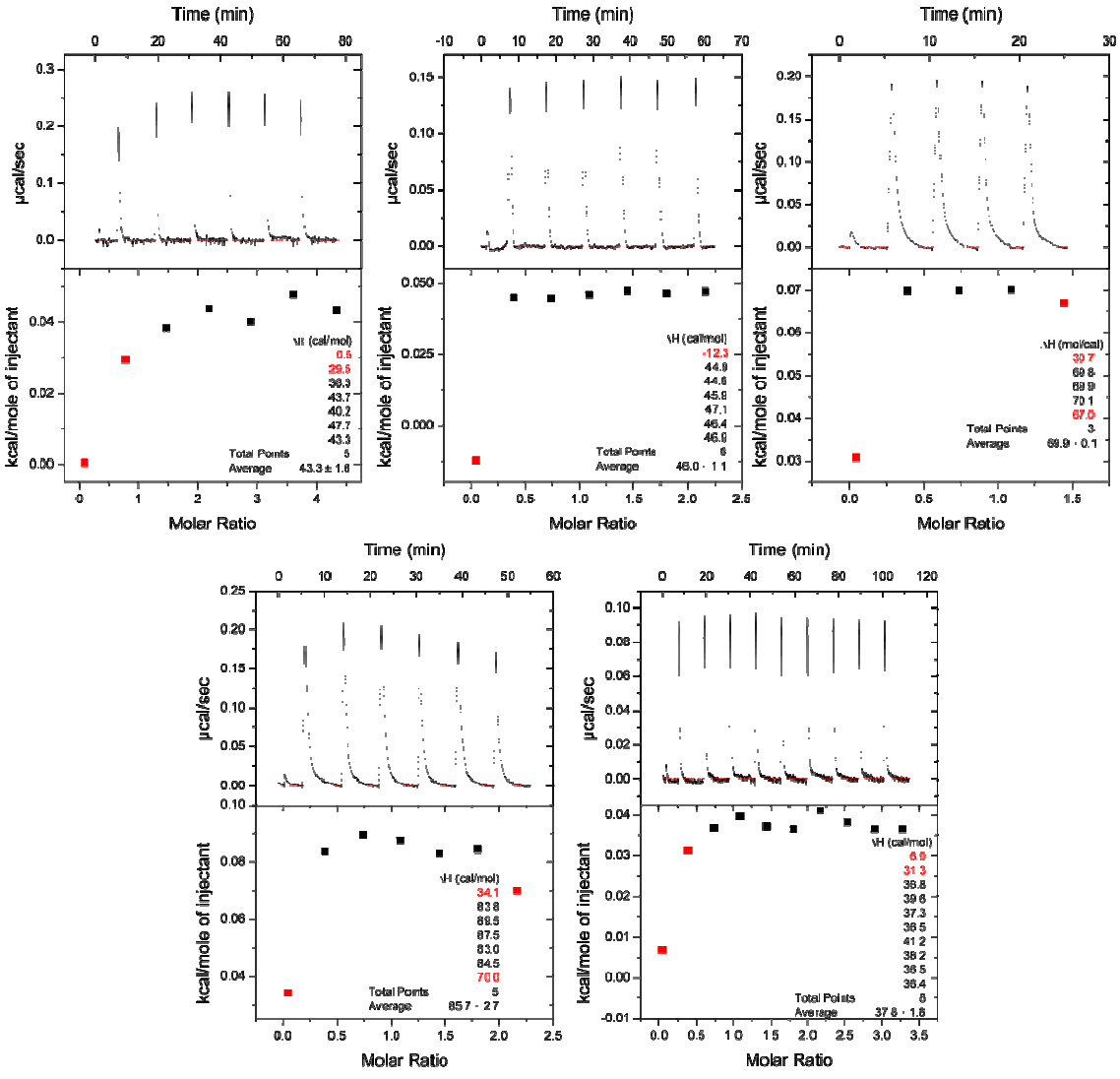

Figure 5.14: Single injection ITC experiments to determine the ΔH of membrane disruption for POPC LUVs. Dilute solutions of 20 mM POPC LUVs were titrated into 300 µM solutions of compound **23** (top left). A 10 mM solution of POPC LUVs was titrated into 300 µM solutions of compounds **43** (top middle), **53** (top right), **45** (bottom left) and **56** (bottom right).

Table 5.6: ΔH (kcal/mol) values for the binding and membrane disruption of 4:1 POPC/POPG and POPC LUVs as determined by single injection ITC experiments.

Compound	4:1 POPC/POPG into Compound	Compound into 4:1 POPC/POPG	POPC into Compound	Compound into POPC
23	0.14 ± 0.03	-1.00 ± 0.04	0.04 ± 0.00	2.10 ± 0.04
43	0.13 ± 0.00	-2.75 ± 0.18	0.05 ± 0.00	1.23 ± 0.03
53	0.16 ± 0.00	-1.85 ± 0.12	0.07 ± 0.00	-1.21 ± 0.07
45	0.02 ± 0.00	-1.86 ± 0.05	0.09 ± 0.00	-3.02 ± 0.14
56	0.15 ± 0.00	-2.90 ± 0.19	0.04 ± 0.00	-1.66 ± 0.09

Calcein Leakage Studies

Peptide induced calcein leakage from POPC LUVs was determined and presented in **Figure 5.15**. The leakage of calcein increased with a decrease in spacer length. Compound **23**, with the longest spacer, produced the least amount of leakage at a concentration of 20 μM with approximately 30%. Compound **43** increased the leakage to approximately 50% followed by compound **53** at 70% total leakage. Even at the lowest peptide concentration of 4 μM, compound **45** induced the maximum leakage for POPC LUVs. As can be seen in **Figure 5.15** and further highlighted in **Figure 5.17** (left), the peptide induced calcein leakage does not appear to be concentration dependent, except for possibly compound **45**, which appears to significantly increase from 8 to 12 μM.

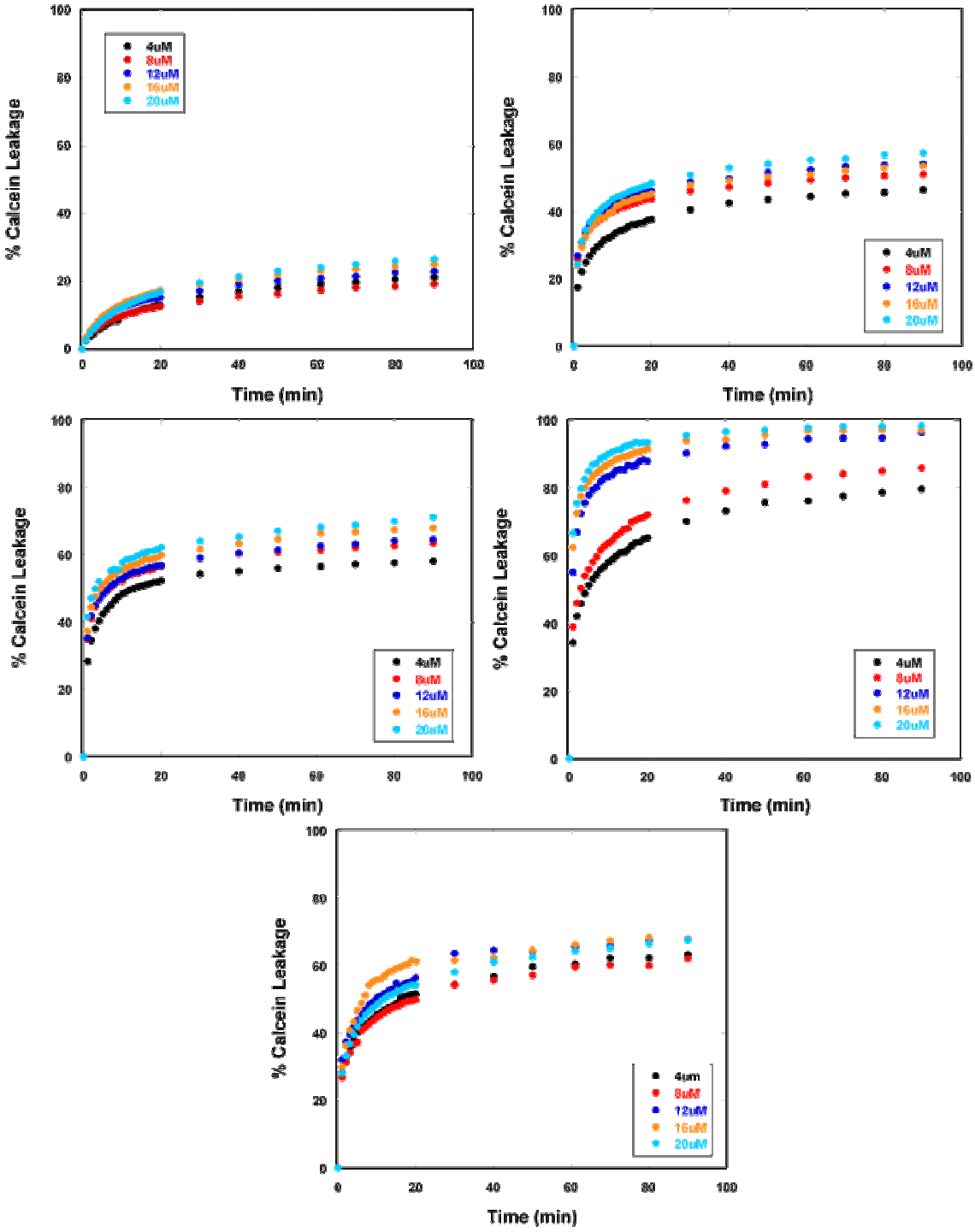

Figure 5.15: The time dependent release of calcein from POPC LUVs induced by increasing concentrations of compounds **23** (top left), **43** (top right), **53** (middle left), **45** (middle right) and **56** (bottom) as measured by fluorescence.[37-39]

This trend, however, was not the case for the peptide induced leakage of calcein from 4:1 POPC/POPG LUVs (**Figure 5.16**). As the concentration of the peptide increases, the leakage of calcein also increases, which is further highlighted in **Figure 5.17** – right. Another obvious trend was the increase of the leakage as the spacer length decreases. Although this does not support the bioactivity data as compounds **23** and **43** were the most biologically active and compound **45** the least, there are two possible explanations. One, the liposomes used are very simple models and do not mimic the surfaces of all bacterial strains that could be presented to the peptides. Another explanation for the increased leakage caused by the compounds which are, biologically, less active could involve the distance between the peptide backbone and the membrane surface. With shorter side-chains, the peptide must reside closer to the surface in order for the hydrophobic side chains to insert, binding the peptide to the liposome. Due to the close proximity, the peptides may be adsorbed into the region of phospholipid head groups causing greater displacement. This process could cause calcein leakage through a membrane "thinning" mechanism similar to that of the "carpet" model,[18, 19, 24] rather than actual pores. With the higher degree of binding observed by the compounds with shorter spacers, there would be an increase the calcein leakage as compared to the other compounds. As for the case of compound **56**, the guanidinium group requires a larger space, thus forming larger pores and increased leakage as compared to the other peptides.

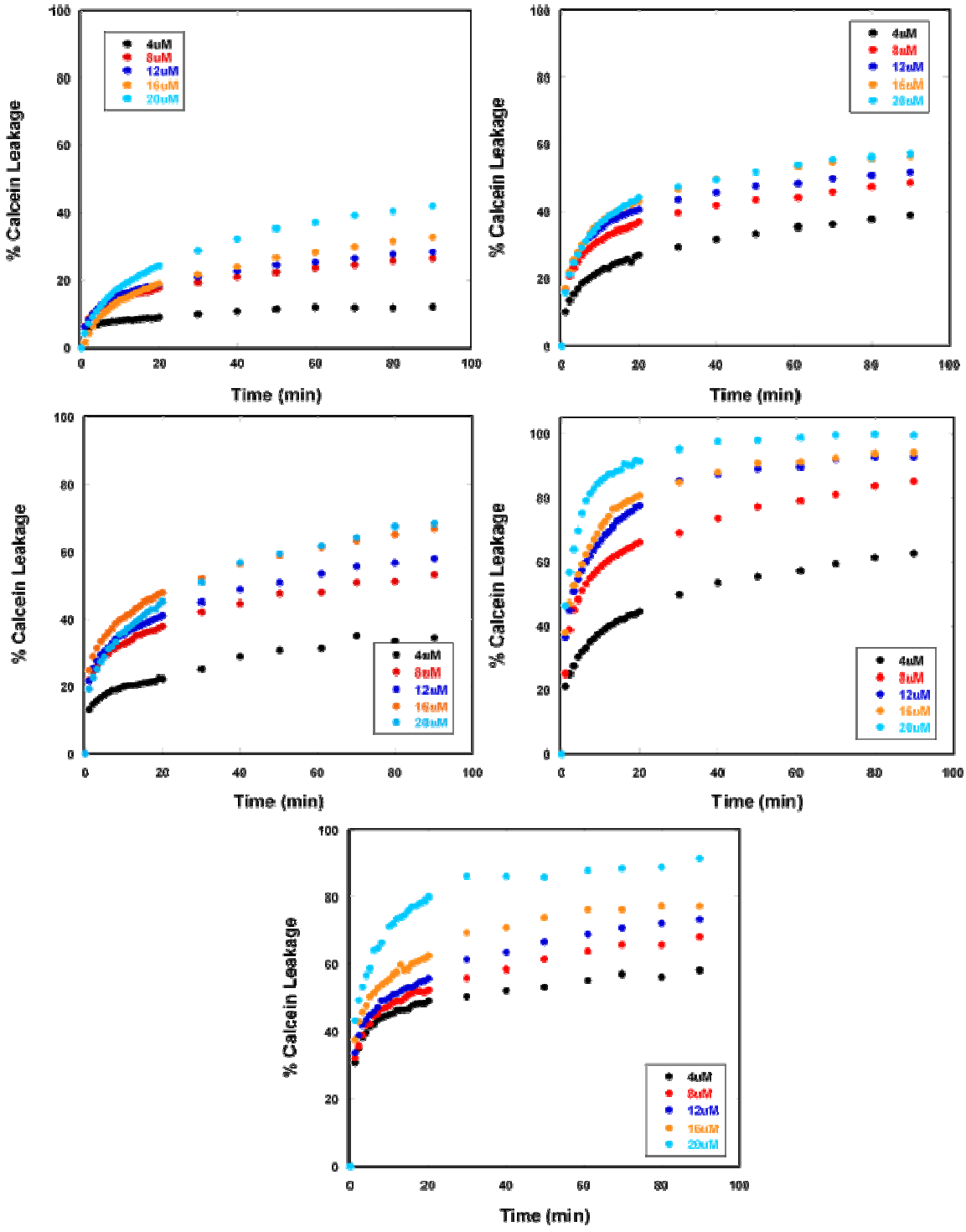

Figure 5.16: The time dependent release of calcein from 4:1 POPC/POPG LUVs induced by increasing concentrations of compounds **23** (top left), **43** (top right), **53** (middle left), **45** (middle right) and **56** (bottom) as measured by fluorescence.[37-39]

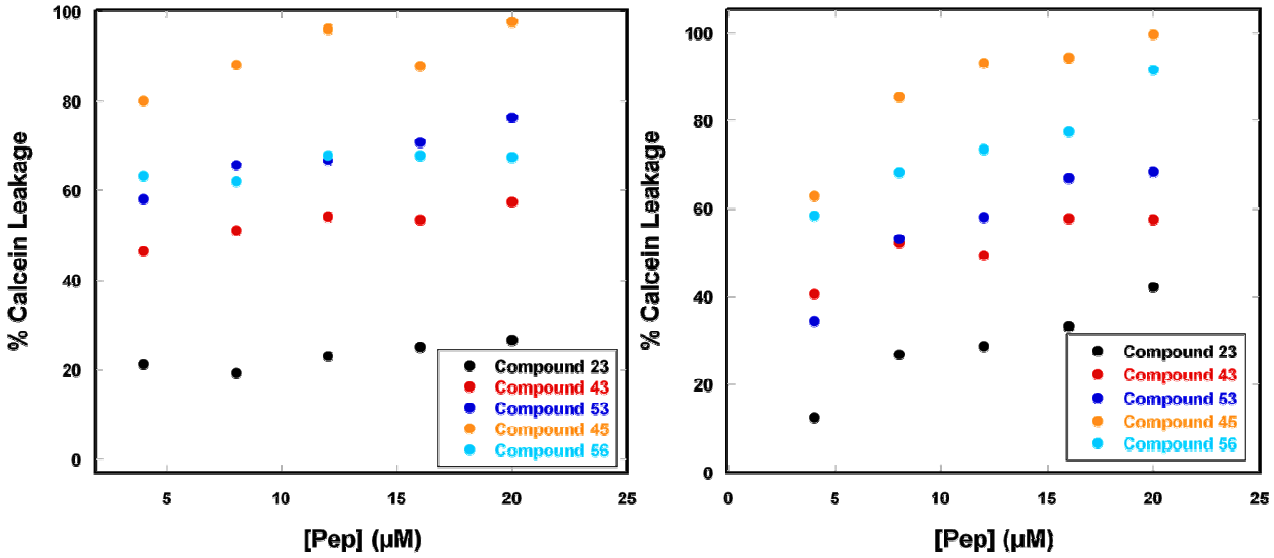

Figure 5.17: The total percent of calcein leakage from POPC (left) and 4:1 POPC/POPG LUVs induced by increasing concentrations of compounds **23**, **43**, **53**, **45** and **56** as measured by fluorescence.

Conclusion

It is clear that the CD, ITC and calcein leakage data support the observed in vitro MIC activity data and serves as evidence that the length of Spacer #2 plays an important role in defining the mechanism of action between this series of peptides and zwitterionic and anionic membrane models. We hypothesized that because Spacer #2 defined the distance between the peptide backbone and the positively charged amine group, it would determine the overall surface charge density of the peptide as well as the distance between the peptide backbone and membrane surfaces. The different conformations adopted as observed by CD coupled with the different thermodynamic mechanisms studied via ITC support this hypothesis.

There is an obvious optimal length of Spacer #2 that promotes antibacterial activity while maintaining minimal interaction with zwitterionic membranes. Compound **43**, with the carbon spacer Orn, exhibited increased antibacterial activity in vitro as well as with the anionic membrane models, but showed minimal interactions with the zwitterionic membranes.

Compound **45**, on the other hand, contained the shortest spacer and also exhibited the greatest interaction with zwitterionic membranes, a therapeutically undesirable quality. Knowing the effect that the length of the positively charge residue will aid in future design and development of novel AMPs as therapeutic agents.

References

(1) Hicks, R. P.; Bhonsle, J. B.; Venugopal, D.; Koser, B. W.; Magill, A. J. De Novo Design of Selective Antibiotic Peptides by Incorporation of Unnatural Amino Acids. *J. Med. Chem.* **2007**, *50*, 3026-3036.

(2) Vogel, H. J.; Schibli, D. J.; Jing, W.; Lohmeier-Vogel, E. M.; Epand, R. F.; Epand, R. M. Towards a structure-function analysis of bovine lactoferricin and related tryptophan- and arginine-containing peptides. *Biochem. Cell Biol.* **2002**, *80*, 49-63.

(3) Haug, B. E.; Strom, M. B.; Svendsen, J. S. The medicinal chemistry of short lactoferricin-based antibacterial peptides. *Curr. Med. Chem.* **2007**, *14*, 1-18.

(4) Venugopal, D.; Klapper, D.; Srouji, A. H.; Bhonsle, J. B.; Borschel, R.; Mueller, A.; Russell, A. L.; Williams, B. C.; Hicks, R. P. Novel antimicrobial peptides that exhibit activity against select agents and other drug resistant bacteria. *Bioorg. Med. Chem.* **2010**, *18*, 5137-5147.

(5) Olofsson, A.; Borowik, T.; Gröbner, G.; Sauer-Eriksson, A. E. Negatively Charged Phospholipid Membranes Induce Amyloid Formation of Medin via an α-Helical Intermediate. *J. Mol. Biol.* **2007**, *374*, 186-194.

(6) Richardson, J. M.; Makhatadze, G. I. Temperature Dependence of the Thermodynamics of Helix–Coil Transition. *J. Mol. Biol.* **2004**, *335*, 1029-1037.

(7) Dathe, M.; Schumann, M.; Wieprecht, T.; Winkler, A.; Beyermann, M.; Krause, E.; Matsuzaki, K.; Murase, O.; Bienert, M. Peptide Helicity and Membrane Surface Charge Modulate the Balance of Electrostatic and Hydrophobic Interactions with Lipid Bilayers and Biological Membranes. *Biochemistry (N. Y.)* **1996**, *35*, 12612-12622.

(8) Glukhov, E.; Stark, M.; Burrows, L. L.; Deber, C. M. Basis for selectivity of cationic antimicrobial peptides for bacterial versus mammalian membranes. *J. Biol. Chem.* **2005**, *280*, 33960-33967.

(9) Nomura, K.; Corzo, G. The effect of binding of spider-derived antimicrobial peptides, oxyopinins, on lipid membranes. *Biochimica et Biophysica Acta (BBA) - Biomembranes* **2006**, *1758*, 1475-1482.

(10) Brahms, S.; Brahms, J.; Spach, G.; Brack, A. Identification of beta,beta-turns and unordered conformations in polypeptide chains by vacuum ultraviolet circular dichroism. *Proc. Natl. Acad. Sci. U. S. A.* **1977**, *74*, 3208-3212.

(11) Ganesh, S.; Jayakumar, R. Circular dichroism and Fourier transform infrared spectroscopic studies on self-assembly of tetrapeptide derivative in solution and solvated film. *The Journal of Peptide Research* **2003**, *61*, 122-128.

(12) Oglęcka, K.; Lundberg, P.; Magzoub, M.; Göran Eriksson, L. E.; Langel, Ü.; Gräslund, A. Relevance of the N-terminal NLS-like sequence of the prion protein for membrane perturbation effects. *Biochimica et Biophysica Acta (BBA) - Biomembranes* **2008**, *1778*, 206-213.

(13) Christiaens, B.; Grooten, J.; Reusens, M.; Joliot, A.; Goethals, M.; Vandekerckhove, J.; Prochiantz, A.; Rosseneu, M. Membrane interaction and cellular internalization of penetratin peptides. *European Journal of Biochemistry* **2004**, *271*, 1187-1197.

(14) Sanavio, B.; Piccoli, A.; Gianni, T.; Bertucci, C. Helicity propensity and interaction of synthetic peptides from heptad-repeat domains of herpes simplex virus 1 glycoprotein H: A circular dichroism study. *Biochimica et Biophysica Acta (BBA) - Proteins & Proteomics* **2007**, *1774*, 781-791.

(15) Wang, P.; Bang, J.; Kim, H. J.; Kim, J.; Kim, Y.; Shin, S. Y. Antimicrobial specificity and mechanism of action of disulfide-removed linear analogs of the plant-derived Cys-rich antimicrobial peptide Ib-AMP1. *Peptides* **2009**, *30*, 2144-2149.

(16) Jing, W.; Demcoe, A. R.; Vogel, H. J. Conformation of a bactericidal domain of puroindoline a: structure and mechanism of action of a 13-residue antimicrobial peptide. *J. Bacteriol.* **2003**, *185*, 4938-4947.

(17) Nielsen, S. B.; Otzen, D. E. Impact of the antimicrobial peptide Novicidin on membrane structure and integrity. *J. Colloid Interface Sci.* **2010**, *345*, 248-256.

(18) Chen, F. Y.; Lee, M. T.; Huang, H. W. Evidence for membrane thinning effect as the mechanism for peptide-induced pore formation. *Biophys. J.* **2003**, *84*, 3751-3758.

(19) Almeida, P. F.; Pokorny, A. Mechanisms of Antimicrobial, Cytolytic, and Cell-Penetrating Peptides: From Kinetics to Thermodynamics. *Biochemistry (N. Y.)* **2009**, *48*, 8083-8093.

(20) Lee, M. T.; Hung, W. C.; Chen, F. Y.; Huang, H. W. Mechanism and kinetics of pore formation in membranes by water-soluble amphipathic peptides. *Proc. Natl. Acad. Sci. U. S. A.* **2008**, *105*, 5087-5092.

(21) Hunter, H. N.; Jing, W.; Schibli, D. J.; Trinh, T.; Park, I. Y.; Kim, S. C.; Vogel, H. J. The interactions of antimicrobial peptides derived from lysozyme with model membrane systems. *Biochimica et Biophysica Acta (BBA) - Biomembranes* **2005**, *1668*, 175-189.

(22) Wen, S.; Majerowicz, M.; Waring, A.; Bringezu, F. Dicynthaurin (ala) Monomer Interaction with Phospholipid Bilayers Studied by Fluorescence Leakage and Isothermal Titration Calorimetry. *The Journal of Physical Chemistry B* **2007**, *111*, 6280-6287.

(23) Wieprecht, T.; Apostolov, O.; Beyermann, M.; Seelig, J. Membrane Binding and Pore Formation of the Antibacterial Peptide PGLa: Thermodynamic and Mechanistic Aspects. *Biochemistry (N. Y.)* **2000**, *39*, 442-452.

(24) Wieprecht, T.; Apostolov, O.; Seelig, J. Binding of the antibacterial peptide magainin 2 amide to small and large unilamellar vesicles. *Biophys. Chem.* **2000**, *85*, 187-198.

(25) Wenk, M. R.; Seelig, J. Magainin 2 Amide Interaction with Lipid Membranes: Calorimetric Detection of Peptide Binding and Pore Formation. *Biochemistry (N. Y.)* **1998**, *37*, 3909-3916.

(26) Wieprecht, T.; Seelig, J. Isothermal Titration Calorimetry for Studying Interactions between Peptides and Lipid Membranes. *Current Topics in Membranes* **2002**, *52*, 31-55.

(27) Abraham, T.; Lewis, R. N. A. H.; Hodges, R. S.; McElhaney, R. N. Isothermal Titration Calorimetry Studies of the Binding of a Rationally Designed Analogue of the Antimicrobial Peptide Gramicidin S to Phospholipid Bilayer Membranes. *Biochemistry (N. Y.)* **2005**, *44*, 2103-2112.

(28) Wieprecht, T.; Beyermann, M.; Seelig, J. Binding of Antibacterial Magainin Peptides to Electrically Neutral Membranes: Thermodynamics and Structure. *Biochemistry (N. Y.)* **1999**, *38*, 10377-10387.

(29) Wieprecht, T.; Beyermann, M.; Seelig, J. Thermodynamics of the coil–α-helix transition of amphipathic peptides in a membrane environment: the role of vesicle curvature. *Biophys. Chem.* **2002**, *96*, 191-201.

(30) Seelig, J.; Nebel, S.; Ganz, P.; Bruns, C. Electrostatic and nonpolar peptide-membrane interactions. Lipid binding and functional properties of somatostatin analogs of charge z = +1 to z = +3. *Biochemistry (N. Y.)* **1993**, *32*, 9714-9721.

(31) Bastos, M.; Bai, G.; Gomes, P.; Andreu, D.; Goormaghtigh, E.; Prieto, M. Energetics and Partition of Two Cecropin-Melittin Hybrid Peptides to Model Membranes of Different Composition. *Biophys. J.* **2008**, *94*, 2128-2141.

(32) Wieprecht, T.; Apostolov, O.; Beyermann, M.; Seelig, J. Thermodynamics of the α-helix-coil transition of amphipathic peptides in a membrane environment: implications for the peptide-membrane binding equilibrium. *J. Mol. Biol.* **1999**, *294*, 785-794.

(33) Seelig, J. Titration calorimetry of lipid-peptide interactions. *Biochim. Biophys. Acta* **1997**, *1331*, 103-116.

(34) Freire, E. Do enthalpy and entropy distinguish first in class from best in class? *Drug Discov. Today* **2008**, *13*, 869-874.

(35) Shimokhina, N.; Bronowska, A.; Homans, S. W. Contribution of Ligand Desolvation to Binding Thermodynamics in a Ligand?Protein Interaction. *Angewandte Chemie* **2006**, *118*, 6522-6524.

(36) Seelig, J. Thermodynamics of lipid-peptide interactions. *Biochim. Biophys. Acta* **2004**, *1666*, 40-50.

(37) Wieprecht, T.; Dathe, M.; Schumann, M.; Krause, E.; Beyermann, M.; Bienert, M. Conformational and Functional Study of Magainin 2 in Model Membrane Environments Using the New Approach of Systematic Double-D-Amino Acid Replacement. *Biochemisty* **1996**, *35*, 10844-10853.

(38) Wei, S.; Wu, J.; Kuo, Y.; Chen, H.; Yip, B.; Tzeng, S.; Cheng, J. Solution Structure of a Novel Tryptophan-Rich Peptide with Bidirectional Antimicrobial Activity. *J. Bacteriol.* **2006**, *188*, 328-334.

(39) Tamba, Y.; Yamazaki, M. Single Giant Unilamellar Vesicle Method Reveals Effect of Antimicrobial Peptide Magainin 2 on Membrane Permeability. *Biochemistry (N. Y.)* **2005**, *44*, 15823-15833.

CHAPTER SIX: SPACER #3

Introduction

The molecular flexibility and the net positive charge of AMPs play an important role in the bioactivity and selectivity as discussed in previous chapters. Here, we focus on increasing the flexibility of the positive charge cluster at the C-terminus to determine the effect it has on the binding interactions with anionic and zwitterionic membrane models. **Figure 1.2** in Chapter 1 gives the basic skeleton of our AMPs containing three Tic-Oic dipeptide units. Spacer #3, and the focus of this chapter, is denoted in green and refers to the amino acid between the last Tic residue and the C-terminus lysines. Compound **23** does not contain Spacer #3. The three compounds investigated in this chapter are compounds **50**, **51** and **52** with βAla, Gaba and Ahx incorporated as Spacer #3, respectively. Their amino acid sequences are given in **Table 6.1**.

Table 6.1: Amino acid sequences of the peptides used to study the role of spacer #3.

Compound	Amino Acid Sequence
23	Ac-GF-Tic-Oic-GK-Tic-Oic-GF-Tic-Oic-GK-Tic-KKKK-$CONH_2$
50	Ac-GF-Tic-Oic-GK-Tic-Oic-GF-Tic-Oic-GK-Tic-**βAla**-KKKK-$CONH_2$
51	Ac-GF-Tic-Oic-GK-Tic-Oic-GF-Tic-Oic-GK-Tic-**Gaba**-KKKK-$CONH_2$
52	Ac-GF-Tic-Oic-GK-Tic-Oic-GF-Tic-Oic-GK-Tic-**Ahx**-KKKK-$CONH_2$

Spacer # 3 provides molecular flexibility to the cluster of positively charged amino acid residues located at the C-terminus of the AMP. Due to the correlation between flexibility and net charge with the potency and selectivity of AMPs, it was believed that the activity of the compounds could be increased if the flexibility of the large positive charge was increased by inserting amino acid residues of varying lengths before the positive cluster. However, as can be seen in **Tables 6.2** and **6.3**, the overall activity of compounds **50**, **51** and **52** did not increase with

the insertion of Spacer #3. Unfortunately, hemolysis data was not collected for these peptides so there can be no correlation for the data in the presence of zwitterionic membrane models.

Table 6.2: Minimum inhibitory concentration (μM) of select bacteria strains and hemolytic activity.[1]

Compound	Salmonella Typhimurium	Staphylococcus Aureus ME/GM/TC resistant	Mycobacterium Ranae	Bacillus Subtillis	% hemolysis 100/25 mM
23	10 μM	3 μM	10 μM	1 μM	14%
50	30 μM	30 μM	10 μM	not tested	not tested
51	30 μM	10 μM	3 μM	not tested	not tested
52	30 μM	30 μM	10 μM	not tested	not tested

Table 6.3: Minimum inhibitory concentration (μM) of specific Gram negative and other drug resistant bacteria strains.[2]

Compound	23	50	52
Acinetobacter baumanii ATCC 19606	3.2	6.2	3
Acinetobacter baumanii WRAIR	3.2	6.2	6.1
Staphylococcus aureus ATCC 33591	205	199	196
Yersinia pestis CO92	205	199	48.9
Brucella melitensis 16M	205	199	196
Brucella abortus 2308	205	199	198
Brucella suis 23444	205	199	196
Bacillus anthracis AMES	12.8	12.4	48.9
Francisella tularensis SCHUS4	100	199	196
Burkholderia mallei	205	199	196
Burkholderia pseudomallei	205	199	196

Results and Discussion

CD Studies

CD spectra of compounds in buffer and micelle environments. In buffer (**Figure 6.1**), all the CD spectra of the peptides exhibited a similar shape, but exhibited varying intensities. Each spectrum contained a double minimum at approximately 208 and 222 nm, typical of an α-helix.[3-7] The maximum at approximately 195 nm was indicative of a combination of β-turn and α-helical components.[3, 8-10] The differences in their intensities suggest varying degrees of ordered structures in buffer.[4, 5, 11]

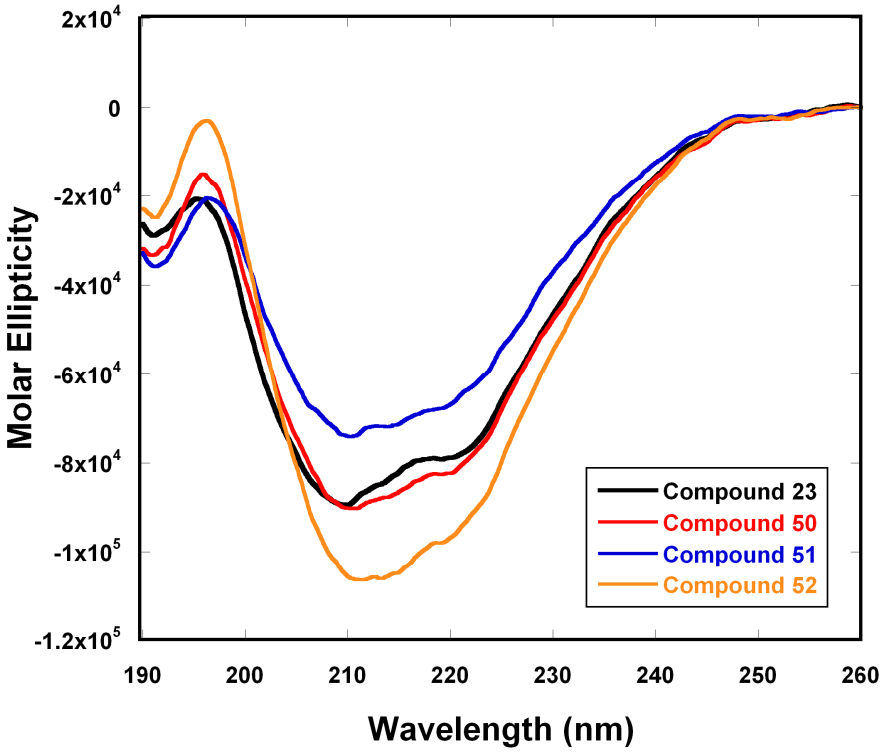

Figure 6.1: Far-UV CD spectra of compounds **23**, **50**, **51** and **52** (peptide concentration approximately 400 μM) in 40 mM phosphate buffer, pH = 6.8.

In the presence of SDS micelles (**Figure 6.2** – left), there was a shift in the CD spectra of these compounds from 195 to 190 nm accompanied with an increase in the intensity. This observation is consistent with the increase in α-helical components.[4, 7, 12-14] Each compound also exhibited a shift from 208 to approximately 202 nm suggesting the combination of α-helical, some type of β-turn and random coil conformations.[6, 15, 16] Only compounds **23** and **51** observed in an increase in intensity for the double minima.

The CD spectra in the presence DPC micelles (**Figure 6.2** – right) exhibited shapes and intensities very similar to those observed in CD spectra in the presence of SDS micelles. This observation leads to the conclusion that the S-state conformations and therefore the binding interactions were not greatly affected by the flexibility of the positively charged lysine cluster at the C-terminus.[3-5]

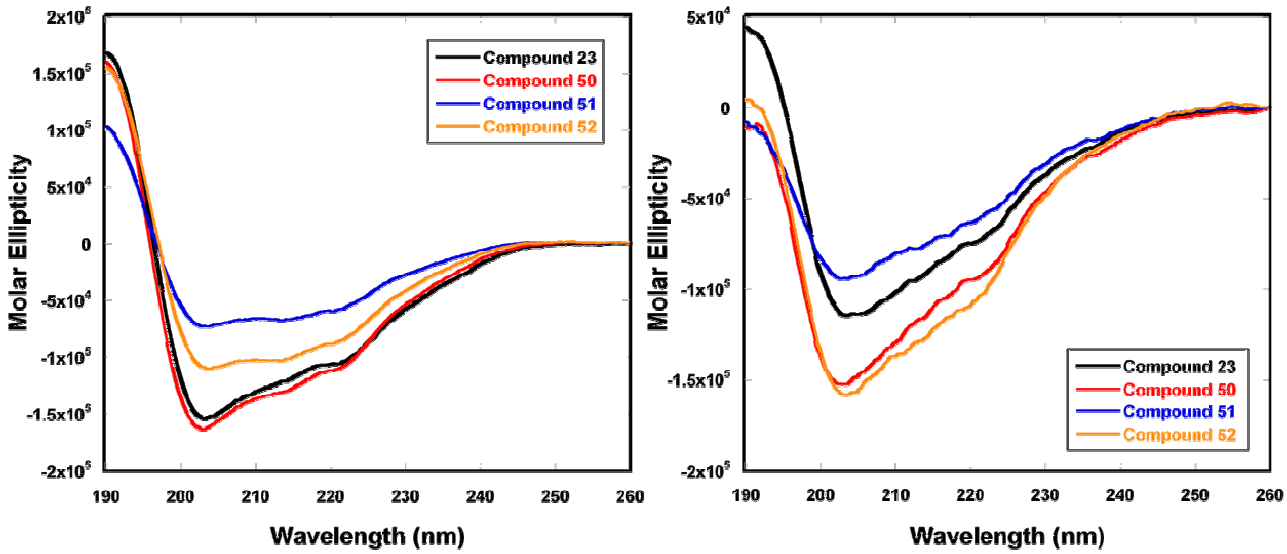

Figure 6.2: Far-UV CD spectra of compounds **23**, **50**, **51** and **52** (peptide concentration approximately 400 μM) in 80 mM SDS (left) and 80 mM DPC (right) micelles in 40 mM sodium phosphate buffer, pH = 6.8.

Transitioning from buffer to the zwitterionic POPC LUVs (**Figure 6.3** – left) exhibited losses in intensity below 200 nm indicating a loss in α-helical characteristics. However, some of this loss may have been compensated for with the increase of the minimum at 208 nm which suggests an increase in α-helicity. [4, 5, 11] The similarity between the CD spectra of these compounds in POPC LUVs and their corresponding spectra in buffer suggests that minimal conformational changes occurred on interaction with zwitterionic membrane models.[3, 5]

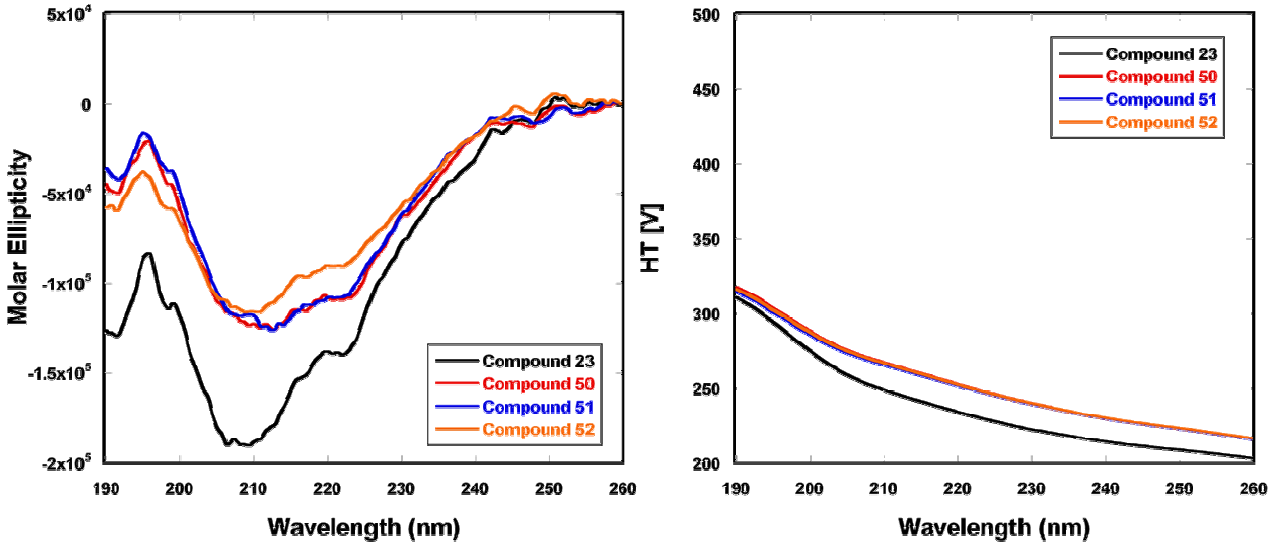

Figure 6.3: Far-UV CD spectra of 75 µM compound **23** and 100 µM solutions of compounds **50**, **51** and **52** in 1.75 mM POPC LUVs (left) in 40 mM phosphate buffer, pH = 6.8, and their corresponding HT values (right).

Obvious shifts in wavelengths in the CD spectra from approximately 195 and 208 to 192 and 202 nm, respectively, are indicative of changes in conformation when in the presence of anionic membrane models (**Figure 6.4** – left).[3-5] The decrease in the intensity of the maximum coupled with the shift in wavelength for the minimum at 208 to 202 nm suggests a decrease in α-helical characteristics. The shift in the maximum and increase in the intensity of the minimum, however, suggests an increase. [3, 5, 6] Overall, the conformation of these peptides was different in

anionic LUVs as compared to buffer and the zwitterionic models concluding there was a different interaction taking place. [5]However, there is no discernable trend that suggests the length of spacer #3 played a role.

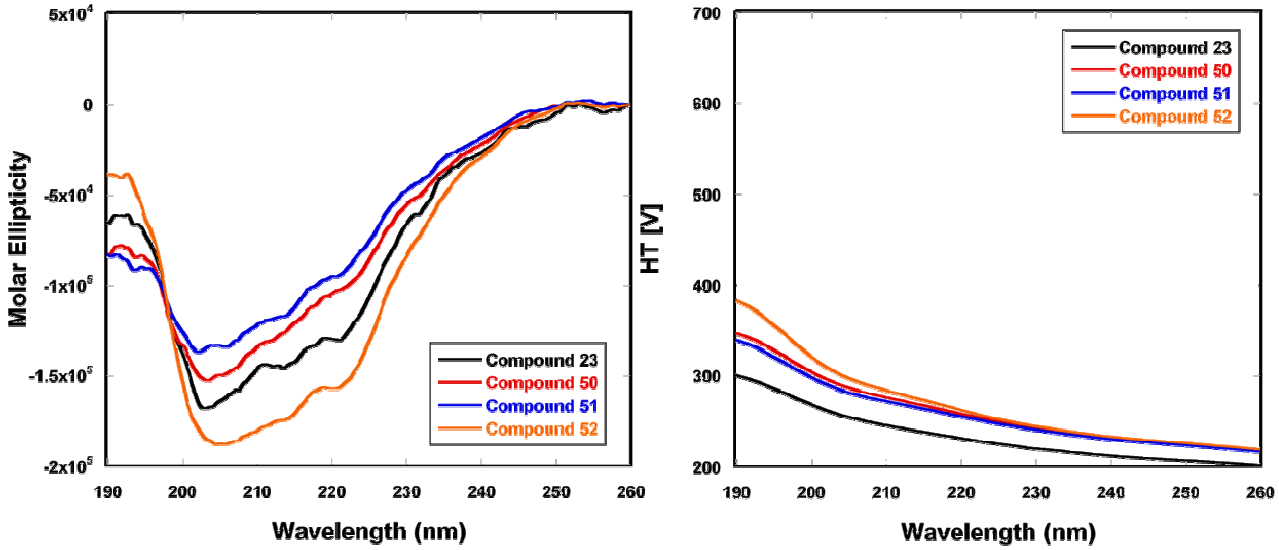

Figure 6.4: Far-UV CD spectra of 200 µM compound **23**, **50**, **51** and **52** in 1.75 mM 4:1 POPC/POPG (left) in 40 mM phosphate buffer, pH = 6.8, and their corresponding HT values (right).

*"Pseudo" CD titrations of compounds **23**, **50**, **51** and **52***. The spectra of compounds **23** and **50** with increasing POPC LUV concentrations (**Figure 6.5**) were very different from their corresponding spectra in buffer, but did not vary much, in regards to shape, as the LUV concentration increased. Compounds **51** and **52** exhibited similar spectra in POPC LUVs as they did with buffer. There were no discernable changes, with the exception of intensity, that would associate the conformational changes with the LUV concentration. These CD spectra lead to the conclusion that the interaction between these peptides and zwitterionic LUVs was minimal, a therapeutically desirable quality.

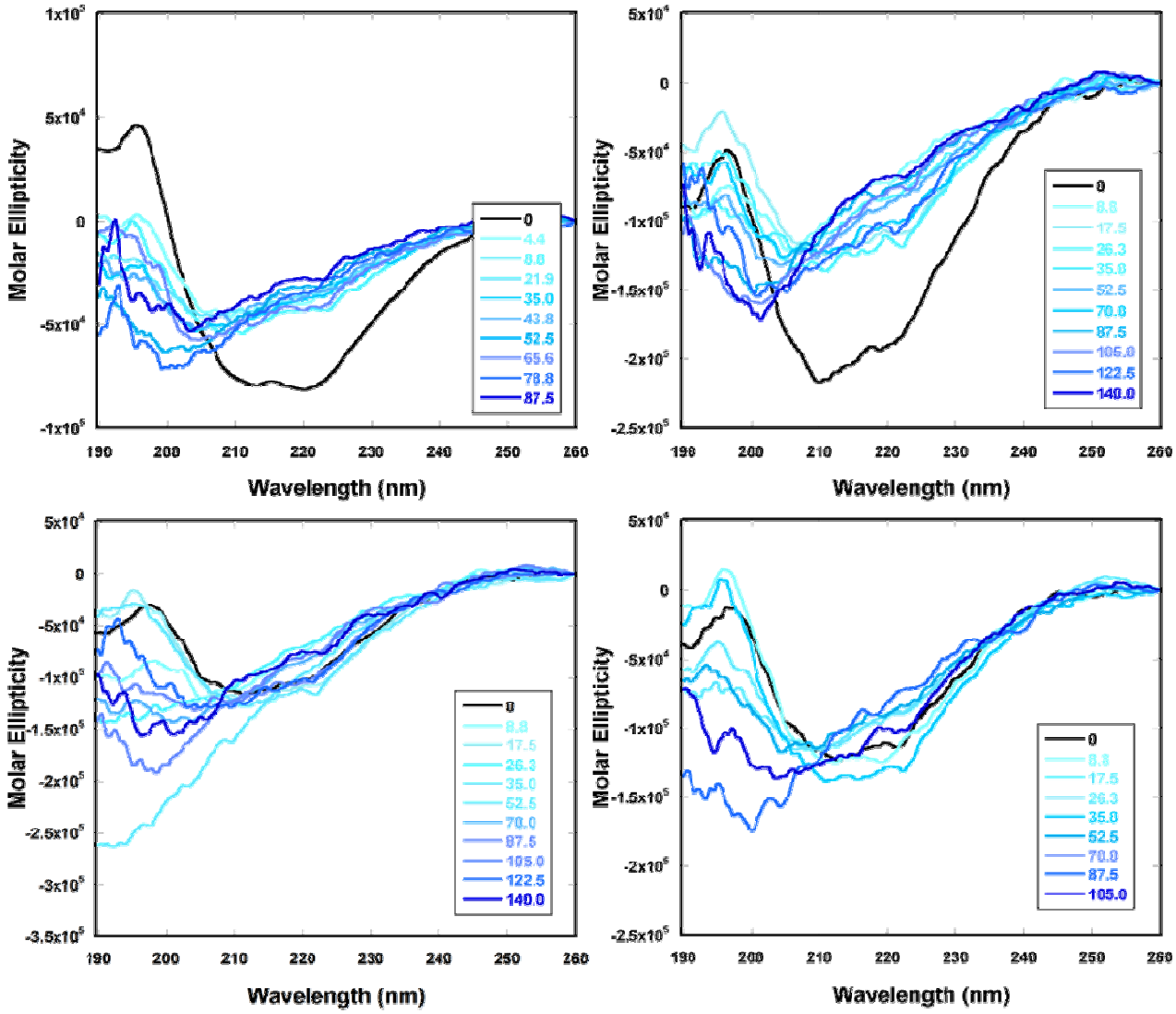

Figure 6.5: Far-UV CD spectra for separate samples of 200 µM solutions of compounds **23** (top left) and 100 µM solutions of compounds **50** (top right), **51** (bottom left) and **52** (bottom right) with increasing concentrations of POPC LUVs in 40 mM phosphate buffer, pH = 6.8.[17, 18]

Different trends were observed for compounds **50**, **51** and **52** in the presence of increasing anionic LUV concentrations as compared to the previously discussed pattern of compound **23** (**Figure 6.6**). The intensity of the spectra for compound **23** decreased with increasing LUV concentration (blue spectra) until a constant level was reached (green spectra)

and all of the peptide was assumed to be bound.[19, 20] As the LUV concentration continued to increase, the intensity of the spectra once again increased (red spectra). As the length of Spacer #3 increased, the mechanism associated with changes in the secondary structure conformations also changed and the peptides with Spacer #3 incorporated exhibited different trends from compound **23**. For compound **50** with a βAla inserted, the intensity of the spectra increased (**Figure 6.6** – top right, blue spectra) with the addition of liposomes until a maximum intensity was reached. Once the maximum intensity was reached, subsequent addition of LUVs resulted in a spectrum with a complete loss of intensity. As the LUV concentration increased, the intensity of the spectra gradually increased. The latter grouping of spectra for compound **50** followed the same trend as the second group of CD for compound **23**, at higher L/P ratios.

For compound **51**, the first group of CD spectra, at low L/P ratios, followed the same trend as those for compound **50** and exhibited an increase in intensity. However, once the maximum intensity was reached for compound **51**, the intensity of the spectra gradually decreased as the L/P ratio increased until the intensity was constant and approximately 0. For the compound with the longest Spacer #3, **52**, the same pattern as compound **51** was observed, but the extent to which the spectra decreased was less.

It appears that as the spacer length increases, the mechanism of action shifts, with compounds **50** and **51** as intermediates between **23** and **52**. The pattern for compound **23** was a decrease in intensity followed by an increase. Compound **50** involved two decreasing trends and **51** an increasing pattern followed by a decrease. The trends for compound **51** were the exact opposite of compound **23**. The longest spacer, Ahx in compound **52**, essentially was the opposite of **23** with a less intense second phase and a completely different mechanism. However, the mechanisms associated with these changes in conformation did not result in an increase in the

biological activity of these peptides in comparison to compound **23**, thus concluding that Spacer #3 does not play a role in the determination of the biological activity.

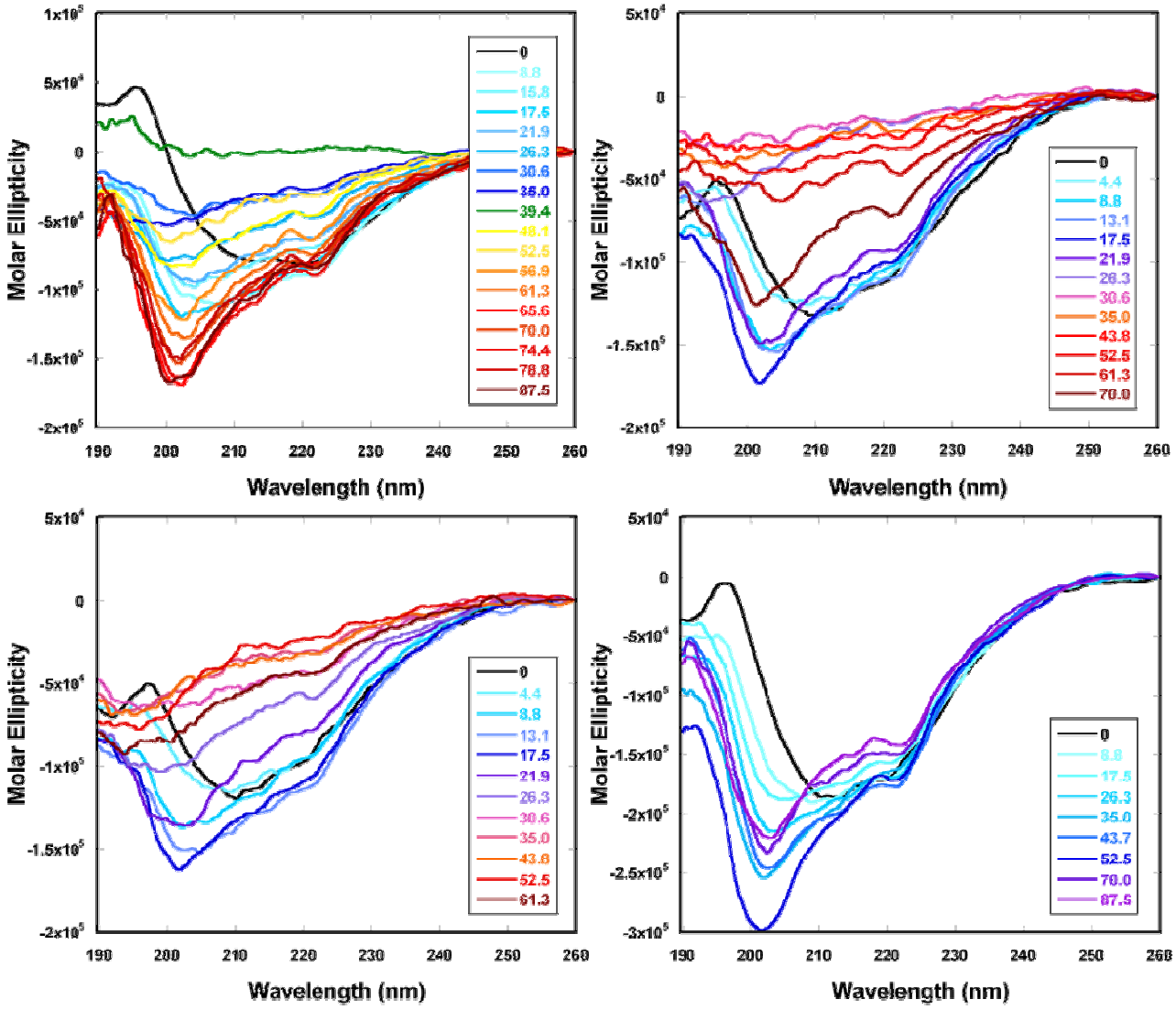

Figure 6.6: Far-UV CD spectra of separate samples of 200 µM solutions of compound **23** (top left) and 100 µM solutions of **50** (top right), **51** (bottom left) and **52** (bottom right) with increasing concentrations of 4:1 POPC/POPG liposomes in 40 mM phosphate buffer, pH = 6.8.[17, 18]

ITC Studies

Anionic LUVs. All four compounds exhibited 2-phase thermograms when titrated with 4:1 POPC/POPG LUVs (**Figure 6.7**) which is indicative of pore formation at low L/P ratios followed by binding as the LUV concentration increased.[19, 21, 22] Endothermic heat is the result of several different processes including, but not limited to, disruption of polar lipid head groups and lipid:lipid interactions, desolvation of structured water molecules on the peptide and membrane surfaces.[20-23] These processes coincide with exothermic processes which describe binding. Attractive electrostatic interactions between the peptide and membrane, conformational changes of the peptide and binding interaction through Van der Waals and hydrogen bonding are a few of these processes.[18, 22-24] Endothermic and exothermic processes occur simultaneously with the more dominate of the two being observed.[22]

At low L/P ratios, pore formation is the dominate interaction as indicated by the endothermic phase.[22] At these ratios, the peptides are in excess of the lipid, oligomerizing and forming pores. As the lipid concentration increases, the pore ↔ binding equilibrium shifts towards binding as the ratio shifts to high L/P.[19, 21, 22] Each of these peptides favors pore formation over binding and their ability to do so increases as the length of Spacer #3 increases. The ratio of the cumulative endothermic components to the cumulative exothermic components increases with the increased flexibility of the positive charges at the C-terminus. Favorability for pore formation in the presence of anionic LUVs suggests these peptides would exhibit some biological activity against bacterial cells. As seen in **Tables 6.2** and **6.3**, these peptides do exhibit biological activity against the common bacterial strains, although no more than compound **23** without Spacer #3 incorporated.

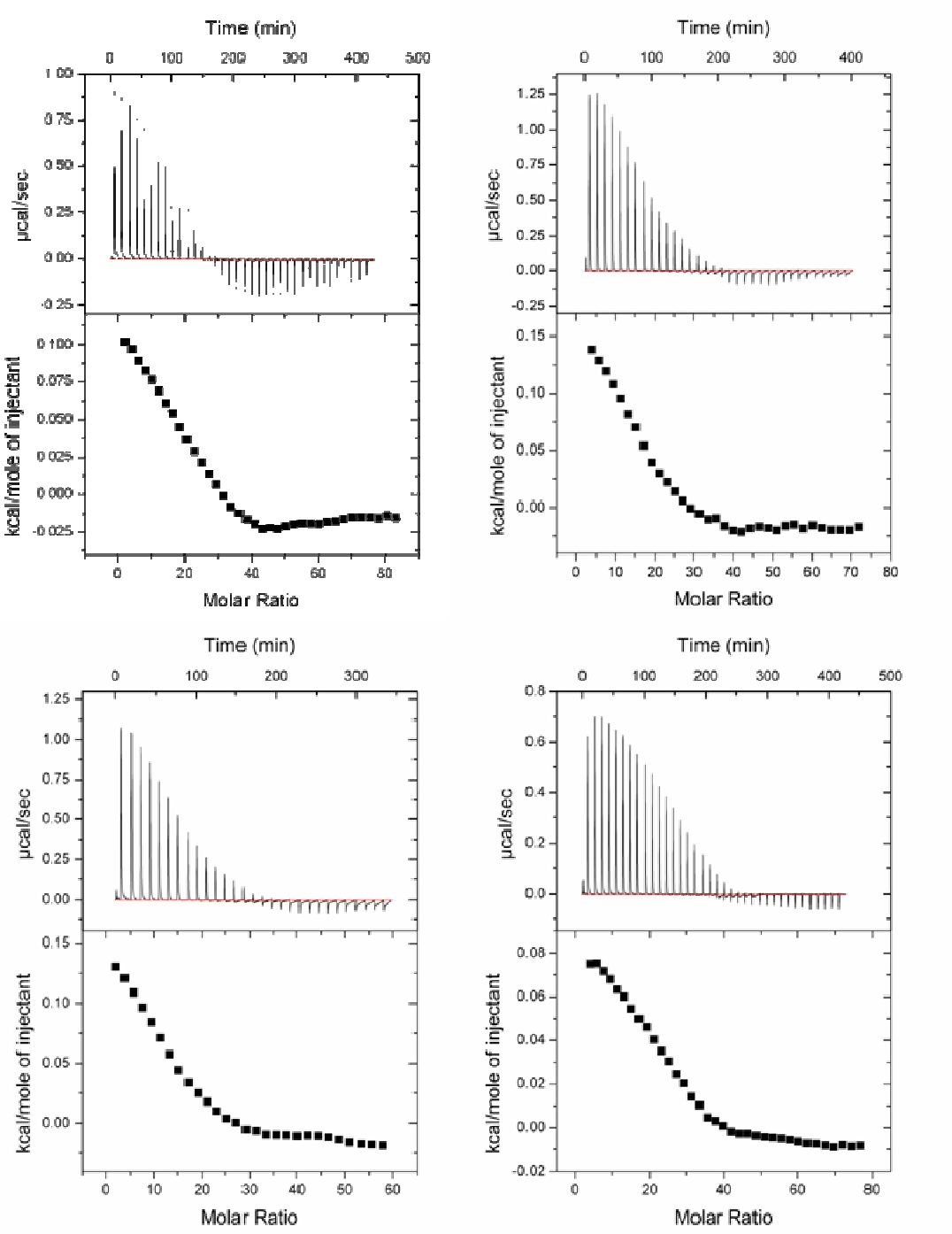

Figure 6.7: ITC data for the full titration of 35 mM 4:1 POPC/POPG LUVs into 200 µM solutions of compounds **23** (top left), **50** (top right), **51** (bottom left) and **52** (bottom right).

Each single titration experiment for the titration of peptide into anionic LUVs exhibited an exothermic event (**Figure 6.8**).[22, 23, 25, 26] The exothermic processes associated with binding are counteracted by corresponding endothermic processes such as desolvation and displacement of polar lipid head groups.[20, 22, 23] As seen in **Figure 6.8**, the exothermic processes were favored. With the exception of compound **23**, the binding enthalpies decreased as the spacer length increased. This result could be attributed to the increased disruption of water molecules and polar head groups caused by the larger space occupied by the cluster of lysines at the C-terminus due to its increased flexibility.[22, 23] Because compound **23** does not follow suit, it appears as though there is not an obvious trend associating binding enthalpies and the length of Spacer #3.

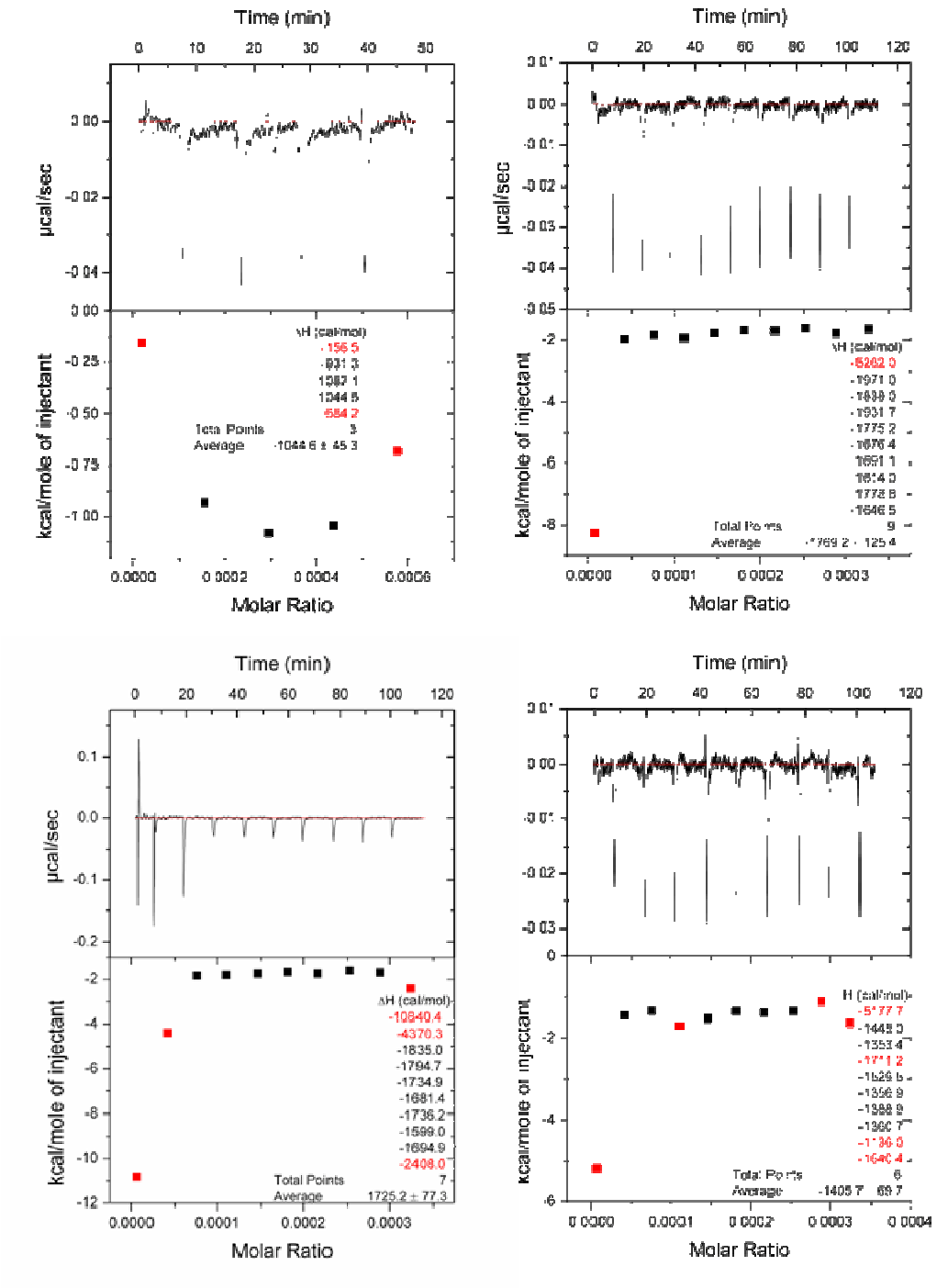

Figure 6.8: Single injection ITC experiments to determine the ΔH of binding. A dilute solution of 200 µM compound **23** (top left) was titrated into 15 mM 4:1 POPC/POPG LUVs. Dilute solutions of 100 µM compound **50** (top right), **51** (bottom left) and **52** (bottom right) were titrated into 20 mM 4:1 POPC/POPG LUVs to give high L/P ratios.[22, 26]

Compound **23** absorbed the largest amount of heat for the single injection experiment of 4:1 POPC/POPG LUVs into peptide in order to determine the ΔH of membrane disruption (**Figure 6.9**).[22, 23, 26] The increase in spacer length did not appear, once again, to have a critical impact on the heat associated with pore formation as compounds **50**, **51**, **52** were similar to each other and less than compound **23**. Pore formation, which is associated to cell lysis, appears to be more favored with compound **23** than the peptides containing Spacer #3, which is supported by the bioactivity.

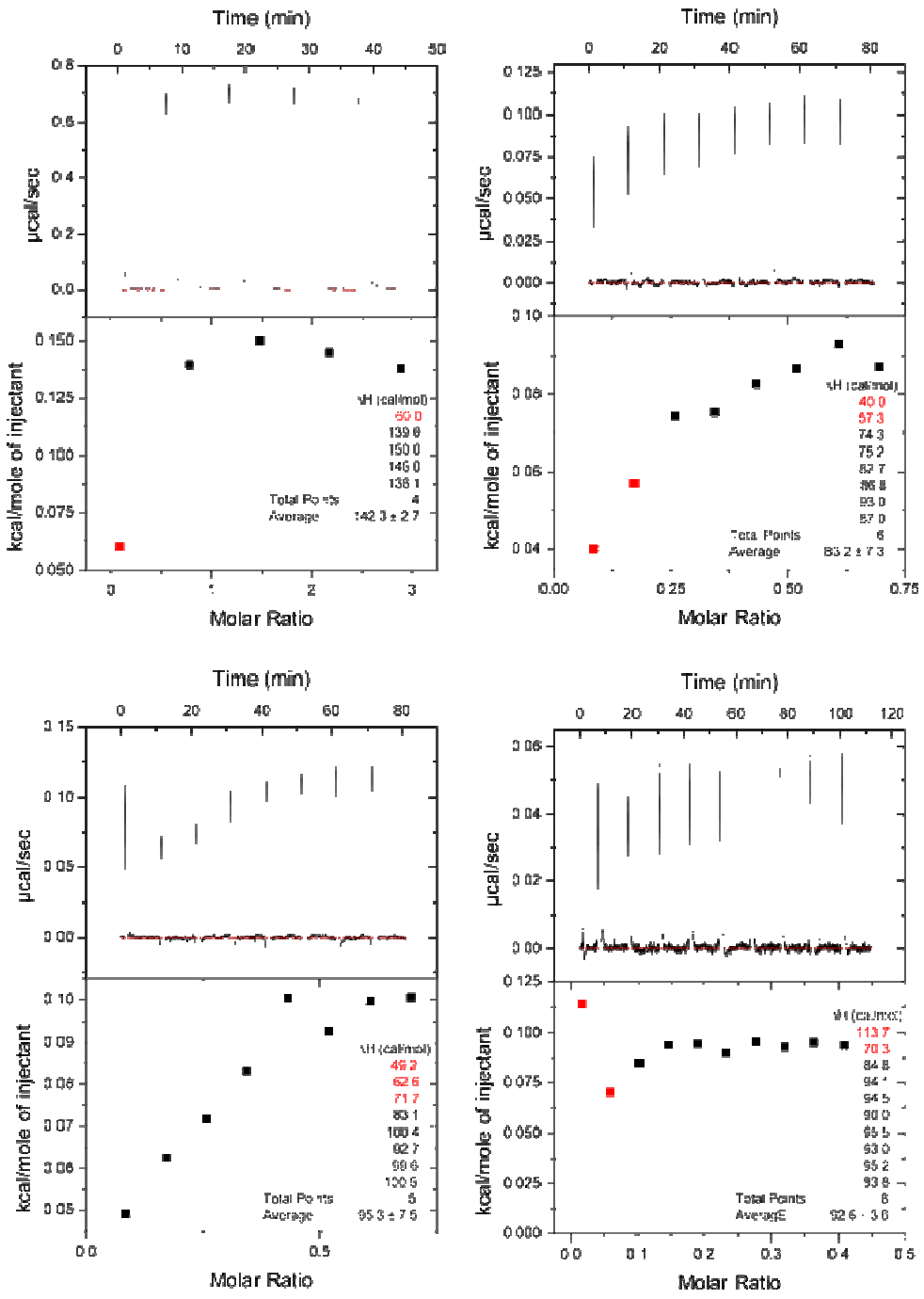

Figure 6.9: Single injection ITC experiments to determine the ΔH of membrane disruption. A 20 mM solution of 4:1 POPC/POPG LUVs was titrated into 300 µM compound **23** (top left). Dilute solutions of 10 mM 4:1 POPC/POPG LUVs were titrated into 400 µM compound **50** (top right) and **51** (bottom left). A dilute solution of 5 mM 4:1 POPC/POPG LUVs was titrated into 400 µM compound **52** (bottom right).[22, 26]

Zwitterionic LUVs. The full titrations of POPC LUVs into each peptide (**Figure 6.10**) yielded one endothermic phase. High L/P ratios were required for the complete binding of the peptide indicating a weak interaction, a therapeutically desirable quality. With the exception compound **23**, the L/P ratios required for 100% binding decreased with the increase in the length of Spacer #3, suggesting that the longer spacers favor binding with POPC LUVs. One explanation for this conclusion could be attributed to the flexibility. By incorporating flexibility into the positively charged C-terminus, it may be possible for the peptide to maneuver around the areas of localized positive charge on the membrane, thus increasing the binding.

By fitting the data to known models allowed us to determine some thermodynamic data so as to make better conclusions regarding the interactions of these peptides with zwitterionic membranes, and thus the role played by Spacer #3, if any. The degree of binding, X_b, and concentration of free peptide in bulk solution, c_f, were calculated using **Equations 1.4** through **1.8** and the raw data from the experiments. The plots of X_b against c_f are given in **Figure 6.11**. Each of the figures exhibited a nonlinear curve which could not be fit by the binding isotherm model described by **Equation 1.3**. The downward bend of the curves have been attributed to the decrease of the surface potential and electrostatic attractions between the membrane and peptides as the concentration of the peptide on the surface increases.[25, 27] This particular model did not account for these electrostatic interactions and, therefore, was not the appropriate model to describe this data.

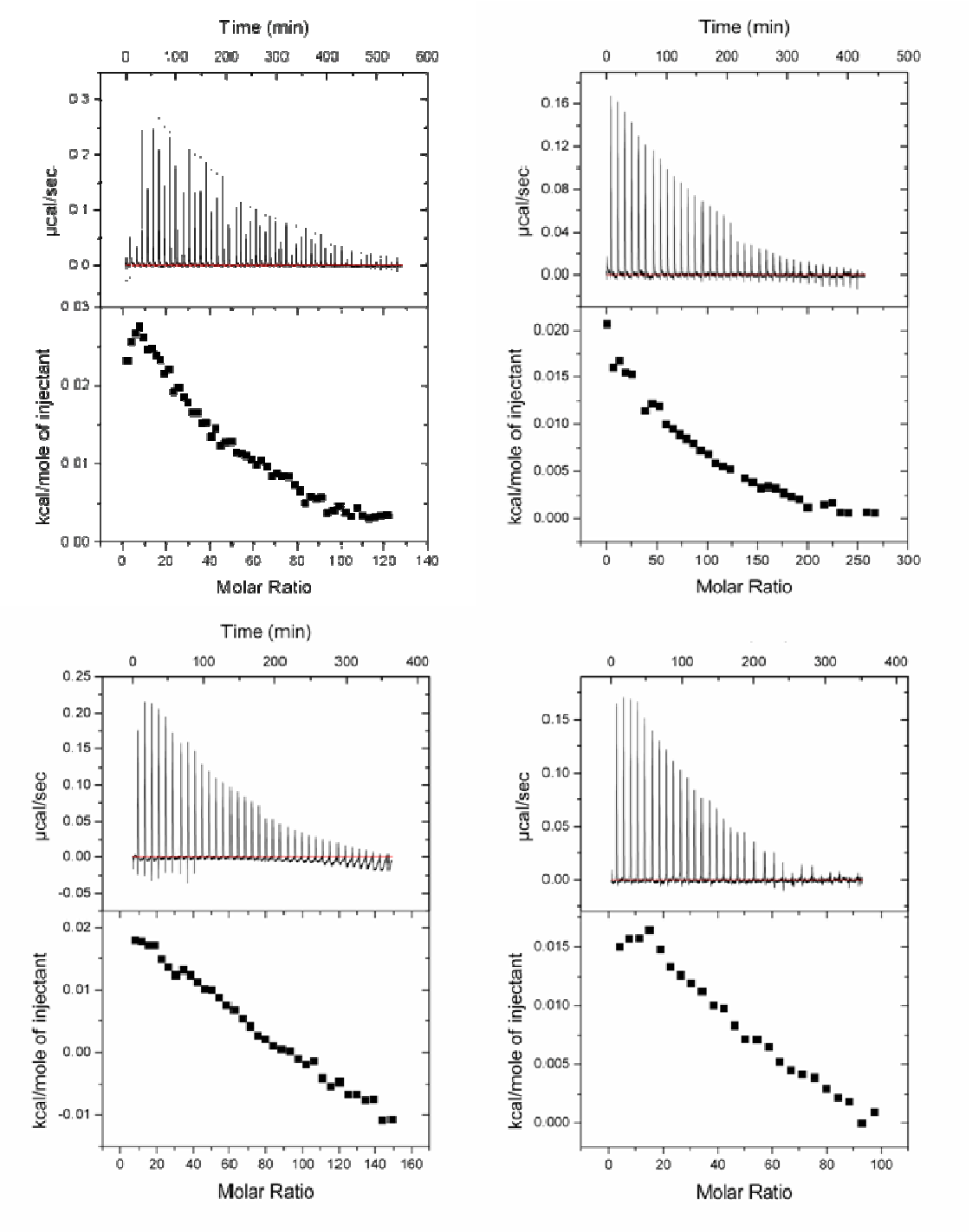

Figure 6.10: ITC experiment for the titration of 35mM POPC LUVs into 200 µM compound **23** (top left), 50 µM compound **50** (top right) and 100 µM solutions of compounds **51** (bottom left) and **52** (bottom right).

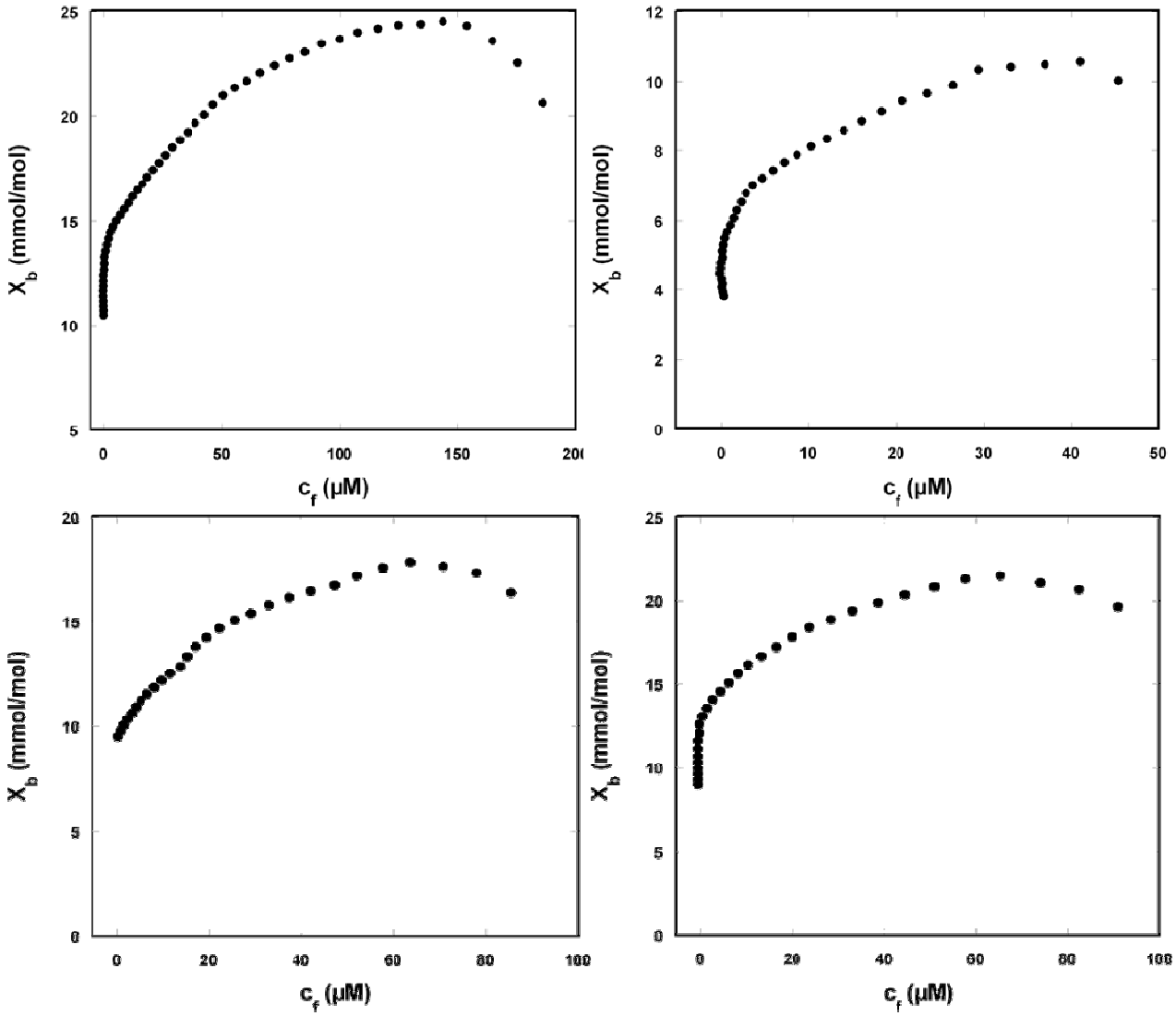

Figure 6.11: Plot for the degree of binding, X_b, as a function of the peptide concentration in bulk solution, c_f. The binding isotherms were derived from the titration of 35 mM POPC LUVs into compounds **23** (top left), **50** (top right), **51** (bottom left) and **52** (bottom right). X_b and c_f were calculated as described in Chapter 1 of the text.[21, 24]

A more sophisticated surface partition equilibrium model for determining the binding isotherms was employed in order to account for the electrostatic interactions between the membrane surface and positively charged peptides. **Equation 1.9** from Chapter 1 factors in the concentration of the free peptide immediately above the surface of the membrane, c_m, as the

attractive electrostatic interactions will cause an in case in this concentration as compared to the peptide concentration in bulk solution. Using **Equations 1.10** through **1.12**, it was possible to calculate cm. plotting X_b against c_m yielded linear curves that could be fit to the binding isotherm model described in **Equation 1.9**. Fitting these curves to straight lines allowed for the determination of the binding constant, K, as it was the slope. Knowing K and the experimentally determined ΔH^0 of the interactions allowed for the determination of ΔG and ΔS using **Equations 1.1** and **1.**2, thus providing a full set of thermodynamic data. The data is summarized in **Table 6.4**.

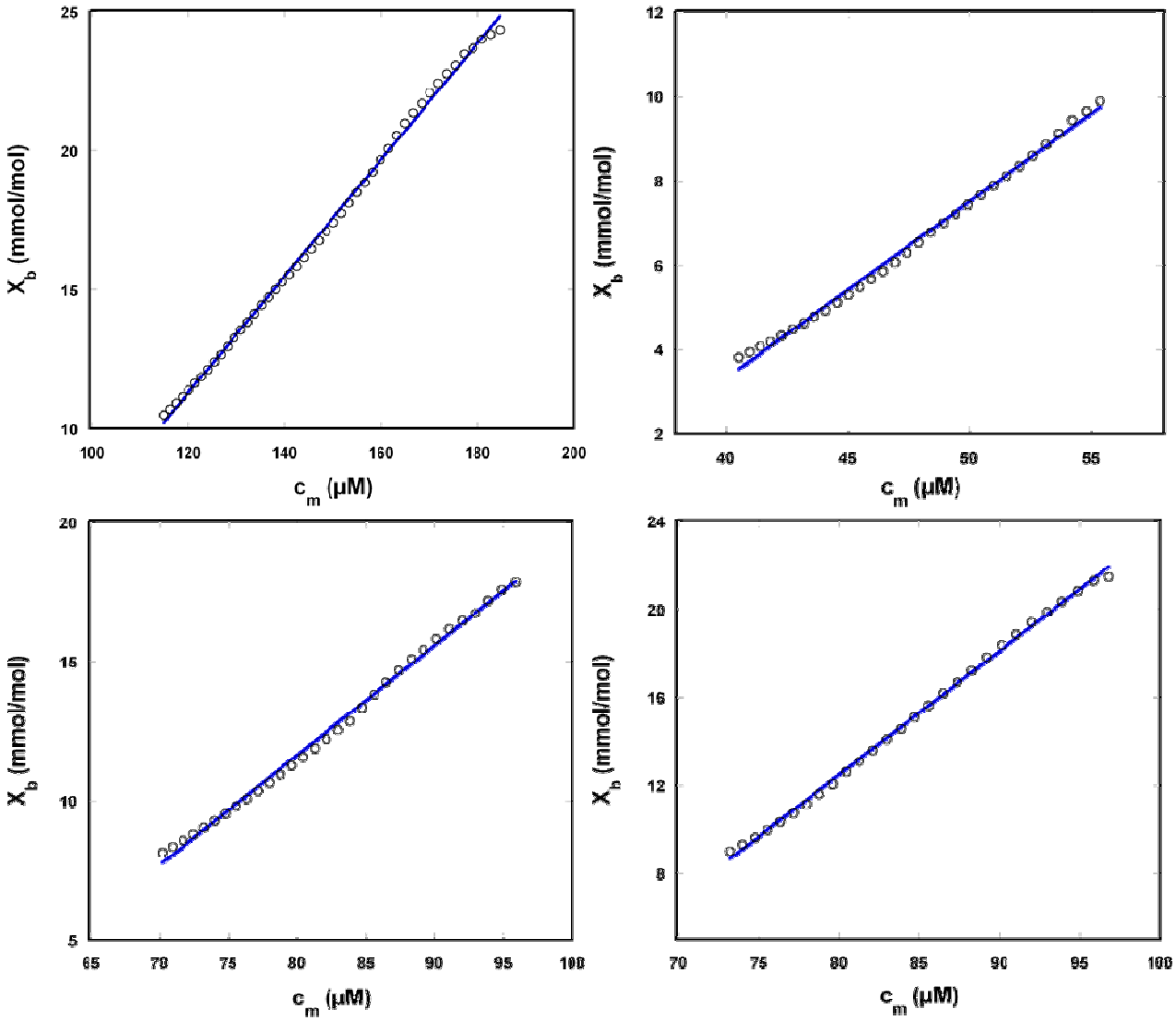

Figure 6.12. Plot for the degree of binding, X_b, as a function of the membrane surface concentration of peptide, c_m. The binding isotherms were derived from the titration of 35 mM POPC LUVs into compounds **23** (top left), **50** (top right), **51** (bottom left) and **52** (bottom right). X_b and c_m were calculated as described in Chapter 1 of the text.[21, 24]

Upon examination of the thermodynamic data in **Table 6.4**, there was not a clear trend between the spacer length and degree of the interaction with POPC LUVs. However, there was one obvious result; the peptides with Spacer #3 incorporated had increased favorable thermodynamic data as compared to compound **23**. With the exception of ΔH^0, which were

overall very similar, compounds **50**, **51** and **52** favored the interaction with POPC LUVs more than compound **23**, in terms of thermodynamics. The binding constants were larger, the ΔG values were more negative and the ΔS values more positive, all favorable results. Based on the thermodynamic data, one can conclude that by increasing the flexibility of the lysine cluster at the C-terminus, the interaction with zwitterionic membrane models is also increased. Increasing the flexibility, as mentioned previously, could allow the peptide the mobility to maneuver around the positive charges on the surface, thus increasing the binding. Such characteristics are not desirable for therapeutic agents.

Table 6.4: Thermodynamic data for a representative titration of 35 mM POPC into the peptides at 25°C as derived from the equations discussed previously.

Compound	$\Delta H^{0,a}$ (kcal/mol)	K^b (M^{-1})	ΔG^c (kcal/mol)	ΔS^d (cal/mol·K)
23	0.67	211.00	-5.54	20.84
50	0.88	418.23	-5.95	22.93
51	0.68	394.85	-5.91	22.14
52	0.56	561.41	-6.12	22.41
Magainin 2 amide[e]				
M2a	-15.9	2000.0	-7.0	-29.4

[a] ΔH^0 values were calculated using **Equation 1.4** from chapter 1 using the binding enthalpies measured directly from the experiment.
[b] K values were generated from the lipid-into-peptide titration using the calculations as described in chapter 1.
[c] ΔG values were calculated using **Equation 1.1** from chapter 1.
[d] ΔS was calculated using **Equation 1.2** from chapter 1.
[e] The thermodynamic parameters for the magainin analogue M2a as presented by Wieprecht et. al.[19, 20]

Fitting the data obtained from the full titration of POPC LUVs into the peptides provided thermodynamic data concerning the entire interaction between the peptides and LUVs. Performing single injection experiments, however, allowed for the isolation of the two extremes

of the interaction, binding and membrane disruption. The titration of dilute solutions of peptide into excess LUVs isolated the binding interaction as the L/P was very high. As seen in **Figure 6.13**, and summarized in **Table 6.5**, increasing the length of Spacer #3 results in a binding enthalpy that becomes more negative, and thus more favorable. This observation supports the theory that increasing the length of Spacer #3 consequently increases the flexibility of the positive cluster. The added flexibility aids in the binding process as the peptide is able to maneuver around the positive charges of the zwitterionic membrane surface.

Reversing the single injection experiment and titrating dilute solutions of LUVs into excess peptide (**Figure 6.14**), the ΔH of membrane disruption was determined. None of the compounds in this series appeared to favor membrane disruption through pore formation more than another, as the ΔHs were almost identical. Although this would appear to be a favorable quality with regards to useful therapeutic agents, pore formation is not the only mechanism by which to disrupt the membrane and cause cell lysis.

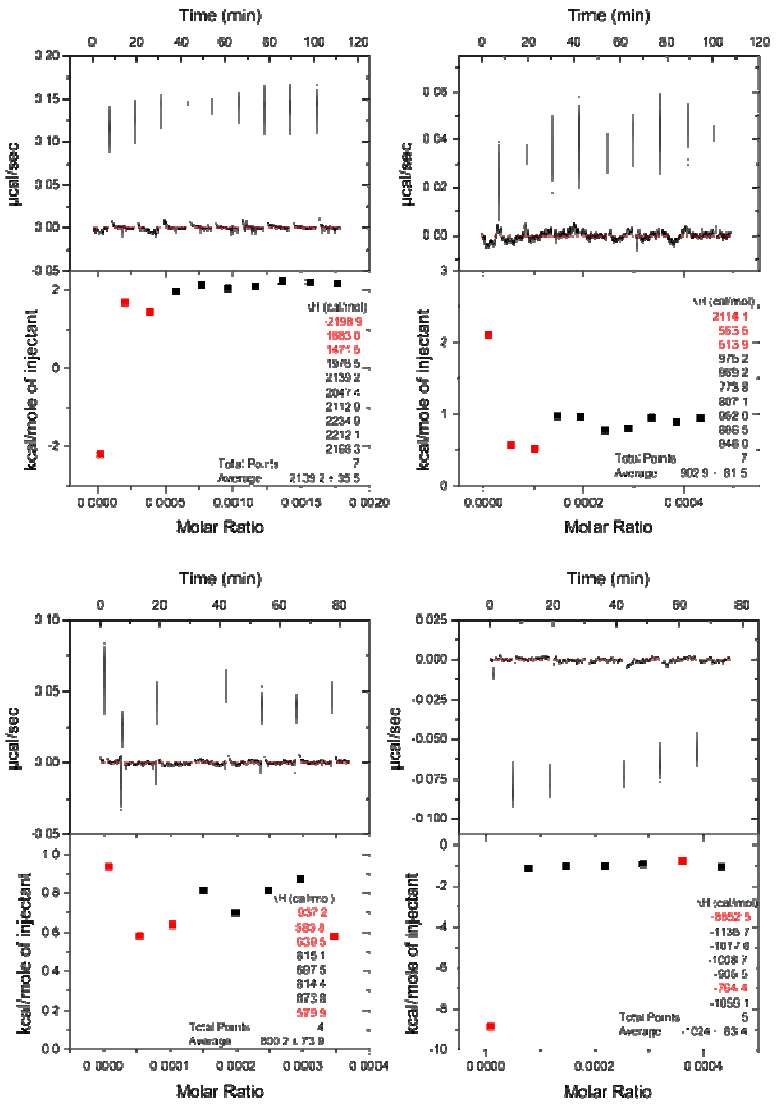

Figure 6.13: Single injection ITC experiments to determine the ΔH of binding. A dilute solution of 200 µM compound **23** (top left) was titrated into 15 mM POPC LUVs. Dilute solutions of 200 µM compounds **50** (top right) and **52** (bottom right) were titrated into 30 mM POPC LUVs. A dilute solution of 200 µM compound **51** (bottom left) was titrated into 35 mM POPC LUVs to give high L/P ratios.[22, 26]

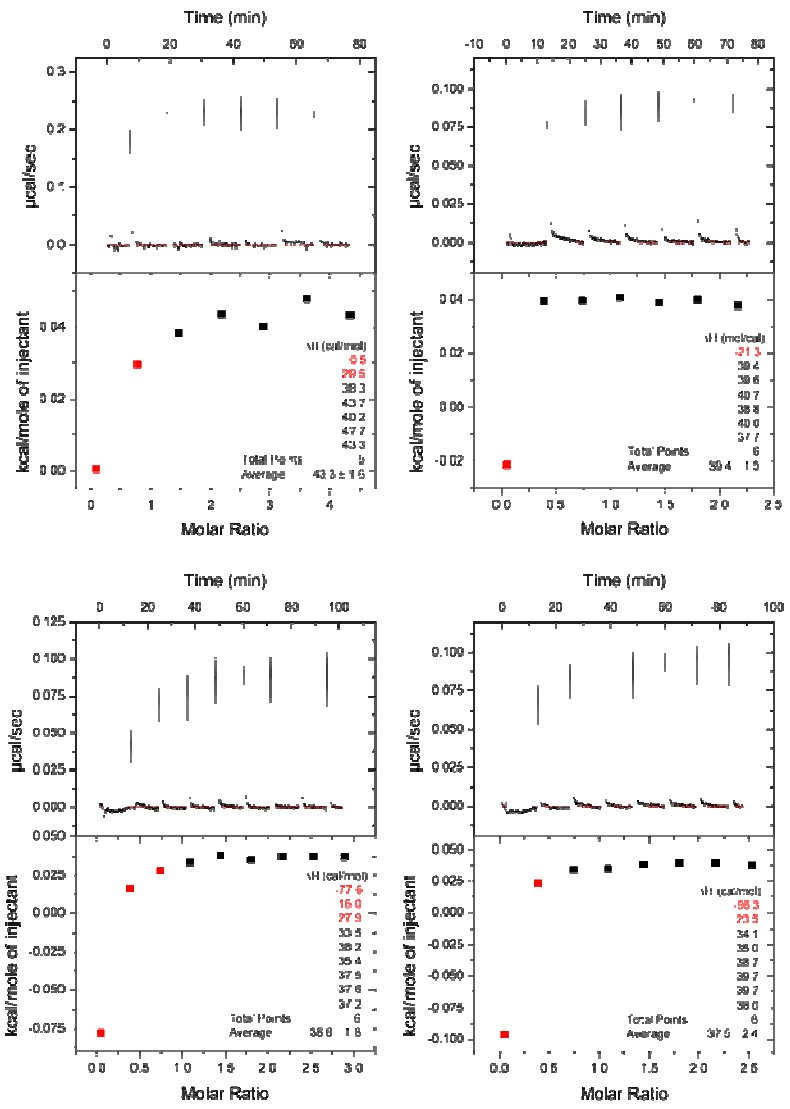

Figure 6:14: Single injection ITC experiments to determine the ΔH of membrane disruption. A 20 mM solution of POPC LUVs was titrated into 300 µM compound **23** (top left). Dilute solutions of 10 mM POPC LUVs were titrated into 400 µM compound **50** (top right), **51** (bottom left) and **52** (bottom right).[22, 26]

Table 6.5: ΔH (kcal/mol) values for the binding and membrane disruption of 4:1 POPC/POPG and POPC LUVs as determined by single injection ITC experiments.[23]

Compound	4:1 POPC/POPG into Compound	Compound into 4:1 POPC/POPG	POPC into Compound	Compound into POPC
23	0.14 ± 0.03	-1.00 ± 0.04	0.04 ± 0.00	2.10 ± 0.04
50	0.08 ± 0.00	-1.77 ± 0.13	0.04 ± 0.00	0.90 ± 0.08
51	0.10 ± 0.00	-1.73 ± 0.08	0.04 ± 0.00	0.80 ± 0.07
52	0.09 ± 0.00	-1.41 ± 0.07	0.04 ± 0.00	-1.02 ± 0.08

Calcein Leakage Studies

The increase in the fluorescence associated with the peptide induced calcein leakage of POPC (**Figure 6.15**) and 4:1 POPC/POPG LUVs (**Figure 6.16**) was monitored over time in an attempt to determine any concentration dependency for the activities or mechanisms of action.[28, 29] In the presence of POPC LUVs, with the exception of a slight increase with compound **51**, these peptides did not appear to interact via a concentration dependent mechanism. In fact, these compounds did not appear to interact with the zwitterionic membranes much at all and this is further highlight in **Figure 6.17** – left. These results lead to the conclusion that the incorporation of Spacer #3 may not affect the binding interaction with mammalian red blood cells either.

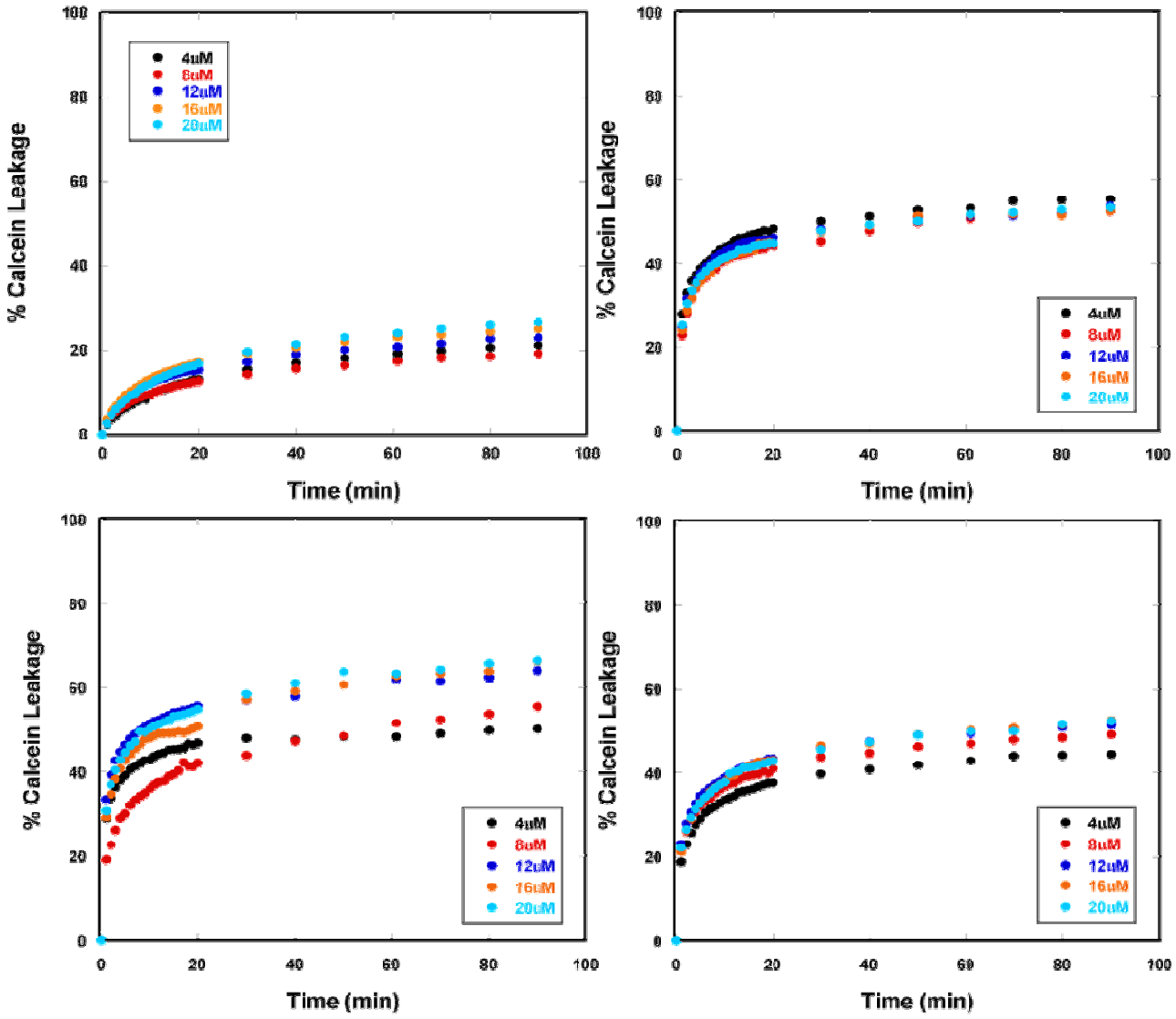

Figure 6.15: The time dependent release of calcein from POPC LUVs induced by increasing concentrations of compounds **23** (top left), **50** (top right), **51** (bottom left), and **52** (bottom right) as measured by fluorescence.[30-32]

The results for the leakage from 4:1 POPC/POPG LUVs presented in **Figure 6.16** exhibited a concentration dependent mechanism. This dependency is further highlighted in **Figure 6.17** – right. Compound **51** displayed the most concentration dependent leakage as well as the most leakage. The increase in leakage as the concentration of peptide increased maybe explained by the formation of a pore.[33-35]Although there was an increase in the overall leakage

with the compounds incorporating Spacer #3 as compared to compound **23** without the spacer, there did not appear to be a great increase. With the exception of compound **51**, which appeared to have an optimal spacer length for the interaction with these simple membrane models, there was no data to suggest that compounds **50** and **52** would be more biologically active than compound **23**. This conclusion is supported by the biological data which suggests, overall, the activity of the peptides is very similar.

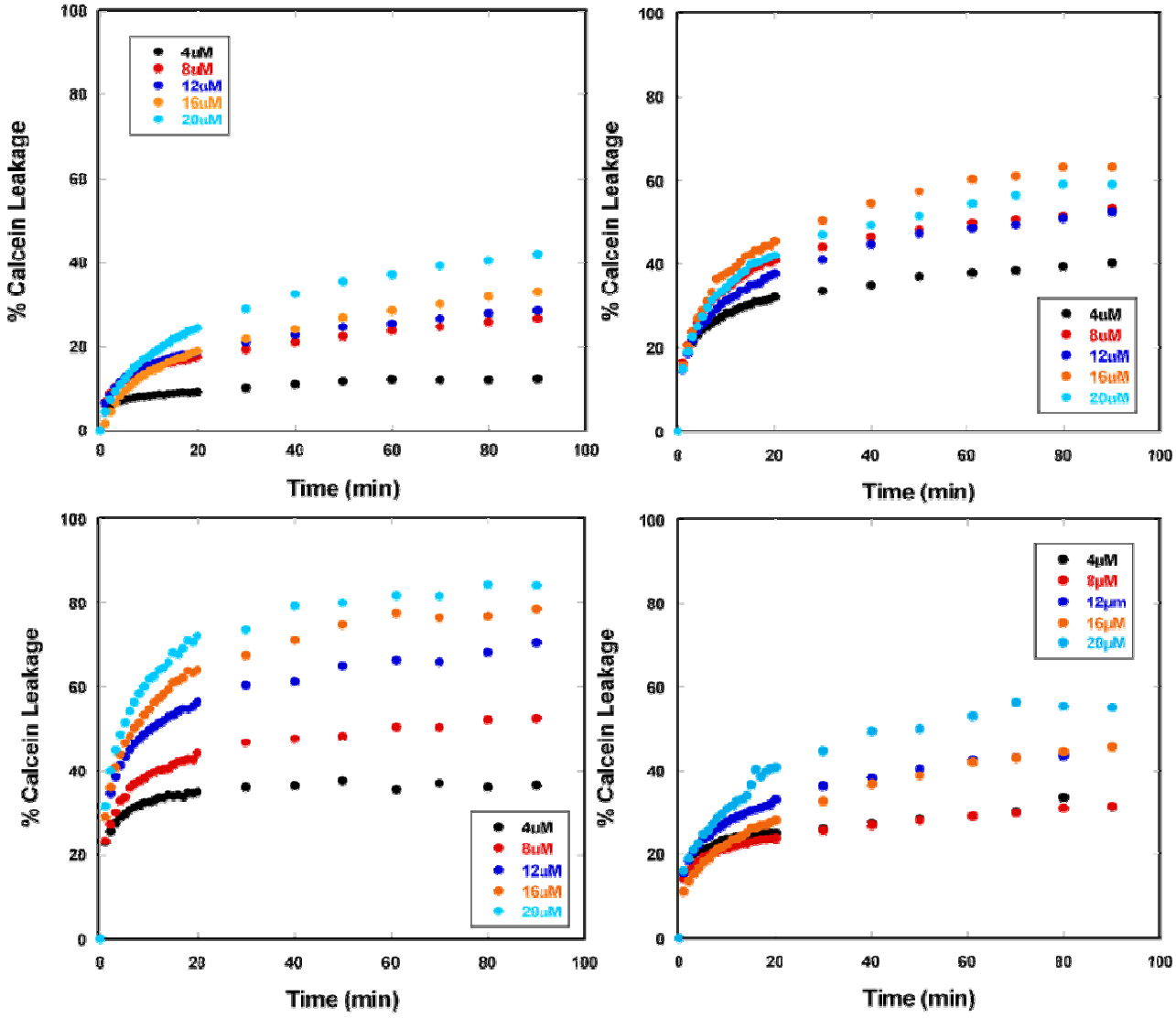

Figure 6.16: The time dependent release of calcein from 4:1 POPC/POPG LUVs induced by increasing concentrations of compounds **23** (top left), **50** (top right), **51** (bottom left), and **52** (bottom right) as measured by fluorescence.[30-32]

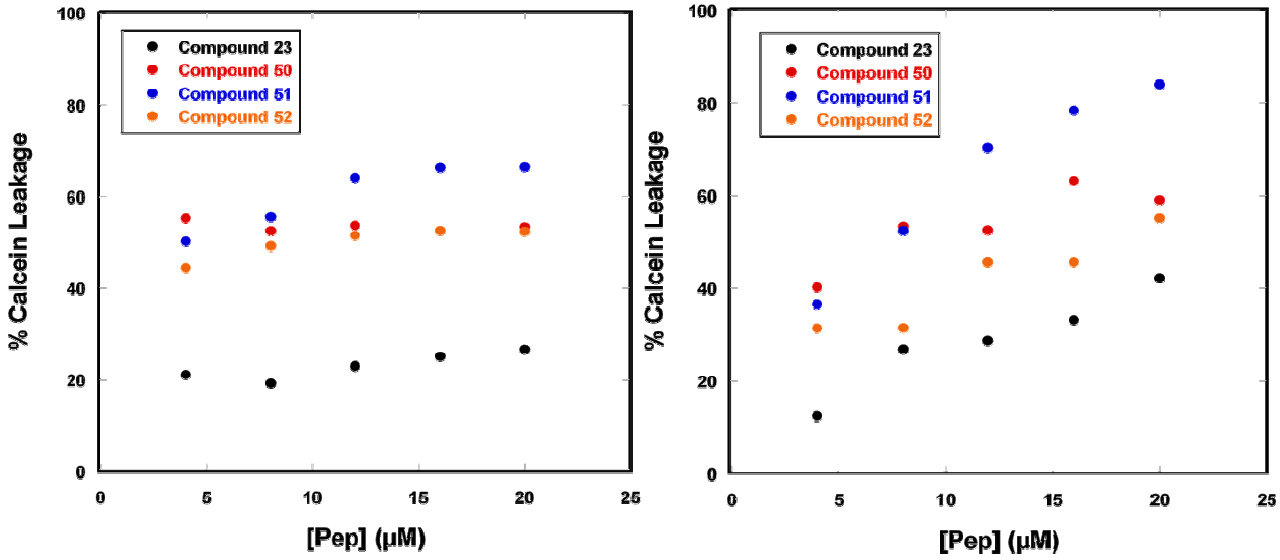

Figure 6.17: The total percent of calcein leakage from POPC (left) and 4:1 POPC/POPG LUVs induced by increasing concentrations of compounds **23**, **50**, **51**, and **52** as measured by fluorescence.

Conclusions

As suggested by the biological activity, the incorporation of Spacer #3 did not have an increased effect on the interactions with anionic membrane models as determined by CD, ITC and fluorescence leakage studies. There were changes in the CD spectra that indicate conformational changes are needed to compensate for the flexibility of the lysine cluster at the C-terminus. ITC and calcein leakage data supported the biological activity data for anionic membranes as the results were slightly different from compound **23** but almost identical to each other. Again, these results support the findings that the changes in the length of Spacer #3 played no role in the biological activity.

There was no hemolytic data available for this series of compounds in order to correlate the results of the CD, ITC and calcein leakage assays for POPC LUVs. However, we were able to hypothesize the interactions based on the studies. CD studies showed that the compounds

adopt very similar conformations in the presence of POPC LUVs to those adopted in buffer. It was determined that thes conformations are not dependent on the concentration of the zwitterionic LUVs suggesting minimal interactions with the LUVs. Based on ITC data, there were indications that the strength of the binding interactions increased with the length of Spacer #3. It is probably that the increased flexibility maximizes the attractive electrostatic interactions for binding. However, the pore forming capability of the compounds with Spacer #3 appeared minimal based on the single injection data and further supported by the calcein leakage studies. Based on the spectroscopic and thermodynamic data for the compounds incorporating Spacer #3 increasing the flexibility of the positively charged C-terminus resulting in increased binding to zwitterionic membranes. Although pore formation was not favored, if this modification was coupled with another that did increase pore formation, the increased binding would cause in increase in hemolysis, an unfavorable characteristic.

References

(1) Hicks, R. P.; Bhonsle, J. B.; Venugopal, D.; Koser, B. W.; Magill, A. J. De Novo Design of Selective Antibiotic Peptides by Incorporation of Unnatural Amino Acids. *J. Med. Chem.* **2007**, *50*, 3026-3036.

(2) Venugopal, D.; Klapper, D.; Srouji, A. H.; Bhonsle, J. B.; Borschel, R.; Mueller, A.; Russell, A. L.; Williams, B. C.; Hicks, R. P. Novel antimicrobial peptides that exhibit activity against select agents and other drug resistant bacteria. *Bioorg. Med. Chem.* **2010**, *18*, 5137-5147.

(3) Olofsson, A.; Borowik, T.; Gröbner, G.; Sauer-Eriksson, A. E. Negatively Charged Phospholipid Membranes Induce Amyloid Formation of Medin via an α-Helical Intermediate. *J. Mol. Biol.* **2007**, *374*, 186-194.

(4) Richardson, J. M.; Makhatadze, G. I. Temperature Dependence of the Thermodynamics of Helix–Coil Transition. *J. Mol. Biol.* **2004**, *335*, 1029-1037.

(5) Sanavio, B.; Piccoli, A.; Gianni, T.; Bertucci, C. Helicity propensity and interaction of synthetic peptides from heptad-repeat domains of herpes simplex virus 1 glycoprotein H: A

circular dichroism study. *Biochimica et Biophysica Acta (BBA) - Proteins & Proteomics* **2007**, *1774*, 781-791.

(6) Glukhov, E.; Stark, M.; Burrows, L. L.; Deber, C. M. Basis for selectivity of cationic antimicrobial peptides for bacterial versus mammalian membranes. *J. Biol. Chem.* **2005**, *280*, 33960-33967.

(7) Dathe, M.; Schumann, M.; Wieprecht, T.; Winkler, A.; Beyermann, M.; Krause, E.; Matsuzaki, K.; Murase, O.; Bienert, M. Peptide Helicity and Membrane Surface Charge Modulate the Balance of Electrostatic and Hydrophobic Interactions with Lipid Bilayers and Biological Membranes. *Biochemistry (N. Y.)* **1996**, *35*, 12612-12622.

(8) Brahms, S.; Brahms, J.; Spach, G.; Brack, A. Identification of beta,beta-turns and unordered conformations in polypeptide chains by vacuum ultraviolet circular dichroism. *Proc. Natl. Acad. Sci. U. S. A.* **1977**, *74*, 3208-3212.

(9) Ganesh, S.; Jayakumar, R. Circular dichroism and Fourier transform infrared spectroscopic studies on self-assembly of tetrapeptide derivative in solution and solvated film. *The Journal of Peptide Research* **2003**, *61*, 122-128.

(10) Nomura, K.; Corzo, G. The effect of binding of spider-derived antimicrobial peptides, oxyopinins, on lipid membranes. *Biochimica et Biophysica Acta (BBA) - Biomembranes* **2006**, *1758*, 1475-1482.

(11) Imura, Y.; Nishida, M.; Matsuzaki, K. Action mechanism of PEGylated magainin 2 analogue peptide. *Biochim. Biophys. Acta* **2007**, *1768*, 2578-2585.

(12) Nielsen, S. B.; Otzen, D. E. Impact of the antimicrobial peptide Novicidin on membrane structure and integrity. *J. Colloid Interface Sci.* **2010**, *345*, 248-256.

(13) Jing, W.; Hunter, H. N.; Hagel, J.; vogel, H. J. The structure of the antimicrobial peptide Ac-RRWWRF-NH2 bound to micelles and its interacitons with phospholipid bilayers. *Journal of Peptide Research* **2003**, *61*, 219-229.

(14) Christiaens, B.; Grooten, J.; Reusens, M.; Joliot, A.; Goethals, M.; Vandekerckhove, J.; Prochiantz, A.; Rosseneu, M. Membrane interaction and cellular internalization of penetratin peptides. *European Journal of Biochemistry* **2004**, *271*, 1187-1197.

(15) Wang, P.; Bang, J.; Kim, H. J.; Kim, J.; Kim, Y.; Shin, S. Y. Antimicrobial specificity and mechanism of action of disulfide-removed linear analogs of the plant-derived Cys-rich antimicrobial peptide Ib-AMP1. *Peptides* **2009**, *30*, 2144-2149.

(16) Wieprecht, T.; Beyermann, M.; Seelig, J. Binding of Antibacterial Magainin Peptides to Electrically Neutral Membranes: Thermodynamics and Structure. *Biochemistry (N. Y.)* **1999**, *38*, 10377-10387.

(17) Hunter, H. N.; Jing, W.; Schibli, D. J.; Trinh, T.; Park, I. Y.; Kim, S. C.; Vogel, H. J. The interactions of antimicrobial peptides derived from lysozyme with model membrane systems. *Biochimica et Biophysica Acta (BBA) - Biomembranes* **2005**, *1668*, 175-189.

(18) Wen, S.; Majerowicz, M.; Waring, A.; Bringezu, F. Dicynthaurin (ala) Monomer Interaction with Phospholipid Bilayers Studied by Fluorescence Leakage and Isothermal Titration Calorimetry. *The Journal of Physical Chemistry B* **2007**, *111*, 6280-6287.

(19) Wieprecht, T.; Apostolov, O.; Beyermann, M.; Seelig, J. Membrane Binding and Pore Formation of the Antibacterial Peptide PGLa: Thermodynamic and Mechanistic Aspects. *Biochemistry (N. Y.)* **2000**, *39*, 442-452.

(20) Wieprecht, T.; Apostolov, O.; Seelig, J. Binding of the antibacterial peptide magainin 2 amide to small and large unilamellar vesicles. *Biophys. Chem.* **2000**, *85*, 187-198.

(21) Wieprecht, T.; Seelig, J. Isothermal Titration Calorimetry for Studying Interactions between Peptides and Lipid Membranes. *Current Topics in Membranes* **2002**, *52*, 31-55.

(22) Wenk, M. R.; Seelig, J. Magainin 2 Amide Interaction with Lipid Membranes: Calorimetric Detection of Peptide Binding and Pore Formation. *Biochemistry (N. Y.)* **1998**, *37*, 3909-3916.

(23) Abraham, T.; Lewis, R. N. A. H.; Hodges, R. S.; McElhaney, R. N. Isothermal Titration Calorimetry Studies of the Binding of a Rationally Designed Analogue of the Antimicrobial Peptide Gramicidin S to Phospholipid Bilayer Membranes. *Biochemistry (N. Y.)* **2005**, *44*, 2103-2112.

(24) Seelig, J. Titration calorimetry of lipid-peptide interactions. *Biochim. Biophys. Acta* **1997**, *1331*, 103-116.

(25) Nomura, K.; Corzo, G. The effect of binding of spider-derived antimicrobial peptides, oxyopinins, on lipid membranes. *Biochimica et Biophysica Acta (BBA) - Biomembranes* **2006**, *1758*, 1475-1482.

(26) Bastos, M.; Bai, G.; Gomes, P.; Andreu, D.; Goormaghtigh, E.; Prieto, M. Energetics and Partition of Two Cecropin-Melittin Hybrid Peptides to Model Membranes of Different Composition. *Biophys. J.* **2008**, *94*, 2128-2141.

(27) Seelig, J. Thermodynamics of lipid-peptide interactions. *Biochim. Biophys. Acta* **2004**, *1666*, 40-50.

(28) Andrushchenko, V. V.; Aarabi, M. H.; Nguyen, L. T.; Prenner, E. J.; Vogel, H. J. Thermodynamics of the interactions of tryptophan-rich cathelicidin antimicrobial peptides with model and natural membranes. *Biochimica et Biophysica Acta (BBA) - Biomembranes* **2008**, *1778*, 1004-1014.

(29) Medina, M. L.; Bolender, J. P.; Plesniak, L. A.; Chapman, B. S. Transient vesicle leakage initiated by a synthetic apoptotic peptide derived from the death domain of neurotrophin receptor, p75NTR. *Journal of Peptide Research* **2002**, *59*, 149-158.

(30) Wei, S.; Wu, J.; Kuo, Y.; Chen, H.; Yip, B.; Tzeng, S.; Cheng, J. Solution Structure of a Novel Tryptophan-Rich Peptide with Bidirectional Antimicrobial Activity. *J. Bacteriol.* **2006**, *188*, 328-334.

(31) Wieprecht, T.; Dathe, M.; Schumann, M.; Krause, E.; Beyermann, M.; Bienert, M. Conformational and Functional Study of Magainin 2 in Model Membrane Environments Using the New Approach of Systematic Double-D-Amino Acid Replacement. *Biochemisty* **1996**, *35*, 10844-10853.

(32) Tamba, Y.; Yamazaki, M. Single Giant Unilamellar Vesicle Method Reveals Effect of Antimicrobial Peptide Magainin 2 on Membrane Permeability. *Biochemistry (N. Y.)* **2005**, *44*, 15823-15833.

(33) Hugonin, L.; Vukojević, V.; Bakalkin, G.; Gräslund, A. Membrane leakage induced by dynorphins. *FEBS Lett.* **2006**, *580*, 3201-3205.

(34) Matsuzaki, K.; Yoneyama, S.; Miyajima, K. Pore formation and translocation of melittin. *Biophys. J.* **1997**, *73*, 831-838.

(35) Benachir, T.; Lafleur, M. Study of vesicle leakage induced by melittin. *Biochimica et Biophysica Acta (BBA) - Biomembranes* **1995**, *1235*, 452-460.

CHAPTER SEVEN: ROLE PLAYED BY NUMBER AND PLACEMENT OF POSITIVELY CHARGED CLUSTER

Introduction

Positive charges are important for the initial attraction of the AMPs to the surface of the target cell's membrane. However, there is an optimal net positive charge that can enhance these electrostatic interactions and exceeding that optimal charge can diminish binding to the surface of the membrane. If the net positive charge is too low the attractive electrostatic interaction between the peptide and the membrane may be insufficient to attract the peptide to the surface of the membrane. If the net positive charge is too high, the repulsive electrostatic interactions between the incoming peptides and peptides already bound to the surface of the membrane may dominate, thus keeping additional peptide away from the surface of the membrane and preventing the peptide from reaching the critical concentration necessary for pore formation to occur. This chapter focuses on the number of positively charged residues clustered at either end of the peptide sequence. Compound **23** has four lysines at the C-terminus following a Tic residue. This number is decreased to three in compound **64** and increased to five for compound **39**. The cluster is relocated to the N-terminus in compound **61**, preceding a glycine amino acid. The amino acid sequences are given in **Table 7.1**.

Table 7.1: Amino acid sequences of the peptides used to study the rold played by the number and placement of the lysine cluster[1]

Compound	Amino Acid Sequence
23	Ac-GF-Tic-Oic-GK-Tic-Oic-GF-Tic-Oic-GK-Tic-KKKK-$CONH_2$
64	Ac-GF-Tic-Oic-GK-Tic-Oic-GF-Tic-Oic-GK-Tic-KKK-$CONH_2$
39	Ac-GF-Tic-Oic-GK-Tic-Oic-GF-Tic-Oic-GK-Tic-KKKK**K**-$CONH_2$
61	Ac-**KKKK**-GF-Tic-Oic-GK-Tic-Oic-GF-Tic-Oic-GK-Tic-$CONH_2$

The in vitro antibacterial activity of these compounds clearly documents the critical role played by the placement and number of positively charged residues in defining activity. The in vitro activity of compounds **23**, **39** and **61** against common bacterial strains (**Table 7.2**), are very similar. Overall, each compound exhibited low MIC values and their activity is very similar with the exception of the decreased activity of compound **61** against *Salmonella typhimurium*. However, in the presence of several Gram negative and Gram positive bacteria strains (**Table 7.3**), there appears to be a range of activity for compounds **23**, **64** and **61**. Compound **23** is the least active of the series except in the case of *Acinetobacter baumanii*. Either compound **64** or **61**, if not both, have increased activity against each strain as compared to compound **23**. Unfortunately, antibacterial activity against select agents is not available for compound **39**, so any conclusions made will be based on its activity with the common bacterial strains.

Table 7.2: Minimum inhibitory concentration (μM) of select bacteria strains and hemolytic activity.[1]

Compound	***Salmonella typhimurium***	***Staphylococcus aureus* ME/GM/TC resistant**	***Mycobacterium ranae***	***Bacillus subtillis***	**% hemolysis 100/25 μM**
23	10 μM	3 μM	10 μM	1 μM	14%
39	10 μM	3 μM	3 μM	1μM	24.9/ 18.9%
61	100 μM	30 μM	3 μM	not tested	not tested

Table 7.3: Minimum inhibitory concentration (μM) of Gram negative and other drug resistant bacteria strains.[2]

Compound	23	64	61
Acinetobacter baumanii ATCC 19606	3.2	6.7	12.8
Acinetobacter baumanii WRAIR	3.2	3.4	12.8
Staphylococcus aureus ATCC 33591	205	54	102
Yersinia pestis CO92	205	27	13.1
Brucella melitensis 16M	205	54	51
Brucella abortus 2308	205	27	51
Brucella suis 23444	205	>216	25.6
Bacillus anthracis AMES	12.8	27	0.4
Francisella tularensis SCHUS4	100	0.02	51
Burkholderia mallei	205	0.02	204
Burkholderia pseudomallei	205	0.02	204

Results and Discussion

CD Studies

CD spectra in buffer and micelle environments. In buffer, the shapes of of the CD spectra of compounds **23**, **64** and **61** were very similar with some differences in their intensities. The maximum at approximately 195 nm was indicative of α-helical components. [1, 3-7] Compound **64** exhibited the most intense CD spectrum followed by **61** and **23**. However, the CD spectrum of compound **61** exhibited the most intense double minima suggesting an increase in α-helical

character.[8-12] The increase in lysines at the C-terminus, compound **39**, did not appear to adopt any discernable structure in buffer.

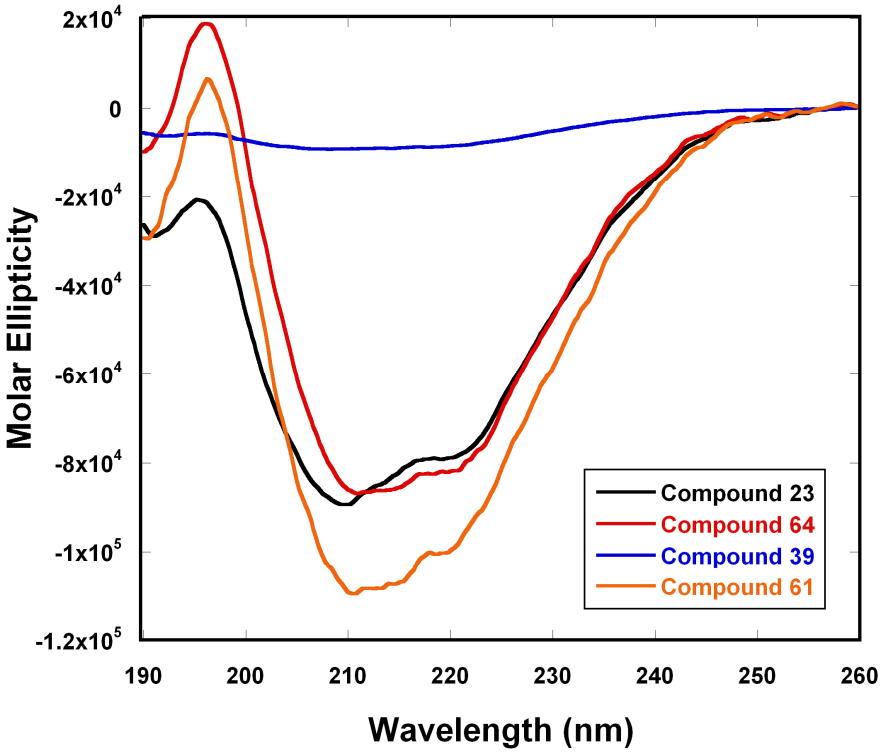

Figure 7.1: Far-UV CD spectra of compounds **23**, **64**, **39** and **61** (peptide concentration of approximately 400 μM) in 40 mM phosphate buffer, pH = 6.8.

Transitioning from a buffer environment to SDS micelles (**Figure 7.2** - left), the CD spectra exhibited two obvious changes. A shift from the λ_{max} 195 to 190 nm accompanied by an increase in the intensity for each peptide, a minimal increase in intensity was observed for compound **39**, indicated an increase in the helicity of the peptides.[5, 8-10, 12] There was also a shift of the λ_{min} at approximately 210 to 202 nm suggesting a decrease in the α-helical component.[5, 11, 13] However, except for compound **23**, the intensities of the minima did not change, although the

order of the spectral intensities did. Compound **61** exhibited the most intense spectra followed by **23** and **64** with similar intensities in buffer. However, in the presence of SDS micelles, compound **23** exhibited the most intense spectra followed by **61** then **64**. The CD spectrum of compound **39** was the least intense in both environments. The CD spectra of all of the peptides, except for **39**, exhibited shifts in wavelength and changes in intensity in comparison to their spectra in buffer, concluding that they were adopting different conformations in the presence of anionic micelles.[5, 8-10]

Similar shapes were observed in CD spectra of the peptides in the presence of DPC micelles (**Figure 7.2 -** right) as well, although, once again a change in the increase of the intensities accompanied the CD spectra. The CD spectrum of compound **23** was the least intense in the presence of DPC micelles, decreasing from intensities observed in the CD spectra in SDS micelles, but increasing in comparison to its spectra in buffer. The CD spectra of compounds **64** and **61** were similar below 200 nm and in the intensities of their double minima, with compound **61** being the most intense. The CD spectrum of compound **39** retained the same shape in both DPC and SDS concluding that its S-state interactions, and therefore conformations, do not vary.[5, 9] Changes in the intensities of the spectra led to the conclusion that the peptides were changing the amount of ordered structure when interacting with DPC and SDS micelle surfaces.[8, 9, 11, 12]

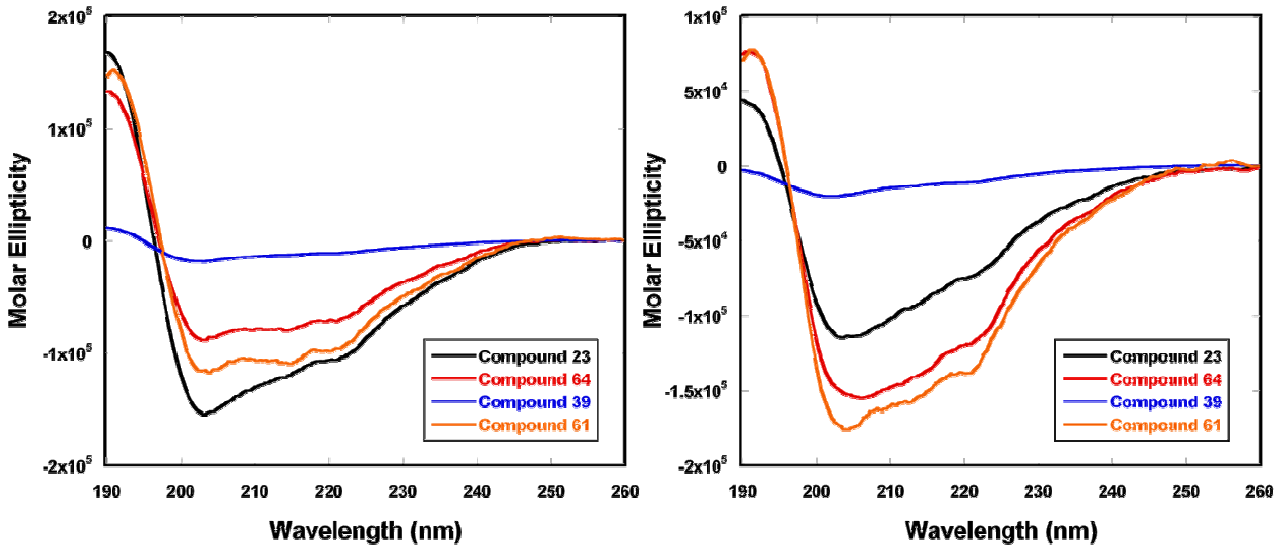

Figure 7.2: Far-UV CD spectra of compounds **23**, **64**, **39,** and **61** (peptide concentration of approximately 400 μM) in 80 mM SDS (left) and 80 mM DPC (right) in 40 mM sodium phosphate buffer, pH = 6.8.

CD spectra of peptides in LUV environments. Introducing POPC LUVs (**Figure 7.3** – left) induced significant changes in the shapes and intensities in the CD spectra of all peptides, including compound **39**. When compared to their corresponding spectra in buffer, there was a decrease in the intensity of the λ_{max} at 195 nm. The increase in intensity and varying shifts in the λ_{min} from 208 in buffer to 210 nm for compound **23** and 212 nm for compounds **64** and **61** was evidence of conformational changes in the presence of POPC LUVs.[9-11] As compared to their S-state conformations in DPC micelles, compounds **23** and **39** were the only peptides which increased in their intensity at their minima.

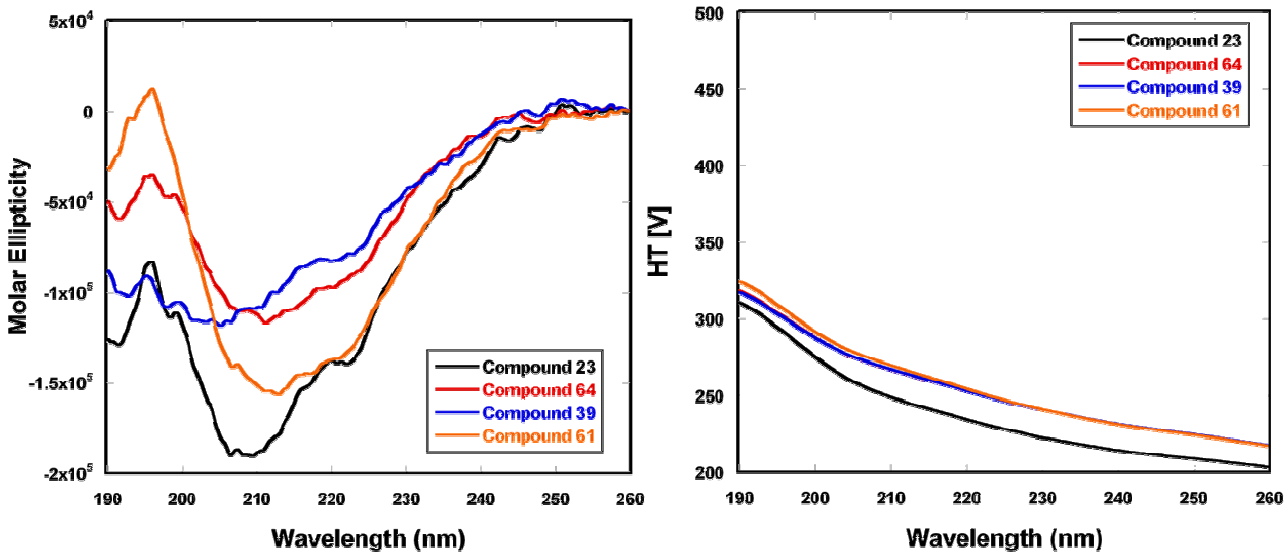

Figure 7.3: Far-UV CD spectra of 75 µM compound **23** and 100 µM solutions of compounds **64**, **39** and **61** in 1.75 mM POPC (left) in 40 mM phosphate buffer, pH = 6.8, and their corresponding HT values (right).

The variations in the positively charged clusters had a great effect on the conformations observed in the presence of 1.75 mM 4:1 POPC/POPG LUVs (**Figure 7.4** – left). Compound **23** exhibited shifts from approximately 196 and 208 nm to 192 and 202 nm, respectively, suggesting an increase in α-helical, β-turn and unstructured components.[3, 9, 11, 13] The CD spectrum of compound **39** was very similar to compound **23**, but with a decrease in intensity suggesting less structures.[8, 9, 12] Compounds **64** and **61** were very different from their spectra in buffer as well as the peptides in this series. The minimum below 200 nm for compound **64** was indicative of a random coil conformation.[3, 6, 11] Though there is not a component of positive charge at approximately 220 nm, which is characteristic of random coil, [8, 9, 11] the disappearance of the minimum typical of an α-helix confirms the significant decrease of an ordered structure in the presence of anionic LUVs. It has been suggested through molecular modeling that peptides do not possess a high degree of ordered structure when inserted into a bilayer as part of a pore.[14]

This observation could explain the unordered appearance of the spectra of compound **64** in the presence of anionic membranes. The compound is biologically active as supported by the biological data and should in fact, for pores. Compound **61**, on the other hand, exhibited a minimum at approximately 202 nm with great intensity as compared to the other minimum at 222 nm. This increased ellipticity coupled with the maximum at approximately 195 nm supports the conclusion that compound **61** adopted a conformation containing high amounts of β-turn and α-helical components.[3, 11, 13, 15]

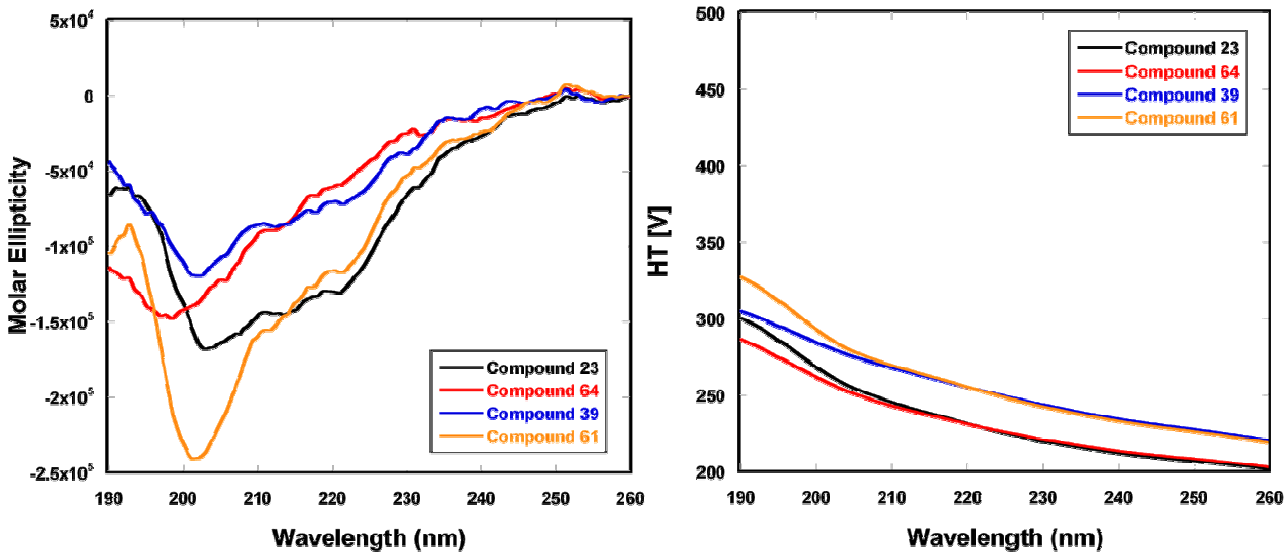

Figure 7.4: Far-UV CD spectra of 75 µM compound **23** and 100 µM solutions of compounds **64**, **39** and **61** in 1.75 mM 4:1 POPC/POPG LUVs (left) in 40 mM phosphate buffer, pH = 6.8, and their corresponding HT values (right).

CD spectra for "pseudo" titrations. The "pseudo" titration of POPC LUVs into these peptides did not yield any results that would suggest a concentration dependent interaction, as can be seen in **Figure 7.5**. The number or placement of the lysine cluster does not appear to

dramatically change the spectra as the concentration of POPC LUVs increased. Compound **23** was the only compound that was significantly different from its spectra in buffer. The remaining three peptides vary in intensity, suggesting some level of interaction.[8, 9, 12]

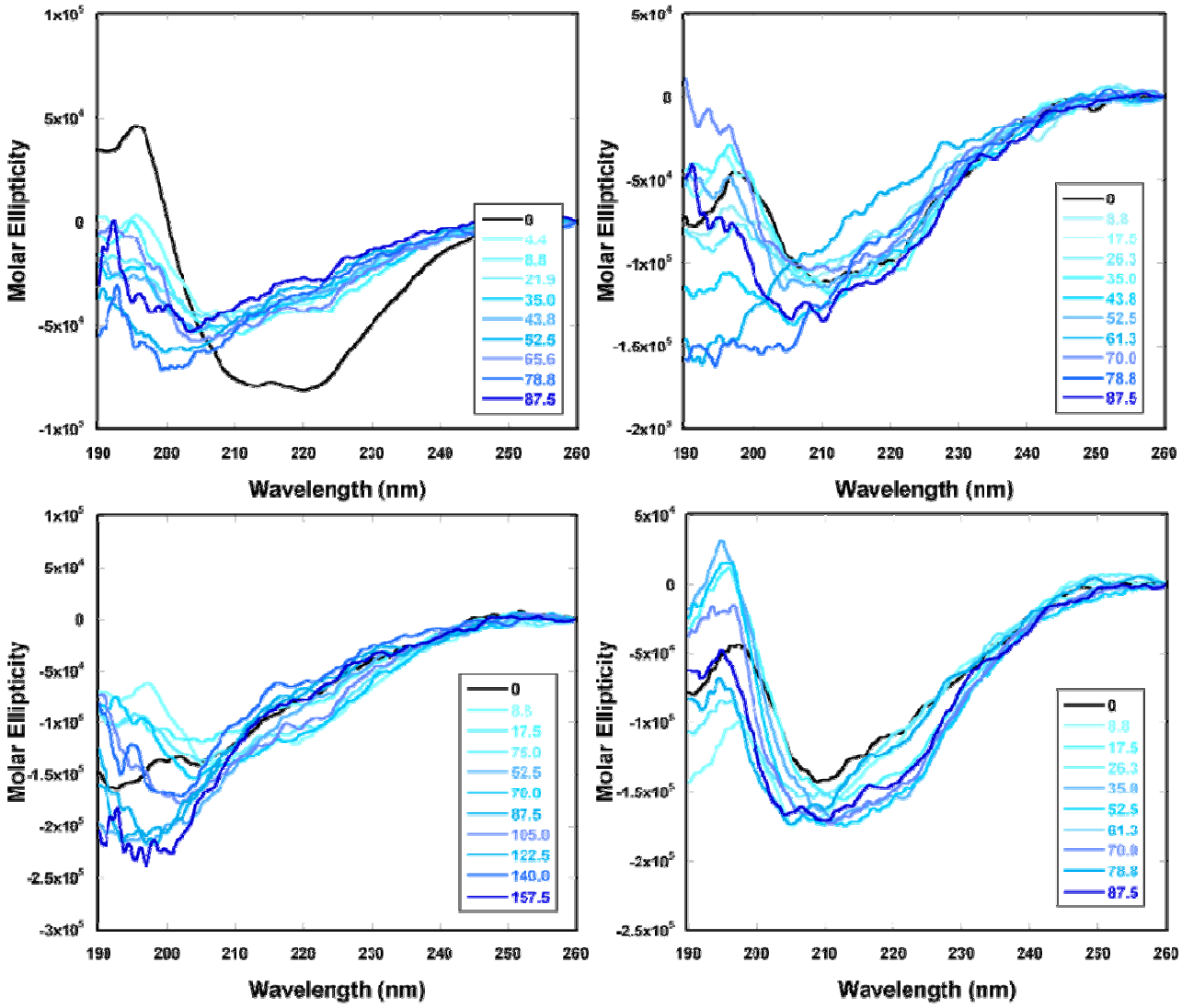

Figure 7.5: Far-UV CD spectra of separate samples of 200 µM solutions of compounds **23** (top left) and compound **61** (bottom right) and 100 µM solutions of compounds **64** (top right) and compound **39** (bottom left) with increasing concentrations of POPC LUVs in 40 mM phosphate buffer, pH = 6.8.[16, 17]

The “pseudo” titrations of compounds **23** and **39** with the anionic liposomes 4:1 POPC/POPG LUVs (**Figure 7.6**) yielded the trend that was discussed previously in chapter 3. A decrease in ellipticity occurred as the L/P ratio increased until a spectra of leveling intensity was reached, followed by an increase. Very different results were observed for the “pseudo” titrations with 4:1 POPC/POPG LUVs for compounds **64** and **61**. As can be seen from the figure, neither compound **64** nor **61** exhibited a spectrum transitioning from decreasing to increasing spectral intensity as was observed with other peptides in this series. This transition spectrum denotes a “critical point” or transition from predominately I-state to S-state. Both compounds, however, exhibited opposite trends in their changing intensities as compared to compounds **23** and **39**. The intensity of their spectra initially decreased with the first addition of anionic LUVs and proceeded to increase (blue spectra) to a spectra of maximum intensity. At this point, the trend reversed and the intensity began to decrease (purple to red spectra). This data was evidence that compounds **64** and **61** interact with anionic membranes via different mechanisms than compounds **23** and **39**, which could support the increased bioactivity.

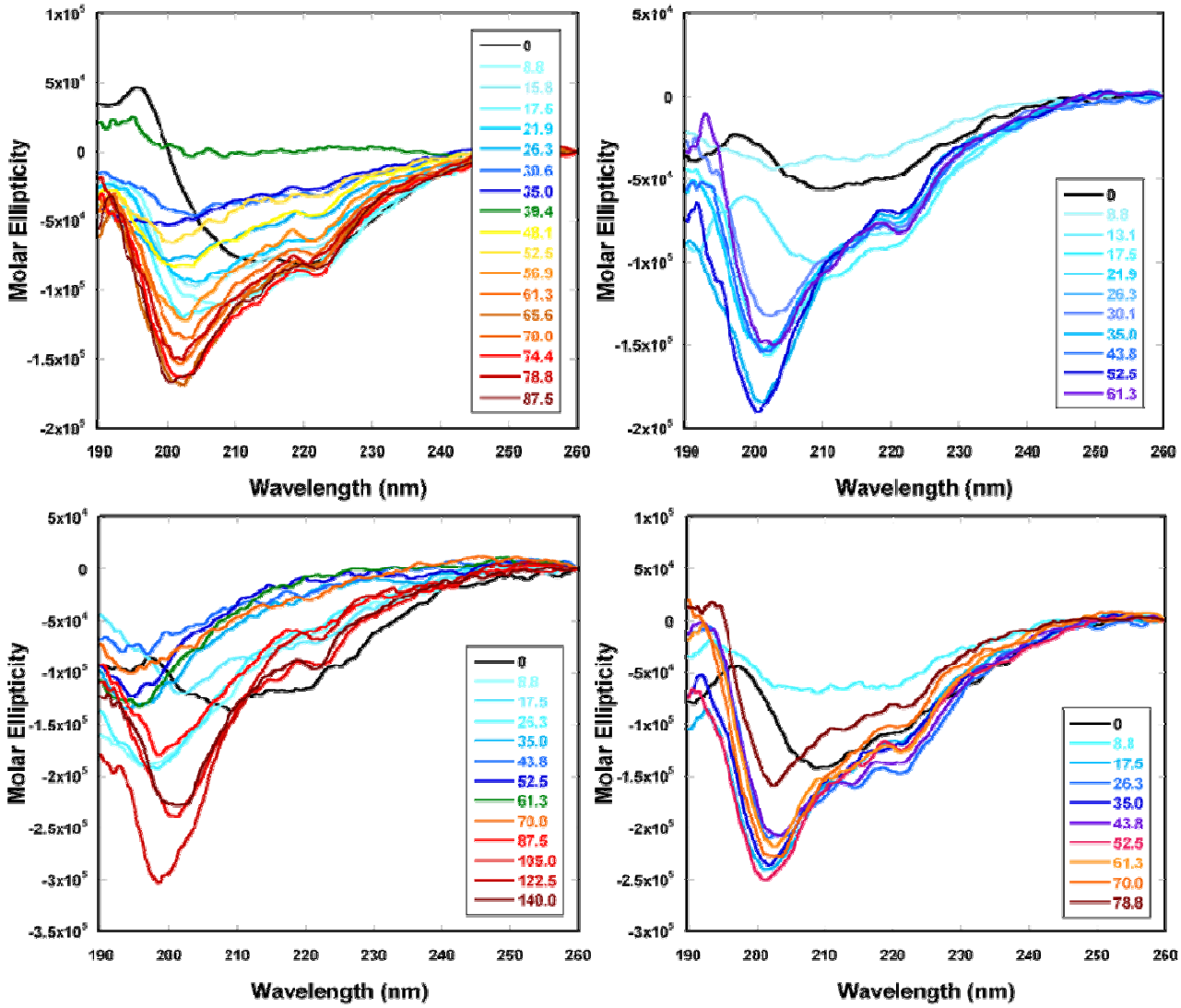

Figure 7.6: Far-UV CD spectra of separate samples of 200 µM solutions of compound **23** (top left), **64** (top right), **39** (bottom left) and **61** (bottom right) with increasing concentrations of 4:1 POPC/POPG LUVs in 40 mM phosphate buffer, pH = 6.8.[16, 17]

ITC Studies

Anionic LUVs. Upon first observation of the full titration experiment for 4:1 POPC/POPG LUVs into these peptides, noticeable observations included a very small exothermic component for compound **39** , and the even smaller, almost undetectable for

compound **64**. It would appear that the slight increase and/or decrease of the charge density at the C-terminus played an important role in the interaction of the peptide with anionic membranes. We were unable to fit thermodynamic data to an existing model, however, by breaking down the thermograms into their separate components, endothermic and exothermic, it was possible to make conclusions in regards to the interactions. The cumulative endothermic heats decreased as the number of lysines increased.[18-21] An endothermic process has been attributed to pore formation.[20, 22] Formation of a pore encompasses several different processes that contribute to positive and negative ΔH values, with the positive components dominating.[20] Positive ΔH contributions include, but are not limited to, the desolvation of structured water molecules on the surfaces of the peptides and membrane, disruption of the phospholipid head groups and lipid:lipid interactions, as well as the release of the water molecules from inside the bilayer model.[17, 21, 23-26] Attractive electrostatic interactions, conformational changes, and reorganization of the head groups and lipid acyl chains are contributors to the negative ΔH associated with the binding process.[17, 20, 21] The resulting peaks observed in the thermogram after each injection reflect the dominate process, pore formation or binding, and therefore the more favorable of the two.[20] The decrease in the endothermic cumulative heats as the number of lysines decreases, 0.79, 0.78 and 0.75 kcal/mol for compounds **64**, **23** and **39** respectively, suggests that pore formation is slightly more favorable with less net positive charge. One possibility for this result could involve the repulsion that is caused by the binding of peptides that are highly positively charged. Accumulation of positively charged peptides on the surface of the LUV during binding may causes an increase in the surface charge of the membrane, consequently increasing the repulsion of additional peptides.[18, 27] In addition, the transition from the endothermic to exothermic phases has been attributed to the shift in the formation ↔ pore

disintegration equilibrium towards to the right. Pore disintegration corresponds to the exothermic phase, and therefore, processes that refer to binding.[20, 22, 28] The L/P ratio that corresponds to the transition from the endothermic to exothermic phase also refers to the point at which all of the peptide is assumed to be bound.[17, 20, 21] The low molar ratios required for this transition to occur supports the theory that the compounds with less net positive charge favor pore formation.

The exothermic components refer to the portion of the titrations that favor binding.[17, 20, 24, 29] As the L/P molar ratios continued to increase, and peptide-free liposomes were added to a solution that was assumed to have no free peptide available, a maximum exothermic point is reached where the processes transition from predominately I-state to S-state. Previously, the L/P ratio corresponding to this transition point could be correlated to the "critical point" in the "pseudo" CD titrations with POPC/POPG LUVs, as was the case for compounds **23** and **39**. For The blue spectra of **Figure 7.6** correspond to the endothermic phase and pore formation of the full titration ITC thermograms for 4:1 POPC/POPG LUVs. The red spectra, therefore, represent the binding and exothermic phases that occur with increased lipid concentration. Compounds **23** and **39** clearly had both phases as seen in CD and ITC, which was not the case for compound **64**. ITC exhibited one clear endothermic phase corresponding with pore formation and the "pseudo" CD titration supports this data with one grouping of CD spectra. These two experiments combined suggest a different mechanism of action for compound **64**.

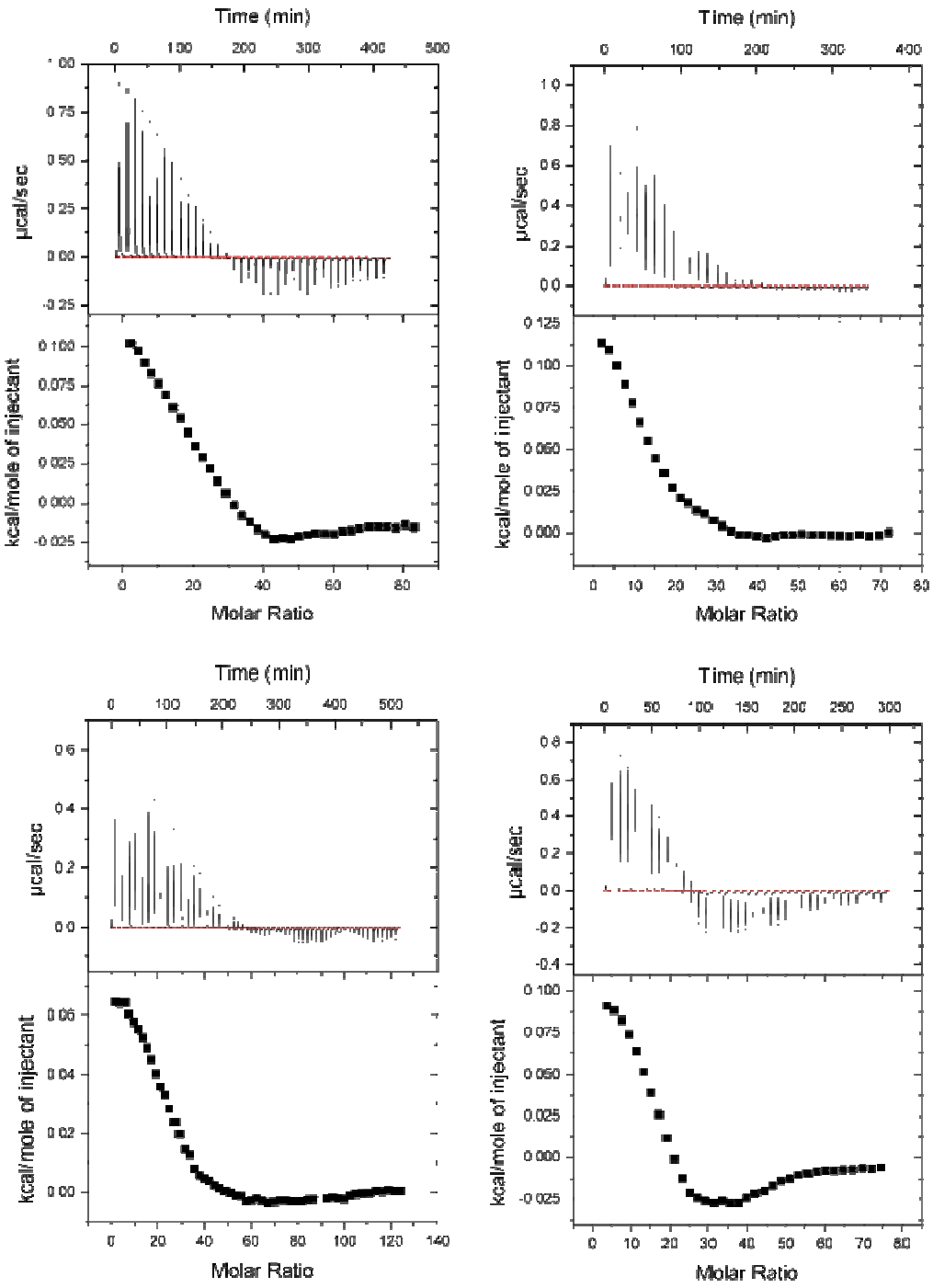

Figure 7.7: ITC data for the full titration of 35 mM 4:1 POPC/POPG LUVs into 200 µM solutions of compounds **23** (top left), **64** (top right)**, 39** (bottom left) and **61** (bottom right).

Repositioning the cluster of lysines at the N-terminus as in Compound **61** (**Figure 7.7** - bottom right) also exhibited a different mechanism of action which is supported by the full

titration ITC experiment and "pseudo" CD titrations with 4:1 POPC/POPG LUVs. The thermogram was very similar in shape to compound **23**. Both exhibited clear endothermic and exothermic components. Their cumulative endothermic ΔHs[18-21] were however, different with 780 and 530 cal/mol for compounds **23** and **61**, respectively. Compound **23** may have produced more "pore forming" heat, but compound **61** bound all of the free peptide at a L/P ratio of approximately 20 compared to 36 for compound **23**.[17, 18, 20, 21] The sum of their exothermic components, however, were very similar in magnitude at approximately -0.37 and -0.38 kcal/mol, respectively, for compounds **23** and **61**. The similarity of these values suggests that their abilities to bind to the membrane surface were comparable. Further evidence that the two compounds, whose only difference is the position of their lysine cluster, were the L/P molar ratios associated with their maximum exothermic component. The maximum exothermic point observed in the thermogram for the titration of compound **23** with anionic LUVs corresponds to the green spectrum in **Figure 7.6** of the CD titration. This particular spectrum refers to the transition from predominately I-state to S-state. Compound **61**, however, does not have a spectrum comparable to that of the transitioning green spectrum observed for compound **23** due to the reversed direction of the changes in the intensity of the spectra. For compound **61**, the intensity of the spectra increased with the first addition of anionic liposomes until a maximum intensity was reached and then began to decrease, a completely different trend from that which was observed for compound **23**. The ITC thermogram of compound **61** supports the CD results in that the placement of the lysine cluster plays an important role in the interaction with anionic LUVs.

Both compounds **64** and **61** interacted via different mechanism from the other two peptides in this series, as well as each other. This conclusion supports the biological activity

(**Table 7.3**) and the ability for these particular compounds to exhibit activity against several different bacteria strains with varying membrane compositions. It is possible that an overall net charge of +5, with a concentration of +3 at the C-terminus as in compound **64**, is ideal for increased activity against *Yersinia pestis* CO92, *Francisella tularensis* SCHUS4 and some strains of *Burkholderia*. The change in mechanism of action for compound **61** could be due to the increased flexibility of the lysine tail at the N-terminus versus the C-terminus. The lysine cluster precedes a glycine residue when positioned at the N-terminus, but follows a very rigid Tic residue at the C-terminus. The neighboring residue in the sequence could play a role in the flexibility of the positive cluster that allows it to adopt certain conformations in the presence of particular bacteria cell membranes such as *Bacillus anthracis* AMES and strains of *Brucella*.

Zwitterionic LUVs. At first inspection of the full titrations of POPC LUVs into compounds **23**, **64**, **39** and **61** (**Figure 7.8**), their thermograms are very similar. All have endothermic components that require very high L/P molar ratios before all of the peptide is assumed bound to the LUV. This high molar ratio is indicative of weak interactions with zwitterionic LUVs. The degree of binding, X_b, associated with these interactions was calculated and plotted against the concentration of peptide free in solution, c_f, using the equations described previously. These plots are given in **Figure 7.9**.

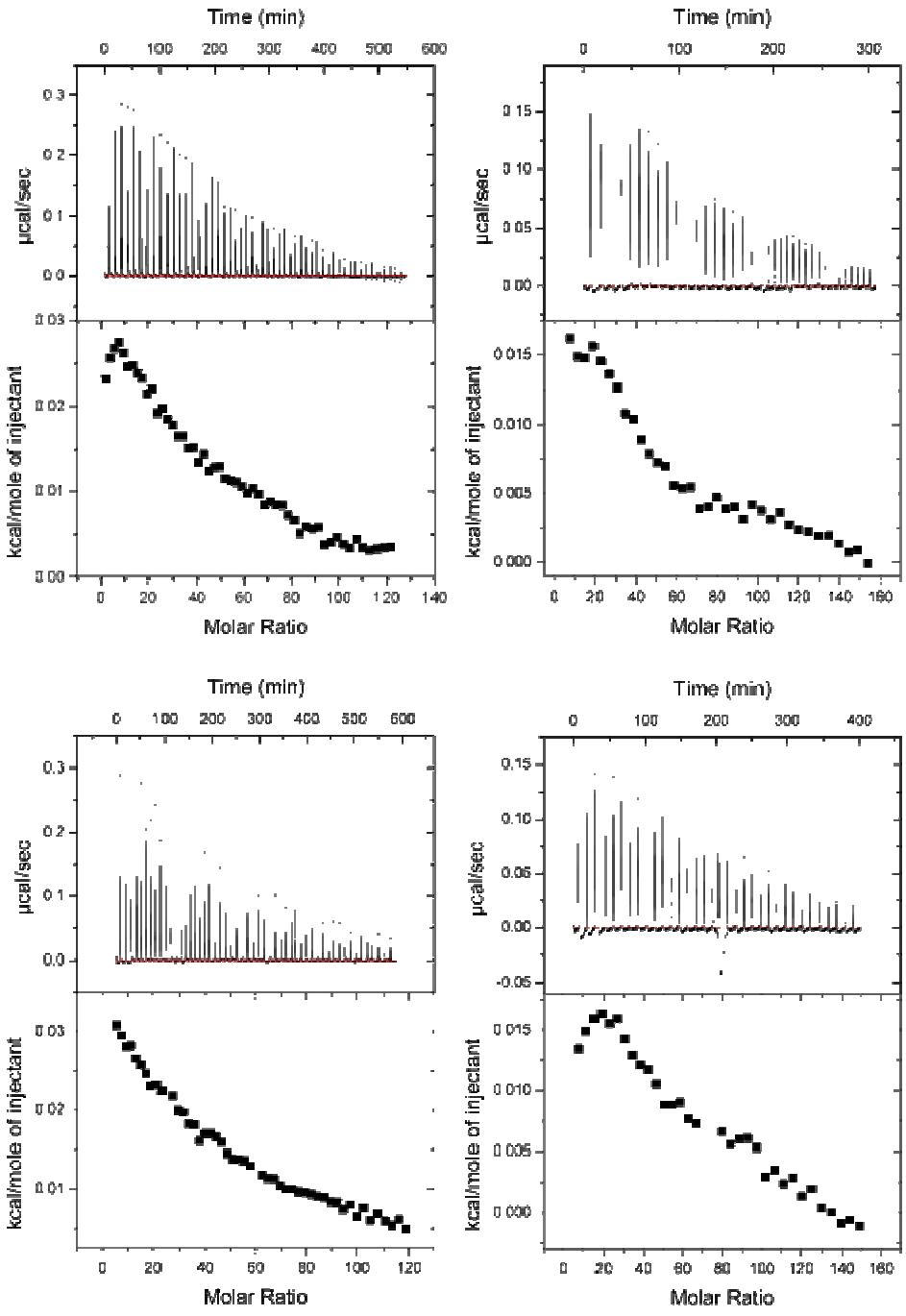

Figure 7.8: ITC data for the full titration of 35 mM POPC LUVs into 200 µM compound **23** (top left), and 100 µM solutions of compounds **64** (top right)**, 39** (bottom left) and **61** (bottom right).

There were two obvious sets of plots. Compounds **23** and **61** exhibited dramatic downward bends at high peptide concentrations. This result has been attributed to repulsion. As

the cationic peptides become bound, the surface of the membrane becomes more positively charged, thus hindering the binding of other peptides. Compound **61** portrayed a more drastic downward bend than compound **23**, suggesting an increase in the repulsive interactions. One possible explanation for this could be the increased flexibility of the lysine cluster at the N-terminus due to the increased flexibility of the neighboring glycine versus the rigid Tic residue at the C-terminus. With the added flexibility, the peptide has increased mobility to move over the surface of the membrane, thus repelling other peptides over a larger area. Compound **23**, when bound, may remain more or less stationary and does not have the capability to repel over a large surface area.

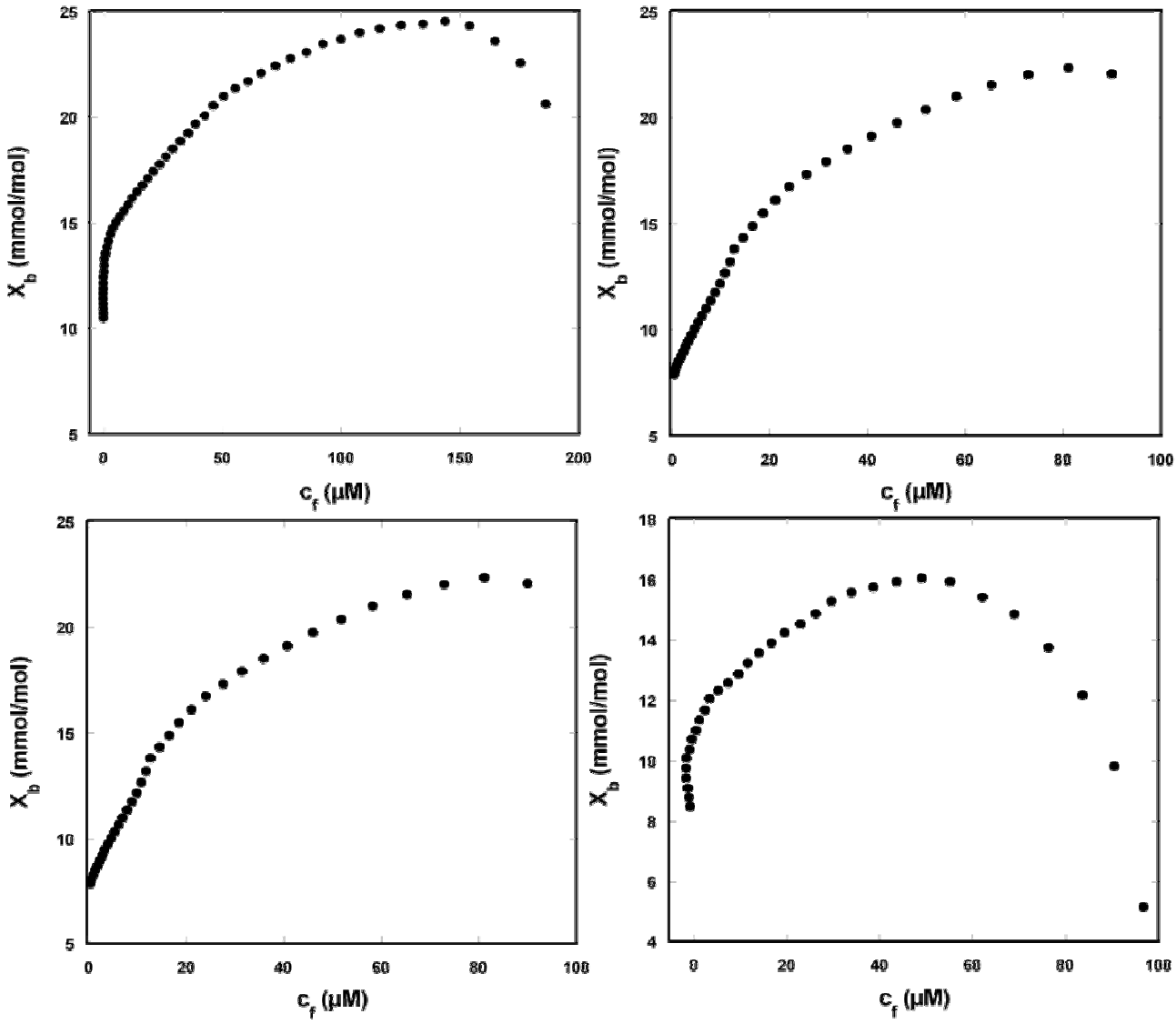

Figure 7.9: Plot for the degree of binding, X_b, as a function of the peptide concentration in bulk solution, c_f. The binding isotherms were derived from the titration of 35 mM POPC LUVs into compounds **23** (top left), **64** (top right), **39** (bottom left) and **61** (bottom right). X_b and c_f were calculated as described in chapter 1 of the text.

Compounds **64** and **39**, the analogues of **23** with a decrease and increase in the number of lysines in the C-terminus cluster, respectively, do not exhibit a drastic bending of their isotherm. The lack of a downward bend is indicative that a different interaction is taking place. This

conclusion is supported when a more sophisticated model, surface partition equilibrium, was applied to the data to account for the electrostatic interactions.

Plots of the degree of binding against the concentration of peptide at the membrane surface, c_m, are given in **Figure 7.10**. Again, there were two obvious trends. Compounds **23** and **61** both exhibited one line fitting the model from **Equation 1.9**. This suggests that these two peptides follow the expected mechanism involving the electrostatic interactions to the surface of the membrane and their binding constants, K, were determined. The other two compounds, however, did not appear to follow the typical interaction as their binding isotherms exhibited two distinct phases, one at a lower peptide concentration and one as the concentration increased. Both of the lines were for to the model described by **Equation 1.9**, allowing for the determination of two separate binding constants. Know the binding constants for the peptides allowed for the calculation of ΔG and ΔS using **Equations 1.1** and **1.2**. These values coupled with the experimentally measure ΔH gave a full set of thermodynamic data for the interaction of these peptides and POPC LUVs.

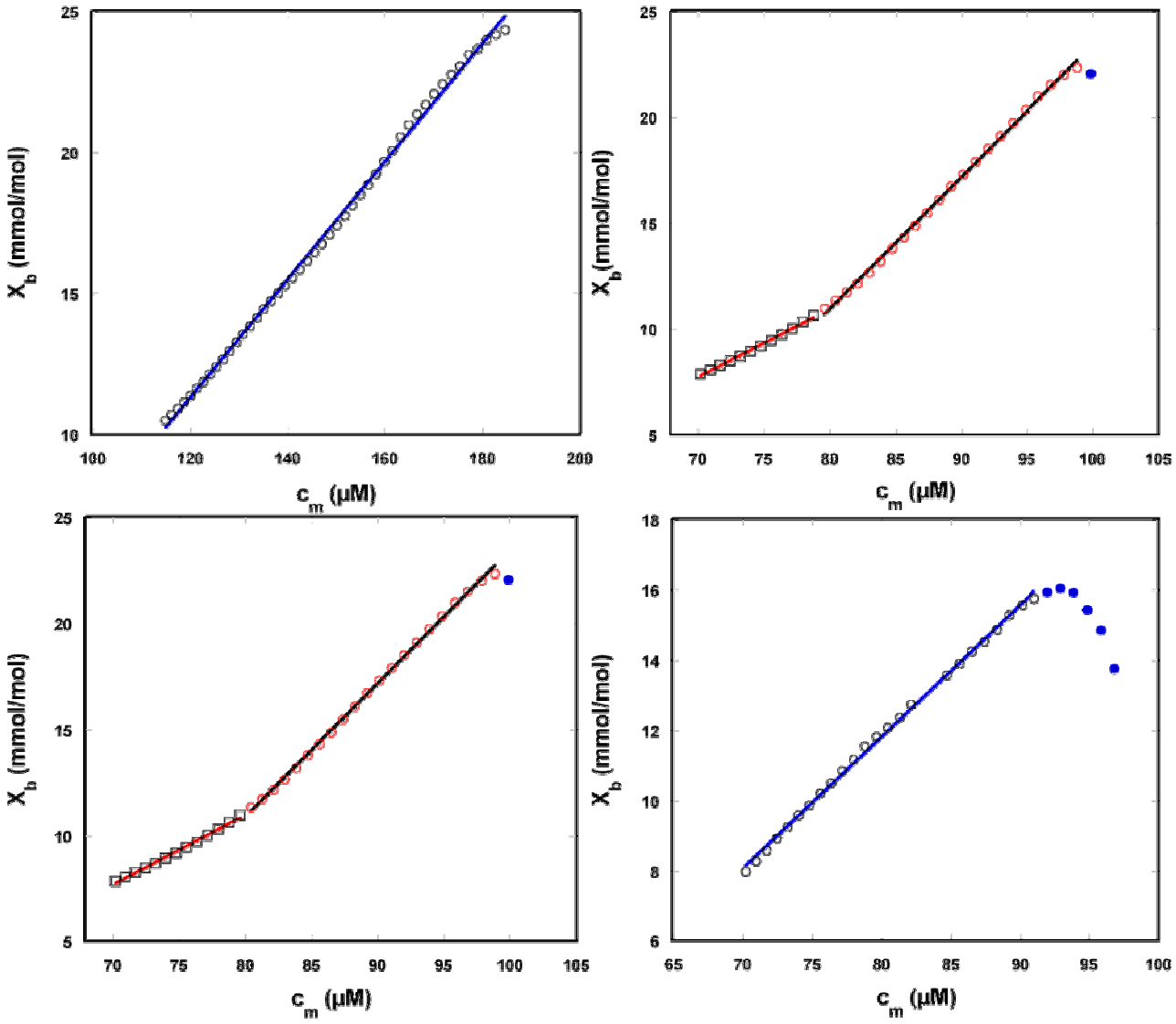

Figure 7.10: Plot for the degree of binding, X_b, as a function of the membrane surface concentration of peptide, c_m. The binding isotherms were derived from the titration of 35 mM POPC LUVs into **23** (top left), **64** (top right), **39** (bottom left) and **61** (bottom right). X_b and c_m were calculated as described in Chapter 1 of the text.

Compounds **23** and **61**, with one set of data, exhibited the least favorable interaction with POPC LUVs, a therapeutically desirable characteristic. All of their thermodynamic data, ΔH^0, K, ΔG and ΔS, were the least favorable of the series, with the exception of the ΔH of compound **61**. The other two compounds, **64** and **39**, did exhibit increased affinity for zwitterionic LUVs, as

compared to compounds **23** and **61**. However, there was not a large amount of interaction taking place. At low peptide concentrations, the thermodynamic data were minimal, but become more favorable as the peptide concentration increases. Even at their highest concentration, however, compounds **64** and **39** interact much less with POPC LUVs than magainin. The thermodynamic data is summarized in **Table 7.4**.

Table 7.4: Thermodynamic data for a representative titration of 35mM POPC into the peptides at 25°C as derived from the equations discussed previously.

Compound	$\Delta H^{0,a}$ (kcal/mol)	K^b (M^{-1})	ΔG^c (kcal/mol)	ΔS^d (cal/mol·K)
Lower Peptide Concentration				
23	na	na	na	na
64	0.05	320.0	-3.41	11.62
39	0.06	327.8	-3.43	11.69
61	na	na	na	na
Higher Peptide Concentration				
23	0.67	211.0	-3.17	12.86
64	0.49	623.0	-3.81	14.43
39	0.49	627.2	-3.81	14.43
61	0.35	374.1	-3.51	12.95
Magainin 2 amide[e]				
M2a	-15.90	2000.00	-7.00	-29.40

[a] ΔH values are directly measured binding enthalpies and calculated using **Equation 1.4**.
[b] Binding constants were generated from the lipid-into-peptide titrations using the model as described in the text.
[c] Free energies were calculated using **Equation 1.1**.
[d] Entropy was calculated using **Equation 1.2**.
[e] Thermodynamic parameters for Magainin analogue M2a as presented by Wieprecht and coworkers.[23, 28]

Calcein Leakage Studies

As can be seen in **Figure 7.11**, with the exception of compound **61**, the peptides induced calcein leakage of POPC LUVs did not appear to be concentration depending for any of the compounds in this series. Compounds **64** and **61** induced the most leakage with is consistent with

the thermodynamic data presented previously. The decrease in the electric charge in compound **64** could allow for the peptide to maneuver around the positive charges of the head groups more easily, thus increasing the binding and causing leakage. The added flexibility of the lysine cluster in compound **61** due to the neighboring glycine, as suggested earlier in this chapter, could allow it to bind more easily to the surface of the membrane. With the N-terminus associated with the polar lipid head groups of the surface, the C-terminus with the larger Tic residue will insert into the bilayer. The larger residue could possibly form a larger pore, which consequently, would cause more leakage as observed in **Figure 7.11**.

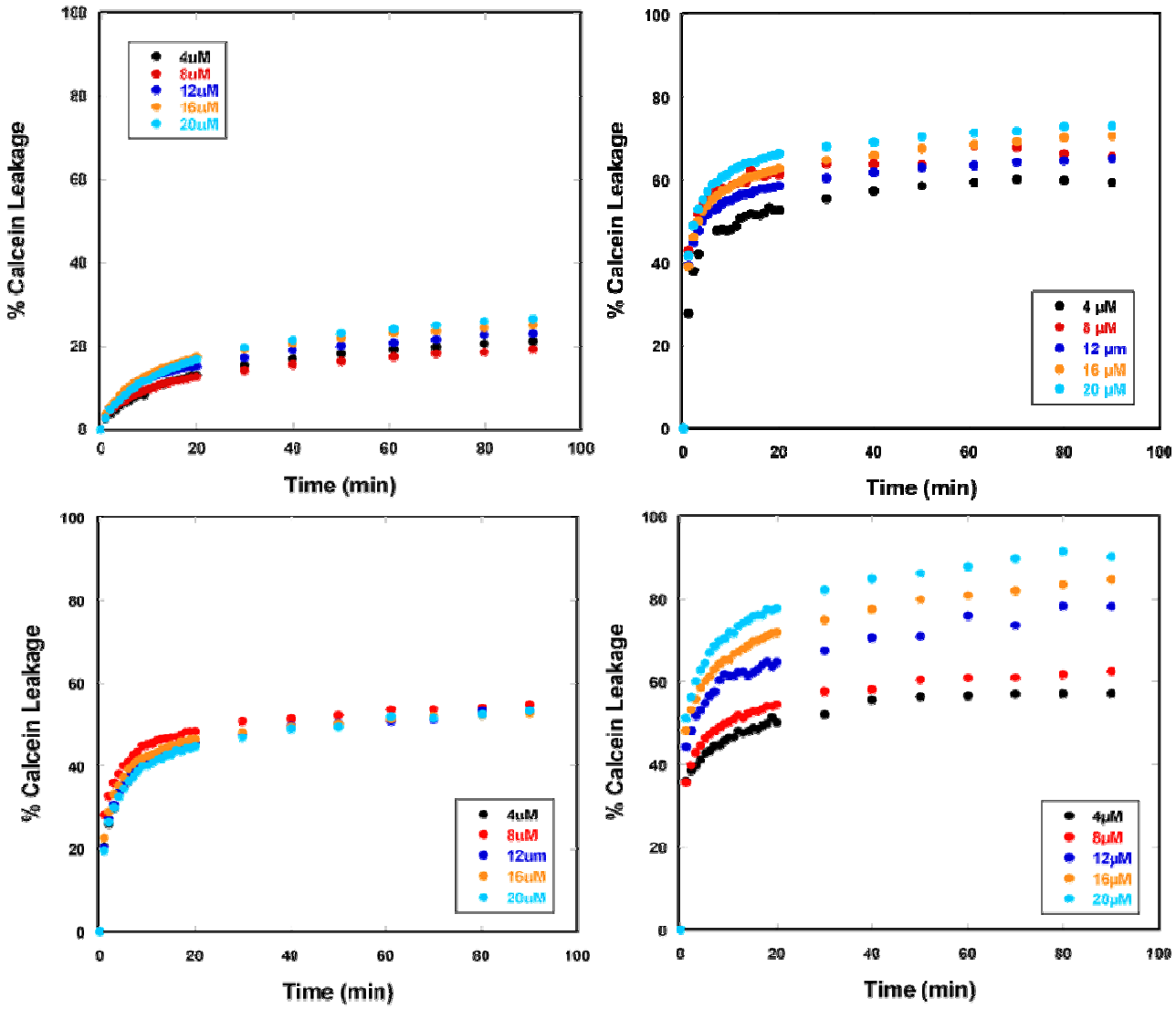

Figure 7.11: The time dependent release of calcein from POPC LUVs induced by increasing concentrations of compounds **23** (top left), **64** (top right), **39** (bottom left), and **61** (bottom right) as measured by fluorescence.[30-32]

Peptide induced leakage of the 4:1 POPC/POPG LUVs was concentration dependent as can be seen in **Figure 7.12** and further highlighted in **Figure 7.13**. Each compound, with the exception of compound **39**, exhibited significant increase in the leakage as the peptide concentration increased. Compound **39**, on the other hand, did not display an obvious dependence on the peptide concentration. One possible explanation is the increased charge

resulted in the repulsion of incoming peptides. As the charge decreased, the leakage increased. The increased leakage of compounds **64** and **61** is supported by the biological data as active compounds in the presence of anionic LUVs.

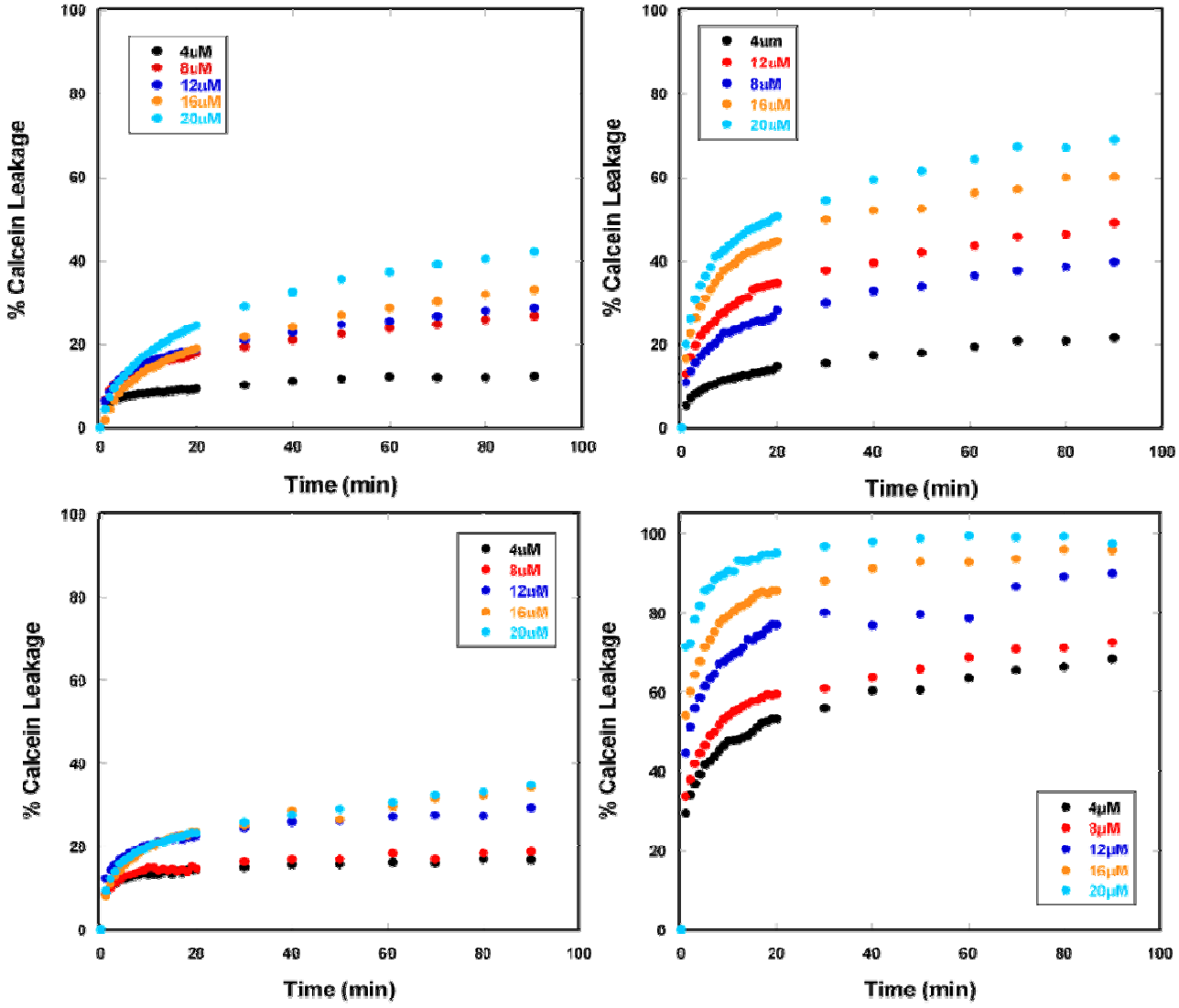

Figure 7.12: The time dependent release of calcein from 4:1 POPC/POPG LUVs induced by increasing concentrations of compounds **23** (top left), **64** (top right), **39** (bottom left), and **61** (bottom right) as measured by fluorescence.[30-32]

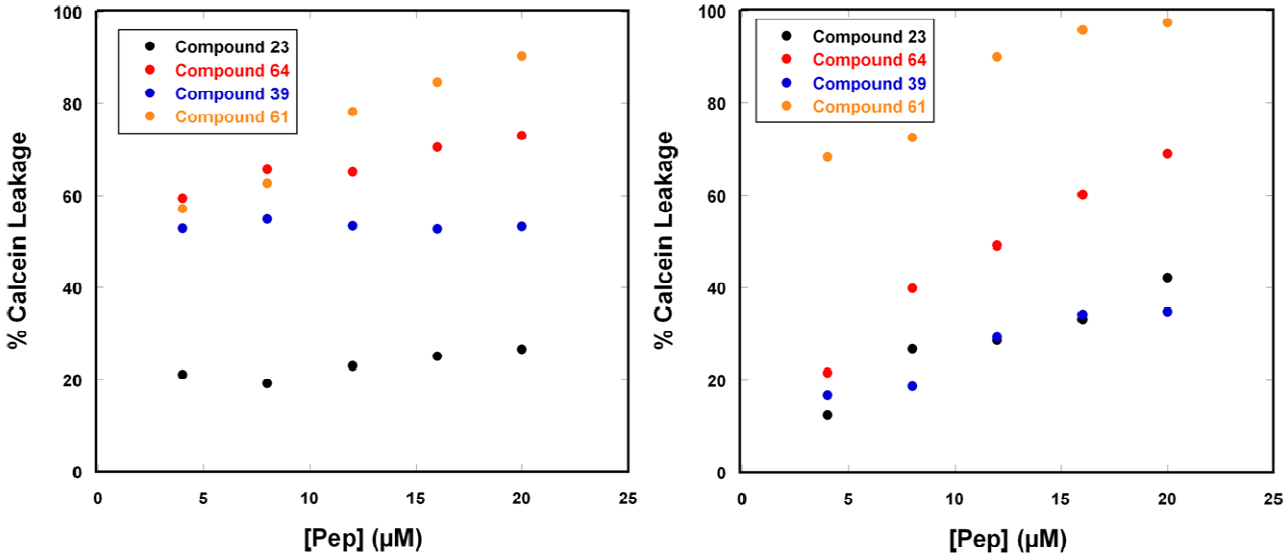

Figure 7.13: The total percent of calcein leakage from POPC (left) and 4:1 POPC/POPG LUVs (right) induced by increasing concentrations of compounds **23**, **61**, **39** and **61** as measured by fluorescence.

Conclusions

The biological activity of these compounds is consistent with the observed CD, ITC and fluorescence data. Compounds **64** and **61** exhibited increased interactions in the presence of anionic LUVs as compared to compound **23**. The increased activity has been attributed to the decreased charge of compound **64** which reduces the repulsive electrostatic interactions between the peptide and membrane surface. It was concluded that the increased flexibility of the lysine cluster at the N-terminus due to the neighboring Gly as compared to the C-terminus with a Tic residue, resulted in the increased activity of compound **61**. The increased charge of compound **39** resulted in the repulsion of the peptide and therefore decreased its activity.

Compounds **64** and **61** exhibited different CD spectra, ITC thermograms and leakage assays from each other supporting the conclusion that they interact with anionic LUVs via different mechanisms. These different mechanisms could be attributed to the selectivity of these

peptides for bacteria strains with varying membrane compositions. Therefore, it is reasonable to believe that it is possible to design and build selectivity and potency into compounds in order to produce therapeutically useful agents.

References

(1) Hicks, R. P.; Bhonsle, J. B.; Venugopal, D.; Koser, B. W.; Magill, A. J. De Novo Design of Selective Antibiotic Peptides by Incorporation of Unnatural Amino Acids. *J. Med. Chem.* **2007**, *50*, 3026-3036.

(2) Venugopal, D.; Klapper, D.; Srouji, A. H.; Bhonsle, J. B.; Borschel, R.; Mueller, A.; Russell, A. L.; Williams, B. C.; Hicks, R. P. Novel antimicrobial peptides that exhibit activity against select agents and other drug resistant bacteria. *Bioorg. Med. Chem.* **2010**, *18*, 5137-5147.

(3) Wang, P.; Bang, J.; Kim, H. J.; Kim, J.; Kim, Y.; Shin, S. Y. Antimicrobial specificity and mechanism of action of disulfide-removed linear analogs of the plant-derived Cys-rich antimicrobial peptide Ib-AMP1. *Peptides* **2009**, *30*, 2144-2149.

(4) Brahms, S.; Brahms, J.; Spach, G.; Brack, A. Identification of beta,beta-turns and unordered conformations in polypeptide chains by vacuum ultraviolet circular dichroism. *Proc. Natl. Acad. Sci. U. S. A.* **1977**, *74*, 3208-3212.

(5) Olofsson, A.; Borowik, T.; Gröbner, G.; Sauer-Eriksson, A. E. Negatively Charged Phospholipid Membranes Induce Amyloid Formation of Medin via an α-Helical Intermediate. *J. Mol. Biol.* **2007**, *374*, 186-194.

(6) Oglęcka, K.; Lundberg, P.; Magzoub, M.; Göran Eriksson, L. E.; Langel, Ü.; Gräslund, A. Relevance of the N-terminal NLS-like sequence of the prion protein for membrane perturbation effects. *Biochimica et Biophysica Acta (BBA) - Biomembranes* **2008**, *1778*, 206-213.

(7) Ganesh, S.; Jayakumar, R. Circular dichroism and Fourier transform infrared spectroscopic studies on self-assembly of tetrapeptide derivative in solution and solvated film. *The Journal of Peptide Research* **2003**, *61*, 122-128.

(8) Richardson, J. M.; Makhatadze, G. I. Temperature Dependence of the Thermodynamics of Helix–Coil Transition. *J. Mol. Biol.* **2004**, *335*, 1029-1037.

(9) Sanavio, B.; Piccoli, A.; Gianni, T.; Bertucci, C. Helicity propensity and interaction of synthetic peptides from heptad-repeat domains of herpes simplex virus 1 glycoprotein H: A circular dichroism study. *Biochimica et Biophysica Acta (BBA) - Proteins & Proteomics* **2007**, *1774*, 781-791.

(10) Imura, Y.; Nishida, M.; Matsuzaki, K. Action mechanism of PEGylated magainin 2 analogue peptide. *Biochim. Biophys. Acta* **2007**, *1768*, 2578-2585.

(11) Glukhov, E.; Stark, M.; Burrows, L. L.; Deber, C. M. Basis for selectivity of cationic antimicrobial peptides for bacterial versus mammalian membranes. *J. Biol. Chem.* **2005**, *280*, 33960-33967.

(12) Christiaens, B.; Grooten, J.; Reusens, M.; Joliot, A.; Goethals, M.; Vandekerckhove, J.; Prochiantz, A.; Rosseneu, M. Membrane interaction and cellular internalization of penetratin peptides. *European Journal of Biochemistry* **2004**, *271*, 1187-1197.

(13) Dathe, M.; Schumann, M.; Wieprecht, T.; Winkler, A.; Beyermann, M.; Krause, E.; Matsuzaki, K.; Murase, O.; Bienert, M. Peptide Helicity and Membrane Surface Charge Modulate the Balance of Electrostatic and Hydrophobic Interactions with Lipid Bilayers and Biological Membranes. *Biochemistry (N. Y.)* **1996**, *35*, 12612-12622.

(14) Leontiadou, H.; Mark, A. E.; Marrink, S. J. Antimicrobial Peptides in Action. *J. Am. Chem. Soc.* **2006**, *128*, 12156-12161.

(15) Nomura, K.; Corzo, G. The effect of binding of spider-derived antimicrobial peptides, oxyopinins, on lipid membranes. *Biochimica et Biophysica Acta (BBA) - Biomembranes* **2006**, *1758*, 1475-1482.

(16) Hunter, H. N.; Jing, W.; Schibli, D. J.; Trinh, T.; Park, I. Y.; Kim, S. C.; Vogel, H. J. The interactions of antimicrobial peptides derived from lysozyme with model membrane systems. *Biochimica et Biophysica Acta (BBA) - Biomembranes* **2005**, *1668*, 175-189.

(17) Wen, S.; Majerowicz, M.; Waring, A.; Bringezu, F. Dicynthaurin (ala) Monomer Interaction with Phospholipid Bilayers Studied by Fluorescence Leakage and Isothermal Titration Calorimetry. *The Journal of Physical Chemistry B* **2007**, *111*, 6280-6287.

(18) Nomura, K.; Corzo, G. The effect of binding of spider-derived antimicrobial peptides, oxyopinins, on lipid membranes. *Biochimica et Biophysica Acta (BBA) - Biomembranes* **2006**, *1758*, 1475-1482.

(19) Bastos, M.; Bai, G.; Gomes, P.; Andreu, D.; Goormaghtigh, E.; Prieto, M. Energetics and Partition of Two Cecropin-Melittin Hybrid Peptides to Model Membranes of Different Composition. *Biophys. J.* **2008**, *94*, 2128-2141.

(20) Wenk, M. R.; Seelig, J. Magainin 2 Amide Interaction with Lipid Membranes: Calorimetric Detection of Peptide Binding and Pore Formation. *Biochemistry (N. Y.)* **1998**, *37*, 3909-3916.

(21) Abraham, T.; Lewis, R. N. A. H.; Hodges, R. S.; McElhaney, R. N. Isothermal Titration Calorimetry Studies of the Binding of a Rationally Designed Analogue of the Antimicrobial Peptide Gramicidin S to Phospholipid Bilayer Membranes. *Biochemistry (N. Y.)* **2005**, *44*, 2103-2112.

(22) Wieprecht, T.; Seelig, J. Isothermal Titration Calorimetry for Studying Interactions between Peptides and Lipid Membranes. *Current Topics in Membranes* **2002**, *52*, 31-55.

(23) Wieprecht, T.; Apostolov, O.; Seelig, J. Binding of the antibacterial peptide magainin 2 amide to small and large unilamellar vesicles. *Biophys. Chem.* **2000**, *85*, 187-198.

(24) Wieprecht, T.; Beyermann, M.; Seelig, J. Binding of Antibacterial Magainin Peptides to Electrically Neutral Membranes: Thermodynamics and Structure. *Biochemistry (N. Y.)* **1999**, *38*, 10377-10387.

(25) Freire, E. Do enthalpy and entropy distinguish first in class from best in class? *Drug Discov. Today* **2008**, *13*, 869-874.

(26) Shimokhina, N.; Bronowska, A.; Homans, S. W. Contribution of Ligand Desolvation to Binding Thermodynamics in a Ligand?Protein Interaction. *Angewandte Chemie* **2006**, *118*, 6522-6524.

(27) Seelig, J. Thermodynamics of lipid-peptide interactions. *Biochim. Biophys. Acta* **2004**, *1666*, 40-50.

(28) Wieprecht, T.; Apostolov, O.; Beyermann, M.; Seelig, J. Membrane Binding and Pore Formation of the Antibacterial Peptide PGLa: Thermodynamic and Mechanistic Aspects. *Biochemistry (N. Y.)* **2000**, *39*, 442-452.

(29) Abraham, T.; Lewis, R. N. A. H.; Hodges, R. S.; McElhaney, R. N. Isothermal Titration Calorimetry Studies of the Binding of the Antimicrobial Peptide Gramicidin S to Phospholipid Bilayer Membranes. *Biochemistry (N. Y.)* **2005**, *44*, 11279-11285.

(30) Wieprecht, T.; Dathe, M.; Schumann, M.; Krause, E.; Beyermann, M.; Bienert, M. Conformational and Functional Study of Magainin 2 in Model Membrane Environments Using the New Approach of Systematic Double-D-Amino Acid Replacement. *Biochemisty* **1996**, *35*, 10844-10853.

(31) Tamba, Y.; Yamazaki, M. Single Giant Unilamellar Vesicle Method Reveals Effect of Antimicrobial Peptide Magainin 2 on Membrane Permeability. *Biochemistry (N. Y.)* **2005**, *44*, 15823-15833.

(32) Wei, S.; Wu, J.; Kuo, Y.; Chen, H.; Yip, B.; Tzeng, S.; Cheng, J. Solution Structure of a Novel Tryptophan-Rich Peptide with Bidirectional Antimicrobial Activity. *J. Bacteriol.* **2006**, *188*, 328-334.

CHAPTER EIGHT: INACTIVE COMPOUNDS AS NEGATIVE CONTROLS

Introduction

Several peptides were designed and synthesized that exhibited a broad range of activity against several strains of bacteria.[1] Of these novel peptides, there were also peptides that did not show in-vitro activity against bacteria or mammalian cells. Compounds **14** and **34** are two of the inactive peptides and their sequences are given in **Table 8.1**. In compound **34** the Tic residues have been replaced with Gly residues and therefore this analog doesn't not contain the conformationally restrained Tic-Oic dipeptide unit required to impart local rigidity to the peptide backbone. The lack of antimicrobial activity for compound **34** confirms that the Tic-Oic dipeptide units are critical for biological activity. Compound **14** contains the Tic-Oic dipeptide unit, however the amino acid sequence between the Tic-Oic dipeptide units is different. Instead of the sequence Spacer #1-charge residue or Spacer #1-hydrophobic residue as followed in the active analogs, the intervening sequence for compound **14** is as follows: Spacer #1-hydrophobic residue-Spacer #1-charged residue. Also the C-terminus of compound **14** consists of the C-terminal residues found in magainin instead of a cluster of positively charged residues. This analog is also inactive in antimicrobial assays confirming that the integrity of the sequence that has been designed for these AMPs is important for antimicrobial activity. Although these two peptides did not exhibit biological activity they still provided critical comparative information.

Table 8.1: Amino acid sequences of the peptides used as negative controls.

Compound	Amino Acid Sequence
23	Ac-GF-Tic-Oic-GK-Tic-Oic-GF-Tic-Oic-GK-Tic-KKKK-$CONH_2$
14	Ac-GK-Tic-Oic-GLGKE-Tic-Oic-GLGK-Tic-Oic-ELMGER-$CONH_2$
34	Ac-GF-G-Oic-GK-G-Oic-GF-G-Oic-GK-G-KKKK-$CONH_2$

Because compound **14** does not exhibit activity against bacteria (**Table 8.2**), clear differences in the data obtained from it and the data obtained from the active analogs would allow for the determination of the defining of parameters and behavior associated with biological activity.

The other inactive peptide (**Table 8.2**), compound **34**, is an analogue of compound **23** with the Tic residues replaced with the more flexible and less hydrophobic Gly. Compound **34**, therefore, served as a negative control as well as provided reinforcement that the Tic residue in the dipeptide turn unit is pertinent for biological activity.

Table 8.2: Minimum inhibitory concentration (μM) of select bacteria strains and hemolytic activity.[1]

Compound	Salmonella Typhimurium	Staphylococcus Aureus ME/GM/TC resistant	Mycobacterium Ranae	Bacillus Subtillis	% hemolysis 100/25 μM
23	10 μM	3 μM	10 μM	1 μM	14%
14	not active	not active	not tested	not tested	not tested
34	not active	not active	100 μM	30 μM	3.30%/ 3.3%

Results and Discussion

CD Studies

*CD spectra of compounds **14** and **34** in buffer and micelle environments.* As emphasized in the previous chapters, the conformations adopted by the peptides in the presence of anionic and zwitterionic membrane models should be different than those observed in a buffer environment if the compound has the potential to selectively interact with bacteria verse mammalian cells. As can be seen in **Figure 8.1**, the spectra of compounds **14** and **34** in buffer

were not significantly different than those in their corresponding micelle environments. Both compounds **14** and **34** contained random coil components with a minimum at approximately 200 nm and a maximum with almost positive intensity at what 220 nm.[2-6] In the presence of SDS and DPC micelles, the CD spectra of compound **14** exhibited changes in the intensity at approximately 220 nm suggesting an increase in unordered structures.[7, 8] The CD spectra in the presence of both DPC and SDS micelles were very similar to each other suggesting that there is no difference in the conformations adopted on binding to either micelle.

The CD spectra of compound **34** exhibited fewer changes in the micelle environments than CD spectra of compound **14**. There was a loss in the intensity in the presence of both DPC and SDS micelles when compared to the buffer spectra. Again, the DPC and SDS spectra were not only similar to the spectra of the peptide in buffer, but they were also similar to each other.

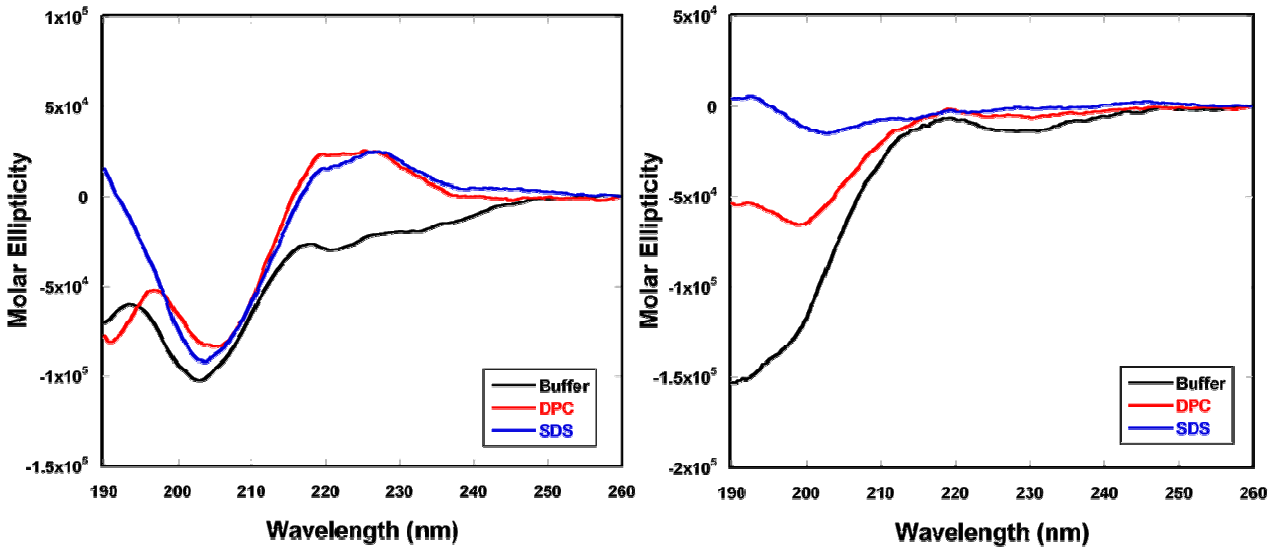

Figure 8.1: Far-UV CD spectra of compound **14** (left) and compound **34** (right) in 40 mM phosphate buffer, pH = 6.8 (black), 80 mM DPC micelles in buffer (red) and 80 mM SDS in buffer (blue).

*"Pseudo" titration of LUVs into compounds **14** and **34***. Zwitterionic and anionic LUVs were titrated into solutions of compounds **14** and **34** in an attempt to observe conformational changes with concentration dependencies. In the presence of POPC LUVs (**Figure 8.2**), CD spectra indicated that the conformations adopted by each compound were very similar to their corresponding spectra in buffer in regards to shape and intensity. These similarities, even at high L/P ratios, support the conclusion that these peptides do not interact with the zwitterionic membrane models.

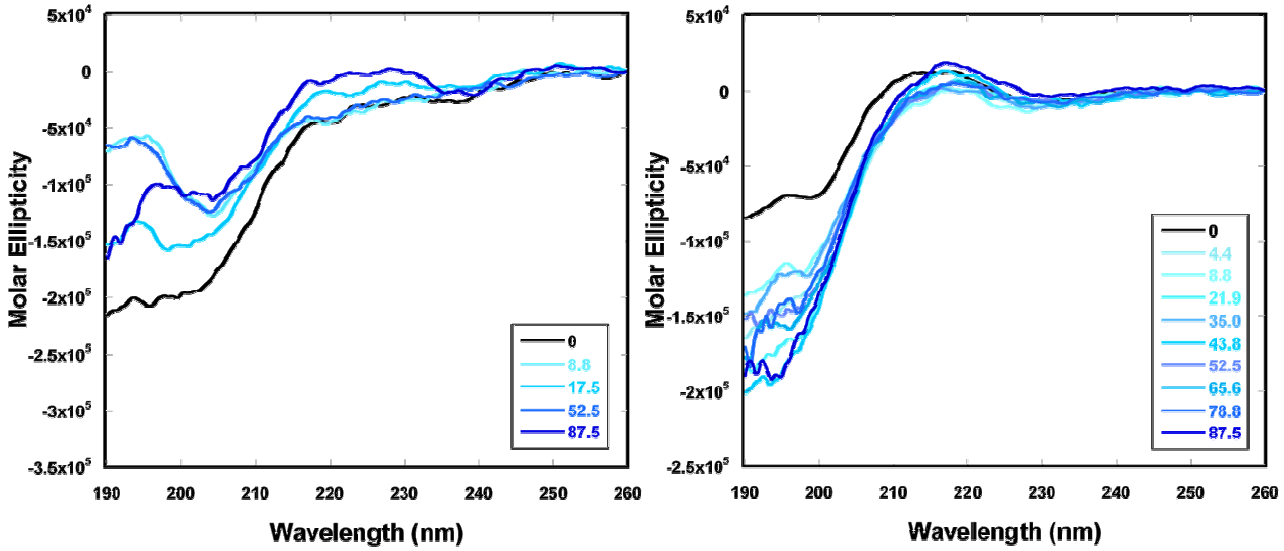

Figure 8.2: Titration of 35 mM POPC LUVs into 100 µM compound **14** (left) and 200 µM compound **34** (right).

Similar results were observed in the presence of the anionic membrane model 4:1 POPC/POPG LUVs (**Figure 8.3**). With the active compounds, the spectra with increasing L/P ratios exhibited changes in their CD spectra with respect to the spectrum in buffer as well as to each other. Also, there was a transition from I-state to S-state observer and referred to as the "critical point." Neither of these characteristics was observed with compounds **14** or **34**. With the

exception of an emergence of a peak at approximately 195 nm for compound **14**, neither peptide showed significant changes from their buffer spectrum. In fact, the spectra of compound **34** were essentially identical to the spectrum in buffer. Again, this data supports the conclusion that these peptides are inactive and serve as negative controls.

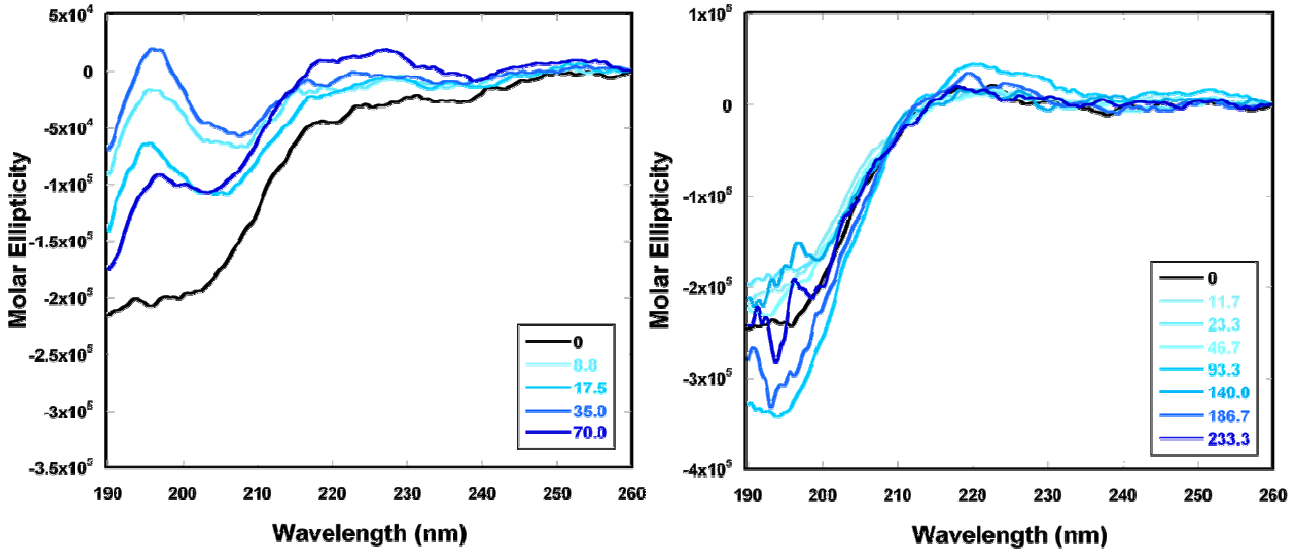

Figure 8.3: Titration of 35 mM 4:1 POPC/POPG LUVs into 100 µM compound **14** (left) and 75 µM compound **34** (right).

ITC Studies

The titration of 35 mM POPC LUVs into compounds **14** and **34** (**Figure 8.4**) supported the claim that these peptides do not interact with membrane models in a manner that would cause membrane disruption. Although the top panels of the thermograms appear to show some interaction, the integrated data in the bottom panel showed that the heat associated with each injection was minimal, less than 4.0 x 10^{-3} kcal/mol of injectant for compounds **14** and **34**. Also,

the integrated heats were so small for the interaction that they were barely discernable from the background noise, supporting the conclusion that there is minimal binding to observe.

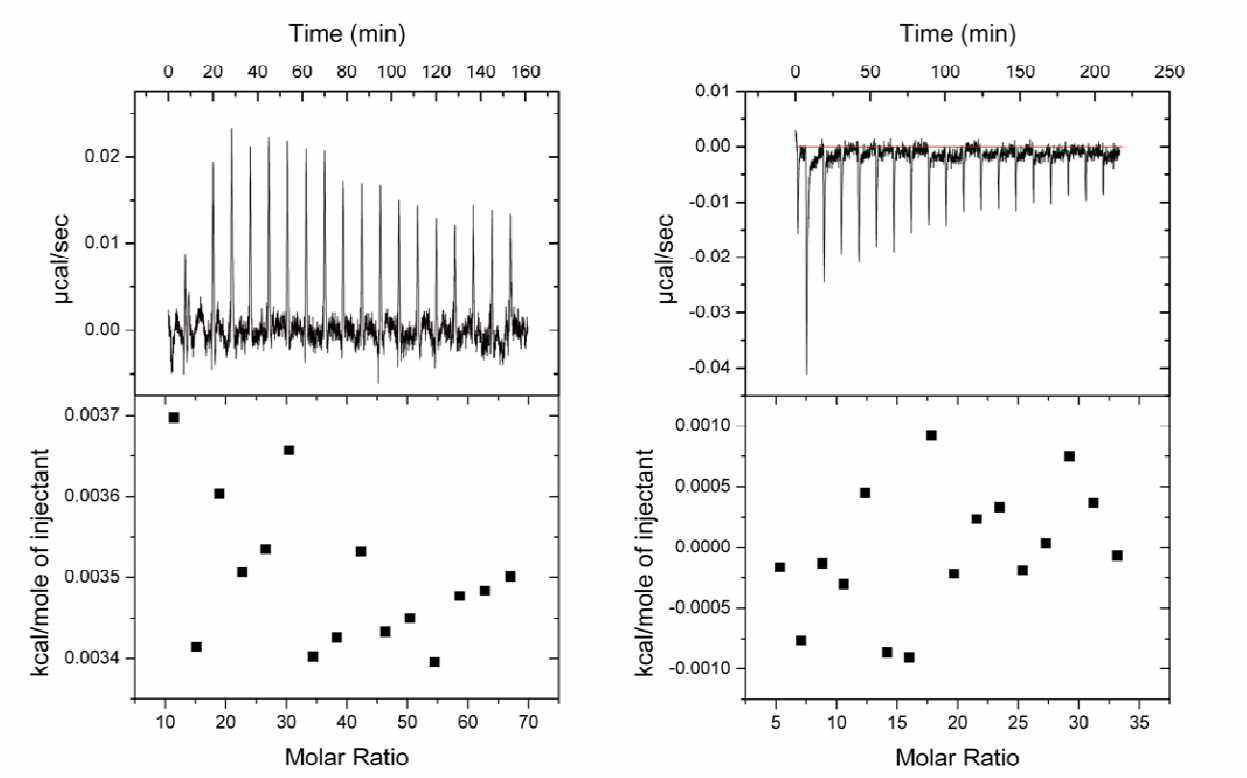

Figure 8.4: ITC experiment of 35 mM POPC LUVs titrated into 100 µM compound **14** (left) and 200 µM compound **34** (right).

The interactions of these two peptides with anionic liposome models (**Figure 8.5**) displayed a slightly different result, but the same conclusion was reached. Compound **14** exhibited a thermogram with less interference from the background noise than was observed with POPC LUVs; however, the maximum amount of heat observed was approximately 4 cal/mol of injectant. The thermogram for compound **34** portrayed a very similar interaction to other peptides in membrane environments with a distinct endothermic phase. The thermograms of the active compounds typically exhibited one of two characteristics, if not both. The

thermograms possessed an endothermic phase followed by an exothermic phase, as was the case of compound **23** (**Figure 3.10**). The second required characteristic was the absorption or release of a large amount of heat. Compound **34** did not possess an exothermic phase and the largest amount of heat absorbed was approximately 0.03 kcal/mol of injectant. Also, the interaction required a L/P molar ratio of approximately 150 before the peptide was completely bound, supporting the conclusion that there was a weak interaction taking place. [9, 10]

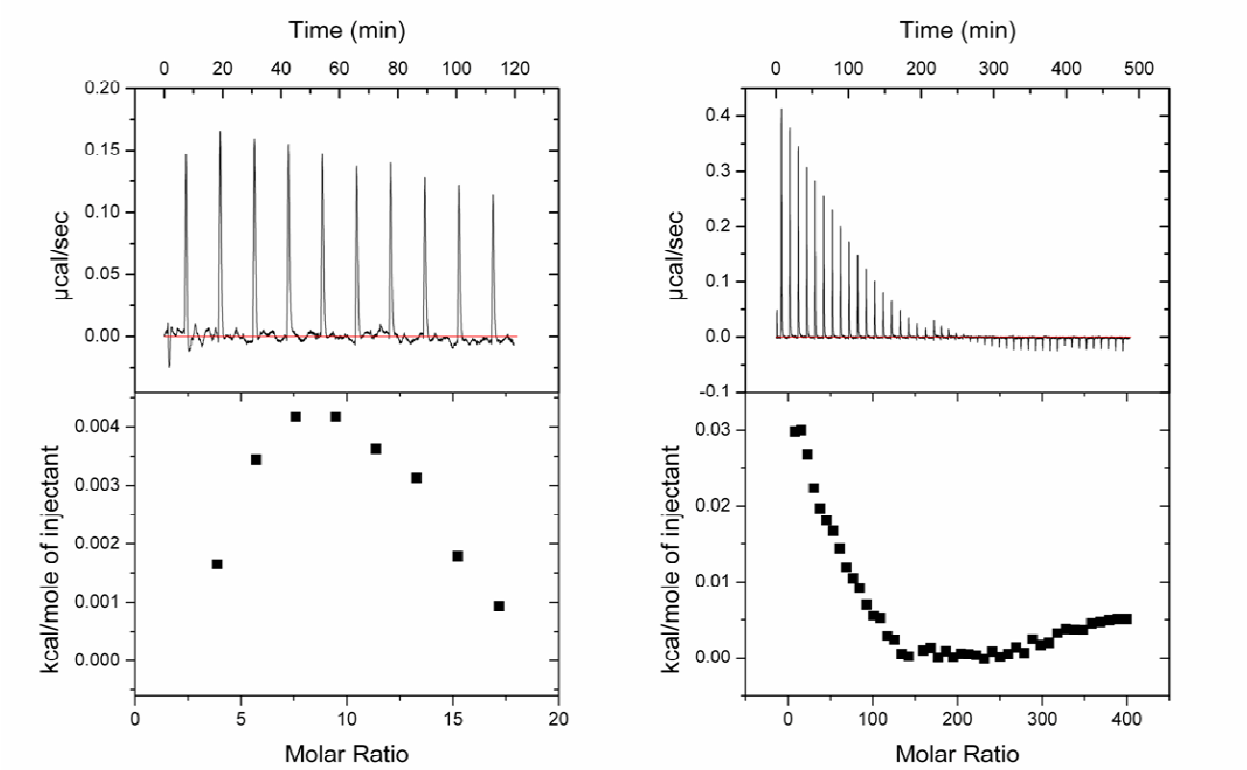

Figure 8.5: ITC experiment of 35 mM POPC LUVs titrated into 100 µM compound **14** (left) and 50 µM compound **34** (right).

Calcein Leakage Studies

Peptide induced calcein leakage studies were used to determine if these peptides were membrane disruptors, and thus, biologically active. [11, 12] Studies were performed only at the maximum concentration of 20 µM (**Figure 8.6**). If these peptides were truly inactive, then they

would produce minimal leakage at the maximum concentration. Also, any peptide concentrations lower than 20 µM would induce less leakage. Interestingly enough, both compounds induced more leakage in the presence of POPC LUVs than 4:1 POPC/POPG LUVs. However, 50% leakage for compound **14** and approximately 30% for compound **34** in POPC was lower than most of the other compounds. An intriguing observation was that both compounds produced 10% or less leakage in the presence of the anionic membrane model. Again, these two compounds have proven to show little activity against membrane model systems, anionic or zwitterionic.

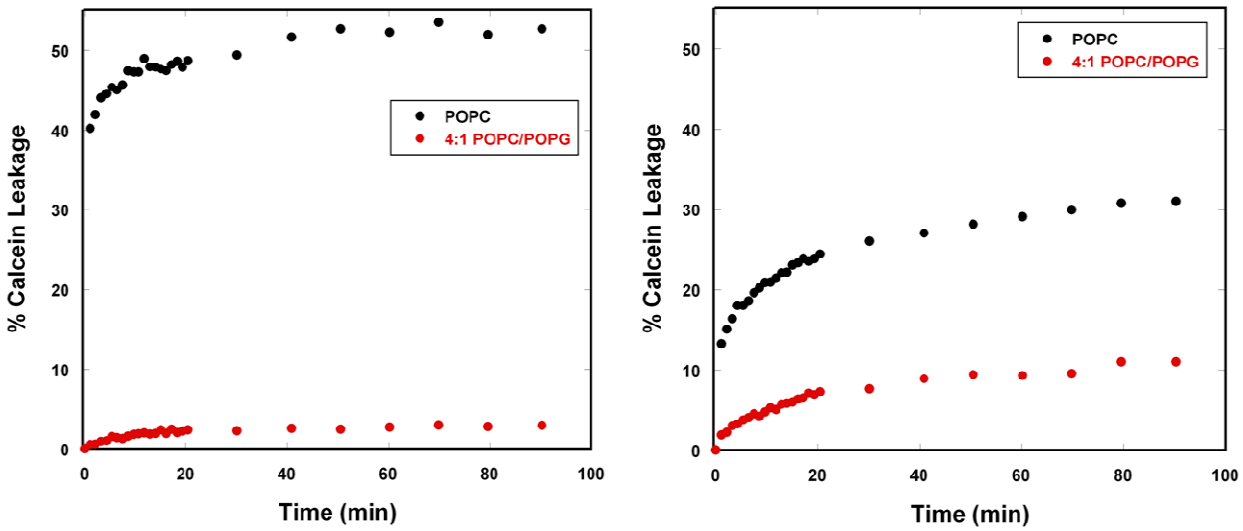

Figure 8.6: The time dependence of the calcein leakage fluorescence of POPC (black) and 4:1 POPC/POPG LUVs (red) induced by 20 µM compounds **14** (left) and **34** (right) as measured by fluorescence.[4, 13, 14]

Conclusions

Compounds **14** and **34** served as negative controls for our peptides. Neither compound exhibited in-vitro activity against different bacteria strains or mammalian red blood cells. Due to their inactive nature, different results should be, and were, observed in regards to CD, ITC and

fluorescence experiments when compared to active compounds. CD spectra of these compounds clearly indicated that they were not interacting with zwitterionic or anionic membrane model systems. The minimal heat and high L/P ratios required for completion of the reaction observed in the ITC thermograms supports the CD data. Also, the low percentage of calcein leakage from the liposomes suggests minimal interaction with the liposomes.

The results for these inactive compounds were extremely different from all of the data presented thus far for the active compounds. CD, ITC and fluorescence experiments proved suitable and more than capable of detecting changes in the interactions between our peptides and membrane models due to small systematic modifications to the peptides. In addition to proving the usefulness of these techniques and compounds **14** and **34** as negative controls, addition to the use of these compounds as negative controls, the loss of activity for Compound **34** due to the deletion of the Tic residue only strengthens the argument that the incorporation of Tic in the dipeptide unit is required for activity.

References

(1) Hicks, R. P.; Bhonsle, J. B.; Venugopal, D.; Koser, B. W.; Magill, A. J. De Novo Design of Selective Antibiotic Peptides by Incorporation of Unnatural Amino Acids. *J. Med. Chem.* **2007**, *50*, 3026-3036.

(2) Jing, W.; Demcoe, A. R.; Vogel, H. J. Conformation of a bactericidal domain of puroindoline a: structure and mechanism of action of a 13-residue antimicrobial peptide. *J. Bacteriol.* **2003**, *185*, 4938-4947.

(3) Perczel, A.; Hollosi, M. In *Turns;* Fasman, G. D., Ed.; Circular dichroism and the conformational analysis of biomolecules; Plenum Press: New York, N.Y., 1996; pp 285-380.

(4) Wieprecht, T.; Dathe, M.; Schumann, M.; Krause, E.; Beyermann, M.; Bienert, M. Conformational and Functional Study of Magainin 2 in Model Membrane Environments Using the New Approach of Systematic Double-D-Amino Acid Replacement. *Biochemisty* **1996**, *35*, 10844-10853.

(5) Christiaens, B.; Grooten, J.; Reusens, M.; Joliot, A.; Goethals, M.; Vandekerckhove, J.; Prochiantz, A.; Rosseneu, M. Membrane interaction and cellular internalization of penetratin peptides. *European Journal of Biochemistry* **2004**, *271*, 1187-1197.

(6) Wang, P.; Bang, J.; Kim, H. J.; Kim, J.; Kim, Y.; Shin, S. Y. Antimicrobial specificity and mechanism of action of disulfide-removed linear analogs of the plant-derived Cys-rich antimicrobial peptide Ib-AMP1. *Peptides* **2009**, *30*, 2144-2149.

(7) Richardson, J. M.; Makhatadze, G. I. Temperature Dependence of the Thermodynamics of Helix–Coil Transition. *J. Mol. Biol.* **2004**, *335*, 1029-1037.

(8) Sanavio, B.; Piccoli, A.; Gianni, T.; Bertucci, C. Helicity propensity and interaction of synthetic peptides from heptad-repeat domains of herpes simplex virus 1 glycoprotein H: A circular dichroism study. *Biochimica et Biophysica Acta (BBA) - Proteins & Proteomics* **2007**, *1774*, 781-791.

(9) Abraham, T.; Lewis, R. N. A. H.; Hodges, R. S.; McElhaney, R. N. Isothermal Titration Calorimetry Studies of the Binding of a Rationally Designed Analogue of the Antimicrobial Peptide Gramicidin S to Phospholipid Bilayer Membranes. *Biochemistry (N. Y.)* **2005**, *44*, 2103-2112.

(10) Wenk, M. R.; Seelig, J. Magainin 2 Amide Interaction with Lipid Membranes: Calorimetric Detection of Peptide Binding and Pore Formation. *Biochemistry (N. Y.)* **1998**, *37*, 3909-3916.

(11) Medina, M. L.; Bolender, J. P.; Plesniak, L. A.; Chapman, B. S. Transient vesicle leakage initiated by a synthetic apoptotic peptide derived from the death domain of neurotrophin receptor, p75NTR. *Journal of Peptide Research* **2002**, *59*, 149-158.

(12) Andrushchenko, V. V.; Aarabi, M. H.; Nguyen, L. T.; Prenner, E. J.; Vogel, H. J. Thermodynamics of the interactions of tryptophan-rich cathelicidin antimicrobial peptides with model and natural membranes. *Biochimica et Biophysica Acta (BBA) - Biomembranes* **2008**, *1778*, 1004-1014.

(13) Tamba, Y.; Yamazaki, M. Single Giant Unilamellar Vesicle Method Reveals Effect of Antimicrobial Peptide Magainin 2 on Membrane Permeability. *Biochemistry (N. Y.)* **2005**, *44*, 15823-15833.

(14) Wei, S.; Wu, J.; Kuo, Y.; Chen, H.; Yip, B.; Tzeng, S.; Cheng, J. Solution Structure of a Novel Tryptophan-Rich Peptide with Bidirectional Antimicrobial Activity. *J. Bacteriol.* **2006**, *188*, 328-334.

CHAPTER NINE: APPLICATION OF A RATIONAL DRUG DESIGN

Introduction

Most chemists and biologist are very familiar with the 20 naturally occurring RNA encoded amino acids, however the incorporation of unnatural amino acids into peptides and proteins is making a major impact on biochemical research and are becoming more common place. Research involving the incorporation of unnatural amino acids has focused on a wide array of applications from drug discovery [1] to site(s) specific incorporation of unnatural amino into proteins.[2-4] This protocol will focus on the rationale and logic used to incorporate unnatural amino acids into the design of novel antimicrobial peptides.

The selectivity of AMPs for prokaryotic versus eukaryotic cells is believed to be derived from the differences in the chemical compositions of their respective membranes.[5-8] Bacterial cells contain a high percentage of negatively charged phospholipids while mammalian cells contain a much higher concentration of zwitterionic phospholipids.[9] Other differences include the incorporation of sterols, lipopolysaccharide, peptidoglycan etc into the membrane composition which induces changes in structure,[8] transmembrane potential and polarizability. The membranes of different strains of bacteria also exhibit differing chemical compositions.[5, 10, 11] The lipid bilayer of Gram positive bacteria is covered by a porous layer of peptidoglycan, while the structure of Gram negative bacteria is more complex with two lipid membranes containing lipopolysaccharides and porins.[5, 10] The outer membrane of mycobacteria is the most complex consisting of a very thick mycolate-rich outer coat[11] which is very difficult to penetrate. There is an increasing amount of evidence in the literature supporting the concept that the selectivity and potency of a specific AMP is determined, in a large measure, by the chemical composition of the target membrane.[8, 12] Thus it is reasonable to postulate that the membrane's

physicochemical surface interactions with the physicochemical surface of the AMP defines organism selectivity.[5, 10, 12-15]

Antimicrobial peptides have been extensively investigated as therapeutic agents to possibly replace current antibiotics because of their novel mechanism of killing bacteria.[6, 16, 17] An international health care crisis has arisen due to the dramatic and continued evolution of drug resistant strains of bacteria.[18, 19] This ever evolving increase in resistance has been the driving force behind the intensive research effort to develop a new class of compounds that exhibit novel mechanisms of antibacterial activity.[17, 18, 20, 21] Both natural and synthetic antimicrobial peptides exhibit a very high potential as new therapeutic agents because of their novel mechanisms of antibiotic activity coupled with the difficulty of bacteria to develop resistance to them.[6, 17, 22, 23] The most promising applications of AMPs thus far are focused on their clinical development as topical antibiotics.[23]

Unnatural amino acids offer several major advantages over the 20 naturally ocurring amino acids including limited conformational flexibility,[1, 24, 25, 25-28] improved enzymatic stability,[29] pharmacodynamics,[1] as well as control over charge distribution[15, 30, 31] and electron density.[3] Having such control over these amino acids will hopefully allow AMPs to be designed and built to perform in specific ways. In the case of our research, react with potency and selectivity.

The Design Process

Selection of Target or Model Natural Antimicrobial Peptide

The first step in the de novo design of selective antimicrobial peptides involves selecting a naturally occurring antimicrobial peptide as a model. In this approach the primary amino acid

sequence is not a major focus, but knowledge of the secondary structure adopted by the peptide on interacting with a zwitterionic and an anionic micelle or a liposome and the resulting physiochemical surface properties is very critical. It is a very difficult process to sit down with a blank sheet of paper and design a series of potent selective antimicrobial peptides without some three-dimensional physicochemical model. Thus the starting point for such a design process is either to determine using 2D-NMR and molecular modeling methods the SDS and DPC micelle bound conformations of an antimicrobial in your own laboratory [14] or use similar structural data reported in the literature. From these structures the electrostatic surface potential maps may be developed.

In order to obtain the desired potency and selectivity for prokaryotic and eukaryotic cells it is critical that the peptide interact with zwitterionic and anionic membrane models via different mechanisms, i.e. adopt different conformations on binding to zwitterionic and anionic membrane models.[15, 16, 32, 33] The physicochemical properties that lead to different mechanisms of binding are not clearly understood.[33] However, factors such as hydrophobicity, structure, electronic charge, hydrophobic moment etc appear to play major roles in defining selectivity.[10, 15, 33, 34] Therefore in our design methodology it is more important to focus on the overall shape of the molecule and the spatial distribution of physicochemical properties, such as charge density and hydrophobicity, than the amino acid composition or sequence.[14, 15]

In our laboratory we selected (Ala [8,13,18])magainin-2 amide, an analog of the magainin family of host defense peptides as our model because this peptide is active against Gram positive and negative bacteria, fungi and protozoa while exhibiting little mammalian cell toxicity.[35] The magainin family has been extensively investigated and has been characterized as α-helical amphipathic cell-selective membrane-disruptors.[36-38] The investigation of AMPs with model

membrane systems has provided a great deal of insight into the role played by physicochemical properties in the mechanisms of the anti-bacterial activity of these compounds.[39] For our investigation of (Ala [8,13,18])magainin-2 amide, DPC micelles[40] were selected as a simple model for zwitterionic lipids and SDS micelles[41] were selected as a simple model for anionic lipids. Due to our previous experience in investigating peptide-micelle interactions,[42-44, 44] we selected NMR as the method of choice for this study. Two-dimensional NMR and molecular modeling[45] investigations indicated that (Ala[8,13,18])magainin-2 amide bound to DPC micelles adopts an α-helical structure involving residues 2 to 16 with the four C-terminal residues converging to a loose β-turn like structure, while (Ala[8,13,18])magainin-2 amide bound to SDS micelles adopts an α-helical structure involving residues 7 to 18 with the C- and N-terminal residues exhibiting a great deal of conformational flexibility. The most plausible explanation for (Ala [8,13,18])magainin-2 amide adopting different conformations on binding with SDS and DPC micelles is that different non-covalent (electrostatic and hydrophobic) interactions are occurring between the surface of the peptide and the two micelle surfaces.[45] The observation of different binding conformations on interaction with anionic and zwitterionic micelles and or liposomes is critical for the development of cell-selective AMP.[32, 45] The ultimate goal of the design process is to develop AMPs that will form membrane-disrupting pores in anionic liposomes while leaving zwitterionic liposomes intact.[14]

Using the NMR determined SDS and DPC micelle bound conformations of (Ala [8,13,18])magainin-2 amide, the electrostatic surface potential maps for these conformers were calculated indicating that the surface electron density of these peptides are very different and conformationally dependent.

In our laboratory we have focused on developing antimicrobial peptides that contain unnatural amino acids to control the conformation and physicochemical properties of the resulting peptide[14] while also taking advantage of the inherent metabolic stability of unnatural amino acids.[6] The guiding hypothesis for our work has evolved from the assertion that the 3D-physicochemical surface properties of a cell's membrane (bacterial or mammalian) interact with the 3D-physicochemical surface properties of the approaching AMP in a very specific way, thus defining the resulting organism selectivity and potency. For the AMPs developed in our laboratory this hypothesis was supported by the development of 3D-QSAR which defines the physicochemical properties required for activity against *Staphylococcus aureus* (***SA***) and *Mycobacterium ranae* (***MR***) bacteria. The AMPs developed in our laboratory exhibited different *in vitro* activity against ***SA*** and ***MR*** bacteria. The cell membranes of *Staphylococcus aureus* and *Mycobacterium ranae* are chemically different. Therefore, we hypothesized that the differences in the observed biological activity was a direct manifestation of the different physicochemical interactions that occur between the peptides and the cell membranes of the ***SA*** and ***MR*** bacteria.[15] For this hypothesis to be correct different physicochemical descriptors must correlate with the anti-bacterial activity of these compounds against ***SA*** and ***MR*** bacteria. There were five physicochemical descriptors specific to the ***SA*** QSAR. These five physicochemical descriptors are: Jurs–Fractional-Positive-Surface-Area–3 (Jurs-FPSA-3), Jurs-Relative-Positive-Charge-Surface-area (Jurs-RPCS), Jurs-Differential-Positively-charged-Surface-Area-3 (Jurs-DPSA-3), Jurs-total-Solvent-Accessible-Surface-Area (Jurs-SASA) and Jurs-TotAl-hydrophobic-Surface-Area (Jurs-TASA). The five physicochemical descriptors specific to the ***MR*** QSAR model are: sum-of-all-atomic-polarizabilities (Apol), Conformer Energy, Jurs-Partial-Positively-charged-Surface-Area-2 (Jurs-PPSA-2), Jurs-Relative-Negative-CharGe (Jurs-RNCG), and Jurs-Total-

Polar-Surface-Area (Jurs-TPSA). This result supports the hypothesis that for any particular AMP, organism selectivity and potency are controlled by the chemical composition of the target cell membrane.[15] Therefore, we believe that by varying the physicochemical and conformational properties of a peptide, it should be possible to design selectivity and potency for a particular membrane composition.

Making a Cartoon Model

The next step in the design process is to identify which of the following functionalities are critical for the desired biological potency and selectivity.

1. Secondary Structure
2. Molecular flexibility between regions of limited conformational flexibility
3. Molecular charge
4. Charge density
5. Flexibility between the regions of limited conformational flexibility and charge clusters.

In **Figure 9.1** an example of this cartoon representation is given. The cartoon starts at the far left with an N-capping residue. This residue is normally a natural amino acid of neutral charge and may be a free amine or acetylated. The second residue in the sequence is a natural amino acid that is either positively charged (Arg, Lys, His) or hydrophobic in nature (Phe, Trp, Tyr, Leu). This particular residue defines the physicochemical character of the N-terminus. The next two amino acids, residues 3 and 4, are unnatural amino acids that form a conformationally restrained dipeptide unit which is used to control local secondary structure and molecular

flexibility. The use of conformationally restrained amino acids, such as Tic and Oic residues in our case, reduces the flexibility of the local peptide backbone and thus reduces the total conformational space that may be sampled by the peptide during lipid binding. The selection of the unnatural amino acids to be incorporated as the dipeptide will be discussed in a later section.

If included, the fifth amino acid residue also referred to as a spacer, can be a Gly residue or an unnatural amino acid such as βAla, GABA or longer amino acid. This spacer, if included in the sequence, provides molecular flexibility between the preceding conformationally restrained dipeptide and the following positively charged amino acid. Increasing the number of $-CH_2-$ groups in the spacer, in our case by including unnatural amino acids such as β-Ala, Gaba or Ahx, the length of the peptide backbone increases, thus increasing the molecular flexibility of the local peptide chain. This results in an increase in the total conformational space that may be sampled by the peptide during lipid binding. By combining regions containing conformationally restrained amino acids and regions of conformational flexibility into the peptide backbone regions of high and low molecular flexibility are created providing a fine tuning of the local verses total conformational space that may be sampled by the peptide during lipid binding.

The next amino acid, residue 6, is a positively charged residue which maybe either a natural or unnatural amino acid. By varying the number of $-CH_2-$ groups in the positively charged residue from 1 to 4 in the side chain of the basic residues (Lys, Orn, Dab, Dpr residues) the distance between the positive charge and the peptide backbone will decrease. This results in a less flexible side chain during binding, which is more important in the binding with zwitterionic lipids than with anionic lipids, and the positive charge density will reside closer to the peptide backbone. The reason that side chain flexibility is more important in the binding of zwitterionic lipids than with anionic lipids is the following. Electrostatic interactions are responsible for

peptide-membrane binding while hydrophobic interactions are responsible for inducing a stable secondary structure onto the peptide.[42, 46] The electrostatic interactions that occur between cationic peptides and zwitterionic lipids are more "complex" than those that occur with anionic lipids.[46] The counter ions in solution are covalently bound to zwitterionic lipids, but are free flowing in an anionic lipid solution, thus their positive and negative charges have limited freedom of motion. As the positive charges of the incoming peptide approaches the surface of the zwitterionic lipid, the positive counter ions of the lipid can not be displaced from the surface and diffuse into solution away from the lipid, as is the case with the free flowing ions in anionic lipid solutions. Therefore, both attractive electrostatic interactions between the positive charges of the peptide and the negative charges on the lipid, as well as the repulsive electrostatic interactions between the positive charges on the peptide and the positive charges of the lipid will be inversely synergistic in nature.[46] Consequently, the binding process will require the conformation of the incoming peptide to adapt in response to these interactions so as to maximize the attractive interactions while concurrently minimizing these repulsive interactions. The selection of this residue is critically important and will be discussed in a later section.

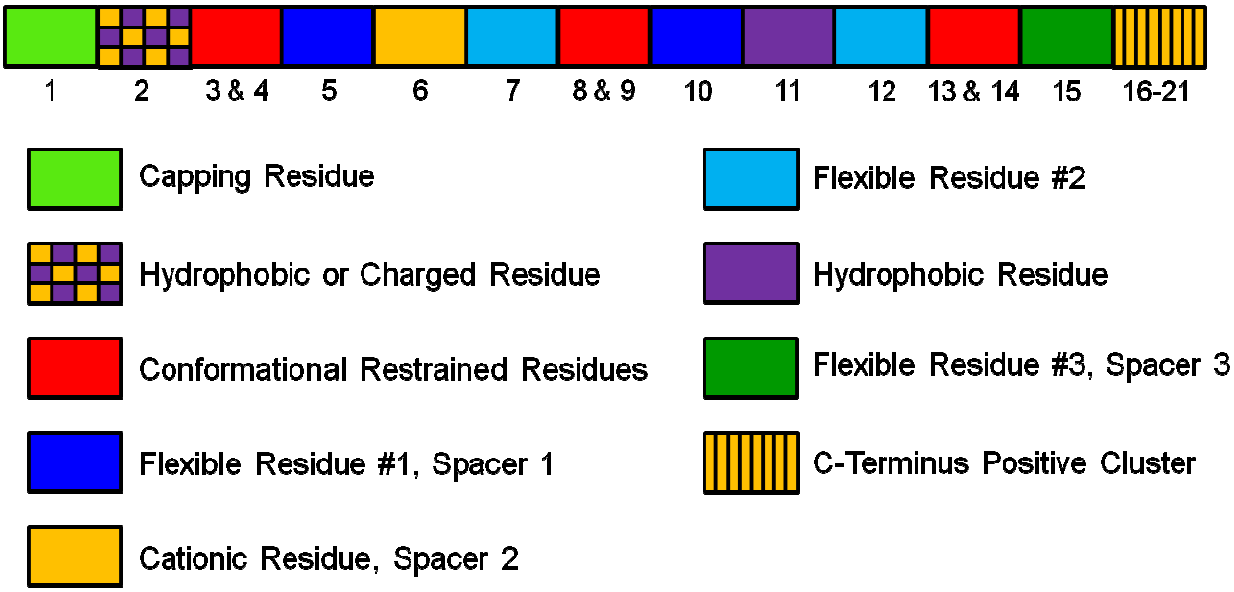

Figure 9.1: A cartoon representation of the important structural and physicochemical features to be incorporated into the new antimicrobial peptide is shown to aid in the design process.

The seventh amino acid residue is another spacer and, if included, is the second spacer in the sequence. As with the previous spacer, it provides molecular flexibility between the preceding cationic residue and residues 8 and 9, the second conformationally restrained dipeptide unit. The next amino acid residue, 10, is also an optional spacer that provides molecular flexibility between the preceding dipeptide and the following hydrophobic amino acid, residue 11. The selection of the hydrophobic residue, which maybe natural or unnatural, is critical and size, aromatic character and electron density are factors that must be taken into consideration. The selection of the hydrophobic residue will be discussed later.

The hydrophobic residue is followed by another spacer, which can be incorporated to provide molecular flexibility between the preceding hydrophobic residue and the following dipeptide unit, which is the third conformationally restrained unit of the sequence and incorporates residues 13 and 14. The amino acid sequence from the first dipeptide unit to the

third dipeptide unit is considered a repeat unit. This repeat unit may recur one to two more times and is followed by the fifth spacer, residue 15. Residue 15 is the last spacer of the sequence and if included provides molecular flexibility between the last conformationally restrained dipeptide and a cluster of positively charged amino acids at the C-terminus. The last three to six amino acids at the C-terminus make up the highly positively charged cluster at the C-terminus. The position of the positively charged and hydrophobic residues may be switched depending on the charge and hydrophobic character of the physicochemical surface properties of the antimicrobial being modeled. The net result of these modifications is to induce semi-rigid conformations onto the peptide backbone, as well as to induce specific regions of hydrophobicity and charge in hopes of dramatically changing the physicochemical surface properties presented to the lipid on binding.

Converting the Cartoon Model into Amino Acid Sequence

The conversion of a carton model of a potential peptide into an amino acid sequence consists of several steps. The first step is to select the conformationally restrained dipeptide building block.

Selection of Conformationally Restrained Dipeptide Units

Once a cartoon representation of the desired structure and physicochemical properties is created, it must be converted to an amino acid sequence. The first step in this process is to select the conformationally restrained dipeptide unit. Our original skeletal design of an un-natural AMP incorporated placement of multiple L-Tic-L-Oic dipeptide units into the polypeptide backbone to induce an ordered structure onto the peptide.[14] Kyle and co-workers reported, using

NMR and molecular modeling methods, that the dipeptide consisting of the un-natural amino acids (D)-Tetrahydroisoquinolinecarboxylic acid (Tic) and (L)-Octahydroindolecarboxylic acid (Oic) when placed in positions *i+1* and *i+2* of a four amino acid sequence induced a β-turn.[27] The AMPs developed in our laboratory have several Tic-Oic dipeptide units connected via one or two amino acid spacers with defined properties of charge and hydrophobicity. Knowing such properties about the amino acids allows for the design of peptides with well defined physiochemical properties that are able to maintain sufficient conformational flexibility, allowing the peptide to adopt different conformations when interacting with membranes of different chemical composition.[14, 15, 31]

The structure of the Tic-Oic dipeptide conformationally restrained unit used in the AMPs designed in our laboratory is given in **Figure 9.2**. The basic skeleton of he AMPs developed in our laboratory is given in **Figure 1.3** from Chapter 1. Spacer #1 defines the distance between successive Tic-Oic dipeptide units, and refers to amino acids 5 and 10 of the cartoon representation. It is involved in defining the flexibility of any induced turn or helical structure. Spacer #2 defines the distance between the polypeptide backbone residues and the positively charged side chain amine. It is involved in determining the overall surface charge density as well as the distance between the membrane surface and the polypeptide backbone and is residue 6 in the cartoon.

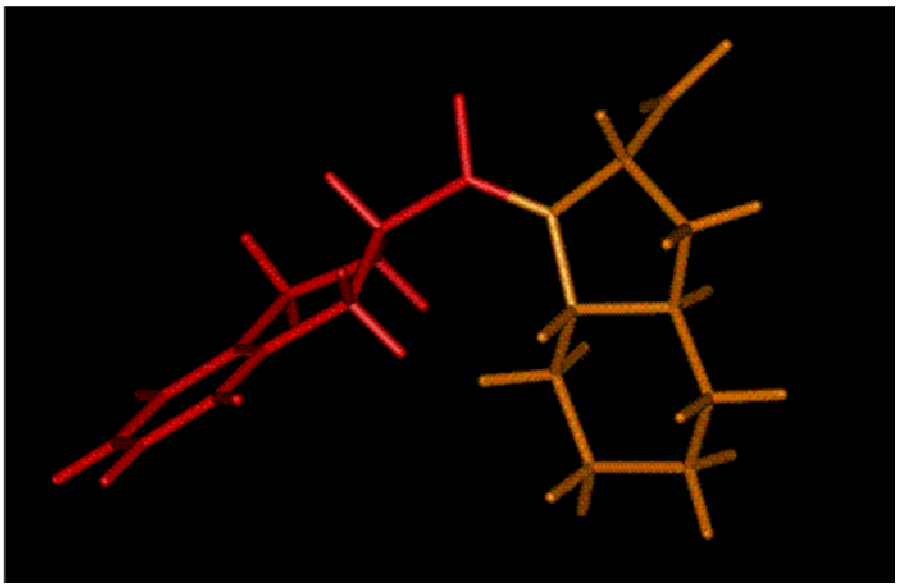

Figure 9.2: The structure of the Tic-Oic dipeptide conformationally restrained unit used in the AMPs designed in our laboratory

The cartoon representation discussed a repeating unit that started and stopped with the dipeptide unit. However, in the case of our peptides, the end of the last repeat unit only includes the first residue of the dipeptide unit, Tic. More specifically, our peptides contain one and a half repeat units, concluding with half of a dipeptide unit. Spacer #3 follows the last repeat unit and defines the distance between the last Tic residue and the C-terminal Lys residues, providing additional conformational flexibility on surface binding.[14]

The purpose of a conformationally restrained dipeptide unit is to induce an ordered structure onto the peptide. With this in mind, the first logical step in the selection of a conformationally restrained dipeptide unit would be constructing a simple tetra peptide to determine whether or not the dipeptide in fact provides the desired conformational rigidity. The stereochemistry, using D or L isomers, as well as the placement of the amino acid residues in the sequence may be of great importance in determining the conformations of the dipeptide unit.

Five separate simple tetrapeptides, with the basic sequence Ala-Tic-Oic-Ala-NH_2, were modeled using ChemDraw 3D. The tetrapeptides were designed by incorporating both the D and L stereoisomer as well as interchanging their order. A very simple approximation of the minimum energy conformations adopted by the five tetrapeptides Ala- L -Tic- L -Oic-Ala-NH_2, Ala- D -Tic- L -Oic-Ala-NH_2 , Ala-L-Tic- D -Oic-Ala-NH_2 , Ala- L -Oic- L -Tic-Ala-NH_2, and Ala- L -Oic- D -Tic-Ala-NH_2 were compared using ChemDraw 3D and can be seen in **Figure 9.3**.

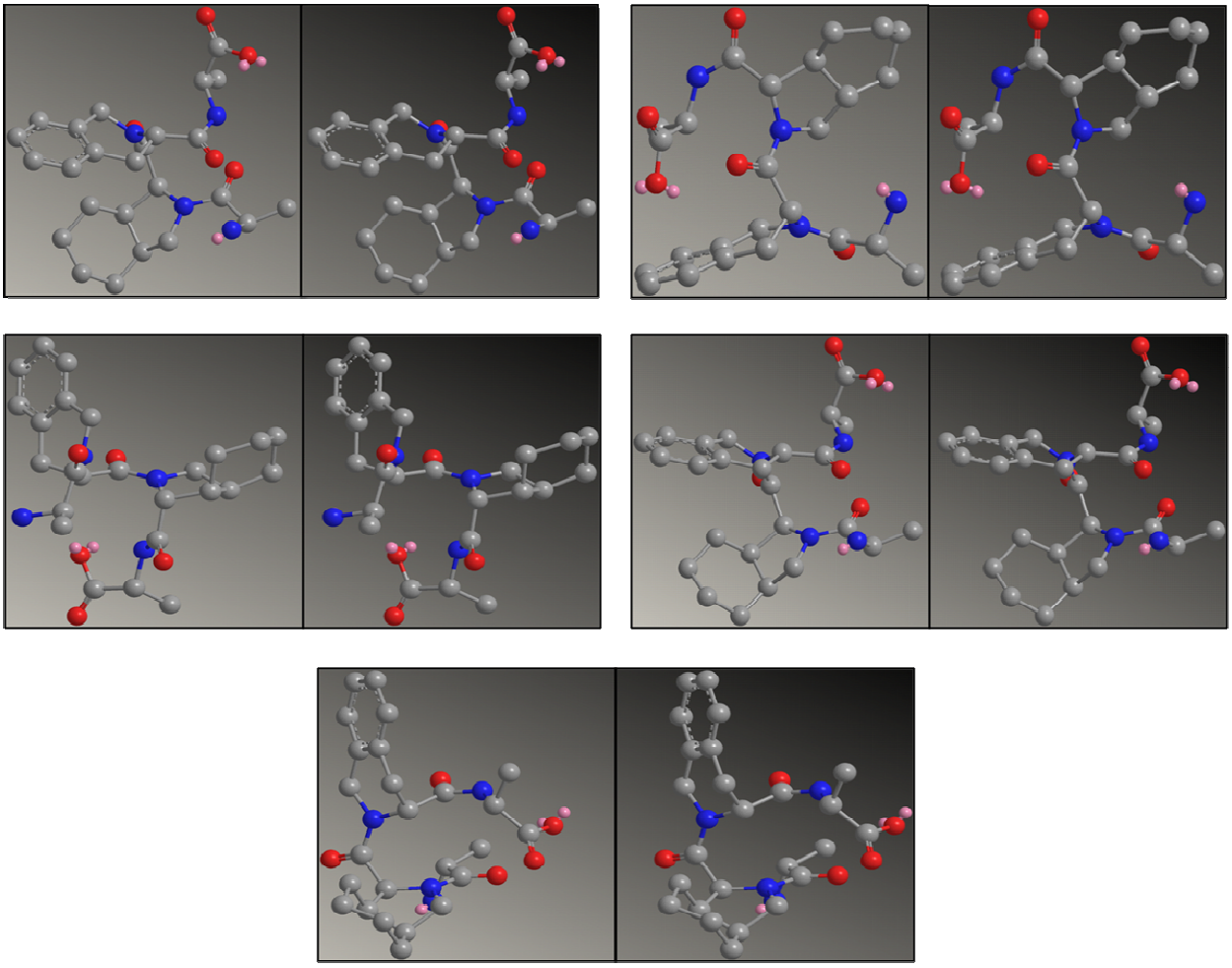

Figure 9.3: Stereoview of the ChemDraw 3D minimum energy structures for the tetrapeptide (hydrogen atoms not shown for clarity) Ala- L -Tic- L -Oic-Ala-NH_2 (top left), Ala- D -Tic- L -Oic-Ala-NH_2 (top right), Ala- L -Tic-D-Oic-Ala-NH_2 (middle left), Ala- L -Oic- L -Tic-Ala-NH_2 (middle right) and Ala-L-Oic- D -Tic-Ala-NH_2 (bottom)

The CD spectra of three of these tetra peptides Ac-Ala-Tic-Oic-Ala-NH_2, Ac-Ala-D-Tic-Oic-Ala-NH_2 and Ac-Ala-Oic-D-Tic-Ala-NH_2 are shown in **Figure 9.4**. These CD spectra clearly demonstrate that the stereochemistry of the alpha carbon can effect the solution conformation of the conformationally restrained dipeptide units.

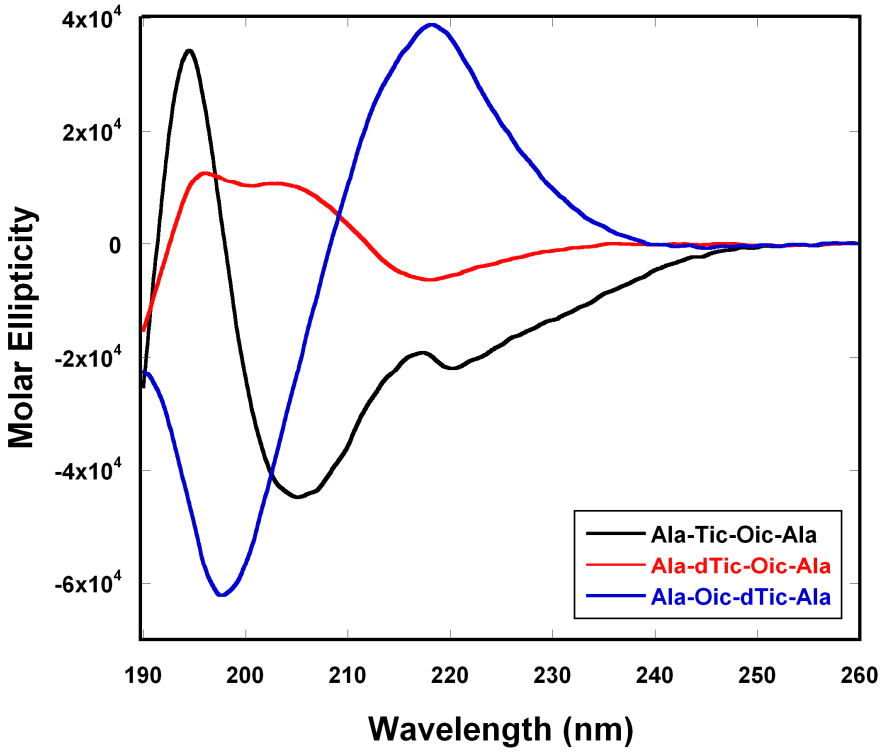

Figure 9.4: The Far-UV Circular Dichroism spectra of the three tetrapeptides (1 mg/mL) dissolved in 40mM phosphate buffer (pH = 6.8). All CD spectra were obtained by acquiring 8 scans on a Jasco J-815 CD Spectrometer using a 0.1mm cylindrical quartz cell (Starna Cells, Atascadero, CA) from 260 to 178nm at 20 nm/min, 1 nm bandwidth, data pitch 0.2nm, response time 0.25 sec and 5 mdeg sensitivity at room temperature (~25°C). The CD spectrum (shown in BLACK) of the tetrapeptide Ac-Ala-Tic-Oic-Ala-NH_2 exhibits an ordered turn containing secondary structure as indicated by the double minima in the CD spectrum at about 195 and 205 nm, which is consistent with the presence of β-turn and helical conformers.[47-49] The CD spectrum (shown in BLUE) of the tetrapeptide Ac-Ala-D-Tic-Oic-Ala-NH_2 exhibits an ordered turn containing secondary structure as indicated by the double maximum in the CD spectrum at about 195 and 205 nm, and a minimum at 185 nm, which is consistent with the presence of possible β-turn conformers.[47-49] The CD spectrum (shown in RED) of the tetrapeptide Ac-Ala-Oic-D-Tic-Ala-NH_2 exhibits an maximum in the CD spectrum at about 220 nm, and a minimum at about 198 nm, which is consistent with a random coil conformers.[47, 48]

The Tic-Oic dipeptide is by no means the only choice for a conformationally restrained dipeptide unit. Of the C^{α}-tetrasubstituted α-amino acids available, α-aminoisobutyric acid (Aib) is the most commonly employed and studied residue and is limited to constrained right and left-handed helical structures.[50] However, additional C^{α}-tetrasubstituted α-amino acids are being developed and investigated. Grauer and Konig[26] have reported the syntheses of a series of novel C^{α}-tetrasubstituted α-amino acids to reduce the conformational flexibility of a peptide. Incorporation of C^{α}-tetrasubstituted α-amino acids derivatives into a peptide sequence can induce stable β-turns[51] or 3_{10} or α-helices.[26, 52, 53] The novel C^{α}-tetrasubstituted α-amino acids developed by Grauer and Konig[26] are given in **Figure 9.5**.

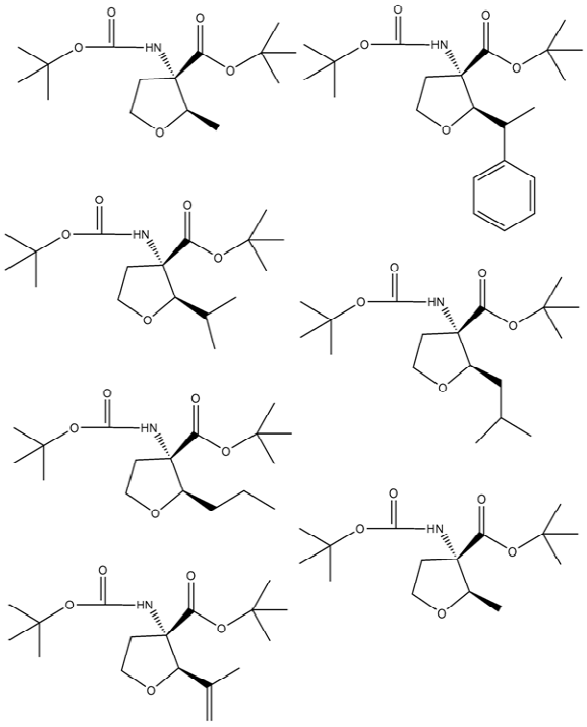

Figure 9.5: Representative novel C^{α}-tetrasubstituted α-amino acids developed by Grauer and Konig[26]

There are several C^{α}-tetrasubstituted α-amino acids that are commercially available as either the Fmoc of tBoc protected analogs or the free amino acids and these are shown in **Figure 9.6**. (R)-2-amino-1,2,3,4,-tetrahydronaphthalene-2-caroxylic acid and (S)-2-amino-1,2,3,4,-tetrahydronaphthalene-2-caroxylic acid shown in **Figure 9.6** are very interesting alicyclic α-amino acids and have the potential to act as conformationally restrained dipeptide units. The advantage the 2-amino-1,2,3,4,-tetrahydronaphthalene-2-caroxylic acid has over the Tic residue is that it contains an amide proton in the peptide which makes NMR studies much easier.

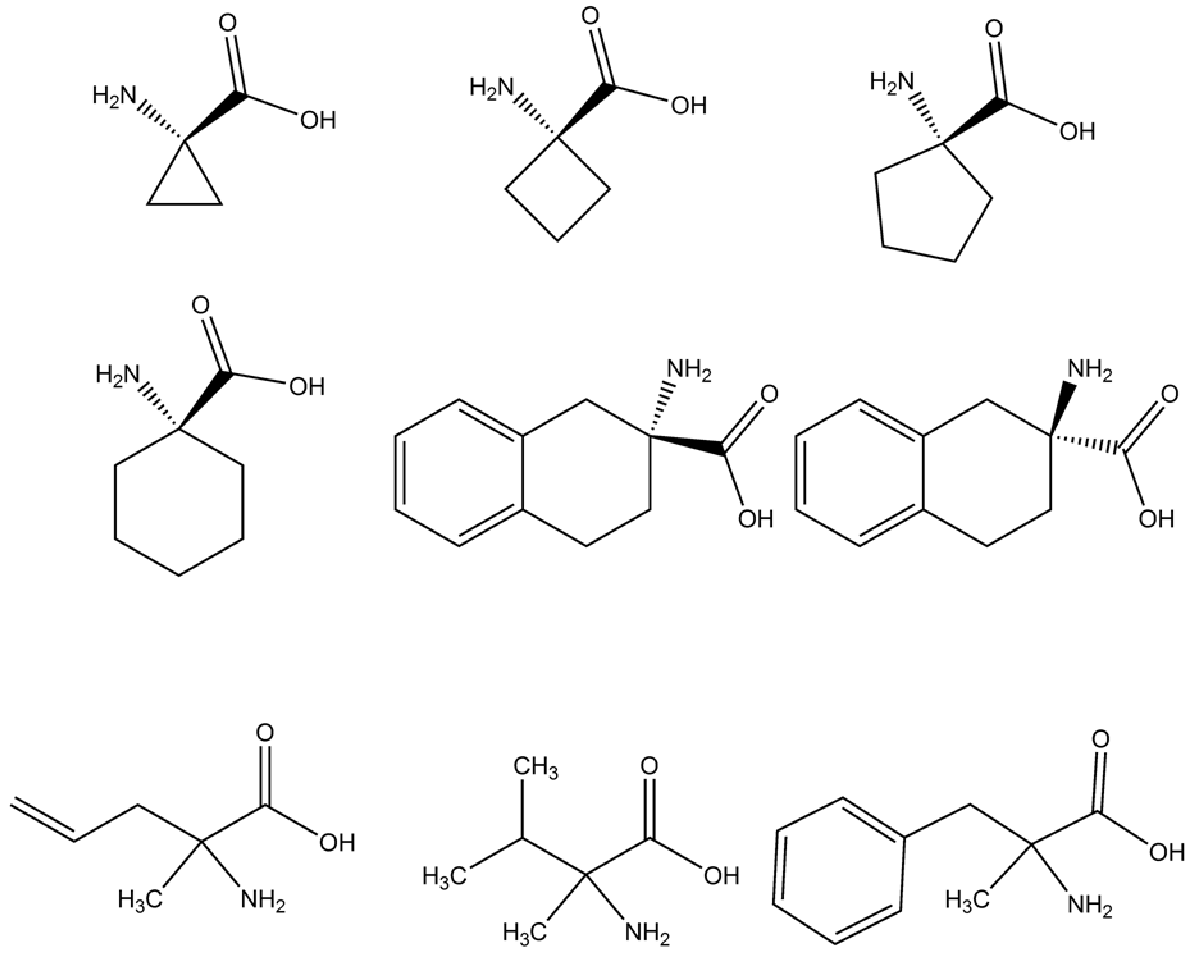

Figure 9.6: Six alicyclic α-amino acids commercially available as either the Fmoc of tBoc protected analogs or the free amino acids.

In **Figure 9.7** stereoviews (using ChemDraw 3D version 10) of hexapeptides with the sequence of Ala-Ala-(2-amino-1,2,3,4,-tetrahydronaphthalene-2-caroxylic acid)-(2-amino-1,2,3,4,-tetrahydronaphthalene-2-caroxylic acid)-Ala-Ala are given. In the top panel of **Figure 9.7** the 2amino-1,2,3,4,-tetrahydronaphthalene-2-caroxylic acid stereochemistry has the RR stereochemistry , in the middle panel the stereochemistry is SS and in the stereochemistry is SR in the bottom panel. As can be seen in the Figures stereochemistry plays an important role in the resulting three dimensional structure and conformational flexibility of the peptide. For an excellent review on the structure of extended and expanded amino acids including C^{α}-tetrasubstituted α-amino acids see Vasudev et. al.[50]

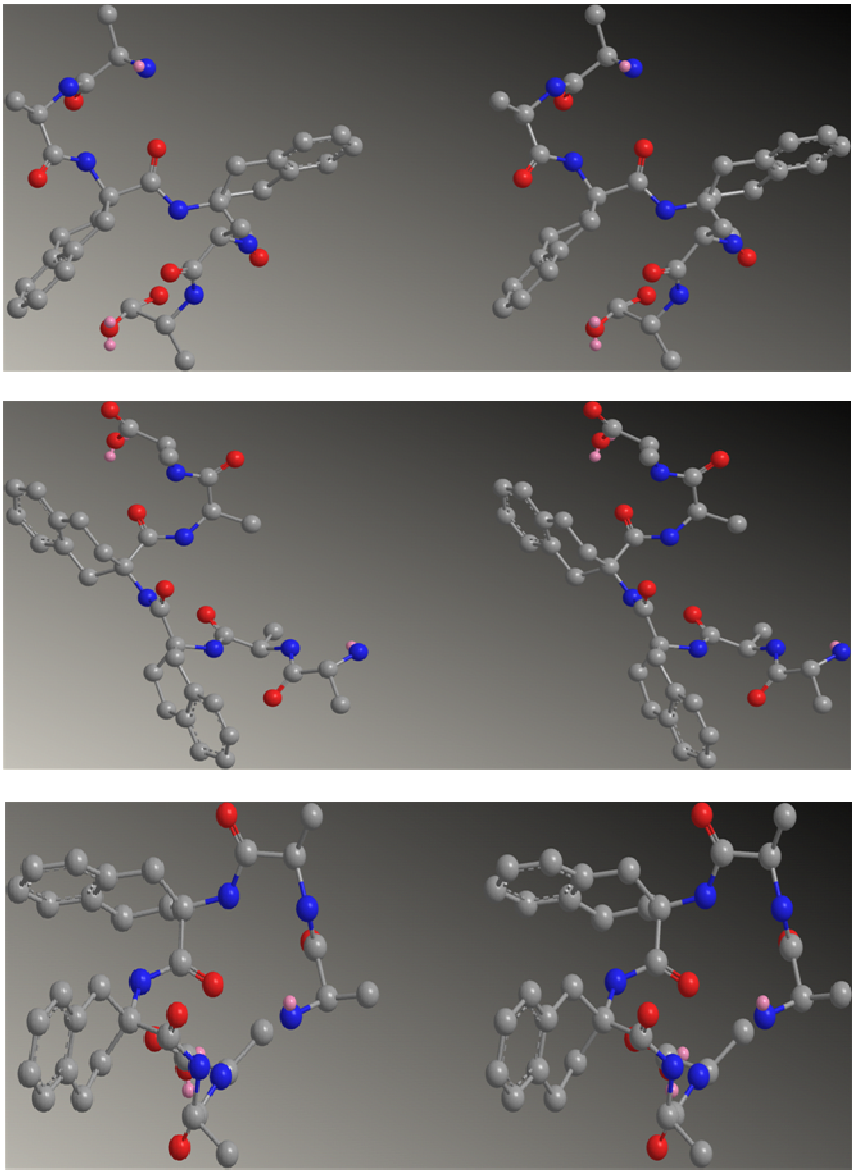

Figure 9.7: Stereoviews of hexapeptides with the sequences of Ala-Ala-((R)-2-amino-1,2,3,4,-tetrahydronaphthalene-2-caroxylic acid)-((R)-2-amino-1,2,3,4,-tetrahydronaphthalene-2-caroxylic acid)-Ala-Ala (top), Ala-Ala-((S)-2-amino-1,2,3,4,-tetrahydronaphthalene-2-caroxylic acid)-((S)-2-amino-1,2,3,4,-tetrahydronaphthalene-2-caroxylic acid)-Ala-Ala (middle) and Ala-Ala-((R)-2-amino-1,2,3,4,-tetrahydronaphthalene-2-caroxylic acid)-((S)-2-amino-1,2,3,4,-tetrahydronaphthalene-2-caroxylic acid)-Ala-Ala (bottom)

Selection of number, position and type of flexible spacers

The amino acid sequences for the flexible spacers in our previous work were the natural amino acid glycine, which contains one carbon atom between the carbonyl carbon and the amide nitrogen, the β-peptide βAla with two carbons, the unnatural amino acids Gaba (gamma-aminobutyric acid) and Ahx (6-aminohexanoic acid) with three and five carbons atoms, respectively. The average distance between the carbonyl carbon atom and the amid nitrogen atom is 2.46, 2.94, 4.68 and 6.91 Å for Gly, βAla, Gaba and Ahx, respectively. Other longer alkyl spacers include the commercially available, 9-aminooctanoic acid (9-Aoa), 10-aminodecanoic acid (10Ada), 12-aminododecanoic acid (12-Adda), and 16-aminopalmitic acid (16-Apa). The longer the amino acid backbone the more flexible the amino acid will be which allows it to occupy a larger amount of conformational space and participate in different intra-molecular hydrogen bonding sequences.[50] An excellent review of the structure of extended and expanded amino acids has been provided by Vasudev et. al.[50]

A number of different α-amino acids have been used to control the conformation of antimicrobial peptides.[33, 54, 55] In our approach we limit their use to the role of a flexible spacer. In addition to β-Ala, analogs of β-Leu and β-Phe, shown in **Figure 9.8,** could also be considered as flexible spacers. These analogs, which are commercially available, have the additional advantage of introducing hydrophobicity into the spacer, along with flexibility.

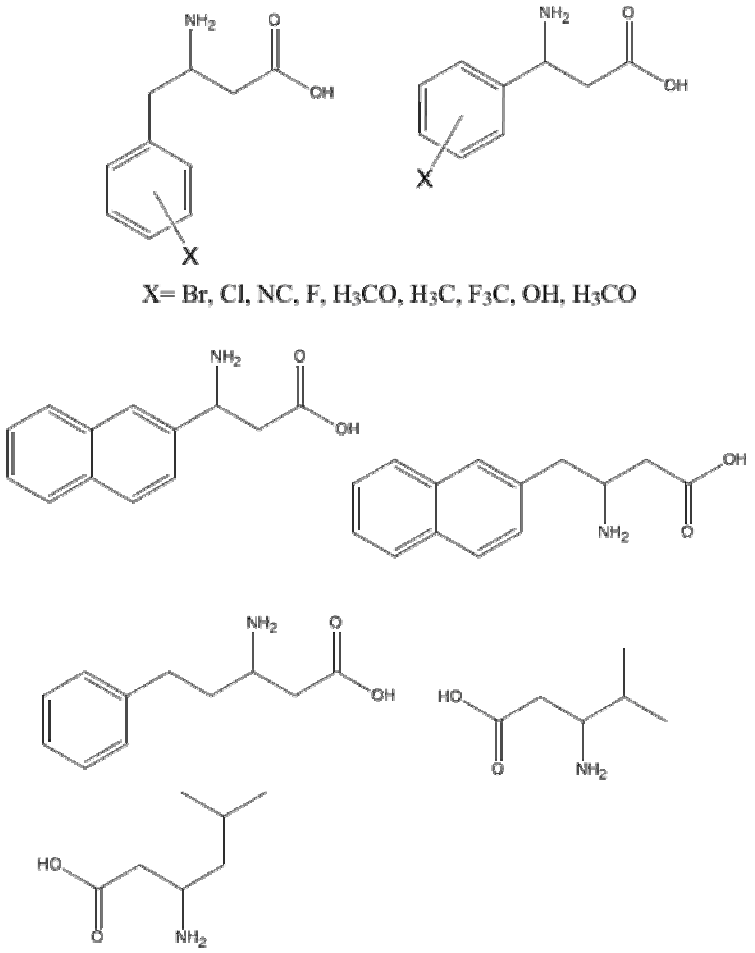

Figure 9.8: Commercially available analogs of β-Leu and β-Phe

The substituted analogs of β-Phe are particularly interesting. The availability of both electron withdrawing and donating groups on the phenyl ring allows for the control of the electron density of the aromatic ring, thus granting the β-Phe analogs the ability to play a dual role as both a flexible spacer and as a hydrophobic residue with varying electronic properties. These spacers can also be used to induce a rigid region onto the peptide backbone using derivatives of amino benzoic acid shown in **Figure 9.9** (other possible derivatives may not

shown). These analogs provide both rigidity and aromatic character, or hydrophobicity, into the backbone. Incorporation of these residues as spacers, however, should be done with care.

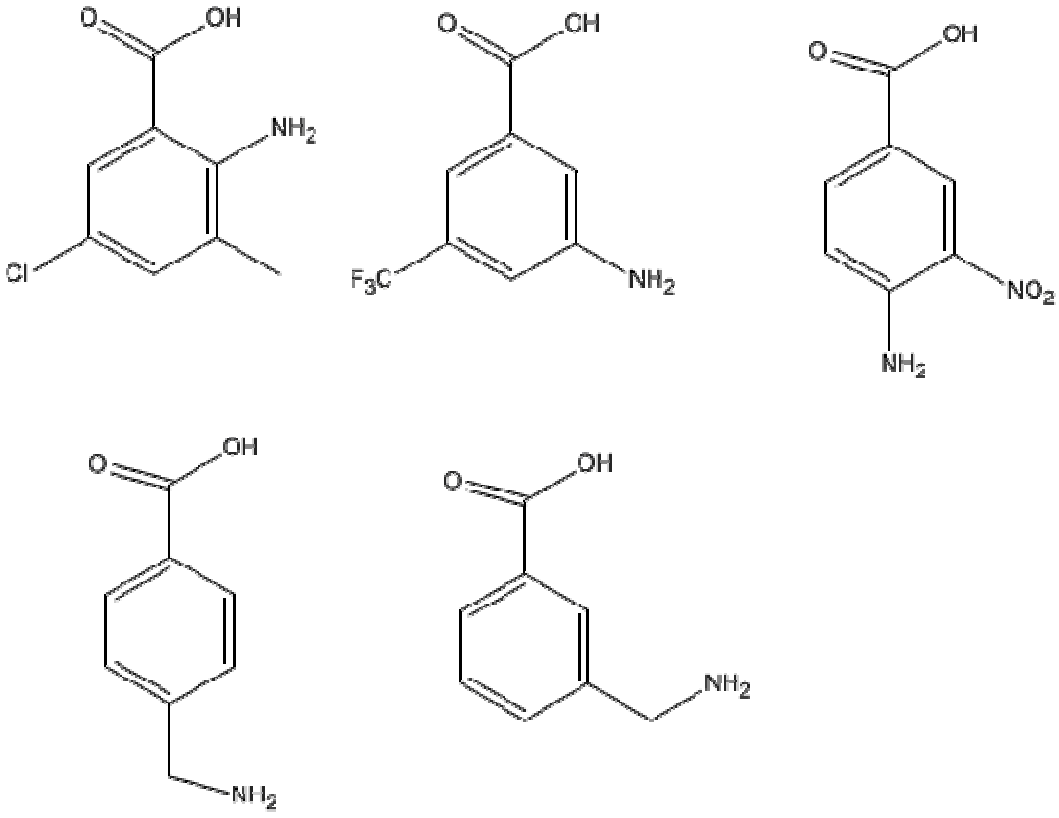

Figure 9.9: A partial listing of the commercially available rigid spacers derived from benzoic acid

Selection of number and position of hydrophobic properties

The next step in the design process is the selection of hydrophobic residues to incorporate into the peptide. There are two basic types of hydrophobic residues 1) aromatic and 2) non-aromatic. Hydrophobic residues are known to play a role in anchoring an antimicrobial peptide

to the membrane by inserting itself into the hydrophobic core of the membrane.[30] Of all the naturally occurring amino acids, Wimley and White determined tryptophan to be the most hydrophobic.[30, 30, 56, 57] It is believed to that the tryptophan residue remains located near the membrane interface and does not partition into deep into the hydrophobic core of the lipid.[30] Haug and co-workers developed a series of short lactoferricin based antimicrobial peptides incorporating different analogs of tryptophan.[30] The net result of this investigation was the development of a novel class of shorter peptides with high antibacterial activity against several resistant strains of bacteria. Some of the hydrophobic and tryptophan analogs used by Haug and co-workers are given in **Figure 9.10**.[30] **Figure 9.10** gives a partial list of commercially available hydrophobic amino acids which may be used to modify the electronic character of the aromatic ring of Phe.

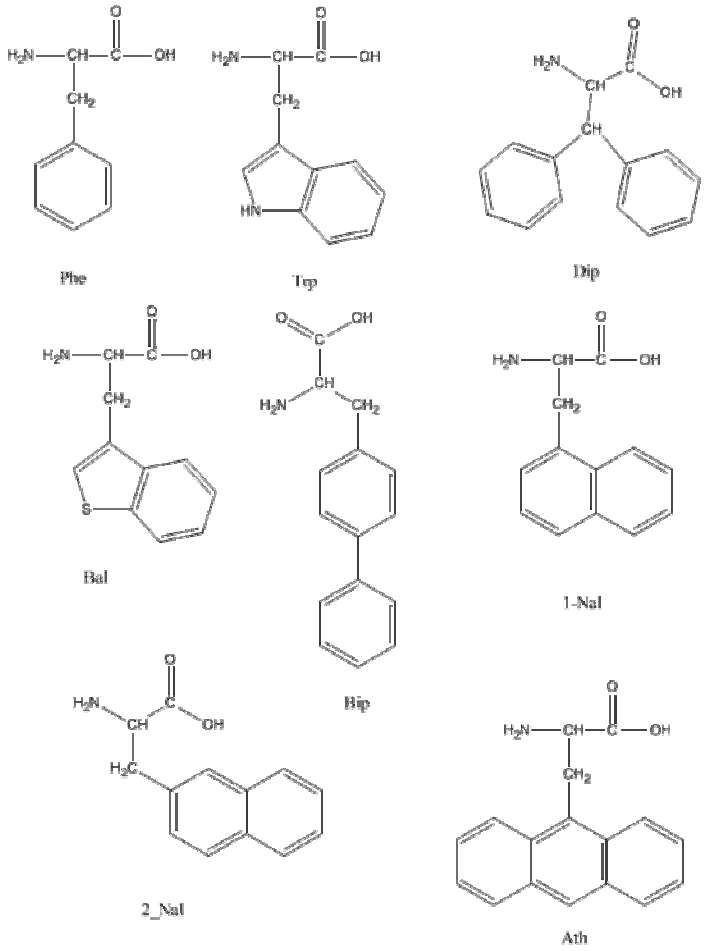

Figure 9.10: Some of the hydrophobic and tryptophan analogs used by Haug and co-workers[30] to developed a series of short lactoferricin based antimicrobial with high antibacterial activity against several resistant strains of bacteria.

Non-aromatic residues include the natural amino acids Leu, and Ile. Also derivatives of β-Leu shown in **Figure 9.11** could be used as hydrophobic residues. However it has been our experience that aromatic residues are preferable.

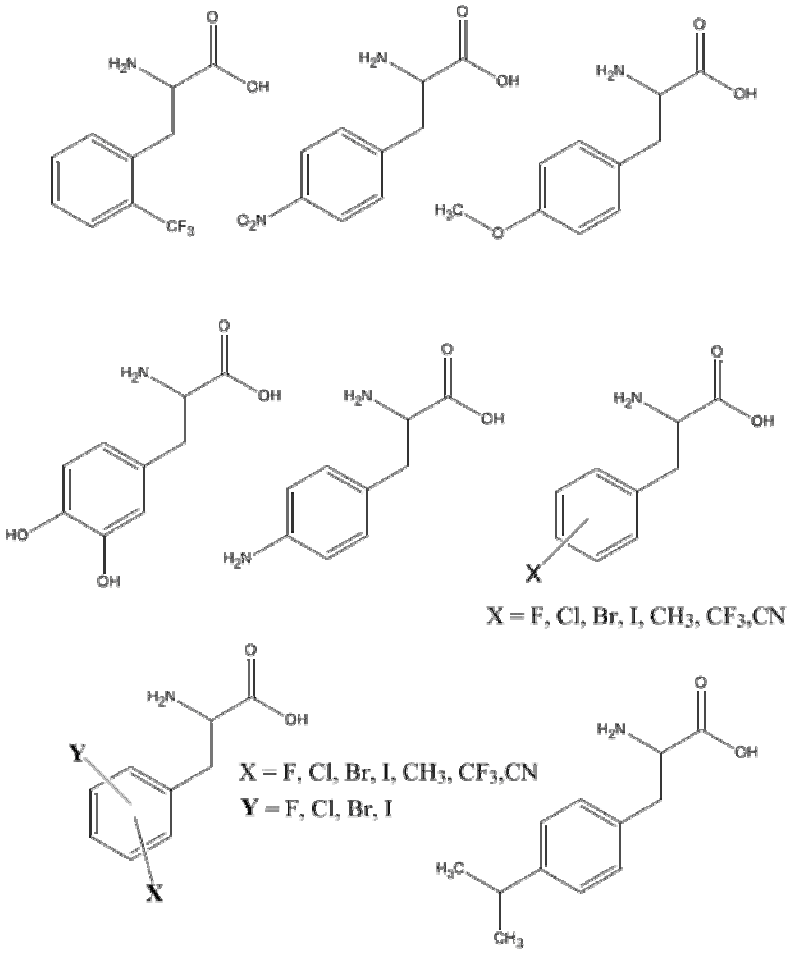

Figure 9.11: A partial list of commercially available hydrophobic amino acids which may be used to modify the electronic character of the aromatic ring of the amino acid residue Phe.

Selection of number and position of electrostatic properties

In our original work the positively charged amino acid residue was referred to as Spacer # 2 and is synomous with residue 6 of the cartoon representation. Spacer #2 consisted of amino acids Lys, Orn, Dpr or Dab, each decreasing the distance from the side chain nitrogen to the α-carbon atom of the peptide backbone. **Table 9.1** gives the average distances for each amino acid residues (Calculated using ChemDraw 3D, Cambridge Software)

Table 9.1: Distance from side chain nitrogen to α-carbon atom of the peptide backbone

Peptide ID	**23**	**43**	**53**	**45**
Residue	Lys	Orn	Dab	Dpr
Average distance	4.76 Å	3.55 Å	2.99 Å	2.56 Å
# of carbons in side-chain	4	3	2	1

Oh and Lee reported[29] the synthesis and biological evaluation of several antimicrobial peptides containing unnatural analogs of the amino acid Lys. These unnatural analogs of Lys are shown in **Figure 9.12** and were designed to incorporate more positive charge (increased number of amino groups) and increase the side chain bulk.[29 51] The increase in positive charge should result in an increase in the electrostatic attraction of the peptide to the surface of a bacterial membrane and thus greater antibiotic activity.[58, 59]

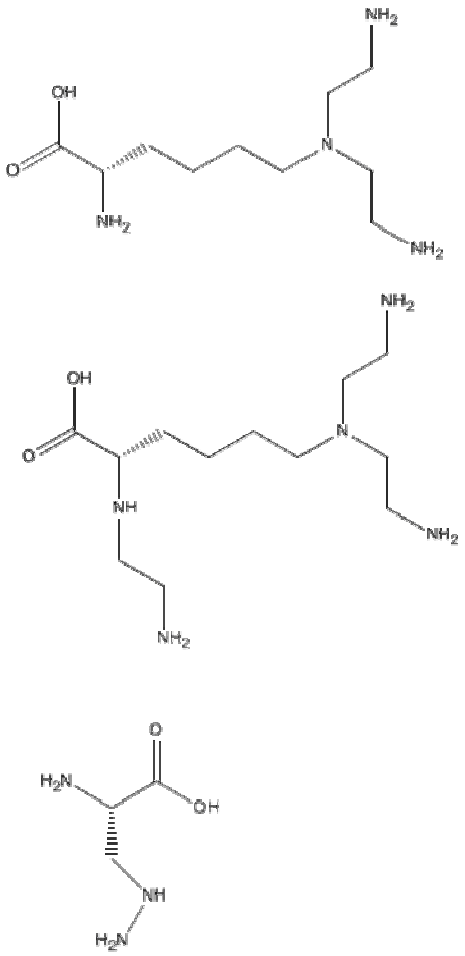

Figure 9.12: Analogs of the amino acid Lys with increased positive charge and side chain bulk developed by Oh and Lee. [51]

One must remember, however, that not all cationic charges are created equal. Arg residues contain a guanidinium group at the end of their side chain. In this planar group the positive charge is delocalized over two different nitrogen atoms. Therefore the positive charge is more dispersed as compared to the localized positive charge on the one nitrogen of the Lys side chain amino group.[30, 60] Also, the work of Haug and co-workers has shown that incorporation of quarternary ammonium groups lead to analogs with similar or lower antimicrobial activity compared to analogs containing Lys residues.[30] one possible explanation for this behaviour is

that by having both positive charge and hydrophobic character in close proximity to one another, an environment is created that interferes with the efficiency of the electrostatic interaction between the peptide and lipid head groups.[30]

Charge Density at the C-Terminus

We have shown that by increasing the number of basic amino acid[15] residues at the C-terminus, the net positive charge density at the C-terminus also increases. It has been previously observed that increased positive charge density, to a point, at the C-terminus can increase antibacterial activity while decreasing hemolytic activity. [14, 15] Organism selectivity has also been observed.[14, 31]

Assemble the Amino Acids to obtain the desired structural and physicochemical properties

In **Figure 9.13** the amino acid sequence of a peptide, compound **46**, (amino acid sequence; Ac-βAla-Fpa-Tic-Oic-βAla-Dpr-Tic-Oic-βAla-Fpa-Tic-Oic-βAla-Dpr-Tic-Dpr-Dpr-Dpr-Dpr-$CONH_2$) that was designed and synthesized in our lab, based on the design principals discussed here in. Although this particular peptide is biologically active, (activity given in **Table 9.2**) this protocol does not guarantee that all peptides designed in this manner will be biologically active and this peptide is used to illustrate the final step before peptide synthesis and purification. In the proceeding section, we will go through each residue from the cartoon representation and offer possible amino acids to incorporate.

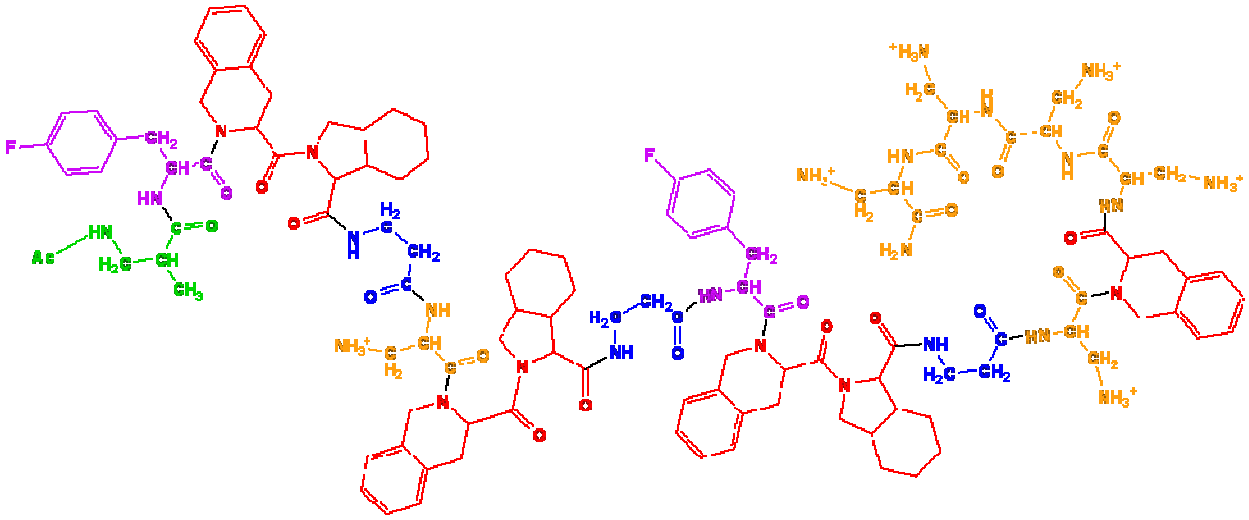

Figure 9.13: Designed amino acid sequence incorporating the desired structural and physicochemical properties.

Table 9.2: Minimum inhibitory concentration (μM) of select bacteria strains for compound **46**[14, 31]

Compound	*Salmonella typhimurium*	*Staphylococcus aureus* ME/GM/TC resistant	*Mycobacterium ranae*	*Bacillus subtillis*
46	3 μM	30 μM	100 μM	0.3 μM

Table 9.3: Minimum inhibitory concentration (μM) of specific Gram negative and other drug resistant bacteria strains for compound **46**.[14, 31]

Compound	46
Acinetobacter baumanii ATCC 19606	3.4
Acinetobacter baumanii WRAIR	3.4
Staphylococcus aureus ATCC 33591	109
Yersinia pestis CO92	219
Brucella melitensis 16M	219
Brucella abortus 2308	219
Brucella suis 23444	219
Bacillus anthracis AMES	6.8
Francisella tularensis SCHUS4	219
Burkholderia mallei	219
Burkholderia pseudomallei	219

The first residue, as previously mentioned, is normally a natural amino acid with neutral charge and it may be the free amine or acetylated. In the case of our example, the N-capping residue, and residue 1, is βAla. The second residue defines the physicochemical character of the N-terminus and is a natural amino acid residue that is either positively charged (Arg, Lys, His, or an unnatural basic residue) or is hydrophobic in nature (Phe, Trp, Tyr, Leu). Residue 2 (striped purple and gold) can also be a derivative of any of the above listed residues, such as Fpa, as in Compound **46**.

Residues 3 and 4 are unnatural amino acids that form a conformationally restrained dipeptide unit. For compound **46** we selected two C^{α}-tetrasubstituted α-amino acids, Tic and Oic, as our dipeptide unit and together they control the local secondary structure and molecular flexibility of our peptide. The use of conformationally restrained amino acids, such as Tic and Oic, reduces the flexibility of the peptide backbone, consequently decreasing the total conformational space that may be sampled by the peptide. It should be noted that the two amino acids used as the conformationally restrained unit may be the same or different depending on the situation.

The fifth residue is an optional spacer, as are all the spacers. In our series of peptides, the spacer immediately following the conformationally restrained dipeptide is referred to as Spacer #1 and can be a Gly residue or an unnatural amino acid such as β-Ala, GABA or longer amino acid, as previously mentioned. There are two Spacer #1 amino acids in the cartoon representation, residues 5 and 10, and when included in the sequence they provide molecular flexibility between the preceding conformationally restrained dipeptide and the following. By increasing the number of $-CH_2-$ groups in the spacer, in our case by including unnatural amino acids such as, βAla, Gaba or Ahx, the length of the peptide backbone increases, thus increasing the molecular flexibility of the local peptide chain. Other longer alkyl spacers that may also be employed include the commercially available, 9-aminooctanoic acid (9-Aoa), 10-aminodecanoic acid (10Ada), 12-aminododecanoic acid (12-Adda), or 16-aminopalmitic acid (16-Apa). The longer the amino acid backbone the more flexible the peptide will be, allowing it to occupy a larger conformational space and participate in different intramolecular hydrogen bonding sequences.[50] For compound **46**, the two Spacer #1 amino acids (residues 5 and 10, royal blue), are βAla which provides two -CH2- groups to the peptide backbone.

Residue 6 is either a positively charge natural or unnatural amino acid, and is also referred to as Spacer #2. By varying the number of $–CH_2-$ groups in the positively charged residue from 1 to 4 in the side chain of the basic residues (Lys, Orn, Dab, Dpr residues) the distance between the positive charge and the peptide backbone will decrease. Dpr has only one methylene group in its side for Compound **46**, decreasing the flexibility greatly when compared to the naturally occurring Lysine. As the length of the side chain decreases the positive charge density will reside closer to the peptide backbone resulting in a less flexible side chain during membrane binding. As previously discussed, this flexibility is more important in the binding with zwitterionic lipids than with anionic lipids due to the covalently bound counter ions.

Another optional spacer follows the positively charged residue. The seventh residue (teal), although excluded in Compound **46**, would precede the dipeptide unit and provide molecular flexibility between the positively charged residue and the next dipeptide unit residues 8 and 9. As before, the dipeptide is followed by a spacer. This spacer, residue 10, is the second Spacer #1 of the sequence and is also β-Ala. It provides molecular flexibility between the preceding dipeptide and the following hydrophobic amino acid, residue 11 (purple). When selecting a hydrophobic residue, which maybe natural or unnatural, factors including size, aromatic character and electron density must be considered. For our example peptide, compound **46**, Fpa was chosen and it must be noted, that Fpa was also the hydrophobic amino acid chosen for residue 2.

The hydrophobic residue is followed by another spacer, residue 12, which can be incorporated to provide additional molecular flexibility between the hydrophobic residue and the third Tic-Oic dipeptide unit, residues 13 and 14. Residue 12, like residue 7, was excluded from Compound **46**.

As mentioned previously, the section of the amino acid sequence from the first dipeptide unit to the third dipeptide unit is considered one repeat unit and a peptide can consist of up to three repeat units, although our peptides only incorporate 1.5. Following the last repeat unit is the final spacer, residue 15, and it is referred to as Spacer #3 in our series of peptides. Spacer #3 is not always included, as in compound **46**, but when it is included it usually consists of the same amino acid residue that is used for Spacer #1. This particular spacer provides molecular flexibility between the last conformationally restrained dipeptide and the cluster of positively charged amino acids that can be found at the C-terminus. The last three to six amino acids of the sequence make up a highly positively charged cluster. These residues may be selected from the common basic residues (Lys, Orn, Dab, Dpr residues) or other unnatural basic amino acid residues and usually, but not always, the same as the amino acid used for Spacer #2, as is the case for compound **46**.

Preliminary Evaluation

Once the peptide(s) have been synthesized and purified their potential as antimicrobial peptides must be evaluated. In vitro screening against several strains of bacterial is critical in determining the activity of these compounds. However, in most research laboratories these assays are not readily available. Therefore samples must be submitted to commercial research organizations for testing. This process can take 4-6 weeks to obtain results and depending on the number of peptides and assays to be screened, this can prove to be a relatively expensive operation. We, there for, recommend the use of CD spectroscopy and calcein leakage studies as a first evaluation of these peptides. If the CD spectra of the peptides do not exhibit different conformations in membrane model systems than they do in buffer, it is most likely that they are

not interacting with the membrane models, and therefore, it is unlikely they will interact with the membrane of a bacterial cell.[32] The results from the calcein leakage assays are critical in determining if the peptide disrupts the membrane.[31, 32, 61] Failure to induce calcein leakage, however, does not mean that the peptide will exhibit no antibiotic activity, but rather that any observed in vitro activity is derived interacting with an intracellular target.

Preparation of POPC and POPC/POPG Liposomes

Refer to chapter 2, Materials and Methods for procedures used.

Dye release experiments

Refer to chapter 2, Materials and Methods for procedures used.

Circular Dichroism

All CD spectra for preliminary evaluations were obtained using the parameters and procedures discussed in chapter 2.

For an example of the observed differences in the CD spectra in these five different environments for compound **46** please see **Figure 9.14**. The shifts in wavelengths and changes in the intensity of the spectra in the anionic and zwitterionic micelle and bilayer membrane models as compared to the spectrum in buffer leads to the conclusion that this AMP does interact with membrane environments. Also, small changes in λ_{max} and λ_{min} were observed between the anionic and zwitterionic models suggesting that this compound may interact differently with the membrane system. If the biological activity of this particular compound were not already known,

this result would act as positive reinforcement that this peptide could possibly exhibit biological activity and selectivity.

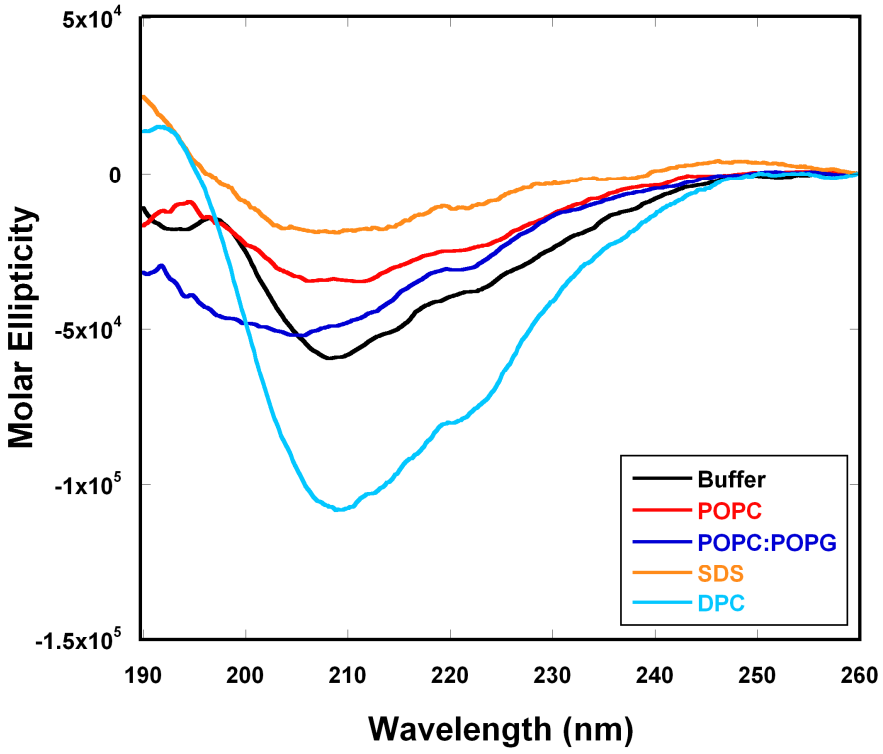

Figure 9.14: The Far-UV CDichroism spectra of compound **46** (1 mg/mL) dissolved in either 40 mM phosphate buffer (pH = 6.8), 80 mM SDS or DPC micelles in buffer, or 10 mM POPC or POPC/POPG (4:1) LUVs in buffer.

Calcein Leakage Assays

Peptide induced calcein leakage was investigated using the praramters and procedures previously discussed in Chapter 2, materials and methods.

The observed differences in calcein leakage from POPC and 4:1 POPC/POPG LUVs caused by compound **46** can be seen in **Figure 9.15**. The clear difference in the concentration dependency for the two types of membrane model systems suggests that there are two different

mechanisms of action occurring. This data supports the CD data in **Figure 9.15** as positive enforcement for the possible use of this compound as a useful therapeutic agent.

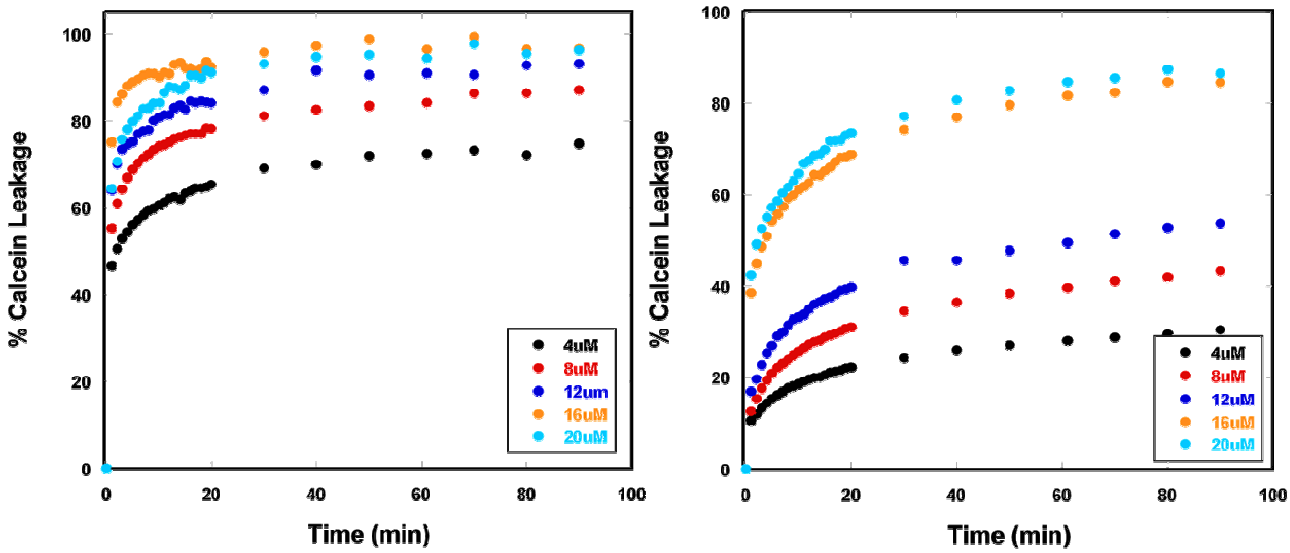

Figure 9.15: The time dependent release of calcein from POPC (left) and 4:1 POPC/POPG LUVs induced by increasing concentrations of compound **46** as measured by fluorescence.[62-64]

Conclusion for preliminary evaluation

In this protocol the procedures and logic used in our laboratory to design antimicrobial peptides containing unnatural amino acids has been outlined. This protocol does not guarantee to lead to potential selective antimicrobial agents on the first attempt. However, careful selection and placement of amino acids with specific physicochemical properties in an iterative process of refinement based on information obtained from the CD and calcein leakage studies should ultimately lead to analogs exhibiting antimicrobial activity. Once compounds are designed that have shown possible bioactivity, in depth characterization investigations involving Circular Dichroism, Isothermal titration calorimetry and calcein spectroscopy should be performed as described in previous chapters.

References

(1) Ma, J. S. Unnatural amino acids in drug discovery. *Chemistry Today* **2003**, 65-68.

(2) Hendrickson, T. L.; de Crecy-Lagard, V.; Schimmel, P. Incorporation of nonnatural amino acids into proteins. *Annu. Rev. Biochem.* **2004**, *73*, 147-176.

(3) Padgett, C. L.; Hanek, A. P.; Lester, H. A.; Dougherty, D. A.; Lummis, S. C. Unnatural amino acid mutagenesis of the GABA(A) receptor binding site residues reveals a novel cation-pi interaction between GABA and beta 2Tyr97. *J. Neurosci.* **2007**, *27*, 886-892.

(4) Rodriguez, E. A.; Lester, H. A.; Dougherty, D. A. In vivo incorporation of multiple unnatural amino acids through nonsense and frameshift suppression. *Proc. Natl. Acad. Sci. U. S. A.* **2006**, *103*, 8650-8655.

(5) Dennison, S. R.; Wallace, J.; Harris, F.; Phoenix, D. A. Amphiphilic alpha-helical antimicrobial peptides and their structure/function relationships. *Protein Peptide Lett.* **2005**, *12*, 31-39.

(6) Toke, O. Antimicrobial peptides: New candidates in the fight against bacterial infections. *Peptide Science* **2005**, *80*, 717-735.

(7) Hancock, R. E. W.; Lehrer, R. Cationic peptides: a new source of antibiotics. *Trends Biotechnol.* **1998**, *16*, 82-88.

(8) Yeaman, M. R.; Yount, N. Y. Mechanisms of Antimicrobial Peptide Action and Resistance. *Pharmacol. Rev.* **2003**, *55*, 27-55.

(9) Papo, N.; Shai, Y. New Lytic Peptides Based on the d,l-Amphipathic Helix Motif Preferentially Kill Tumor Cells Compared to Normal Cellsâ€. *Biochemistry (N. Y.)* **2003**, *42*, 9346-9354.

(10) Giangaspero, A.; Sandri, L.; Tossi, A. Amphipathic alpha helical antimicrobial peptides. *Eur. J. Biochem.* **2001**, *268*, 5589-5600.

(11) Azuma, I.; Yamamura, Y.; Tanaka, Y.; Kosaka, K.; Mori, T. Cell wall of Mycobacterium lepraemurium strain Hawaii. *J. Bacteriol.* **1973**, *113*, 515-518.

(12) Powers, J. -. S.; Hancock, R. E. W. The relationship between peptide structure and antibacterial activity. *Peptides* **2003**, *24*, 1681-1691.

(13) Glukhov, E.; Stark, M.; Burrows, L. L.; Deber, C. M. Basis for selectivity of cationic antimicrobial peptides for bacterial versus mammalian membranes. *J. Biol. Chem.* **2005**, *280*, 33960-33967.

(14) Hicks, R. P.; Bhonsle, J. B.; Venugopal, D.; Koser, B. W.; Magill, A. J. De Novo Design of Selective Antibiotic Peptides by Incorporation of Unnatural Amino Acids. *J. Med. Chem.* **2007**, *50*, 3026-3036.

(15) Bhonsle, J. B.; Venugopal, D.; Huddler, D. P.; Magill, A. J.; Hicks, R. P. Application of 3D-QSAR for Identification of Descriptors Defining Bioactivity of Antimicrobial Peptides. *J. Med. Chem.* **2007**, *50*, 6545-6553.

(16) Conlon, J. M.; Al-Ghaferi, N.; Abraham, B.; Leprince, J. Strategies for transformation of naturally-occurring amphibian antimicrobial peptides into therapeutically valuable anti-infective agents. *Methods* **2007**, *42*, 349-357.

(17) Shlaes, D. M.; Projan, S. J.; Edwards, J. E. Antibiotic Discovery: State of the State. *ASM News* **2004**, *70*, 275.

(18) Bush, K. Why it is important to continue antibacterial drug discovery. *ASM News* **2004**, *50*, 3026-3026.

(19) Klevens, R. M.; Edwards, J. R.; Richards, C. L.; Horan, T. C.; Gaynes, R. P.; Pollock, D. A.; Cardo, D. M. Estimating Health Care-Associated Infections and Deaths in U.S. Hospitals, 2002. *Public Health Reports* **2007**, *122*, 160-166.

(20) Wang, G.; Li, X.; Wang, Z. APD2: the updated antimicrobial peptide database and its application in peptide design. *Nucleic Acids Res.* **2009**, *37*, D933-7.

(21) Hancock, R. E.; Patrzykat, A. Clinical development of cationic antimicrobial peptides: from natural to novel antibiotics. *Curr. Drug Targets Infect. Disord.* **2002**, *2*, 79-83.

(22) Kamysz, W. Are antimicrobial peptides an alternative for conventional antibiotics? *Nucl. Med. Rev. Cent. East. Eur.* **2005**, *8*, 78-86.

(23) Zhang, L.; Falla, T. J. Host defense peptides for use as potential therapeutics. *Curr. Opin. Investig Drugs* **2009**, *10*, 164-171.

(24) Nowick, J. S.; Chung, D. M.; Maitra, K.; Maitra, S.; Stigers, K. D.; Sun, Y. An Unnatural Amino Acid that Mimics a Tripeptide Î²-Strand and Forms Î²-Sheetlike Hydrogen-Bonded Dimers. *J. Am. Chem. Soc.* **2000**, *122*, 7654-7661.

(25) Nowick, J. S. Exploring beta-sheet structure and interactions with chemical model systems. *Acc. Chem. Res.* **2008**, *41*, 1319-1330.

(26) Grauer, A. A.; Konig, B. Synthesis of new Calpha-tetrasubstituted alpha-amino acids. *Beilstein J. Org. Chem.* **2009**, *5*, 5.

(27) Kyle, D. J.; Blake, P. R.; Smithwick, D.; Green, L. M.; Martin, J. A.; Sinsko, J. A.; Summers, M. F. NMR and computational evidence that high-affinity bradykinin receptor antagonists adopt C-terminal beta-turns. *J. Med. Chem.* **1993**, *36*, 1450-1460.

(28) Kyle, D. J.; Green, L. M.; Blake, P. R.; Smithwick, D.; Summers, M. F. A novel beta-turn mimic useful for mapping the unknown topology of peptide receptors. *Pept. Res.* **1992**, *5*, 206-209.

(29) Oh, J. E.; Lee, K. H. Synthesis of novel unnatural amino acid as a building block and its incorporation into an antimicrobial peptide. *Bioorg. Med. Chem.* **1999**, *7*, 2985-2990.

(30) Haug, B. E.; Strom, M. B.; Svendsen, J. S. The medicinal chemistry of short lactoferricin-based antibacterial peptides. *Curr. Med. Chem.* **2007**, *14*, 1-18.

(31) Venugopal, D.; Klapper, D.; Srouji, A. H.; Bhonsle, J. B.; Borschel, R.; Mueller, A.; Russell, A. L.; Williams, B. C.; Hicks, R. P. Novel antimicrobial peptides that exhibit activity against select agents and other drug resistant bacteria. *Bioorg. Med. Chem.* **2010**, *18*, 5137-5147.

(32) Russell, A. L.; Kennedy, A. M.; Spuches, A. M.; Venugopal, D.; Bhonsle, J. B.; Hicks, R. P. Spectroscopic and thermodynamic evidence for antimicrobial peptide membrane selectivity. *Chem. Phys. Lipids* **2010**, *163*, 488-497.

(33) Porter, E. A.; Weisblum, B.; Gellman, S. H. Mimicry of host-defense peptides by unnatural oligomers: antimicrobial beta-peptides. *J. Am. Chem. Soc.* **2002**, *124*, 7324-7330.

(34) Tossi, A.; Sandri, L.; Giangaspero, A. Amphipathic alpha-helical antimicrobial peptides. *Biopolymers* **2000**, *55*, 4-30.

(35) Zasloff, M. Antimicrobial peptides of multicellular organisms. *Nature* **2002**, *415*, 389-395.

(36) Matsuzaki, K. Magainins as paradigm for the mode of action of pore forming polypeptides. *Biochim. Biophys. Acta* **1998**, *1376*, 391-400.

(37) Wenk, M. R.; Seelig, J. Magainin 2 Amide Interaction with Lipid Membranes: Calorimetric Detection of Peptide Binding and Pore Formation. *Biochemistry (N. Y.)* **1998**, *37*, 3909-3916.

(38) Yang, L.; Weiss, T. M.; Lehrer, R. I.; Huang, H. W. Crystallization of antimicrobial pores in membranes: magainin and protegrin. *Biophys. J.* **2000**, *79*, 2002-2009.

(39) Brogden, K. A. Antimicrobial Peptides: Pore formers or metabolic inhibitors in bacteria? *Nature Reviews.Microbiology* **2005**, *3*.

(40) Jing, W.; Hunter, H. N.; Hagel, J.; vogel, H. J. The structure of the antimicrobial peptide Ac-RRWWRF-NH2 bound to micelles and its interacitons with phospholipid bilayers. *Journal of Peptide Research* **2003**, *61*, 219-229.

(41) Watson, R. M.; Woody, R. W.; Lewis, R. V.; Bohle, D. S.; Andreotti, A. H.; Ray, B.; Miller, K. W. Conformational changes in pediocin AcH upon vesicle binding and approximation of the membrane-bound structure in detergent micelles. *Biochemistry* **2001**, *40*, 14037-14046.

(42) Whitehead, T. L.; Jones, L. M.; Hicks, R. P. Effects of the incorporation of CHAPS itno SDS micelles on neuropeptide-micelles binding: separation of the role of electrostatic interactions from hydrophobic interactions. *Biopolymers* **2001**, *58*, 593-605.

(43) Whitehead, T. L.; McNair, S. D.; Hadden, C. E.; Young, J. K.; Hicks, R. P. Membrane-induced secondary structures of neuropeptides: a comparison of the solution conformations adopted by agonists and antagonists of the mammalian tachykinin NK1 receptor. *J. Med. Chem.* **1998**, *41*, 1497-1506.

(44) Perrine, S. A.; Whitehead, T. L.; Hicks, R. P.; Szarek, J. L.; Krause, J. E.; Simmons, M. A. Solution structures in SDS micelles and functional activity at the bullfrog substance P receptor of ranatachykinin peptides. *J. Med. Chem.* **2000**, *43*, 1741-1753.

(45) Hicks, R. P.; Mones, E.; Kim, H.; Koser, B. W.; Nichols, D. A.; Bhattacharjee, A. K. Comparison of the conformation and electrostatic surface properties of magainin peptides bound to SDS and DPC micelles: Insight into possible modes on antimicrobial activity. *Biopolymers* **2003**, *68*, 459-470.

(46) Whitehead, T. L.; Jones, L. M.; Hicks, R. P. PFG-NMR investigations of the binding of cationic neuropeptides to anionic and zwitterionic micelles. *J. Biomol. Struct. Dyn.* **2004**, *21*, 567-576.

(47) Turner, J.; Cho, Y.; Dinh, N. N.; Waring, A. J.; Lehrer, R. I. Activities of LL-37, a cathelin-associated antimicrobial peptide of human neutrophils. *Antimicrob. Agents Chemother.* **1998**, *42*, 2206-2214.

(48) Fuchs, P. F. J.; Bonvin, A. M. J. J.; Bochicchio, B.; Pepe, A.; Alix, A. J. P.; Tamburro, A. M. Kinetics and Thermodynamics of Type VIII β-Turn Formation: A CD, NMR, and Microsecond Explicit Molecular Dynamics Study of the GDNP Tetrapeptide. *Biophys. J.* **2006**, *90*, 2745-2759.

(49) Perczel, A.; Fasman, G. D. Quantitative analysis of cyclic beta-turn models. *Protein Sci.* **1992**, *1*, 378-395.

(50) Vasudev, P. G.; Chatterjee, S.; Shamala, N.; Balaram, P. Structural Chemistry of Peptides Containing Backbone Expanded Amino Acid Residues: Conformational Features of beta, gamma, and Hybrid Peptides. *Chem. Rev.* **2011**, *111*, 657-687.

(51) Crisma, M.; Moretto, A.; De Zotti, M.; Formaggio, F.; Kaptein, B.; Broxterman, Q. B.; Toniolo, C. Turn stabilization in short peptides by C(alpha)-methylated alpha-amino acids. *Biopolymers* **2005**, *80*, 279-293.

(52) Crisma, M.; Saviano, M.; Moretto, A.; Broxterman, Q. B.; Kaptein, B.; Toniolo, C. Peptide alpha/3(10)-helix dimorphism in the crystal state. *J. Am. Chem. Soc.* **2007**, *129*, 15471-15473.

(53) Toniolo, C.; Crisma, M.; Formaggio, F.; Peggion, C. Control of peptide conformation by the Thorpe-Ingold effect (C alpha-tetrasubstitution). *Biopolymers* **2001**, *60*, 396-419.

(54) Epand, R. F.; Raguse, L.; Gellman, S. H.; Epand, R. M. Antimicrobial 14-Helical Î²-Peptides: Potent Bilayer Disrupting Agents. *Biochemistry (N. Y.)* **2004**, *43*, 9527-9535.

(55) Seebach, D.; Matthews, J.,L. β-Peptides: a surprise at every turn. *Chem. Commun.* **1997**, 2015-2022.

(56) White, S. H.; Wimley, W. C. Hydrophobic interactions of peptides with membrane interfaces. *Biochim. Biophys. Acta* **1998**, *1376*, 339-352.

(57) Wimley, W. C.; White, S. H. Membrane partitioning: distinguishing bilayer effects from the hydrophobic effect. *Biochemistry* **1993**, *32*, 6307-6312.

(58) Dathe, M.; Wieprecht, T.; Nikolenko, H.; Handel, L.; Maloy, W. L.; MacDonald, D. L.; Beyermann, M.; Bienert, M. Hydrophobicity, hydrophobic moment and angle subtended by charged residues modulate antibacterial and haemolytic activity of amphipathic helical peptides. *FEBS Lett.* **1997**, *403*, 208-212.

(59) Kiyota, T.; Lee, S.; Sugihara, G. Design and Synthesis of Amphiphilic Î±-Helical Model Peptides with Systematically Varied Hydrophobicâ^'Hydrophilic Balance and Their Interaction with Lipid- and Bio-Membranesâ€ . *Biochemistry (N. Y.)* **1996**, *35*, 13196-13204.

(60) Vogel, H. J.; Schibli, D. J.; Jing, W.; Lohmeier-Vogel, E. M.; Epand, R. F.; Epand, R. M. Towards a structure-function analysis of bovine lactoferricin and related tryptophan- and arginine-containing peptides. *Biochem. Cell Biol.* **2002**, *80*, 49-63.

(61) Medina, M. L.; Bolender, J. P.; Plesniak, L. A.; Chapman, B. S. Transient vesicle leakage initiated by a synthetic apoptotic peptide derived from the death domain of neurotrophin receptor, p75NTR. *Journal of Peptide Research* **2002**, *59*, 149-158.

(62) Wei, S.; Wu, J.; Kuo, Y.; Chen, H.; Yip, B.; Tzeng, S.; Cheng, J. Solution Structure of a Novel Tryptophan-Rich Peptide with Bidirectional Antimicrobial Activity. *J. Bacteriol.* **2006**, *188*, 328-334.

(63) Tamba, Y.; Yamazaki, M. Single Giant Unilamellar Vesicle Method Reveals Effect of Antimicrobial Peptide Magainin 2 on Membrane Permeability. *Biochemistry (N. Y.)* **2005**, *44*, 15823-15833.

(64) Wieprecht, T.; Dathe, M.; Schumann, M.; Krause, E.; Beyermann, M.; Bienert, M. Conformational and Functional Study of Magainin 2 in Model Membrane Environments Using

the New Approach of Systematic Double-D-Amino Acid Replacement. *Biochemisty* **1996**, *35*, 10844-10853.

CONCLUSIONS

Spectroscopic and thermodynamic studies have been conducted in order to gain a better understanding of the mechanisms for the lipid binding that occurs between an AMP and zwitterionic and/or anionic membrane models. The intent of these investigations was to determine which physicochemical characteristics of an AMP increased or decreased biological activity and then use that knowledge to design and synthesize novel AMPs with optimized parameters for increase organism selectivity and potency.

Each of the compounds investigated in this research exhibited different degrees of interactions with anionic and zwitterionic membrane models. The activity that the compounds exhibited against different bacteria strains also varied. We concluded this to be due of the different physicochemical properties of the peptides resulting from the varying structural modifications made to the sequence of the reference peptide, compound **23**. This peptide showed broad spectrum activity at low micromolar ranges while exhibiting minimal activity against mammalian red blood cells. Compound **23** appeared to interact predominately with the surface of zwitterionic POPC LUVs (S-state), while all of the evidence supports the formation of a toroidal pore into the bilayer of the anionic 4:1 POPC/POPG LUVs (I-state).

Lengthening the peptide backbone of compound **23** and incorporating unnatural amino acids as Spacer #1 does in fact play a role in the interactions with model membrane systems. CD spectra of compounds **23**, **36**, **29** and **37** clearly indicate that these peptides interact with zwitterionic and anionic micelles and liposomes differently and the different conformations adopted by the peptides are indicative of different mechanisms. The differences in the ITC data as compared to natural AMPs are due, in large part, to the fact that our peptides incorporate a high percentage of unnatural amino acids and were specifically designed to have regions of

limited conformational flexibility, as well as, region on increased conformational flexibility. The Spacer #1 peptides are believed to interact with POPC LUVs via a modified version of the "carpet" mechanism, as with compound **23**, while forming pores in the presence of 4:1 POPC/POPG LUVs. We have also presented evidence suggesting that the peptides with the shorter spacers, compounds **23** and **36**, require a higher number of peptides to form a leakage inducing pore than compounds **29** and **37** with the longer backbones.

The length of Spacer #2 plays an important role in defining the mechanism of action between this series of peptides and zwitterionic and anionic membrane models. We hypothesized that because Spacer #2 defines the distance between the peptide backbone and the positively charged amine group, it determines the overall surface charge density of the peptide as well as the distance between the peptide backbone and membrane surfaces. The different spectra observed by CD coupled with the different thermodynamic mechanisms studied via ITC support this hypothesis. Also, there appears to be an optimal length for Spacer #2 which promotes antibacterial activity while maintaining minimal interaction with zwitterionic membranes. Compound **43**, with the carbon spacer Orn, exhibited increased antibacterial activity in vitro as well as with the anionic membrane models when compared to compound **23**, but also showed minimal interactions with the zwitterionic membranes. Compound **45**, on the other hand, contained the shortest spacer and interacted the most with zwitterionic membranes, a therapeutically undesirable quality.

Incorporating Spacer #3 into the peptide sequence of compound **23** did not have an increased effect on the interactions with anionic membrane models as concluded by CD, ITC and fluorescence leakage studies. There were similarities to each other and compound **23** in their

results to support the theory that the changes in the length of Spacer #3 played no role in the biological activity.

Changing the number and location of the lysines in the positively charged cluster played an important role the in biological activity of compounds **64**, **39** and **61**. Compounds **64** and **61** exhibited increased interactions via two different mechanisms in the presence of anionic LUVs as compared to compound **23**. The increased activity has been attributed to the decreased charge of compound **64** which reduces the repulsive electrostatic interactions between the peptide and membrane surface. The increased flexibility of the lysine cluster at the N-terminus for compound 61 was determined to attribute to its increased activity. The increased charge of compound **39** resulted in the repulsion of the peptide and therefore decreased its activity.

It was shown in **Figure 3.2** that the percentage of anionic lipids present in the liposomes plays a critical role in the interactions with the peptides, supporting our hypothesis that the chemical composition, and thus the surface physicochemical properties, of the lipid membrane plays a very important role in determining the conformation adopted by these peptides upon binding to the surface. The chemical composition of different strains of bacteria is very different, thus presenting different physicochemical properties to the approaching peptide. By systematically modifying the structure of the peptide, we are able to create peptides with certain physicochemical properties that are compatible with the differing bacterial membrane surfaces. It is therefore reasonable to expect our peptides to be capable of interacting specifically with the membranes of various bacteria strains.

The rational drug design applied to building compound **46** is just one example of how the incorporation of unnatural amino acids into a peptide allows for the control of the physicochemical properties exhibited to bacteria cells. Other peptides that showed varying

selectivity included compounds **37**, **64**, and **61** against several Gram Negative and other drug resistant bacteria strains discussed. Therefore, this study shows that a rational approach may be utilized to design biologically active and selective AMPs.